SEDIMENT-TOXIC SUBSTANCE INTERACTION MODELLING

WAN YIU POR

M.PHIL

THE HONG KONG POLYTECHNIC UNIVERSITY

2003

Memorandum

The accompanying dissertation entitled "Sediment-toxic substance interaction modeling" is submitted for the degree of Master of philosophy in the Department of Civil and Structural Engineering in the Hong Kong Polytechnic University.

The dissertation is based on an independent work carried out by the author from November 1999 to July 2003, with the supervision of Prof. Y. S. Li and Dr. W. H. Wai. The work and the ideas are original and all contributions from others are duly acknowledged in the text by reference.

Yiu Por, Wan

Abstract

Water quality models with analytical solutions are developed to simulate the transport of toxic substances in different aquatic environments. The models take into account both the physical transport processes such as the transport by water flows and dispersion mixings, and the chemical processes such as the sorption kinetics between the toxic substances and the sediment. Analytical forms in this research are being derived because analytical solutions can act as fast predicting tools in relatively simple cases. They also offer fundamental insights into the contributions of particular physical or chemical parameters to the transport process. However, in order to solve the models analytically, the governing systems must be formulated in relatively simple forms, while still retaining sufficient physics and chemistry to be realistic. In accordance with the above requirements, a one dimensional, time varying governing system has been studied and solved analytically.

The vertical axis z is chosen as the controlling dimension in the governing system in order to include the settling and the resuspension of sediment and toxic substances in the water column. An instantaneous equilibrium of sorption kinetics between dissolved and particulate toxic substances is assumed and a governing equation is written in terms of the total toxic substance concentration. The governing system is further studied by assuming two different flow conditions (constant and parabolic distribution of the turbulent mixing coefficient) and the equilibrium distribution of suspended sediment in the whole transport process.

Three analytical water quality models with constant or specific coefficients in the governing equations are developed based on the governing system. The analysis of different parameters in the governing system is carried out to identify the parameter ranges under which the transport of toxic substances can be modeled by the developed models.

Analysis is also conducted to identify the effects of particular parameters on toxic substance transports. Since the particulate toxic substances has an additional downward motion due to the particle settling. The overall concentration is smaller for cases that have a larger fraction of toxic substances in the particulate forms. Thus, a larger partition coefficient and settling velocity or a smaller mixing coefficient leads to lower concentrations.

Finally, three cases studies are presented to demonstrate the applications of the developed models for toxic substance transports and also in other areas. It is found that the models are also useful for simulating the transport of sediment in the water column and of chemicals in soil layers.

Acknowledgements

The author would like to thank those who have provided much assistance in various ways to complete this research project. My chief supervisor, Dr. Y. S. Li. and co-supervisor, Dr. W. H. Wai., both gave valuable advice and professional judgement on the project.

I would also like to thank my parents, brother and sister for their love and moral support during the completion of my thesis. I would like to send my sincere appreciation to all my friends for all their support and assistance during my low periods.

Finally I would like to express strong appreciation of the financial support given by the Hong Kong Polytechnic University.

Notations

a = reference level

A = a/H, dimensionless reference level

$\overline{A}$ = coefficient in Equation (3.4.5.8)

$\overline{A}_{ave}$ = depth average value of $\overline{A}$

A_b = area of bed sediment layer,

A_c = coefficient associated with the averaged area of turbulent bursts per unit bed area = 0.02

$\overline{A}_e$ = coefficient in Equation (3.4.6.1.7)

$\overline{A}_R$ = coefficient in governing equation assuming sediment distribution in the form of Rouse profile

b = maximum sorption capacity of solids

b_1, b_2, b_3 and b_4 = coefficients for settling or resuspension of sediment or contaminant at boundaries in Model 3

B = dimensionless coefficient for deposition velocity of contaminant at sediment water interface in Model 2

$\overline{B}$ = coefficient in Equation (3.4.5.8)

B_1 = dimensionless coefficient for deposition velocity of contaminant at sediment water interface

B_2 = dimensionless coefficient for resuspension velocity of contaminant at sediment water interface

$\overline{B}_{ave}$ = depth average value of $\overline{B}$

B_c = calibrated coefficients in Equation (2.4.3.18)

$\overline{B}_e$ = coefficient in Equation (3.4.6.1.7)

B_i = found from the initial conditions and in Equation (2.4.4.2.7a)

$\overline{B}_R$ = coefficient in governing equation assuming sediment distribution in the form of Rouse profile

$Bta(x,y)$ = Beta function

c = concentration of dissolved toxicant

c_0 = initial concentration of dissolved toxic substance

c_a = reference level concentration of dissolved toxicant

c_c = concentration of toxicants in colloidal organic matter

c_d = dissolved concentration in water

c_e = concentration of dissolved toxicant at equilibrium state

$ce_n(x,q)$ = one of the Mathieu functions

c_s = calibrated coefficient in Equation (2.4.3.18)

c_T = total concentration of toxic substance

c_{TO} = initial total concentration

c_{Tb} = total toxic concentration in bed layer,

$\overline{C}$ = coefficient in Equation (3.4.5.8)

$\overline{C}_{ave}$ = depth average value of $\overline{C}$

$\overline{C}_e$ = coefficient in Equation (3.4.6.1.7)

$\overline{C}_R$ = coefficient in governing equation assuming sediment distribution in the form of Rouse profile

$C'' = 18\log(12H/3d_{90})$

d = sediment diameter,

d_2, d_4 = decay rate of contaminant as boundary to Model 3

d_{50} = median particle diameter

d_{90} = particle diameter that 90% particles have diameters less than d_{90}

$D = \gamma/\phi$

D_* = dimensionless particle parameter

D_i = coefficient in Equation (2.4.4.2.7a)

$D_v(z)$ = Weber parabolic cylinder function

DA = depth average value of difference between magnitude of $\overline{A}$ along water depth and its depth average value, $\overline{A}_{ave}$

DB = depth average value of difference between magnitude of $\overline{B}$ along water depth and its depth average value, $\overline{B}_{ave}$

DC = depth average value of difference between magnitude of $\overline{C}$ along water depth and its depth average value, $\overline{C}_{ave}$

Ent = entrainment flux

f_d = partition fraction of dissolved toxic substance

f_{db} = dissolved fractions in the bed layer

$f_{kd} = k_p/(k_c + k_p)$

$f_{kp} = k_c/(k_c + k_p)$

f_p = partition fraction of particulate toxic substance

f_{pb} = particulate fractions in the bed layer

$\tilde{f}(u)$ = Fourier Transform of a function f(x)

f_s = volume fraction of sediment in mud

F(a,b,c,Z) = hypergeometric function

F_x = flux enters to the control volume in the x direction

F_y = flux enters to the control volume in the y direction

F_z = flux enters to the control volume in the z direction

g = gravitational acceleration

$$h \cong -\frac{k_c k_4 + k_p k_3 + k_p k_4}{k_T}$$

H = water depth

H_b = depth of bed layer

$H_n = H_n(x)$ = Hermite polynomial

I = water surface slope or energy gradient

$J_v(x)$ = Bessel function of first kind

κ = von Karman coefficient

$k = k_p/k_c$

$k_0 = 0.000147$

k_3 = adsorption coefficient for transfer of toxicants from c_d to c_c

k_4 = adsorption coefficient for transfer of toxicants from c_c to c_d

k_c = sorption rate constant of toxic substance to sediment particle

k_d = partition coefficient

k_{dc} = first order decay coefficients of dissolved toxicant

k_{dd} = coefficient estimated by $k_c / k_T \cong k_{dd} s / (1 + k_{dd} s)$

k_{dp} = first order decay coefficients of particulate toxicant

k_{dT} =Decay rate of total toxic substance

k_{DOC} = DOC partition coefficient

k_H = the Henry constant

k_{mz} = turbulent mixing coefficient in the vertical direction

k_p = desorption rate constant of toxic substance to sediment particle

k_r = coefficient in Equation (2.4.3.15)

k_s = sediment partition coefficient

$k_{s0} = k_{s2} s_{I0}$

k_{s2} = second order settling coefficient of sediment

k_{sx} = mixing coefficient of sediment along the x axis

k_{sy} = mixing coefficient of sediment along the y axis

$\bar{k}_{sz}$ = depth average value of k_z

k_{sz} = mixing coefficient of sediment along the z axis

$k_t = k_c + k_p + \upsilon_v / H$

$k_T = k_c + k_p + k_3 + k_4$

k_x = mixing coefficient of dissolved toxicant along the x axis

k_y = mixing coefficient of dissolved toxicant along the y axis

k_z = mixing coefficient of dissolved toxicant along the z axis

K = dimensionless term for contaminant mixing coefficient

$$K_T = f_p \frac{\omega_s}{H} + f_d \frac{\upsilon_f}{H}$$

$$K_{Tb} = \frac{\upsilon_b}{H_b} + \frac{\gamma}{H_b} + f_{db} \frac{\upsilon_f}{H_b}$$

$L\{f\}$ = Laplace transform of a function f

$L^{-1}\left(\tilde{M}(Z,q)\right)$ = Inverse Laplace Transform for a function $\tilde{M}(Z,q)$ with respect to q

$L_n = L_n(x)$ = Laguerre polynomials

$L_n^{\alpha} = L_n^{\alpha}(x)$ = generalized Laguerre polynomials

m = concentration of the intrinsic property

m_{I0} = initial contaminant concentration

m_a = reference level contaminant concentration

M = dimensionless contaminant concentration

M_{I0} = dimensionless initial contaminant concentration

M_a = dimensionless reference level contaminant concentration

$M_{k,\mu}(x)$ = one of Whittaker functions

n = coefficient.

$N_{o1} = \bar{B}H / \bar{A}$

$N_{o2} = \bar{C}H^2 / \bar{A}$

$N_{o3} = \bar{C}H / \bar{B}$

p = concentration of particulate toxicant

p_a = reference level concentration of particulate toxicant

p_e = concentration of particulate toxicant at equilibrium state

ρ_s = density of sediment.

ρ_w = density of water,

P_e = Peclet number

$P_n = P_n(x)$ = Legendre polynomials

$P_n^{\alpha,\beta}(x)$ = Jacobi polynomials

r = toxicant concentration sorbed onto unit mass of sediment

r_e = sorption capacity of solid at equilibrium state,

r_m = first order coefficient for source/sink term

R = dimensionless coefficient for source/sink term

R_c = coefficient in Equation (2.4.4.2.20)

R_d = retardation factor

$Re = \omega_s d/\nu$ = particle's Reynolds number

s = sediment concentration

s_{0max} = maximum volume concentration

s_{l0} = the initial sediment concentration in water

s_a = reference level sediment concentration

s_{DOC} = DOC concentration in sediment

s_e = equilibrium sediment concentration in water

$se_n(x,q)$ = one of the Mathieu functions

t = time

t_0 = detention time of the instantaneous source

t_{50} = half life of a radionuclide

T = dimensionless time

T_b^+ = nondimensional bursting period = 100.

T_c = temperature in °C

T_{ed}, T_{ep} = tolerance values appearing in Section (5.2.2)

$T_n = T_n(x)$ = Chebyshev polynomials

$T_r = (\tau_{b,c} - \tau_{b,cr})/\tau_{b,cr}$

u = instantaneous velocity of water along the x axis

u_s = velocitiy of sediment along the x axis

u_* = shear velocity

$\bar{u}$ = depth-average flow velocity

U_∞ = flow velocity at free surface

v = instantaneous velocity of water along the y axis

ν = kinematics viscosity of water.

v_s = velocity of sediment along the y axis.

V_b = volume of bed sediment layer

w = instantaneous velocity of water along the z axis

W_0 = initial value of source,

$W(t)$ = an exponentially decreasing function

$W_{k,\mu}(x)$ = one of the Whittaker functions

x = x coordinate

$\bar{x}$ = mean sediment diameter

y = y coordinate

$Y_v(x)$ = Bessel function of second kind

z = z coordinate

Z = dimensionless z coordinate

$Z_v(x) = C_1 J_v(x) + C_2 Y_v(x)$ = general solution of the Bessel equation

ω = settling velocity of contaminant

ω_s = settling velocity of sediment

ω_s' = effective sediment settling velocity

α_K = arbitary constant appearing in Model 1

β = ratio of sediment mixing coefficient to momentum diffusion coefficient

β_c = correction factor in Equation (2.4.4.2.19)

β_m = ratio of contaminant mixing coefficient to mixing coefficient

$\beta_s = 1 + 2(\omega_s / u_*)^2$

γ = resuspension velocity of sediment from water-sediment interface

γ_m = resuspension velocity of contaminant from water-sediment interface

γ_s = specific weights of sediment

γ_w = specific weights of water,

σ = dimensionless factor reflecting the effect of the particle's shape on settling velocity

σ_d = standard deviation of sediment distribution

θ' = mobility parameter

θ_{cr} = particle mobility parameter at initiation of motion (Shields)

ϕ = deposition velocity of sediment at the sediment-water interface

ϕ_m = the deposition velocity of contaminant at level a

ϕ_s = factor expresses the influence of the sediment particles on the turbulence structure of the fluid

$\Gamma(z)$ = The Gamma function

$\lambda = \frac{\omega_s}{\beta \kappa u_*}$ = *dimensionless constant for settling velocity*

$\lambda_1 = 1 - \upsilon_v / \omega_s$ *in Equation (2.4.4.2.14)*

$\lambda_2 = 1 + k_d s_{l0} \frac{\upsilon_v}{\omega_s}$ *in Equation (2.4.4.2.18)*

$\varepsilon = \beta \kappa u_* / \overline{u}$

υ_b = *sedimentation velocity*

υ_f = *diffusive exchange velocity of dissolved toxicant*

υ_v = *rate of volatilization loss of the dissolved component*

$\tau_{b,c}$ = *effective current-related bed shear stress*

$\tau_{b,cr}$ = *critical bed-shear stress according to Shields criterion*

Contents

List of figures

List of tables

Chapter 1: Introduction

1.1 Background of water quality modeling related to toxic substance transport in water environment

The issue of chemicals released into the environment in toxic concentrations is a major concern in the maintenance of the integrity of the ecosystem. The toxic substances related to the water quality problems can be defined as the discharge of chemicals into the aquatic environment, which results in concentrations in water or aquatic food chains at levels determined to be hazardous. De Pinto et al (1994, p.1), Ng (2000) and other researchers mentioned that such phenomena have both acute and chronic effects on the ecosystem.

The environmental scientists have serious concerns for the environmental impacts due to the toxic substances because of their special chemical properties in the water. The toxic chemicals may be absorbed onto the particles in the water body. Such contaminated particles after being transported to other locations release toxic chemicals back to the aquatic environment. Therefore, an instantaneous disposal of toxic chemicals may generate acute impacts for several days to chronic impacts in time scales ranging from several years to several decades. The toxic chemicals concentrated in aquatic organisms may also be transferred up to the food chain. Humans, thus often consume a significant level of toxic substances from fish and other aquatic organisms. Lastly, some toxic substances can significantly pollute the aquatic environment at relatively low concentrations.

The environmental engineers should thus seriously consider the impacts from the disposals of toxic substances.

It is impossible to provide a dense measurement network to monitor the extremely vast aquatic environment. Instead, measurements can only be taken at a limited number of points in the area of concern. Water quality models are then used to predict the distribution of contaminants in the whole area. Actions may subsequently be formulated to alleviate the adverse effects of the pollution. Water quality models, thus, always play an important role in providing the whole picture of the pollution.

Using mathematical models to investigate the water quality problems related to toxic substances is a relatively difficult task. The "prediction" capability of a model is always related to the properties of the problem to be investigated. In toxic substance problems, it is important to predict the proportions of dissolved and particulate components of toxic chemicals. The difficulties in the formulation of a water quality model for toxic substances include the modeling of adsorption/desorption interactions between chemicals and particles, particle settlings and re-mobilizations within estuaries.

Toxic substances are prone to several physio-chemical interactions in water such as the diffusive exchange between the sediment and the water column, the loss due to the biodegradation and volatilization, the sorption and desorption between dissolved and particulate forms of toxic substances. Not all required chemicals are affected by all these physio-chemical interactions. Some chemicals are more volatile and less absorbable to solids while the

converse is also true for other chemicals. Since some chemicals are sorbed into solids and particles, the sediments of the water body become particularly significant as a potential long-term reservoir of the chemicals. Sediments are thus responsible for the transport of many toxic substances in the aquatic environment. Therefore, transport models for sediment particles in a water body can be incorporated into the toxic substance transport models.

It is important to understand the reactivity of toxic substances in aquatic sediment for environmental planning assessment. Some research work such as that of O'Conner (1988) focused on predicting the concentration distribution of toxic substances in the water environment and on reaction kinetics of toxic substances in the environment. The distribution pattern of a chemical in the aquatic environment, however, is also affected by the dynamic transport phenomena such as the advection transport and the turbulent mixing. In this research project, mathematical water quality models, by taking both chemical reactions and hydrodynamic transport phenomena into consideration, are developed.

The contaminant transport in the aquatic environment is typically modeled by using the generalized advection and dispersion equation (ADE). The solution of ADE's, in most applications, requires discretized numerical methods in order to simulate the transport phenomena in the coastal regions of complex geometry. The rapid development of computer technology in the last few decades enhances the possibility and the flexibility of using numerical modeling for the simulation of contaminants in a complex coastal environment. Although analytic solutions exist for only a few idealized cases,

they have important roles in water quality modeling. Some of these roles are briefly described here. Firstly, analytic solutions offer fundamental insights into the governing physical processes and facilitate the delineation of the effects of contaminants of a particular physical/chemical parameter. Secondly, they offer validation of results using numerical methods and fast prediction methods for relatively simple cases. Thirdly, closed form solutions provide a generalization of solutions without the worries of different discretisation parameters.

1.2 Objective of the project

In this project, a detailed study for the transport of toxic substances in the aquatic environment is provided. The purpose of the study is to examine a governing system, which describes most common transport phenomena of toxic substances in the aquatic environment. The governing system takes account of the sorption kinetics between toxic substances and sediment, the hydrodynamic transport of sediment and toxic substances and the contribution of sediment and toxic concentrations by the settling / resuspension processes at the sediment-water interface.

Several relatively simpler models with analytic solutions are developed. The purpose is to formulate some analytical models for toxic substance transportation in a dynamic water environment and to predict the water quality after the discharge of toxic substances. The proposed research provides some useful analytic tools for scientists and engineers to predict the

vertical concentration distribution patterns of toxic substances in the aquatic environment of various situations.

While the developed models in the project have constant input parameters or parameters in specific functions, they do not always adequately represent the governing system. The governing system has been analyzed to find the ranges of different input parameters in which the governing system can be further simplified with the objective to evaluate the developed models to adequately represent the system.

Sensitivity analysis of some physical, chemical and mathematical parameters in the governing system and in the developed models are carried out. The purpose is to examine the effect on the toxic substance transport by varying these physical and chemical parameters.

1.3 Scope of the project

In the project, several topics are studied to achieve the goal. Firstly, the physics of hydrodynamics and the transport of contaminants in water are reviewed for understanding each physical process and the physical equations used in the simulation. Secondly, different mathematical techniques are studied for obtaining solutions from the governing system formed in this project. Thirdly, the limitations and the complexity of the governing equations are examined.

A detailed study of the interaction between toxic substances and sediment is also provided. Included are the different physical and chemical

parameters involved in the interaction and the effects of such physical and chemical parameters on the transport of toxic substances in water.

A review is given of previous studies of advection-dispersion equations solved by analytical solutions. The recent development in this research area, particularly the mathematical techniques used to solve the governing system and possible applications of such techniques, are also included.

A review is given of previous experimental studies related to transport of contaminants in water. It allows the identification of useful cases or data for verification and application of the models developed in this thesis.

1.4 Methodology used in the thesis

The thesis concentrates on the theoretical study of the interaction between sediment and toxic substances and the solutions of the differential equations adopted for the interaction models. Equations are written for describing the interaction between sediment and toxic substances in terms of sorption and desorption. The governing equations include the transport terms such as advection, diffusion, settling velocity. The settling and re-suspension of sediment and toxic substances and the diffusive exchange of dissolved toxic substances between the water column and the bottom sediment layer are also considered in the governing equations or as boundary conditions. Other kinetics reactions, such as the volatilization of dissolved toxicity and decay are selectively applied either in the equations or as boundary conditions based on the nature of toxic substances in each case.

The governing equations, which are generally second order partial differential equations, are then solved by different mathematical techniques. This thesis emphasizes the derivation of closed form solutions from the governing equations, and therefore some assumptions / simplifications are inevitable in order to simplify the governing equations to such a level that the equations may be solved analytically. In addition, the parameter sensitivity analysis has been conducted to identify how changing the magnitude of each parameter affects the fate of contaminants. The solutions are verified by available experimental results in the literature. Efforts have been made to identify the application areas of the developed models.

Chapter 2: Literature review of sediment and toxic substance transport modeling

2.1 Literature review of sediment transport modeling

The distinguishing property of many toxic substances is their affinity to surfaces that are provided by solids in suspension and in the sea bed. The correlative effects of the toxic substance transport and sediment transport in the aquatic environment should be taken into account. Several theoretical models for sediment transports have been solved by analytical techniques. These models provide the foundation for the present research. The physical parameters used in sediment transport modeling and models collected from the former researches are presented in this section. The assumptions, including the form of the governing equations, the initial and boundary conditions and solution techniques are described.

2.1.1 Physical parameters

There are a number of important physical parameters in the transport of sediment particles in a water body. Their physical properties and their representations must be carefully understood in order to ensure an accurate estimation of their values or indeed to have acceptable formulae for their evaluation for inputting into the governing equations of a model.

2.1.2 Sediment settling velocity, ω_s

The settling velocity of sediment is a function of the sediment size, shape, density and water viscosity. The sizes of suspended solids found in natural water lie between 0.0005mm (fine clay) and 6mm (fine gravel). The

simplest formula for the settling velocity of a particle is the Stokes' law (Chapra, 1997, (p.300)):

$$\omega_s = \sigma \frac{g}{18}\left(\frac{\gamma_s - \gamma_w}{\gamma_w}\right)\frac{d^2}{\nu} \qquad (2.1.2.1)$$

where g =gravitational acceleration, γ_s = specific weight of sediment, γ_w = specific weight of water, d = sediment diameter, σ = a dimensionless factor reflecting the effect of the particle's shape on the setting velocity (for a sphere it is 1.0), and ν = kinematic viscosity of water in m^2/s. The settling velocity calculated by Stokes' law, lies between 10^{-7} m/s and 0.6 m/s. The value of the kinematic viscosity is a function of water temperature (Van Rijn, 1993 (p3.2)):

$$\nu = 10^{-6}(1.14 - 0.031(T_c - 15) + 0.00068(T_c - 15)^2) \qquad (2.1.2.2)$$

where T_c = temperature in °C. The terminal fall velocity of spherical sediment particles can also be determined by the following formulae (Van Rijn,1984):

$$\omega_s = \frac{g}{18}\left(\frac{\gamma_s - \gamma_w}{\gamma_w}\right)\frac{d^2}{\nu} \qquad for \quad 1 < d \le 100\mu m \qquad (2.1.2.3a)$$

$$\omega_s = \frac{10\nu}{d}\left[\left(1 + \frac{0.01(s_s - 1)gd^3}{\nu^2}\right)^{0.5} - 1\right] \quad for\ 100 < d \le 1000\mu m \qquad (2.1.2.3b)$$

$$\omega_s = 1.1[(s_s - 1)gd]^{0.5} \qquad for \quad d \ge 1000\mu m \qquad (2.1.2.3c)$$

$$s_s = 2.65$$

Richardson and Zaki (1954) developed an equation for effective settling velocity (ω_s'), considering the effect of sediment concentration (s):

$$\omega_s' = \omega_s(1 - (s/\rho_s))^j \qquad (2.1.2.4a)$$

$$j = (4.45 + 18d/H)\mathrm{Re}^{-0.1} \qquad (2.1.2.4b)$$

where ω_s' = effective settling velocity, s = sediment concentration, Re = $\omega_s d/\nu$ = particle's Reynolds number, H = depth of flow, ρ_s = density of sediment. Oliver (1961) also formulated an expression for the settling velocity as affected by the effective sediment concentration (s) and is shown as follows:

$$\omega_s' = (1 - 2.15(s/\rho_s))(1 - 0.75(s/\rho_s)^{0.33})\omega_s \qquad (2.1.2.5)$$

Cheng (1997) developed a formula for the settling velocity of natural sediment particles over a wide range of particle Reynolds number *Re:*

$$\omega_s = \frac{\nu}{d}\left(\sqrt{25 + 1.2(D_*)^2} - 5\right)^{1.5} \qquad (2.1.2.6)$$

in which $D_* = d((\rho_s/\rho - 1)g/\nu^2)^{1/3}$ = dimensionless particle parameter

2.1.3 Sediment turbulent mixing coefficient, k_{sz}

Four commonly used distributions for the sediment turbulent mixing coefficient with depth, namely constant, linear, parabolic and parabolic-constant distributions, are found. The parabolic distribution is the most physically satisfactory one because it is based on a linear shear stress distribution and a logarithmic velocity profile. The expression for the parabolic distribution of the sediment turbulent mixing coefficient is as follows (Van Rijn, 1993 (p7.53)):

$$k_{sz} = \beta\kappa u_* z\left(1 - \frac{z}{H}\right) \qquad (2.1.3.1)$$

in which H is the water depth, κ is the von Karman coefficient (= 0.4 for clear water), β is the ratio of sediment mixing coefficient to momentum diffusion

coefficient (can simply be assumed to be unity) and u_* is shear velocity. Based on the expression for the parabolic distribution of the sediment turbulent mixing coefficient, the range of the sediment turbulent mixing coefficients obtained by the distribution lies between 0 and $0.25\beta\kappa u_*$.

The parabolic form has a weakness that the value of the mixing coefficient near the free water surface is close to zero. This means that there is nearly no sediment mixing near the free surface level, which is an unrealistic situation. The expression of the parabolic-constant form assumes that the value of the mixing coefficient from the middle level to the free surface to be constant and equal to the value at the middle level of the water column.

The value of the shear velocity can be found by the following formulae (Van Rijn, 1993 (p7.27)):

$$u_* = \sqrt{\tau_{b,c}/\rho_w} \qquad (2.1.3.2)$$

or $u_* = \sqrt{gHI}$ for open channel flow (2.1.3.3)

in which I = water surface slope or energy gradient, ρ_w = density of water, and $\tau_{b,c}$ = effective current-related bed shear stress. Han and He (1999) provided the following formula for the shear velocity:

$$u_* = \frac{\overline{u}}{6.5\left(\frac{H}{d}\right)^{1/\{4+\log(H/d)\}}} \qquad (2.1.3.4)$$

in which: $\bar{u}$ = depth-average flow velocity. Equation (2.1.3.3) is difficult to apply since the value of *l* is not easy to identify. Equations (2.1.3.2) and (2.1.3.4) are more useful.

The value of β is contributed to by two parts β_s and ϕ_s as follows (Van Rijn, 1993 (p7.55)):

$$\beta = \beta_s \phi_s \tag{2.1.3.5}$$

The value of β_s can be found by the following formula:

$$\beta_s = 1 + 2\left(\frac{\omega_s}{u_*}\right)^2 \qquad for \quad 0.1 < \frac{\omega_s}{u_*} < 1 \tag{2.1.3.6}$$

The factor ϕ_s expresses the influence of the sediment particles on the turbulence structure of the fluid and is important for cases in which the overall suspended sediment concentration (*s*) is higher than 10 kg/m^3. ϕ_s can be determined as follows:

$$\phi_s = 1 + \left(\frac{s}{0.65\rho_s}\right)^{0.8} - 2\left(\frac{s}{0.65\rho_s}\right)^{0.4} \qquad \text{for } s > 2.5 \text{ kg/m}^3 \tag{2.1.3.7}$$

2.1.4 Sediment deposition flux to bottom layer, *De*

The amount of sediment, which settles from a water column to a bed sediment layer and entrains from the bed sediment layer to the water column, should be accounted for in specifying the boundary conditions in a toxic substance transport model. The most common approach to simulate the deposition flux, *De*, is to calculate the product of the effective settling velocity (ω_s) and sediment concentration at the bottom level ($s|_{z=0}$). Some examples using the approach include Celik and Rodi (1989) and Cheng (1984).

$$De = \omega_s \times s\big|_{z=a} \qquad (2.1.4.1)$$

Thus, the value of *De* depends on the sediment concentration at the bottom level and it varies with time owing to the changes in $s\big|_{z=0}$ until the sediment concentration profile becomes steady.

2.1.5. Sediment entrainment flux from bed sediment, *Ent*

A common approach to the bed entrainment is based on the assumption that the entrainment occurrs at the same rate as the deposition in the case under equilibrium conditions (Celik and Rodi, 1989). The equilibrium near-bed concentration can be computed by using empirical relationships or transport capacity formulae with the aid of an equilibrium-concentration profile assumption and velocity distribution.

$$Ent = \omega_s \times s_a \qquad (2.1.5.1)$$

The amount of the entrainment flux highly depends on the value of the reference level equilibrium concentration s_a, which is discussed in the next section.

2.1.6 Reference level equilibrium sediment concentration, s_a and reference level, *a*

The most logical reference level (*a*) of the sediment concentration profile is the upper edge of the bed-load layer (Van Rijn, 1993 (p7.61)), which is defined as the moving layer with rolling, sliding and saltating of the bed sediment (Van Rijn, 1993 (p7.2)). The reference concentration (s_a) is defined as equal to the bed-load concentration. There is a minimum value of *a*, which equals 0.01 times the water depth. The value of *a* should be equal to $0.01H$ if

the estimated value of the reference level by any formula is less than this value. For a flat bed, there are several formulae to estimate the value of *a* and s_a. Van Rijn (1984) assumed that the motions of bed load particles were dominated by particle saltations under the influence of hydrodynamic fluid and the gravity force. He also assumed that the height of the reference level as the saltation height of the bed-load particles. The expression yields a value of the reference level in the range of 2 to $10d_{50}$. Formulae for *a* and s_a are as follows:

$$a = 0.3 d_{50} D_*^{0.7} T_r^{0.5} \tag{2.1.6.1}$$

$$s_a = 0.18 s_{0\max} \rho_s T_r / D_* \tag{2.1.6.2}$$

$s_{0\max}$ = max*imum volume concentration* (= 0.65)
d_{50} = *median particle diameter*
$T_r = (\tau_{b,c} - \tau_{b,cr}) / \tau_{b,cr}$
$\tau_{b,c}$ = *effective current – related bed – shear stress*
$\tau_{b,cr}$ = *critical bed – shear stress according to Shields criterion*
ν = *kinematic viscosity*
$s_s = \rho_s / \rho_w$ = *relative density of particles*
and $D_* = d((\rho_s / \rho - 1) g / \nu^2)^{1/3}$ = dimensionless particle parameter

The value of the critical bed shear stress can be found from the Shields' curves (Van Rijn, 1993 (p.4.4)). The value of the effective bed-shear stress can be found by the following formulae:

$$\tau_{b,c} = \rho_w g (\bar{u} / C'')^2 \tag{2.1.6.3a}$$

$$C'' = 18 \log(12H / 3d_{90}) \tag{2.1.6.3b}$$

d_{90} is a particle diameter such that 90% of the particles have diameters less than d_{90}. $\bar{u}$ is the depth-averaged velocity (m/s) and C" is in $m^{0.5}/s$.

Some other expressions for the reference level and reference level sediment concentration are provided by Einstein (1950), Engelund and FredsØe (1976), Smith and Mclean (1977) and Zyserman and FredsØe (1994).

Cao (1999) computed s_a by the turbulent bursting approach and derived the following formulae:

$$a = 10\theta' d \tag{2.1.6.4}$$

$$\theta' = \frac{\tau_{b,c}}{(\rho_s - \rho_w)gd} = mobility \quad parameter \tag{2.1.6.5}$$

Two approaches, inner-scale law and outer scale law, are used to compute the value of the entrainment flux.

For inner scale law:

$$Ent = \rho_s \sqrt{(s-1)gd}\, \frac{A_c s_{0\max} \sqrt{(s-1)g}}{T_b^+ \nu \theta_{cr}} (\theta' - \theta_{cr})\theta' \tag{2.1.6.6}$$

in which θ_{cr} = particle mobility parameter at initiation of motion (Shields), which is a function of D_*, A_c = coefficient associated with the average area of turbulent bursts per unit bed area = 0.02. T_b^+ = nondimensional bursting period = 100. s_{0max} = 0.65.

For outer scale law:

$$Ent = \rho_s \sqrt{(s-1)gd}\, \frac{A_c s_{0\max} d}{T_b^+ \theta_{cr} H} (\theta' - \theta_{cr}) U_\infty \tag{2.1.6.7}$$

where U_∞ = flow velocity at the free surface.

Cheng (1984) provides a semiempirical formula for the concentration of suspended sediment at the reference level s_a, which is:

$$s_a = k_0 \gamma_s \left[\frac{\gamma_w}{\gamma_s - \gamma_w}\right]^n \left[\frac{\bar{u}^3}{gH\omega_s}\right]^n \quad (2.1.6.8)$$

where $\bar{u}$ = average flow velocity, k_0 = 0.000147; n = 0.92, $\gamma_s = 2.65\gamma$; γ = (1000kg/m^3)g.

2.2 Analytical solutions for advection and dispersion equation (ADE)

The general form of the advection-dispersion equation for describing contaminant transport (m) in three-dimensional space is as follows:

$$\frac{\partial m}{\partial t} = -\frac{\partial um}{\partial x} - \frac{\partial vm}{\partial y} - \frac{\partial wm}{\partial z} + \frac{\partial^2 k_x m}{\partial x^2} + \frac{\partial^2 k_y m}{\partial y^2} + \frac{\partial^2 k_z m}{\partial z^2} \pm sources / sinks \quad (2.2.1)$$

where u, v and w are the instantaneous velocities along the x, y and z axes, respectively. k_x, k_y and k_z are the mixing coefficients along the x, y and z axes, respectively. The governing equation for describing the transport in one-dimensional space is:

$$\frac{\partial m}{\partial t} = -\frac{\partial um}{\partial x} + \frac{\partial^2 k_x m}{\partial x^2} \pm sources / sinks \quad (2.2.2)$$

As indicated in the pervious sections, ADE can often describe the transport of toxic substance. The following paragraphs review the former research studies, which derive analytical solutions from different cases of ADE.

Mei (1969) developed a model for suspended sediment at steady state condition. The model is a two dimensional model in the flow and the vertical directions. The model assumes a constant settling velocity and turbulent mixing coefficient. It also assumes that the effect caused by the turbulent

mixing in the flow direction is much less than the effect of the flow velocity. Thus the term accounting for the mixing can be neglected in the governing equation. There is no suspended sediment initially at $x = 0$. The boundary condition at the bottom is assumed to be uniform and steady. On the water surface level, the model assumes no diffusion exchange of sediment through the surface. The model was finally solved analytically by using Laplace transform as the main mathematical technique.

Hjelmfelt and Lenau (1970) formulated a model similar to that of Mei (1969), but with a major difference in that the turbulent mixing coefficient was changed from a constant value to a parabolic distribution. The model was solved analytically by using the method of separation of variables and the solution of Hypergeometric Differential Equation.

Based on the model of Mei (1969), Zhang (1980) developed a solution taking into consideration for the resuspension of sediment from the bottom sediment layer. The model assumed a normal distribution of the sediment concentration as the condition at the inflow boundary.

Zhang and Xie (1993) provided a model with a parabolic distribution of the vertical turbulent mixing coefficient. The model considered the settling and resuspension exchange of sediment at the bottom. At the entrance, two distribution functions for sediment concentration were considered, 1. a general deposition case and 2. a point source case at some levels of the entrance section.

Cheng (1984) developed a one dimensional, time varying model with analytical solutions for the non-equilibrium transport of sediment. The model

considered the settling and resuspension exchange of sediment at the bottom.

Barry (1989) developed a time varying, one spatial dimension in the water flow direction advection-dispersion model for the transport of conservative substances. The model allowed the flow velocity and turbulent mixing coefficient to be functions of time.

Runkel (1996) developed an analytical solution to the constant parameter advection-dispersion equation for a continuous source with finite duration. A one dimensional, semi-infinite domain and time varying model with first order decay term in the governing differential equation was presented. Zero initial concentration, zero concentration at infinite travel distance and fixed concentration at zero travel distance were set in the governing system.

Choy and Reible (2000) listed several advection-diffusion models with semi-infinite domain. All models assumed zero concentration gradient at infinity. Some models assumed a constant concentration at inlet boundary while some models assumed a constant flux at the inlet boundary. Some models allowed a finite-time pulse of contaminant input to the system. All models allowed an initial value of contaminant concentration and some models allowed uniform initial concentration capped by a finite region of a different uniform initial concentration.

Prakash (2000) developed a one dimensional, time varying advection-diffusion model to simulate contaminant transport in soil, which allowed an exponential growth/decay of contaminants at source. The model used a

semi-infinite boundary and assumed initial zero concentration along the soil column.

2.3 Analytical solution of ADE for multi-layer media

Some diffusion models as well as advection-diffusion models have been developed for contaminant transport through two or several homogeneous media layers. Most are used for the contaminant transport in soil layers. The most difficult task for the development of such models is the consideration of the interaction between layers. A review of these kinds of models is given below.

Al-Niami and Rushton (1979) developed analytical solutions for dispersion in stratified porous media. Two different situations were considered, flow parallel to the stratification and flow perpendicular to the stratification. The first model considered a two-layered porous medium in which the direction of flow was parallel to the interface. A model of two spatial dimensions, time varying transport of contaminants was developed. The governing equation for each layer considered longitudinal velocity and dispersion in both dimensions. Initially zero concentration of contaminants at both layers was set. At the interface, the continuity of concentration and the concentration gradient was set. A zero concentration gradient was set at other boundaries. The system was solved analytically under the assumption of equal magnitudes of lateral dispersion coefficients in both layers. The second analytical model considered contaminant transport through a three-layer medium. A one dimensional, time varying model was developed. The

governing equation for each layer considered flow velocity and diffusion of contaminants in the medium. Zero initially concentration has been set in the system. The model did not consider the interaction at interfaces, but used the concentration profile generated from the first layer as the input to the layer 2 and similarly for the layer 3.

Leji and Van Genuchten (1995) developed an approximate analytical solution for contaminant transport during steady state flow in a two-layer medium requiring continuity of contaminant fluxes and resident concentrations at the interface. A one dimensional, time varying model with semi-infinite boundary was derived. The governing equation for each layer considered the flow and diffusion of contaminants in the layer. The partial differential equations were augmented by a zero initial condition, a flux type (third type) inlet condition, continuity of concentration (first type) or continuity of net fluxes (third type) interface conditions, and a zero gradient at infinity as boundary conditions for the governing system. The solutions were derived with Laplace transformations making use of the binomial theorem.

Liu, Ball and Ellis (1998) used a generalized integral transform method to derive an analytical solution to the one-dimensional solute advection-dispersion equation in multi-layer porous media. The continuity of concentration and the concentration gradient were considered at interfaces. A flux type inlet condition was used and the inlet flux was allowed to change temporally.

Choy and Reible (2000) considered diffusion models for contaminants in two or three homogenous soil layers. Governing equations of each layer

included the diffusion and first order decay of contaminants. All models allowed an arbitrary initial concentration at each layer and assumed a zero flux at the base. Some models assumed a zero concentration at the surface while others considered mass transfer or reaction at the surface.

2.4 Literature reviews of toxic substance transport modeling

In the following sections, the basic parameters in toxic substance transport models, followed by existing toxic substance transport models are reviewed. The assumptions and application limits of these models are noted.

2.4.1 Parameters for modeling of toxicant transport in aquatic environment

The concentration distribution of toxic substances in a flowing aquatic environment depends not only on general hydrodynamic transport factors, such as advection and turbulent mixing, but also on chemical reaction kinetics. The most important characteristic of the transport process of toxic substances is the unsteady sorption interaction between the dissolved and particulate components. Parameters that appear commonly in the transport models are listed below:

1. Parameters for hydraulic transport of toxic substances:

   Advection: $\frac{\partial u c_T}{\partial x}$. This first order derivative term in the governing equation is used to describe the transport of contaminant by water flow.

Diffusion/turbulent mixing: $\frac{\partial}{\partial x}\left[k_x \frac{\partial c_T}{\partial x}\right]$. This second order derivative term in the governing equations is used to describe the transport of contaminants by turbulent mixing, diffusion or dispersion of water.

Settling: $\frac{\partial \omega_s p}{\partial x}$. The particulate toxic substance settles to the bottom layer due to the particle settling. The motion can be described by this first order derivative term in the governing equations.

Source/loading: W. The term for source or loading of toxic substances to the water column can be added to the governing equations or boundary conditions.

2. Parameters for chemical kinetic terms for toxic substance transport in aquatic environment:

   Adsorption/Desorption: $k_c c\,; k_p p$. The first order terms in the governing equations are used to describe the sorption exchange between dissolved and particulate toxic substances.

   Decay due to microbial decay, photolysis and hydrolysis : $k_{dT} c_T$. The first order term in the governing equations describes the loss of toxic substances due to the above chemical processes.

3. Kinetic terms for toxic substance exchanges between an aquatic environment and an air above water surface:

   Volatilization: $\upsilon_v c$. Volatilization loss of dissolved contaminant can be described by this term in the boundary conditions at water surface.

4. Exchange of toxic substances between water and bed layer:

Diffusion exchange: $\upsilon_f c$, $\upsilon_f c_a$

Deposition: ϕp_a

Resuspension: γp_a

The above first order terms in boundary conditions at the water-sediment interface are used to describe the exchange processes of dissolved and particulate toxic substances between the water column and the bed sediment layer, in which c and p are dissolved and particulate toxic substance concentration, and $c + p = c_T$ = total concentration of toxic substance. k_c = sorption rate constant of toxic substances to sediment particles. k_p = desorption rate constant of toxic substances to sediment particles. k_x is the contaminant mixing coefficient in x-direction, u is the flow velocity in x-direction. υ_v is the rate of volatilization loss of dissolved toxic substances. υ_f is the diffusion exchange velocities at water-bed sediment interfaces. c_a and p_a are reference level concentrations of dissolved and particulate toxic substances at bed sediment layers respectively. ϕ is the deposition velocity of sediment at sediment-water interfaces. γ is the resuspension velocity of sediment from water-sediment interfaces.

2.4.2 Instantaneous and noninstantaneous equilibrium for sorption mechanics in toxic substance transport modeling

The sorption interaction between the dissolved and particulate components tends to a state of equilibrium. The time required to achieve this condition markedly depends on the characteristics of the chemical and sorbent. If the rate of achieving equilibrium is much faster than the other

kinetic routes, such as decay and volatilization, a state of instantaneous equilibrium may be assumed.

In an instantaneous equilibrium, the governing equations of the transport of toxic substances in the water column can be reduced to a single equation by applying the concept of partition fractions. If instantaneous equilibrium does not materialize, at least two governing equations must be set for both dissolved and particulate components. The assumption thus separates the transport models into two different kinds. As there is only one partial differential equation when assuming instantaneous equilibrium, the model allows the consideration of more parameters, especially some dynamic transport terms, which are first or even second order partial derivatives in the establishment of the analytical solution.

2.4.3 Existing models for toxic substance transport without assuming instantaneous equilibrium for sorption mechanics

O'Conner (1988) proposed some equations and solutions for the steady-state distribution of sediment and sorption chemicals in freshwater systems. The first model assumes a constant concentration of suspended sediment and considers the partition exchange between dissolved and particulate toxicants, and loss by volatilization. The governing equations are:

$$\frac{dc}{dt} = -(k_c + \frac{\upsilon_v}{H})c + k_p p \qquad (2.4.3.1)$$

$$\frac{dp}{dt} = k_c c - k_p p \qquad (2.4.3.2)$$

The initial condition is:

$$c = c_0 = c_{TO} = \textit{initial total concentration} \qquad \textit{(i.e. } p = 0\textit{)}$$

in which υ_v = coefficient due to volatilization loss of chemical, c = dissolved concentration; p = particulate concentration. The solutions to the two differential equations are:

$$c = c_{TO}(f_{kp}e^{-k_t t} + f_{kd}e^{-f_{kd}t\upsilon_v/H}) \quad (2.4.3.3)$$

$$p = c_{TO}(-f_{kp}e^{-k_t t} + f_{kp}e^{-f_{kd}t\upsilon_v/H}) \quad (2.4.3.4)$$

in which

$$f_{kd} = k_p/(k_c + k_p) \quad (2.4.3.5a)$$

$$f_{kp} = k_c/(k_c + k_p) \quad (2.4.3.5b)$$

$$k_t = k_c + k_p + \frac{\upsilon_v}{H} \quad (2.4.3.5c)$$

The second model is a modification of the first one, and takes further account of the dissolved and colloidal organic matter by assuming this matter is proportional to that of the particulate sediment concentration (s), leading to:

$$\frac{dc_d}{dt} = -(k_c + k_3)c_d + k_p p + k_4 c_c \quad (2.4.3.6)$$

$$\frac{dc_c}{dt} = k_3 c_d - k_4 c_c \quad (2.4.3.7)$$

$$\frac{dp}{dt} = k_c c_d - k_p p \quad (2.4.3.8)$$

in which c_d = dissolved concentration in water, c_c = concentration of toxicants in colloidal organic matter, total concentration = $c_T = c_d + c_c + p = c + p$; k_3 = adsorption coefficient for transfer of toxicants from c_d to c_c and vice versa for k_4. The solutions of these three equations are as follows:

$$\frac{c}{c_T} - \frac{c_e}{c_T} = \left(\frac{1}{1+k_{dd}s} - \frac{1}{1+k_d s} \right) e^{ht} + \frac{k_{dd}s}{1+k_{dd}s} e^{-k_T t} \qquad (2.4.3.9)$$

$$k_T = k_c + k_p + k_3 + k_4 \qquad (2.4.3.10)$$

$$h \cong -\frac{k_c k_4 + k_p k_3 + k_p k_4}{k_T} \qquad (2.4.3.11)$$

$$\frac{k_c}{k_T} \cong \frac{k_{dd}s}{1+k_{dd}s} \qquad (2.4.3.12)$$

and c_e = concentration of dissolved toxicant at equilibrium state.

There are also other models for modeling the sorption of toxic substances to sediment. For the case of extremely low heavy metal ion concentrations, the Henry model is similar to O'Conner's (1988) model except that it does not consider the effect of volatilization and decay. The system and sorption isotherm of the Henry model are given below (Huang and Wan, 1997):

$$\frac{dp}{dt} = k_c c - k_p p \qquad (2.4.3.13)$$

$$p_e = k_H c_e \qquad (2.4.3.14)$$

in which p_e = concentration of particulate toxicant at equilibrium state, k_H = the Henry constant.

Under the condition of toxic substance concentrations in common range, either the Freundlich model or the Langmuir model can be applied. Freundlich model uses the same reaction equation as the Henry model but a different sorption isotherm, that is (Huang and Wan, 1997):

$$p_e = r_e s = k_f s c_e^{1/n} \qquad (2.4.3.15)$$

in which r_e = sorption capacity of sediment at equilibrium state, k_r and n are coefficients. It is a pure empirical formula.

The system of Langmuir model is as follows (Huang and Wan, 1997):

$$\frac{dp}{dt} = k_c c(b-r) - k_p p \tag{2.4.3.16}$$

$$p_e = \frac{bc_e}{ks + c_e} \tag{2.4.3.17}$$

in which r = sorption capacity of sediment, b is the maximum sorption capacity of sediment, and $k = k_p / k_c$.

Another popular model is the BET model as follows (Chapra, 1997, (p.717)):

$$r = \frac{bB_c c}{(c_s - c)[1+(B_c - 1)(c/c_s)]} \tag{2.4.3.18}$$

$$p = rs \tag{2.4.3.19}$$

in which B_c and c_s are calibrated coefficients.

Huang and Wan (1997) developed two sorption models for cases of extremely low and common range heavy metal concentrations in the water phase. The models assume complete mixing of toxicants in the environment for conservative chemicals and given initial values of the dissolved and particulate components of toxic substances.

2.4.4 Existing models for toxic substance transport at instantaneous equilibrium for sorption mechanics

2.4.4.1 Partition fractions

The most important concept for toxic substance transport models is the assumption of instantaneous equilibrium for the sorption interaction

between dissolved and particulate components and the resulting definitions of partition coefficients and partition fractions. Partition fractions are fractions of dissolved and particulate toxic substances at local equilibrium conditions. The partition fraction for dissolved components, f_d, and particulate toxic substances, f_p, are respectively expressed as follows (Thomann and Mueller, 1987 (p.508)):

$$f_d = \frac{1}{1+k_d s}; f_p = \frac{k_d s}{1+k_d s} \qquad (2.4.4.1.1)$$

$$c = f_d c_T ; p = f_p c_T \qquad (2.4.4.1.2)$$

$$f_d = 1 - f_p \qquad (2.4.4.1.3)$$

in which k_d is the partition coefficient defined by:

$$k_d = {}^{r_e}\!/_{c_e} \qquad (2.4.4.1.4)$$

where r_e is the sorption capacity of sediment at equilibrium (dimensionless) and c_e is the dissolved toxicant concentration at equilibrium. These two expressions are sufficiently general to cover various situations.

There are also other possible expressions based on sorption interactions between dissolved and particulate toxic substances such as the Henry or Langmuir model. The equilibrium condition of these models can be converted to the partition fractions for dissolved and particulate toxic substances.

2.4.4.2 Existing models

Several models have been developed for modeling the fate of toxic substances in water under the complete mixing condition. In natural environments, toxic substances in water often interact with the suspended sediment as well as the bed sediment. The settling/resuspension of particulate toxic substances and diffusion exchanges of dissolved toxic chemicals in the waterbed interface should thus be considered in the models.

O'Conner (1988) developed a model for sorption of toxic substances in well-mixed water environments (such as reservoirs) with a settling / resuspension of sediment at the bed layer. The fraction of the dissolved, f_d, and particulate toxic substances, f_p, in water are related to the concentration of suspended sediment in water, and should be functions of time as the sediment concentration changes with time by settling / resuspension at the bed layer. The concentration of suspension sediment (s) is found by solving the following governing equations:

$$\frac{ds}{dt} = -\frac{\omega_s}{H} s + \frac{\gamma}{H} s_a \qquad (2.4.4.2.1)$$

The solution is:

$$s = s_e + (s_{I0} - s_e) e^{-\frac{\omega_s}{H} t} \qquad (2.4.4.2.2)$$

in which $s_{I0}, s_a, s_e = \frac{\gamma s_a}{\omega_s}$ are the initial, reference level and equilibrium sediment concentration in water. ω_s and γ are the settling and resuspended velocities of sediment, and H is the water depth.

The equations for total toxic concentrations in water, c_T, and bed sediment layers, c_{Tb}, are given as follows:

$$\frac{dc_T}{dt} = -f_d \frac{\upsilon_v}{H} c_T - f_p \frac{\omega_s}{H} c_T + \frac{\upsilon_f}{H}\left[f_{db} c_{Tb} - f_d c_T\right] + \frac{\gamma}{H} c_{Tb} \qquad (2.4.4.2.3)$$

$$\frac{d(V_b c_{Tb})}{dt} = f_p \omega_s A_b c_T - \gamma f_{pb} A_b c_{Tb} - \upsilon_f A_b \left[f_{db} c_{Tb} - f_d c_T\right] \qquad (2.4.4.2.4)$$

in which: V_b = volume of bed sediment layer, A_b = area of bed sediment layer, $f_{db} \approx 1/k_{db} s_a$; $f_{pb} \approx 1$ are dissolved and particulate fractions in the bed layer and are constant for constant s_a, υ_f is the transfer coefficient of dissolved exchange. Assuming the value of c_{Tb} is a constant and equal to that at equilibrium, the system can then be simplified to a single equation for c_T.

O'Conner (1988) also developed another model for constant values of f_d and f_p, and instantaneous releasing of a conservative substance with the suspension sediment at equilibrium.

$$\frac{dc_T}{dt} = -\frac{c_T}{t_0} - f_p \frac{\omega_s}{H} c_T + \frac{\omega_f}{H}\left[f_{db} c_{Tb} - f_d c_T\right] + \frac{\gamma}{H} c_{Tb} \qquad (2.4.4.2.5)$$

$$\frac{dc_{Tb}}{dt} = f_p \frac{\omega_s}{H_b} c_T - \frac{\gamma}{H_b} f_{pb} c_{Tb} - \frac{\upsilon_f}{H_b}\left[f_{db} c_{Tb} - f_d c_T\right] - \frac{\upsilon_b}{H_b} c_{Tb} \qquad (2.4.4.2.6)$$

in which υ_b is the sedimentation velocity, H_b is the depth of bed layer and, t_0 is the detention time of the instantaneous source. The solution of c_T is as follows:

$$c_T = B_i e^{lt} + D_i e^{ht} \qquad (2.4.4.2.7a)$$

$$l,h = -\frac{\left(1/t_0 + K_T + K_{Tb}\right)}{2}(1 \pm N) \qquad (2.4.4.2.7b)$$

$$N = \left[1 - \frac{4\left(K_{Tb}/t_0 + \upsilon_b K_T/H_b\right)}{\left(1/t_0 + K_T + K_{Tb}\right)^2}\right]^{1/2} \qquad (2.4.4.2.7c)$$

$$K_T = f_p \frac{\omega_s}{H} + f_d \frac{\upsilon_f}{H} \qquad (2.4.4.2.7d)$$

$$K_{Tb} = \frac{\upsilon_b}{H_b} + \frac{\gamma}{H_b} + f_{db} \frac{\upsilon_f}{H_b} \qquad (2.4.4.2.7e)$$

The values of B_i and D_i may be found from the initial conditions.

The above two models assume constant sediment concentration in water. If the sediment concentration changes with time, such models are much more difficult to be solved analytically. However, for a conservative substance in a system with zero inflow of solid and toxic concentration, and the solids that are introduced as a delta function settle without scour (i.e. $s_e = 0; t_0 = \infty$), the system can then be simplified by applying the initial condition $c_T = c_{T0}$ and becomes as follows:

$$\frac{dc_T}{dt} = -f_p(t)\frac{\omega_s}{H} c_T \qquad (2.4.4.2.8)$$

$$f_p = \frac{k_d s}{1 + k_d s} \qquad (2.4.4.2.9)$$

$$s = s_{i0} e^{-\frac{\omega_s}{H} t} \qquad (2.4.4.2.10)$$

The solution is:

$$\frac{c_T}{c_{T0}} = f_d\big|_{t=0} + f_p\big|_{t=0} e^{-\frac{\omega_s}{H}t} \qquad (2.4.4.2.11)$$

For the case of an instantaneous release of sediment and a volatile non-conservative chemical without diffusive exchange with the bed in a system with infinite detention, the governing PDE for c_T is changed as follows:

$$\frac{dc_T}{dt} = -\left[k_{dT} + f_d \frac{\upsilon_v}{H} + f_p \frac{\omega_s}{H}\right] c_T \qquad (2.4.4.2.12)$$

The solution is:

$$\frac{c_T}{c_{T0}} = e^{-\left(k_{dT}+\frac{\upsilon_v}{H}\right)t} (f_d\big|_{t=0} + f_p\big|_{t=0} e^{-\frac{\omega_s}{H}t})^{\lambda_1} \qquad (2.4.4.2.13)$$

$$\lambda_1 = 1 - \upsilon_v / \omega_s \qquad (2.4.4.2.14)$$

in which k_{dT} is the decay coefficient of the total chemical concentration.

In the case where the settling of suspended sediment follows the second order dynamics, then we have:

$$\frac{ds}{dt} = -k_{s2} s^2 \qquad (2.4.4.2.15)$$

$$\frac{s}{s_{I0}} = \frac{1}{1 + k_{s0} t} \qquad (2.4.4.2.16)$$

$$k_{s0} = k_{s2} s_{I0} \qquad (2.4.4.2.17)$$

in which k_{s2} is the second order settling coefficient of sediment.

Substituting this solution of the suspended sediment to the governing equation of the above case for non-conservative chemical fields, the following solution of c_T can be obtained.

$$\frac{c_T}{c_{T0}} = \exp\left[-(k_{dT} + \frac{\upsilon_v}{H})t\right]\frac{(1+f_d|_{t=0}k_{s0}t_0)^{\lambda_2}}{1+k_{s0}t} \qquad (2.4.4.2.18)$$

in which: $\lambda_2 = 1 + k_d s_{l0}\frac{\upsilon_v}{\omega_s}$.

O'Conner (1988) also developed a model for a non-conservative chemical as a continuous, but time varying input to the system. An exponentially decreasing function $W(t)$ for the input source was assumed. The sediment concentration was assumed to be constant. The exchange of the dissolved chemical between the water and the bed was considered. Thus, the governing equation and solution are as follows:

$$\frac{dc_T}{dt} = \frac{W(t)}{H} - \frac{c_T}{t_0} - k_{dT}c_T - \beta_c f_p \frac{\omega_s}{H}c_T \qquad (2.4.4.2.19)$$

$$W(t) = W_0 e^{-R_c t} \qquad (2.4.4.2.20)$$

$$c_T = \frac{W_0\left[e^{-R_c t} - \exp\left[-\left(\frac{1}{t_0} + k_{dT} + \beta_c f_p \frac{\omega_s}{H}\right)t\right]\right]}{H\left(\frac{1}{t_0} + k_{dT} + \beta_c f_p \frac{\omega_s}{H} - R_c\right)} + c_{T0}\exp\left[-\left(\frac{1}{t_0} + k_{dT} + \beta_c f_p \frac{\omega_s}{H}\right)t\right]$$

(2.4.4.2.21)

in which W_0 = initial value of source, β_c is a correction factor, and R_c is a coefficient.

Chen and Tay (1996) developed a numerical model taking diffusive exchanges of toxic substances between water and the bottom layers into consideration. The model considers dissolved toxic concentrations, particulate concentrations, concentrations in active bottom layers, and inactive bottom layers. Hwang, Jun, Lee and Lung (1998), investigated the

effects of DOC, a filterable colloidal phase on the toxic concentration in the water column. DOC binds chemicals and makes them unavailable for vertical diffusive exchanges. A three-phase partitioning model that consists of free-dissolved, DOC-bound, particulate-bound components of the chemicals is developed. The three-phase partition fractions for dissolved free chemical, f_d^f, DOC-complexed chemical, f_d^{DOC}, and particulate, f_p, are as follows:

$$f_p = \frac{sk_s}{sk_s + 1 + s_{DOC}k_{DOC}} \qquad (2.4.4.2.22)$$

$$f_d^f = \frac{1}{sk_s + 1 + s_{DOC}k_{DOC}} \qquad (2.4.4.2.23)$$

$$f_d^{DOC} = \frac{s_{DOC}k_{DOC}}{sk_s + 1 + s_{DOC}k_{DOC}} \qquad (2.4.4.2.24)$$

in which: k_s = sediment partition coefficient, k_{DOC} = DOC partition coefficient, and s_{DOC} = DOC concentration in sediment.

O'Conner (1988) also introduced a model for steady –state distribution of sediment and sorptive substances in freshwater streams and rivers. The model considers a volatile, non-degradable chemical in water in the main flowing direction of water. The suspended sediment disperses along the water flow direction with constant flow velocity. Analytical solutions are derived for constant values of the coefficient of volatilization, the partition fractions for the bottom sediment layer and constant total toxic concentration in the bottom sediment layer.

2.5 Mathematical techniques for solving second order partial differential equations (PDE)

In the fields of water quality modeling and hydrodynamics, the governing equations used to simulate the fate of contaminants are often advection-dispersion equations (ADE). ADE is a type of second order PDE and therefore corresponding mathematical techniques should be reviewed. Some common solution methods are mentioned in the following paragraphs. Generally, the way to solve a second order PDE system is to first apply appropriate mathematical methods, such a transform method to the governing system. The governing system will then be transformed into a number of ordinary differential equations (ODE) and hence can be solved analytically.

2.5.1 Separation of variables

One of the most common techniques for solving PDEs is the separation of variables. The approach assumes the dependent variable in a system to be a product of several functions, each of which depends on only one of the independent variables. For example, consider a governing system which has a dependent variable, c and independent variables, x and t. The solution of c is then assumed as follows:

$$c(x,t) = F(x)G(t) \qquad (2.5.1.1)$$

By differentiating the above equation we obtain

$$\frac{\partial^2 c}{\partial t^2} = F\ddot{G} \quad \text{and} \quad \frac{\partial^2 c}{\partial x^2} = \ddot{F}G \qquad (2.5.1.2)$$

in which the dots represent derivatives

We then substitute such partial derivatives (first and second order) into the governing equation. The method works if all derivatives of functions *F* and *G* can be separately grouped each group equaling the same constant. The resulting ordinary differential equations can then be solved by standard methods.

2.5.2 Integral Transform Method

Other than the method of separating variables, various integral transforms are widely used to solve second order PDEs. Common integral transforms include Laplace, Fourier, Mellin, Hankel and Meijer transforms. Some are described in the following paragraphs.

2.5.2.1 Laplace Transform

The Laplace transform is a useful tool to solve ADEs cases of PDEs. Governing systems of models appeared in Mei (1969), Cheng (1984) and many other former works are mainly solved by Laplace Transform. The Laplace transform, $L\{f\}$, of a function $f(x)$ defined on $(0,\infty)$ is (Lokenath, 1995, (p.83)):

$$F(s) = L\{f\} = \int_0^\infty e^{-sx} f(x)dx \qquad (2.5.2.1.1)$$

A function depending on more than one variable, such as, the transform of a function $M(Z,T)$ with respect to T, is defined as $\tilde{M}(Z,q)$,

$$\tilde{M}(Z,q) = \int_0^\infty e^{-qT} M(Z,T)dT \qquad (2.5.2.1.2)$$

The main properties of the Laplace transform include linearity and expressivity of transforms of higher order derivatives in terms of those of the lower order. For linearity, the Laplace Transform of the linear sum of two or

several Laplace transformable functions is (Polyamin and Manzhirov, 1998, (p.710)):

$$L\{af(t)+bg(t)\}=aL\{f(t)\}+bL\{g(t)\} \qquad (2.5.2.1.3)$$

in which a and b are constants.

The properties of Laplace Transform for derivatives are:

$$L\{\frac{\partial^n M}{\partial T^n}\}=q^n\tilde{M}(Z,q)-q^{n-1}M(Z,0)-q^{n-2}M'(Z,0)-\ldots-M^{n-1}(Z,0)$$

(Polyamin and Manzhirov, 1998, (p.710)) (2.5.2.1.4)

$$L\left\{a\frac{\partial^2 M}{\partial Z^2}\right\}=a\frac{\partial^2}{\partial Z^2}L\{M\}=a\frac{\partial^2\tilde{M}(Z,q)}{\partial Z^2}$$

(Lokenath, 1995, (p.91)) (2.5.2.1.5)

In general, Laplace Transform and its derivative properties are applied to the governing equation in a system. The method converts the governing equation to a second order ODE in the variable Z. The solution of $\tilde{M}(Z,q)$ is found by solving the second order ODE. Finally, the inverse Laplace transform is applied to convert the solution of $\tilde{M}(Z,q)$ to $M(Z,T)$. The definition of inverse Laplace Transform, $L^{-1}\left[\tilde{M}(Z,q)\right]$, for a function $\tilde{M}(Z,q)$ with respect to q is (Lokenath, 1995, (p.84)):

$$L^{-1}\left[\tilde{M}(Z,q)\right]=M(Z,T)=\frac{1}{2\pi i}\int_{\gamma-i\infty}^{\gamma+i\infty}e^{qT}\tilde{M}(Z,q)dq \qquad (2.5.2.1.6)$$

There are only limited analytical solutions for specific functions of $\tilde{M}(Z,q)$ and numerical integrations is needed for other forms of $\tilde{M}(Z,q)$.

In Inverse Laplace transform, there is also a rule that (Polyamin and Manzhirov, 1998, (p.725)):

$$f(x)=\sum_{k=1}^{n}\frac{R(\lambda_k)}{Q'(\lambda_k)}exp^{\lambda_k x} \qquad (2.5.2.1.7)$$

$$\text{for } Q(p) = constant^{*}(p-\lambda_1)\,(p-\lambda_2)\ldots\,(p-\lambda_n) \qquad (2.5.2.1.8)$$

$$\text{And } L[f(x)]=\frac{R(p)}{Q(p)} \qquad (2.5.2.1.9)$$

where the prime denotes derivatives. The above rule can be widely used to find the inverse transform of $L[f(x)]$ in terms of a polynomial. The rule is also useful for finding the approximate solution of $f(x)$ in which the solution of $L[f(x)]$ is expressed as a combination of other functions and each can be represented by a polynomial.

2.5.2.2 Fourier Transform

Fourier Transform is another common tool for solving second order PDEs. The definition of Fourier Transform, $\tilde{f}(u)$, of a function $f(x)$ is:

$$\tilde{f}(u)=\frac{1}{\sqrt{2\pi}}\int_{-\infty}^{\infty}f(x)e^{-iux}dx \qquad i^2=-1 \qquad (2.5.2.2.1)$$

Useful properties of Fourier Transform include Linearity and Scaling.

The definition of inverse Fourier Transform is:

$$f(x)=\frac{1}{\sqrt{2\pi}}\int_{-\infty}^{\infty}\tilde{f}(u)e^{iux}du \qquad (2.5.2.2.2)$$

Fourier Sine and Fourier Cosine transforms are developments from the Fourier Transform and are also and they are also useful for solving second order PDEs.

2.5.3 Special functions and their properties

During the process of solving a second order PDE, it is common to encounter governing equations which include special form terms. Therefore, the solutions and properties of such functions should be reviewed. Examples include Error function, Gamma and Beta functions, Hyperbolic functions, Hypergeometric functions, Bessel functions, Hankel functions, Legendre functions, Chebyshev functions, Hermite polynomials, Whittaker functions and Jocobi polynomials. Some are general functions with special forms while others are solutions of specific second order ODEs. A selection is described in the following paragraphs.

2.5.3.1 Error function

The definition of an Error function, *erf x*, is:

$$erf\, x = \frac{2}{\sqrt{\pi}} \int_0^x exp(-t^2)dt \qquad (2.5.3.1.1)$$

The Error function often appears in the solution of second order PDEs. Examples include the solutions of the models appearing in the work of Alshawabkeh and Adrian (1997), Runkel (1996) and Formica et.al (1988).

2.5.3.2 Gamma and Beta functions

The Gamma function, $\Gamma(z)$, is an analytic function of the complex argument *z* everywhere except at the points *z=0, -1, -2,...*

$$\Gamma(z) = \int_0^\infty t^{z-1} e^{-t} dt \qquad (2.5.3.2.1)$$

The definition of a Beta function, *Bta(x,y)*, is:

$$Bta(x, y) = \int_0^1 t^{x-1}(1-t)^{y-1} dt \qquad (2.5.3.2.2)$$

where x and y are both real and greater than zero. He relationship between the Gamma and Beta Functions is

$$Bta(x,y) = \Gamma(x)\Gamma(y)/\Gamma(x+y) \qquad (2.5.3.2.3)$$

Gamma or Beta functions appear frequently in the solution of second order PDEs. An example is the solution of the model in Hjelmfelt and Lenau (1970).

2.5.3.3 Hyperbolic sine, cosine and tangent functions

The general definitions of hyperbolic sine, *sinh*, hyperbolic cosine, *cosh* and hyperbolic tangent, *tanh* are as follows:

$$sinh(x) = 0.5(e^{x} - e^{-x}) \qquad (2.5.3.3.1)$$

$$cosh(x) = 0.5(e^{x} + e^{-x}) \qquad (2.5.3.3.2)$$

$$tanh(x) = sinh(x)/cosh(x) \qquad (2.5.3.3.3)$$

Some properties of hyperbolic functions are $sinh(ix) = isin(x)$, $cosh(ix) = cos(x)$ *and* $tanh(ix) = itan(x)$, which are useful for modifying Mei's (1969) and Cheng's (1984) solutions and some models developed by authors shown in later sections of this thesis.

2.5.3.4 Hypergeometric functions

The hypergeometric function $F(\alpha,\beta,\gamma;x)$ is a solution of the Gaussian hypergeometric equation:

$$x(x-1)\frac{d^2y}{dx^2} + [(\alpha+\beta+1)x-\gamma]\frac{dy}{dx} + \alpha\beta y = 0, \text{ for } \gamma \neq 0,-1,-2,-3,\ldots \qquad (2.5.3.4.1)$$

The fucntion $F(\alpha,\beta,\gamma;x)$ can be expressed in terms of the hypergeometric series:

$$F(\alpha,\beta,\gamma;x) = 1 + \sum_{k=1}^{\infty}\frac{(\alpha)_k(\beta)_k}{(\gamma)_k}\frac{x^k}{k!}, \quad (\alpha)_k = \alpha(\alpha+1)\ldots(\alpha+k-1) \qquad (2.5.3.4.2)$$

There are special cases in which the hypergeometric function can be expressed in terms of elementary functions. The solutions of the model in Hjelmfelt and Lenau (1970) and a model developed by the author is solved by using the hypergeometric function.

2.5.3.5 Other special functions for solving special second order ODEs

In addition to the hypergeometric functions, other special functions have been developed to solve second order ODEs in specific forms.

The Bessel function of first kind, $J_v(x)$, and second kind $Y_v(x)$ are solutions of the Bessel equation

$$x^2\frac{d^2y}{dx^2}+x\frac{dy}{dx}+(x^2-v^2)y=0 \qquad (2.5.3.5.1)$$

and

$$J_v(x)=\sum_{k=0}^{\infty}\frac{(-1)^k(x/2)^{v+2k}}{k!\Gamma(v+k+1)},\ Y_v(x)=\frac{J_v(x)\cos\pi v-J_{-v}(x)}{\sin\pi v} \qquad (2.5.3.5.2)$$

The formula for $J_v(x)$ is valid for $v\neq 0,\pm1,\pm2,\ldots$. The general solution of the Bessel equation has the form

$$Z_v(x)=C_1J_v(x)+C_2Y_v(x). \qquad (2.5.3.5.3)$$

The Whittaker functions $M_{k,\mu}(x)$ and $W_{k,\mu}(x)$ are linearly independent solutions of the Whittaker equation:

$$\frac{d^2y}{dx^2}+\left[-\frac{1}{4}+\frac{1}{2}k+\left(\frac{1}{4}-\mu^2\right)x^{-2}\right]y=0 \qquad (2.5.3.5.4)$$

The Whittaker functions are expressed in terms of degenerated hypergeometric functions.

The Legendre polynomials $P_n = P_n(x)$ and the Legendre functions $Q_n(x)$ are solutions of the equation:

$$(1-x^2)\frac{d^2y}{dx} - 2x\frac{dy}{dx} + n(n+1)y = 0 \qquad (2.5.3.5.5)$$

The Weber parabolic cylinder function $D_v(z)$ is a solution of the linear differential equation:

$$\frac{d^2y}{dx^2} + \left(-\frac{1}{4}z^2 + v + \frac{1}{2}\right)y = 0 \qquad (2.5.3.5.6)$$

where the parameter v and the variable z can assume arbitrary real or complex values.

The Mathieu functions $ce_n(x,q)$ and $se_n(x,q)$ are periodical solutions of the Mathieu equation

$$\frac{d^2y}{dx^2} + (a - 2q\cos 2x)y = 0 \qquad (2.5.3.5.7)$$

Modified Mathieu functions $Ce_n(x,q)$ and $Se_n(x,q)$ which are solutions of the modified Mathieu equation:

$$\frac{d^2y}{dx^2} + (a - 2q\cosh 2x)y = 0 \qquad (2.5.3.5.8)$$

The Laguerre polynomials $L_n = L_n(x)$ satisfy the equation:

$$x^2\frac{d^2y}{dx^2} + (1-x)\frac{dy}{dx} + ny = 0 \qquad (2.5.3.5.9)$$

while the generalized Laguerre polynomials $L_n^{\alpha} = L_n^{\alpha}(x)$ $(\alpha > -1)$ satisfy the equation:

$$x^2\frac{d^2y}{dx^2} + (\alpha + 1 - x)\frac{dy}{dx} + ny = 0 \qquad (2.5.3.5.10)$$

The Chebyshev polynomials $T_n = T_n(x)$ satisfy the equation

$$(1-x^2)\frac{d^2y}{dx^2} - x\frac{dy}{dx} + n^2 y = 0 \qquad (2.5.3.5.11)$$

The Hermite polynomial $H_n = H_n(x)$ satisfies the equation

$$\frac{d^2y}{dx^2} - 2x\frac{dy}{dx} + 2ny = 0 \qquad (2.5.3.5.12)$$

The Jacobi polynomials $P_n^{\alpha,\beta}(x)$ satisfy the equation

$$(1-x^2)\frac{d^2y}{dx^2} + [\beta - \alpha - (\alpha + \beta + 2)x]\frac{dy}{dx} + n(n + \alpha + \beta + 1)y = 0 \qquad (2.5.3.5.13)$$

The above special functions provide solutions for special cases of second order ODEs. Thus it must be noted that second order ODEs with forms not belonging to one of the above mentioned forms may be cannot analytically solve.

Chapter 3: Approach, assumption and simplifications used for the formulation of the governing system for toxic substance transport modeling

3.1 Instantaneous equations for transport of constituent mass

The fundamental forms of the basic equations for the conservation of momentum, water mass and constituent mass are the same. The equation can be derived by writing a conservation equation for a control volume of a small size. The quantity presented in the control volume is $mdxdydz$, in which m is the concentration of the intrinsic property, dx, dy and dz are sizes of the control volume in x, y and z directions, respectively. The time rate of change of an intrinsic property within the control volume is equal to the sum of the fluxes through all control surfaces. The general governing equation is:

$$\frac{\partial(mdxdydz)}{\partial t} = \text{Sum of fluxes through control surface in each direction} \pm \text{sources/sinks} \quad (3.1.1)$$

For example, the flux enters the control volume ($dxdydz$) in the x direction as F_x. The flux then exiting another surface in the x direction is $F_x + (\partial F_x / \partial x)dx$. The general governing equation, after considering six fluxes through the six control surfaces of the control volume, becomes:

$$\frac{\partial(mdxdydz)}{\partial t} = -\frac{\partial F_x}{\partial x}dx - \frac{\partial F_y}{\partial y}dy - \frac{\partial F_z}{\partial z}dz \pm sources/sinks \quad (3.1.2)$$

The fluxes, F_x, F_y and F_z are contributed by two processes: advection and mixing. When advection occurs, the intrinsic property is transported by

the flow of water through the control volume interfaces. A flux is equal to the product of the volumetric flux times the concentration of the intrinsic property. The volumetric flux or flow of water is equal to the product of the cross-sectional area of the interface, times the water velocity normal to that area. According to Fick's first law of diffusion, the rate of mixing is proportional to the gradient across the interfaces of a control volume and the interfacial area. The flux terms for the three coordinate directions (x, y and z) are:

$$F_x = udydzm - \partial(k_x dydzm)/\partial x \qquad (3.1.3a)$$

$$F_y = vdxdzm - \partial(k_y dxdzm)/\partial y \qquad (3.1.3b)$$

$$F_z = wdxdym - \partial(k_z dxdym)/\partial z \qquad (3.1.3c)$$

where u, v and w are the instantaneous velocities along the x, y and z axes, respectively. k_x, k_y and k_z are the mixing coefficients along the x, y and z axes, respectively. Substituting the fluxes into the general governing equation 3.1.2, it becomes:

$$\frac{\partial m}{\partial t} = -\frac{\partial um}{\partial x} - \frac{\partial vm}{\partial y} - \frac{\partial wm}{\partial z} + \frac{\partial^2 k_x m}{\partial x^2} + \frac{\partial^2 k_y m}{\partial y^2} + \frac{\partial^2 k_z m}{\partial z^2} \pm sources / sinks \qquad (3.1.4)$$

This generalized equation serves as the basis to develop conservation equations for each intrinsic property: water mass, momentum, heat, and constituent mass.

3.2 Generalized instantaneous equations for transport of sediment particles

Since sediment particles will not decay or grow, there should be no source or sink terms added in the governing equation. The velocity of sediment particles along z axis is often dominated by the settling velocity, ω_s, which is downward positive. The generalized equation developed from Equation (3.1.4) for the transport of sediment particles should be:

$$\frac{\partial s}{\partial t} = -\frac{\partial u_s s}{\partial x} - \frac{\partial v_s s}{\partial y} + \frac{\partial \omega_s s}{\partial z} + \frac{\partial}{\partial x}\left(k_{sx}\frac{\partial s}{\partial x}\right) + \frac{\partial}{\partial y}\left(k_{sy}\frac{\partial s}{\partial y}\right) + \frac{\partial}{\partial z}\left(k_{sz}\frac{\partial s}{\partial z}\right) \quad (3.2.1)$$

where s is the sediment concentration. u_s and v_s are velocities of sediment along the x and y axes, respectively. k_{sx}, k_{sy} and k_{sz} are the mixing coefficients of sediment along the x, y and z axes, respectively.

3.3 Generalized instantaneous equations for transport of toxic substances

3.3.1 Forms of toxic substance in the water body

From the general features of the physio-chemical phases of the transport of a toxic substance in the water body, it is common to assume that the toxicant can exist in two basic forms, the dissolved phase and the solid phase. Examples of previous works that use this approach include such as Thomann and Mueller (1987, p505), Schnoor (1996, p390), Chapra (1997, p697), Connolly et al (2000), Ng and Yip (2001), O'Conner (1988). As described in Chapter 2, the total concentration of a toxic substance, c_T, is the sum of the concentration of the dissolved toxicant (c) and the particulate toxicant (p). The term p can be further expressed as the product of the

sediment concentration (s) and toxicant concentration sorbed onto unit mass of sediment (r). Thus, the modeling environment depends on the sediment distribution.

3.3.2 Sorption exchange between dissolved and particulate phase of toxic substances

It is commonly assumed that sorption is a reversible process between aqueous and solid phases of a toxic substance. A simple representation of this interaction is given by a first-order kinetics expression

$$\frac{\partial p}{\partial t} = k_c c - k_p p \qquad (3.3.2.1a)$$

$$\frac{\partial c}{\partial t} = k_p p - k_c c \qquad (3.3.2.1b)$$

in which k_c and k_p are respectively the sorption and desorption rate constant of a toxic substance to sediment particles respectively. This first-order kinetics approach is widely used in different previous models. Examples include the transport models presented by Bahr and Rubin (1987), Cvetkovic and Dagan (1994), Valocchi (1985), Thomann and Mueller (1987, p506), Connolly et al (2000), Ng (2000a and b) and O'Conner (1988).

3.3.3 Generalized instantaneous equations for transport of dissolved and particulate toxicants

First, it is assumed that the disposal and transport of toxicants do not affect the transport of suspended sediment in the water body. Combining the first-order sorption kinetics equations and the generalized, three-dimensional, time varying equation, Equation (3.1.4), for nonconservative toxic substances

with dissolved and particulate components, one may obtain the following expressions:

$$\frac{\partial c}{\partial t} = -\frac{\partial uc}{\partial x} - \frac{\partial vc}{\partial y} - \frac{\partial wc}{\partial z} + \frac{\partial}{\partial x}\left(k_x \frac{\partial c}{\partial x}\right) + \frac{\partial}{\partial y}\left(k_y \frac{\partial c}{\partial y}\right) + \frac{\partial}{\partial z}\left(k_z \frac{\partial c}{\partial z}\right) - k_c c + k_p p - k_{dc} c \tag{3.3.3.1}$$

$$\frac{\partial p}{\partial t} = -\frac{\partial u_s p}{\partial x} - \frac{\partial v_s p}{\partial y} + \frac{\partial \omega_s p}{\partial z} + \frac{\partial}{\partial x}\left(k_{sx} \frac{\partial p}{\partial x}\right) + \frac{\partial}{\partial y}\left(k_{sy} \frac{\partial p}{\partial y}\right) + \frac{\partial}{\partial z}\left(k_{sz} \frac{\partial p}{\partial z}\right) - k_p p + k_c c - k_{dp} p \tag{3.3.3.2}$$

in which k_x, k_y and k_z are the mixing coefficients of a dissolved toxicant in the x, y and z directions respectively. k_{dc} and k_{dp} are first order decay coefficients of dissolved and particulate toxicants, respectively. A first order decay term is also added to each governing equation to take into account contaminants such as radionclides, which will decay. It can be simply assumed that the velocities of dissolved toxicants are the same as the flow velocities of water. Therefore, u, v and w are the flow velocities of water along the x, y and z axes, respectively. The physical hydrodynamic transport phenomena of particulate toxicants can be assumed to be the same as the transport of suspended sediment.

3.4 Simplification of the instantaneous governing system for transport of sediment, dissolved toxicants and particulate toxicants

The general governing equations described in Section (3.2) and Section (3.3.3) are difficult to solve analytically. To avoid excessive mathematical complications, these equations must be simplified but at the same time must ensure the retention of sufficient physics. Different approaches of simplification are used to study different situations of contaminant transport. For a wide range of problems, such as dispersion in a wide open channel flow, one can simplify the general governing equations into the two-dimensional transport equations by considering only the horizontal axis, x, parallel to the resultant horizontal flow direction, such as:

$$\frac{\partial s}{\partial t} = -\frac{\partial u_s s}{\partial x} + \frac{\partial \omega_s s}{\partial z} + \frac{\partial}{\partial x}\left(k_{sx}\frac{\partial s}{\partial x}\right) + \frac{\partial}{\partial z}\left(k_{sz}\frac{\partial s}{\partial z}\right) \qquad (3.4.1)$$

$$\frac{\partial c}{\partial t} = -\frac{\partial uc}{\partial x} - \frac{\partial wc}{\partial z} + \frac{\partial}{\partial x}\left(k_x\frac{\partial c}{\partial x}\right) + \frac{\partial}{\partial z}\left(k_z\frac{\partial c}{\partial z}\right) - k_c c + k_p p - k_{dc} c \qquad (3.4.2)$$

$$\frac{\partial p}{\partial t} = -\frac{\partial u_s p}{\partial x} + \frac{\partial \omega_s p}{\partial z} + \frac{\partial}{\partial x}\left(k_{sx}\frac{\partial p}{\partial x}\right) + \frac{\partial}{\partial z}\left(k_{sz}\frac{\partial p}{\partial z}\right) - k_p p + k_c c - k_{dp} p \qquad (3.4.3)$$

For a wide range of specific problems, one can further assume the advection transport of dissolved toxicants along the vertical axis, $\partial wc/\partial z$, to be zero. However, it is still difficult to solve the above two-dimensional governing equations analytically and further simplification is required in order to formulate one-dimensional governing equations that can be used to reveal the fundamental behaviour. The following sections describe approaches used to formulate the governing system of the present model.

3.4.1 Reasons of choosing vertical axis as the dominate spatial dimension

Because of the limitation of the analytical solution techniques, most existing models consider only one spatial dimension and the choice of the spatial dimension thus becomes an important consideration in the model development. Many existing models consider the main fluid flow direction, for example, Ng (2000a), Runkel (1996), Alshawabkeh and Adrian (1997), Smedt et al (1998) and Prakash (2000). Such models are useful to predict the transport of a toxicant disposed from a point.

In this research, however, the vertical direction, z, is considered in the governing system for the following reasons. The choice of a spatial dimension in a model is based on particular physical and chemical transport parameters that need to be considered carefully. Researchers are concerned with the changes of flow velocity in the horizontal direction, when choosing the horizontal flow direction as the spatial dimension. In this project, the settling of particles, resuspension of particles at the water-bed sediment interface, turbulent mixing and the diffusive exchange of dissolved toxic substances at the water-bed sediment interface are phenomena that are of main concerns. The settling velocity and turbulent mixing coefficients often vary in the vertical direction. The exchange of toxic substances and particles at the water-bed sediment interface is also a vertical transport process. Thus, models choosing vertical directions allow the consideration of the above transport phenomena in detail. In addition, previous work in comparison with models considering the horizontal axis, is relatively scarce thus enhancing the need for vertical models. An additional benefit is that the models with relatively complicated boundary conditions developed in the research can

also be used to study contaminant transport along the horizontal axis by applying suitable transformation of variables and other modifications.

Another important dimension for the governing system is time. Sorption exchanges between toxic substances and particles, decay loss and volatilization are transport phenomena that vary with time. These transport processes separate the transport of toxic substances from other conservative contaminants such as sediment. Therefore, models can only properly simulate the toxic substance transport if such processes have been seriously considered.

3.4.2 One-dimensional, time varying governing system for sediment transports

The one dimensional, time varying governing equation for the transport of sediment in the vertical direction is:

$$\frac{\partial s}{\partial t} = \frac{\partial \omega_s s}{\partial z} + \frac{\partial}{\partial z}\left(k_{sz}\frac{\partial s}{\partial z}\right) \qquad (3.4.2.1)$$

The distribution of settling velocity, ω_s, can be assumed to be a constant. Even some former works (e.g. Oliver 1961) considered that the settling velocity is dependent on the sediment concentration. The distribution of sediment mixing coefficients is assumed in various forms such as in a constant value or the parabolic distribution. The governing equation, assuming a parabolic distribution of sediment mixing coefficient, ($k_{sz} = \beta\kappa u_* z(1-z/H)$) is:

$$\frac{\partial s}{\partial t} = [\omega_s + \beta\kappa u_*(1-2z/H)]\frac{\partial s}{\partial z} + \beta\kappa u_* z(1-z/H)\frac{\partial^2 s}{\partial z^2} \qquad (3.4.2.2)$$

The settling of particles and resuspension of particles at the water-bed sediment interface is the main concern in this research. Thus, such processes should be considered in the setting of the corresponding boundary condition. The boundary condition describing the net sediment flux $-(k_{sz}\partial s/\partial z + \omega_s s)$ which is equal to the difference between the sediment entrainment flux, γs_a, and the sediment deposition flux, ϕs, can be written as:

$$-\left[k_{sz}\frac{\partial s}{\partial z}+\omega_s s\right]=-[\phi s-\gamma s_a] \quad at \quad z=a, \quad \forall t \geq 0 \tag{3.4.2.3}$$

In which a and s_a are the reference level and the reference level sediment concentration respectively. ϕ is the deposition velocity of sediment at level a and γ is the resuspension velocity of sediment from the water-sediment interface. a is set to be zero if a constant mixing coefficient is used. At the water surface, it is assumed that there is no net sediment flux through the surface:

$$-\left[k_{sz}\frac{\partial s}{\partial z}+\omega_s s\right]=0 \quad at \quad z=H, \quad \forall t \geq 0 \tag{3.4.2.4}$$

Different solutions exist, based on substituting different distributions of the sediment mixing coefficient and initial conditions. Cheng (1984) developed an analytical solution with a constant mixing coefficient and constant initial distribution of sediment along the water column. The two-dimensional, steady state model given by Hjelmfelt and Lenau (1970) can be transformed to a one-dimensional, time varying model by transforming the horizontal distance, x, to the product of time, t and flow velocity, u. The model uses a parabolic form of k_{sz} and a zero initial concentration. Model 1 shown in Chapter 4 also

assumes a parabolic form of k_{sz} but allows an arbitrary initial concentration distribution. The model formulations and solutions of Models 1 to Model 3 are shown in Chapter 4.

3.4.3 Instantaneous equilibrium of sorption mechanics

The sorption interaction between the dissolved and particulate components tends to an equilibrium state. The time required to achieve this condition may vary markedly depending on the characteristics of the chemical and sorbent. If the rate at which equilibrium is achieved is much higher than that of other kinetic routes, such as decay, volatilization, settling and exchange with the bed, a state of instantaneous equilibrium may be assumed. As described in Chapter 2, the local equilibrium relations between dissolved and particulate toxicants can be represented by the partition fractions. The partition fractions depend on sediment concentration and thus they may be functions of spatial variables and time, depending on the sediment distribution in a problem. In this research, instantaneous equilibrium and the partition fractions are applied. They are widely used assumptions for the development of toxic substance transport modeling. Examples are found in the work of O'Connor (1988), Ng (2001) and Connolly et al (2000). They are useful for toxic substances such as heavy metals that do not decay or volatile. They are also useful to investigate long-term impacts on aquatic environments by contaminated bed sediment. Few models consider the phenomena of hydrodynamic transport without assuming the instantaneous equilibrium. In fact, it is difficult to solve the system of Equations (3.4.1), (3.4.2) and (3.4.3) analytically without assuming instantaneous equilibrium

even the model is reduced to a one-dimensional model. The simplification and assumptions are described in the following sections.

3.4.4 Generalized equations for toxic substance transport with instantaneous equilibrium

As described in the Section 2.4.4.1, partition fractions are fractions of dissolved and particulate toxic substances at local equilibrium conditions. Applying Equation (2.4.4.1.2) to Equations (3.3.3.1) and (3.3.3.2), we obtain:

$$\frac{\partial f_d c_T}{\partial t} = -\frac{\partial u f_d c_T}{\partial x} - \frac{\partial v f_d c_T}{\partial y} - \frac{\partial w f_d c_T}{\partial z} + \frac{\partial}{\partial x}\left(k_x \frac{\partial f_d c_T}{\partial x}\right) + \frac{\partial}{\partial y}\left(k_y \frac{\partial f_d c_T}{\partial y}\right) + \frac{\partial}{\partial z}\left(k_z \frac{\partial f_d c_T}{\partial z}\right) - k_c f_d c_T + k_p f_p c_T - k_{dc} f_d c_T \tag{3.4.4.1}$$

$$\frac{\partial f_p c_T}{\partial t} = -\frac{\partial u_s f_p c_T}{\partial x} - \frac{\partial v_s f_p c_T}{\partial y} + \frac{\partial \omega_s f_p c_T}{\partial z} + \frac{\partial}{\partial x}\left(k_{sx} \frac{\partial f_p c_T}{\partial x}\right) + \frac{\partial}{\partial y}\left(k_{sy} \frac{\partial f_p c_T}{\partial y}\right) + \frac{\partial}{\partial z}\left(k_{sz} \frac{\partial f_p c_T}{\partial z}\right) - k_p f_p c_T + k_c f_d c_T - k_{dp} f_p c_T \tag{3.4.4.2}$$

If it is further assumed that the vertical flow velocity (w) of water is zero and advection and dispersion transport coefficients of water and suspended sediment are the same, the above system of equations can be reduced to a single partial differential equation in terms of total concentration by adding the above two equations and applying Equation (2.4.4.1.3), i.e.,

$$\frac{\partial c_T}{\partial t} = -u_x \frac{\partial c_T}{\partial x} - v \frac{\partial c_T}{\partial y} + \omega_s \frac{\partial f_p c_T}{\partial z} + \frac{\partial}{\partial x}\left(k_x \frac{\partial c_T}{\partial x}\right) + \frac{\partial}{\partial y}\left(k_y \frac{\partial c_T}{\partial y}\right) + \frac{\partial}{\partial z}\left(k_z \frac{\partial c_T}{\partial z}\right) - k_{dc} f_d c_T - k_{dp} f_p c_T \tag{3.4.4.3}$$

In the two-dimensional case, it becomes:

$$\frac{\partial c_T}{\partial t} = -u_x \frac{\partial c_T}{\partial x} + \omega_s \frac{\partial f_p c_T}{\partial z} + \frac{\partial}{\partial x}\left(k_x \frac{\partial c_T}{\partial x}\right) + \frac{\partial}{\partial z}\left(k_z \frac{\partial c_T}{\partial z}\right) - k_{dc} f_d c_T - k_{dp} f_p c_T \quad (3.4.4.4)$$

The above two equations have only one term, $\omega_s \partial f_p c_T / \partial z$, that depends on the partition fraction, f_p. However, since f_p depends on the suspended sediment distribution, the complexity of solving the above equations depends on the applied suspended sediment distribution.

3.4.5 One-dimensional, time varying governing system for toxic substance transport instantaneous equilibrium

For the one-dimensional case, the governing equations of dissolved and particulate toxicants by further reducing Equations (3.4.4.1) and (3.4.4.2) to equations with only the vertical axis and applying Equation (2.4.4.1.2) are:

$$\frac{\partial f_d c_T}{\partial t} = \frac{\partial}{\partial z}\left(k_z \frac{\partial f_d c_T}{\partial z}\right) - k_c f_d c_T + k_p f_p c_T - k_{dc} f_d c_T \quad (3.4.5.1)$$

$$\frac{\partial f_p c_T}{\partial t} = + \frac{\partial \omega_s f_p c_T}{\partial z} + \frac{\partial}{\partial z}\left(k_{sz} \frac{\partial f_p c_T}{\partial z}\right) - k_p f_p c_T + k_c f_d c_T - k_{dp} f_p c_T \quad (3.4.5.2)$$

Adding Equations (3.4.5.1) and (3.4.5.2) and applying Equation (2.4.4.1.3) forms a single governing equation in terms of the total concentration:

$$\frac{\partial c_T}{\partial t} = \frac{\partial \omega_s f_p c_T}{\partial z} + \frac{\partial}{\partial z}\left(k_z \frac{\partial c_T}{\partial z}\right) + \frac{\partial}{\partial z}\left((k_{sz} - k_z)\frac{\partial f_p c_T}{\partial z}\right) - (k_{dp} f_p + k_{dc} f_d) c_T \quad (3.4.5.3)$$

If we further assume a constant settling velocity and the vertical mixing coefficient of water (k_z) is the same as sediment mixing coefficient (k_{sz}), Equation (3.4.5.3) reduces to:

$$\frac{\partial c_T}{\partial t} = k_z \frac{\partial^2 c_T}{\partial z^2} + \left(\omega_s f_p + \frac{\partial k_z}{\partial z} \right) \frac{\partial c_T}{\partial z} + \left[\omega_s \frac{\partial f_p}{\partial z} - k_{dc} f_d - k_{dp} f_p \right] c_T \qquad (3.4.5.4)$$

The complexity of the governing equation depends highly on the complexity of the concentration profile of the suspended solid and the expressions of f_d and f_p to be substituted into the governing equation.

The simplest assumption is to consider f_d and f_p as constants. In this way, Equation (3.4.5.4) reduces to a linear second-order partial differential equation with constant coefficients. However, the assumption is not sufficient to reveal the physics in many cases. In generally, the following terms can be expanded by applying Equation (2.4.4.1.1):

$$\frac{\partial f_p c_T}{\partial z} = f_p \frac{\partial c_T}{\partial z} + c_T \frac{\partial f_p}{\partial z}$$

$$= f_p \frac{\partial c_T}{\partial z} + c_T \frac{\partial}{\partial z} \left(\frac{k_d s}{1 + k_d s} \right)$$

$$= f_p \frac{\partial c_T}{\partial z} + c_T \frac{k_d}{(1 + k_d s)^2} \frac{\partial s}{\partial z}$$

$$\frac{\partial f_p c_T}{\partial z} = f_p \frac{\partial c_T}{\partial z} + c_T k_d {f_d}^2 \frac{\partial s}{\partial z} \qquad (3.4.5.5)$$

$$\frac{\partial^2 f_p c_T}{\partial z^2} = \frac{\partial}{\partial z} \left(f_p \frac{\partial c_T}{\partial z} + c_T k_d {f_d}^2 \frac{\partial s}{\partial z} \right)$$

$$= f_p \frac{\partial^2 c_T}{\partial z^2} + \frac{\partial c_T}{\partial z} \frac{\partial f_p}{\partial z} + k_d {f_d}^2 \frac{\partial s}{\partial z} \frac{\partial c_T}{\partial z} + c_T \frac{\partial}{\partial z} \left(k_d {f_d}^2 \frac{\partial s}{\partial z} \right)$$

$$= f_p \frac{\partial^2 c_T}{\partial z^2} + 2 k_d {f_d}^2 \frac{\partial s}{\partial z} \frac{\partial c_T}{\partial z} + c_T k_d \left({f_d}^2 \frac{\partial^2 s}{\partial z^2} + \frac{\partial s}{\partial z} \frac{\partial {f_d}^2}{\partial z} \right)$$

$$= f_p \frac{\partial^2 c_T}{\partial z^2} + 2k_d {f_d}^2 \frac{\partial s}{\partial z}\frac{\partial c_T}{\partial z} + c_T k_d \left({f_d}^2 \frac{\partial^2 s}{\partial z^2} + 2f_d \frac{\partial}{\partial z}\left(\frac{1}{1+k_d s}\right)\frac{\partial s}{\partial z}\right)$$

$$= f_p \frac{\partial^2 c_T}{\partial z^2} + 2k_d {f_d}^2 \frac{\partial s}{\partial z}\frac{\partial c_T}{\partial z} + c_T k_d \left({f_d}^2 \frac{\partial^2 s}{\partial z^2} - \frac{2f_d k_d}{(1+k_d s)^2}\left(\frac{\partial s}{\partial z}\right)^2\right)$$

$$= f_p \frac{\partial^2 c_T}{\partial z^2} + 2k_d {f_d}^2 \frac{\partial s}{\partial z}\frac{\partial c_T}{\partial z} + c_T k_d {f_d}^2 \left(\frac{\partial^2 s}{\partial z^2} - 2f_d k_d \left(\frac{\partial s}{\partial z}\right)^2\right) \qquad (3.4.5.6)$$

$$\frac{\partial}{\partial z}\left((k_{sz}-k_z)\frac{\partial f_p c_T}{\partial z}\right) = (k_{sz}-k_z)\frac{\partial^2 f_p c_T}{\partial z^2} + \frac{\partial f_p c_T}{\partial z}\frac{\partial (k_{sz}-k_z)}{\partial z}$$

$$= (k_{sz}-k_z)\left[f_p \frac{\partial^2 c_T}{\partial z^2} + 2k_d {f_d}^2 \frac{\partial s}{\partial z}\frac{\partial c_T}{\partial z} + c_T k_d {f_d}^2 \left(\frac{\partial^2 s}{\partial z^2} - 2f_d k_d \left(\frac{\partial s}{\partial z}\right)^2\right)\right]$$
$$+ \frac{\partial (k_{sz}-k_z)}{\partial z}\left[f_p \frac{\partial c_T}{\partial z} + c_T k_d {f_d}^2 \frac{\partial s}{\partial z}\right]$$

$$= (k_{sz}-k_z) f_p \frac{\partial^2 c_T}{\partial z^2} + \left[2(k_{sz}-k_z)k_d {f_d}^2 \frac{\partial s}{\partial z} + f_p \frac{\partial (k_{sz}-k_z)}{\partial z}\right]\frac{\partial c_T}{\partial z}$$
$$+ k_d {f_d}^2 \left[(k_{sz}-k_z)\left(\frac{\partial^2 s}{\partial z^2} - 2f_d k_d \left(\frac{\partial s}{\partial z}\right)^2\right) + \frac{\partial (k_{sz}-k_z)}{\partial z}\frac{\partial s}{\partial z}\right] c_T \qquad (3.4.5.7)$$

By substituting Equations (3.4.5.5) and (3.4.5.7) into Equation (3.4.5.3), we obtain:

$$\frac{\partial c_T}{\partial t} = \omega_s f_p \frac{\partial c_T}{\partial z} + \omega_s c_T k_d {f_d}^2 \frac{\partial s}{\partial z} + f_p c_T \frac{\partial \omega_s}{\partial z} + \frac{\partial}{\partial z}\left(k_z \frac{\partial c_T}{\partial z}\right) + (k_{sz}-k_z) f_p \frac{\partial^2 c_T}{\partial z^2}$$
$$+ \left[2(k_{sz}-k_z)k_d {f_d}^2 \frac{\partial s}{\partial z} + f_p \frac{\partial (k_{sz}-k_z)}{\partial z}\right]\frac{\partial c_T}{\partial z}$$
$$+ k_d {f_d}^2 \left[(k_{sz}-k_z)\left(\frac{\partial^2 s}{\partial z^2} - 2f_d k_d \left(\frac{\partial s}{\partial z}\right)^2\right) + \frac{\partial (k_{sz}-k_z)}{\partial z}\frac{\partial s}{\partial z}\right] c_T - (k_{dp} f_p + k_{dc} f_d) c_T$$

$$\frac{\partial c_T}{\partial t} = \left(k_z + (k_{sz} - k_z)f_p\right)\frac{\partial^2 c_T}{\partial z^2}$$
$$+\left[\omega_s f_p + 2(k_{sz} - k_z)k_d f_d{}^2 \frac{\partial s}{\partial z} + f_p \frac{\partial (k_{sz} - k_z)}{\partial z} + \frac{\partial k_z}{\partial z}\right]\frac{\partial c_T}{\partial z}$$
$$+\left\{\begin{array}{l} f_p \frac{\partial \omega_s}{\partial z} + k_d f_d{}^2\left[(k_{sz} - k_z)\left(\frac{\partial^2 s}{\partial z^2} - 2f_d k_d\left(\frac{\partial s}{\partial z}\right)^2\right) + \left(\frac{\partial (k_{sz} - k_z)}{\partial z} + \omega_s\right)\frac{\partial s}{\partial z}\right] \\ -(k_{dp} f_p + k_{dc} f_d) \end{array}\right\} c_T$$

or say:

$$\frac{\partial c_T}{\partial t} = \overline{A}(f_p, k_z, k_{sz})\frac{\partial^2 c_T}{\partial z^2} + \overline{B}(f_p, f_d, k_d, k_z, k_{sz}, s)\frac{\partial c_T}{\partial z} \quad (3.4.5.8)$$
$$+\overline{C}(\omega_s, f_p, f_d, k_d, k_z, k_{sz}, s, k_{dp}, k_{dc})c_T$$

in which:

$$\overline{A}(f_p, k_z, k_{sz}) = k_z + (k_{sz} - k_z)f_p \quad (3.4.5.9)$$

$$\overline{B}(f_p, f_d, k_d, k_z, k_{sz}, s) = \omega_s f_p + 2(k_{sz} - k_z)k_d f_d{}^2 \frac{\partial s}{\partial z} + f_p \frac{\partial (k_{sz} - k_z)}{\partial z} + \frac{\partial k_z}{\partial z} \quad (3.4.5.10)$$

$$\overline{C}(\omega_s, f_p, f_d, k_d, k_z, k_{sz}, s, k_{dp}, k_{dc})$$
$$= f_p \frac{\partial \omega_s}{\partial z} + k_d f_d{}^2\left[(k_{sz} - k_z)\left(\frac{\partial^2 s}{\partial z^2} - 2f_d k_d\left(\frac{\partial s}{\partial z}\right)^2\right) + \left(\frac{\partial (k_{sz} - k_z)}{\partial z} + \omega_s\right)\frac{\partial s}{\partial z}\right]$$
$$-(k_{dp} f_p + k_{dc} f_d)$$

(3.4.5.11)

Coefficients in Equation (3.4.5.8) depend on the sediment concentration and hence the distributions of the settling velocity, sediment mixing coefficient and suspended sediment are needed for the solution of the governing equation. It should be noted that the value of $\overline{C}$ may not be zero even the values of k_{dp} and k_{dc} are zeros. Thus, first order growth/decay terms should

be considered in the governing equation for modeling toxic substances even for one that does not decay naturally.

3.4.6 Governing equations with substituting equilibrium distributions of suspended sediment

In order to reveal the physics, a distribution function of suspended sediment (s) should be substituted into the above governing equations. However, relatively simple functions should be considered in order to reduce the complexity of the system. A reasonable approach is that an equilibrium concentration profile of suspended sediment is used. In this approach, there are two assumptions made. Firstly, the aquatic environment in which the sediment distribution has reached equilibrium is completely developed, and remains so during the modeling period. Secondly, the discharge of toxic substances does not affect the transport of sediment particles in the water column.

3.4.6.1 Equilibrium sediment distribution in the form of exponential function

For the equilibrium sediment distribution, two forms are commonly used by environmental engineers and scientists. The first is developed by assuming the settling velocity and sediment mixing coefficient to be constant. The author also assumes the water mixing coefficient (k_z) to be constant based on the reason that both sediments and chemicals are transported in the same environment. The shape of the equilibrium concentration profile is shown in the Cheng's (1984) paper and in Models 2 and 3 developed by the author. The equilibrium sediment distribution function, based on the above

assumptions and developed from governing system, described in Section (3.4.2) is:

$$s = \frac{\gamma s_a}{\phi} e^{\frac{-z\omega_s}{k_{sz}}} \tag{3.4.6.1.1}$$

In this way, f_d and f_p now become:

$$f_p = \frac{k_d \frac{\gamma s_a}{\phi}}{k_d \frac{\gamma s_a}{\phi} + e^{z\omega_z / k_{sz}}} \tag{3.4.6.1.2a}$$

$$f_d = \frac{e^{z\omega_z / k_{sz}}}{k_d \frac{\gamma s_a}{\phi} + e^{z\omega_z / k_{sz}}} \tag{3.4.6.1.2b}$$

From Equation (3.4.6.1.1), the following terms can be expanded:

$$\frac{\partial s}{\partial z} = \frac{\partial \frac{\gamma s_a}{\phi} e^{\frac{-z\omega_s}{k_{sz}}}}{\partial z} = \frac{-\omega_s}{k_{sz}} \frac{\gamma s_a}{\phi} e^{\frac{-z\omega_s}{k_{sz}}} = \frac{-\omega_s}{k_{sz}} s \tag{3.4.6.1.3}$$

$$\frac{\partial^2 s}{\partial z^2} = \frac{\partial}{\partial z}\left(\frac{-\omega_s}{k_{sz}} s\right) = \frac{\omega_s^{\,2}}{k_{sz}^{\,2}} s = \frac{\omega_s^{\,2}}{k_{sz}^{\,2}} \frac{\gamma s_a}{\phi} e^{\frac{-\omega_s z}{k_{sz}}} \tag{3.4.6.1.4}$$

Apply Equations (3.4.6.1.3) and (3.4.6.1.4) to Equations (3.4.5.5) and (3.4.5.7), they become:

$$\frac{\partial f_p c_T}{\partial z} = f_p \frac{\partial c_T}{\partial z} - \frac{\omega_s f_d f_p}{k_{sz}} c_T \tag{3.4.6.1.5}$$

$$\frac{\partial}{\partial z}\left((k_{sz} - k_z)\frac{\partial f_p c_T}{\partial z}\right) = (k_{sz} - k_z) f_p \frac{\partial^2 c_T}{\partial z^2} + \left[f_p \frac{\partial (k_{sz} - k_z)}{\partial z} - \frac{2(k_{sz} - k_z)\omega_s f_d f_p}{k_{sz}}\right]\frac{\partial c_T}{\partial z}$$
$$+ k_d f_d^{\,2}\left[(k_{sz} - k_z)\frac{\omega_s^{\,2} s}{k_{sz}^{\,2}}(1 - 2f_p) - \frac{\partial (k_{sz} - k_z)}{\partial z}\frac{\omega_s s}{k_{sz}}\right] c_T$$

$$= (k_{sz} - k_z) f_p \frac{\partial^2 c_T}{\partial z^2} - \frac{2(k_{sz} - k_z)\omega_s f_d f_p}{k_{sz}} \frac{\partial c_T}{\partial z} + \frac{(k_{sz} - k_z)(1 - 2f_p)\omega_s{}^2 f_d f_p}{k_{sz}{}^2} c_T \quad (3.4.6.1.6)$$

Note that since the author assumes constant values of k_{sz} and k_z. Their derivatives should be zero. By substituting Equations (3.4.6.1.5) and (3.4.6.1.6) into Equation (3.4.5.3), it becomes:

$$\frac{\partial c_T}{\partial t} = \left[k_{sz} + (k_z - k_{sz}) f_d\right] \frac{\partial^2 c_T}{\partial z^2} + (k_{sz} + 2(k_z - k_{sz}) f_d) \frac{\omega_s f_p}{k_{sz}} \frac{\partial c_T}{\partial z}$$
$$- \left[\left[k_z - 2f_p (k_z - k_{sz})\right] \frac{\omega_s{}^2 f_d f_p}{k_{sz}{}^2} + (k_{dp} f_p + k_{dc} f_d) \right] c_T$$

or say:

$$\frac{\partial c_T}{\partial t} = \overline{A}_e(f_d, k_z, k_{sz}) \frac{\partial^2 c_T}{\partial z^2} + \overline{B}_e(\omega_s, f_p, f_d, k_z, k_{sz}) \frac{\partial c_T}{\partial z} - \overline{C}_e(\omega_s, f_p, f_d, k_z, k_{sz}, k_{dp}, k_{dc}) c_T \quad (3.4.6.1.7)$$

in which:

$$\overline{A}_e(f_d, k_z, k_{sz}) = k_{sz} + (k_z - k_{sz}) f_d \quad (3.4.6.1.8)$$

$$\overline{B}_e(\omega_s, f_p, f_d, k_z, k_{sz}) = (k_{sz} + 2(k_z - k_{sz}) f_d) \frac{\omega_s f_p}{k_{sz}} \quad (3.4.6.1.9)$$

$$\overline{C}_e(\omega_s, f_p, f_d, k_z, k_{sz}, k_{dp}, k_{dc}) = \frac{\omega_s{}^2 f_d f_p \left[k_z - 2f_p (k_z - k_{sz})\right]}{k_{sz}{}^2} + k_{dp} f_p + k_{dc} f_d \quad (3.4.6.1.10)$$

Equation (3.4.5.4) becomes:

$$\frac{\partial c_T}{\partial t} = k_z \frac{\partial^2 c_T}{\partial z^2} + \omega_s f_p \frac{\partial c_T}{\partial z} - \left(\frac{\omega_s{}^2 f_d f_p}{k_{sz}} + k_{dc} f_d + k_{dp} f_p \right) c_T \quad (3.4.6.1.11)$$

Equation (3.4.6.1.7) is a linear second-order PDE with all coefficients dependent on the independent variable z while Equation (3.4.6.1.11) has coefficients at first and zero orders of derivatives dependent on z.

3.4.6.2 Equilibrium sediment distribution in the form of Rouse profile

Another equilibrium distribution function of suspended sediment is the well-known Rouse profile. The distribution at equilibrium for the model developed by Hjelmfelt and Lenau (1970) and Model 1, developed by the author, also has this shape. The Rouse profile was developed with the assumptions of the constant settling velocity and parabolic distribution of the sediment mixing coefficient. The concentration profile at steady state based on the above assumptions as described in Section (3.4.2) is:

$$s = s_a \frac{\gamma}{\phi}\left(\frac{a}{H-a}\right)^{\frac{\omega_s}{\beta\kappa u_*}}\left(\frac{H-z}{z}\right)^{\frac{\omega_s}{\beta\kappa u_*}} = s_{am}\left(\frac{H-z}{z}\right)^{\frac{\omega_s}{\beta\kappa u_*}} \qquad (3.4.6.2.1)$$

$$\text{where} \qquad s_{am} = s_a \frac{\gamma}{\phi}\left(\frac{a}{H-a}\right)^{\frac{\omega_s}{\beta\kappa u_*}} \qquad (3.4.6.2.2)$$

By substituting Equation (3.4.6.2.1), the following terms can be obtained:

$$\frac{\partial s}{\partial z} = \frac{-\omega_s H s_{am}}{\beta\kappa u_* z^2}\left(\frac{H-z}{z}\right)^{\frac{\omega_s}{\beta\kappa u_*}-1} = \frac{-\omega_s H}{\beta\kappa u_* z(H-z)} s \qquad (3.4.6.2.3)$$

$$\frac{\partial^2 s}{\partial z^2} = \frac{\omega_s H}{\beta\kappa u_* z^2 (H-z)^2}\left[\frac{\omega_s H}{\beta\kappa u_*} + H - 2z\right] s \qquad (3.4.6.2.4)$$

Recall the parabolic distribution of sediment mixing coefficient:

$$k_{sz} = \beta\kappa u_* z(1 - z/H) \qquad (2.1.3.1)$$

The distribution of mixing coefficient of water should be also a parabolic function as follows:

$$k_z = \kappa u_* z(1 - z/H) \qquad (3.4.6.2.5)$$

By substituting Equations (2.1.3.1) and (3.4.6.2.5), the following terms can be obtained:

$$k_{sz} - k_z = (\beta - 1)k_z \qquad (3.4.6.2.6)$$

$$\frac{\partial k_z}{\partial z} = \kappa u_*(1 - 2z/H) \qquad (3.4.6.2.7)$$

The derivative of ω_s should be zero because of the constant settling velocity. A specific governing equation for using the Rouse profile is formed by applying Equations (3.4.6.2.1) to (3.4.6.2.7) to the governing equation set of Equations (3.4.5.8) to (3.4.5.11). For this case, the author renames the three coefficients $\overline{A}$, $\overline{B}$ and $\overline{C}$ in Equation (3.4.5.8) to $\overline{A}_R$, $\overline{B}_R$ and $\overline{C}_R$ respectively.

The governing Equation (3.4.5.8) is simplified to two specific equations by substituting two different distributions of sediment concentrations (s). However, governing equations described in Sections (3.4.6.1) and (3.4.6.2) are still complex and difficult to solve analytically. Instead, the author developed mathematical models shown in Chapter 4, which have constants or specific forms of input parameters. In order to identify real life situations that the models in Chapter 4 are adequate for modeling toxic substance transport. The real life situations that the coefficient $\overline{A}$, $\overline{B}$ and $\overline{C}$ can be simplified to constants or specific forms, which match the corresponding coefficients in one of the developed models in Chapter 4 should be identified. The identification is described in Chapter 5.

3.4.7 Boundary conditions for transport of toxic substances

At the water-sediment interface, the following mechanics is usually considered to form the boundary conditions. For dissolved toxicants, diffusive exchanges through the interface are considered. For particulate toxicants, deposition from water to bed sediment and resuspension from bed sediment to water column are considered. The sorption mechanics between dissolved and particulate toxicants is also taken into account. The general boundary conditions describing the flux from dissolved and particulate toxicants are:

$$k_z \frac{\partial c}{\partial z} = \upsilon_f (c - c_a) + k_c Hc - k_p Hp \qquad at\ z = a \qquad (3.4.7.1)$$

$$k_{sz} \frac{\partial p}{\partial z} + \omega_s p = \phi p - \gamma p_a - k_c Hc + k_p Hp \qquad at \quad z = a \qquad (3.4.7.2)$$

in which υ_f is diffusive exchange velocity of dissolved toxicant at the interface. a is the reference level. c_a and p_a are the reference level concentration of dissolved and particulate toxicant respectively. ϕ is deposition velocity of sediment at level a and γ is resuspension velocity of sediment from water-sediment interface.

The concept of instantaneous equilibrium of the kinetics can be applied by substituting Equations (2.4.4.1.1), (2.4.4.1.2) and (2.4.4.1.3) to Equations (3.4.7.1) and (3.4.7.2) and then adding together Equations (3.4.7.1) and (3.4.7.2) together, the boundary condition in terms of the total concentration (c_T) is as follows:

$$k_z \frac{\partial c_T}{\partial z} + (k_{sz} - k_z) \frac{\partial f_p c_T}{\partial z} + \omega_s f_p c_T = (\upsilon_f f_d + \phi f_p) c_T - (\upsilon_f c_a + \gamma p_a) at\ z = a \quad (3.4.7.3)$$

The boundary condition can be further simplified by substituting a distribution function of suspended sediment. However, if the sediment distribution function depends on the vertical dimension (z) only, the values of f_d and f_p should be constant at a particular z coordinate and equation (3.4.7.3) becomes:

$$(f_p k_{sz} + f_d k_z)\frac{\partial c_T}{\partial z} + \omega_s f_p c_T = (\upsilon_f f_d + \phi f_p)c_T - (\upsilon_f c_a + \gamma p_a) at\ z = a \qquad (3.4.7.4)$$

If the decay of toxic substances in the bed sediment layer is assumed, the boundary condition is as follows:

$$(f_p k_{sz} + f_d k_z)\frac{\partial c_T}{\partial z} + \omega_s f_p c_T = (\upsilon_f f_d + \phi f_p)c_T - (\upsilon_f c_a e^{-r_{cb}t} + \gamma p_a e^{-r_{pb}t}) at\ z = a \qquad (3.4.7.5)$$

in which r_{cb} and r_{pb} are decay rates of dissolved and particulate toxic substances respectively.

At the water surface, the volatilization loss of the dissolved component is considered and boundary conditions of dissolved and particulate toxicants are:

$$k_z \frac{\partial c}{\partial z} = -\upsilon_v c + k_c Hc - k_p Hp \qquad at\ z = H \qquad (3.4.7.6)$$

$$k_{sz}\frac{\partial p}{\partial z} + \omega_s p = -k_c Hc + k_p Hp \qquad at\ \ z = H \qquad (3.4.7.7)$$

in which υ_v is the rate of volatilization loss of the dissolved component.

The boundary condition in terms of total concentration after applying the concept of instantaneous equilibrium is:

$$k_z \frac{\partial c_T}{\partial z} + (k_{sz} - k_z) \frac{\partial f_p c_T}{\partial z} + \omega_s f_p c_T = -\upsilon_v f_d c_T \quad at\ z = H \qquad (3.4.7.8)$$

A complete governing system for the transport of toxic substance has been developed based on the general governing equations and boundary conditions. Different initial conditions are required according to different modeling situations. However, coefficients in the governing equations defined in previous sections are complex and the governing equations still cannot be solved analytically. Three different models with further simplified coefficients are given in Chapter 4 and solved analytically. In Chapter 5, analysis of the coefficients in the governing system is described. The purpose of the analysis is to identify the scopes of input parameters of the governing system that can be further simplified to show that one of the developed models in Chapter 4 is adequate to model the toxic substance transport in such scopes of input parameters.

Chapter 4: Formulations, solutions and general analysis of developed models

Three contaminant transport models have been developed in this research study to simulate the transport of contaminants in different transport environments. All are one dimensional, time varying models with consideration of the advection-diffusion effects on contaminant transport. The governing system, solution steps and analysis of parameters for each model are described in the following sections.

4.1 Governing system of Model 1

The first model, Model 1, is developed with reference to Hjelmfelt and Lenau (1970) with the initial condition changed from zero concentration to a function along the water depth. Figure 1 shows the modeling environment of Model 1. The model considers the changes of contaminant concentration along the vertical direction with time and the settling of contaminant particles along the water column. It also takes into account the setting and resuspension of contaminants at the bottom sediment layer.

The governing equation is the general advection-diffusion equation as follows.

$$\frac{\partial m}{\partial t} = \frac{\partial}{\partial z}\left(k_{mz}\frac{\partial m}{\partial z}\right) + \omega\frac{\partial m}{\partial z} \qquad (4.1.1)$$

in which m = contaminant concentration, t = time, z = vertical dimension, ω = settling velocity of contaminant and k_{mz} = turbulent mixing coefficient in

vertical direction. A parabolic distribution of the turbulent mixing coefficient is assumed for the modeling as follows:

$$k_{mz} = \beta_m \kappa u_* z\left(1 - \frac{z}{H}\right) \tag{4.1.2}$$

in which κ is the von Karman coefficient, β_m is the ratio of contaminant mixing coefficient to momentum diffusion coefficient, u_* is shear velocity and H is the water depth.

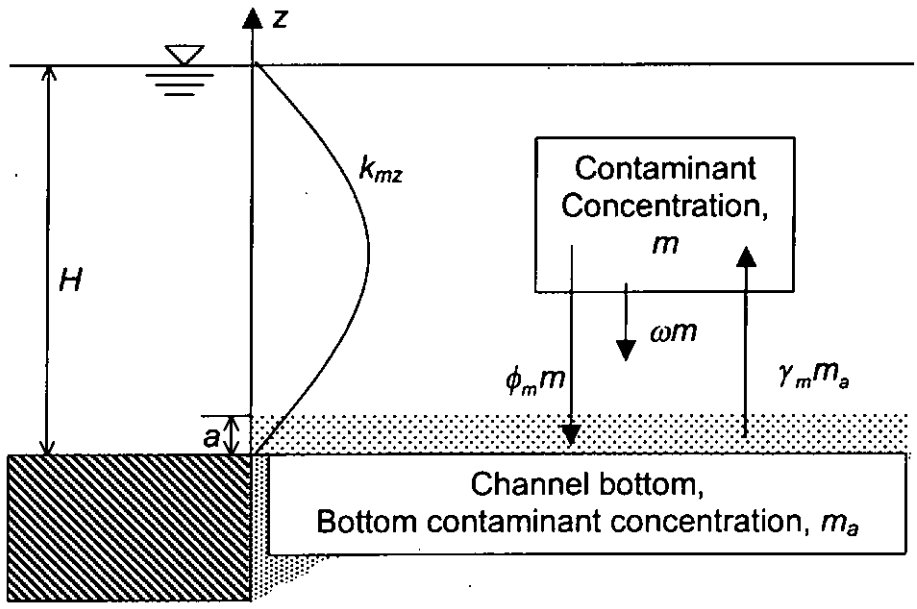

Figure 1: Problem Definition of Model 1

It is assumed that there is no exchange of the contaminant between water and the air layers at water surface. Thus the boundary condition at water surface is as follows:

$$k_{mz}\frac{\partial m}{\partial z} + \omega m = 0 \quad at \quad z = H, \quad \forall t \geq 0 \tag{4.1.3}$$

At water-sediment interface, exchange of the contaminant by settling and resuspension is considered. The boundary condition is as follows:

$$k_{mz}\frac{\partial m}{\partial z} + \omega m = \phi_m m - \gamma_m m_a \quad at \quad z = a, \quad \forall t \geq 0 \tag{4.1.4}$$

in which a and m_a are the reference level and the reference level contaminant concentration respectively. ϕ_m is the deposition velocity of contaminant at the reference level. γ_m is resuspension velocity of the contaminant from water-sediment interface.

The model further allows an arbitrary initial contaminant concentration distribution ($m_{I0}(z)$) in the water column. The initial condition is written as follows:

$$m = m_{I0}(z) \text{ at } \quad a<z<=H, \quad t = 0 \tag{4.1.5}$$

4.2 Summary of solution steps of Model 1

Mathematical techniques involved to solve the system of equations mentioned in the last Section are similar to the techniques used by Hjelmfelt and Lenau (1970). A summary of the solution processes is shown below:

First, introduce the dimensionless variables and parameters:

$$M = m/m_a; \quad M_{I0} = m_{I0}/m_a; \quad \lambda = \frac{\omega}{\beta_m \kappa u_*}; \quad T = \beta_m \kappa u_* t/H$$

$$Z = z/H; \quad A = a/H; \quad B_1 = \frac{\phi_m}{\beta_m \kappa u_*}; \quad B_2 = \frac{\gamma_m}{\beta_m \kappa u_*}$$

Using the dimensionless variables and parameters, the system becomes:

$$\frac{\partial M}{\partial T} = \lambda \frac{\partial M}{\partial Z} + \frac{\partial}{\partial Z}\left[Z(1-Z)\frac{\partial M}{\partial Z} \right] \tag{4.2.1}$$

with boundary conditions:

$$Z(1-Z)\frac{\partial M}{\partial Z} + \lambda M = 0 \quad at\ Z = 1, \quad T \geq 0 \tag{4.2.2}$$

$$Z(1-Z)\frac{\partial M}{\partial Z}+\lambda M=B_1M-B_2 \quad at\ Z=A,\quad T\geq 0 \tag{4.2.3}$$

$$M=M_0 \quad at \quad A\leq Z\leq 1,\quad T=0 \tag{4.2.4}$$

Secondly, method of separating variables is applied to the governing equation:

$$M=P(Z)G(T) \tag{4.2.5}$$

The governing PDE becomes:

$$\frac{G'}{G}=(1+\lambda-2Z)\frac{P'}{P}+Z(1-Z)\frac{P''}{P}=-\alpha^2+\frac{1}{4} \tag{4.2.6}$$

in which $-\alpha^2+0.25$ is an arbitrary constant.

The solution of G is:

$$G=C_1e^{-T(\alpha^2-0.25)} \tag{4.2.7}$$

in which C_1 is an arbitrary constant. Also for $P(Z)$, we have:

$$Z(1-Z)P''+(1+\lambda-2Z)P'+(\alpha^2-1/4)P=0 \tag{4.2.8}$$

Putting $Z' = 1 - Z$, the above equation becomes:

$$Z'(1-Z')P''+(1-\lambda-2Z')P'+(\alpha^2-1/4)P=0 \tag{4.2.9}$$

Noting that a general form of a hypergeometric differential equation is:

$$Z(1-Z)P''+(c-(a+b+1)Z)P'-abP=0 \tag{4.2.10}$$

the above differential equation of $P(Z')$ is a hypergeometric differential equation for:

$$a=1/2+\alpha \tag{4.2.11}$$

$$b=1/2-\alpha \tag{4.2.12}$$

$$c=1-\lambda \tag{4.2.13}$$

The general solution of the above equation, with $c = 1 - \lambda$ not an integer (note: λ cannot be an integer) and by putting back $Z = 1 - Z'$ is:

$$P = \tilde{A}F(0.5+\alpha,0.5-\alpha,1-\lambda,1-Z)+\tilde{B}(1-Z)^{\lambda}F(0.5+\alpha+\lambda,0.5-\alpha+\lambda,1+\lambda,1-Z) \tag{4.2.14}$$

where $\tilde{A}, \tilde{B}$ are arbitrary constants, and F is the hypergeometric function.

$$F(a,b,c,Z) = 1+\sum_{n=1}^{\infty}\frac{(a)_n(b)_n}{(c)_n}\frac{Z^n}{n!}, \quad |Z|<1 \tag{4.2.15}$$

$$(a)_n = a(a+1)(a+2)\cdots(a+n-1) \quad for\ n \geq 1 \tag{4.2.16}$$

Applying the boundary condition at $Z = 1$

$$Z(1-Z)\frac{\partial M}{\partial Z}+\lambda M = 0 \qquad \text{at } Z = 1,\ T \geq 0 \tag{4.2.17}$$

$$\Rightarrow \quad P(Z)G(T) = 0$$

Since $G(T)$ cannot always be zero at any T, this condition means $P(1) = 0$ and then:

$$P = \tilde{A}F(0.5+\alpha,0.5-\alpha,1-\lambda,0)+\tilde{B}(1-1)^{\lambda}F(0.5+\alpha+\lambda,0.5-\alpha+\lambda,1+\lambda,0) = 0 \tag{4.2.18}$$

$$\Rightarrow \quad \tilde{A}\left(1+\sum_{n=1}^{\infty}\frac{(0.5+\alpha)_n(0.5-\alpha)_n}{(1-\lambda)_n}\frac{0^n}{n!}\right) = 0 \tag{4.2.19}$$

and finally we get $\tilde{A} = 0$.

Now, M becomes:

$$M = C_1\tilde{B}e^{-(\alpha^2-0.25)T}(1-Z)^{\lambda}F(0.5+\alpha+\lambda,0.5-\alpha+\lambda,1+\lambda,1-Z) \tag{4.2.20}$$

In the solution, only the term $G(T)$ depends on T. Thus, the equilibrium state forms when $G(T)$ = constant for all T., i.e., $\alpha = 0.5$. In this case, M becomes:

$$M = C_1\tilde{B}(1-Z)^{\lambda}F(1+\lambda,\lambda,1+\lambda,1-Z) \tag{4.2.21}$$

$F(1+\lambda,\lambda,1+\lambda,1-Z)$ is equal to $Y^{-\lambda}$ based on the definition of F.

Applying the boundary condition at $Z = A$, we get:

$$Z(1-Z)\frac{\partial M}{\partial Z}+\lambda M = B_1 M - B_2 \qquad \text{at } Z = A,\ T \geq 0 \tag{4.2.22}$$

$$\Rightarrow \quad -A(1-A)C_1\tilde{B}\lambda\frac{(1-A)^{\lambda-1}}{A^{\lambda+1}}+\lambda C_1\tilde{B}\left(\frac{1-A}{A}\right)^{\lambda} = B_1 C_1\tilde{B}\left(\frac{1-A}{A}\right)^{\lambda} - B_2 \tag{4.2.23}$$

$$C_1\tilde{B} = \frac{B_2}{B_1}\left(\frac{A}{1-A}\right)^{\lambda} \tag{4.2.24}$$

For the non-equilibrium case, it is assumed that:

$$M = \frac{B_2}{B_1}\left(\frac{A}{1-A}\right)^{\lambda}\left(\frac{1-Z}{Z}\right)^{\lambda}+\sum_{K=1}^{\infty} a_K e^{-T(\alpha_K{}^2-\frac{1}{4})}P(Z;\alpha_K) \tag{4.2.25}$$

$$P(Z;\alpha_K) = (1-Z)^{\lambda}F(0.5+\lambda+\alpha_K,0.5+\lambda-\alpha_K 1+\lambda,1-Z) \tag{4.2.26}$$

where $\alpha_K > 1/2$ are roots of $F(0.5+\lambda+\alpha_K,0.5+\lambda-\alpha_K,1+\lambda,1-Y) = 0$.

(Note: The first term of the above solution is widely known as the Rouse profile which represents the equilibrium concentration profile of contaminants.)

Applying the initial condition $M = M_{I0}$ at $A < Z \leq H$, $T = 0$, we can get:

$$\sum_{K=1}^{\infty} a_K P(Z;\alpha_K) = M_{I0} - \frac{B_2}{B_1}\left(\frac{A}{1-A}\right)^{\lambda}\left(\frac{1-Z}{Z}\right)^{\lambda} \tag{4.2.27}$$

It can be shown that the function $P(Z;\alpha_K)$ forms an orthogonal system with respect to the weight function $Z^{\lambda}(1-Z)^{-\lambda}$ i.e.,

$$\int_A^1 P(Z;\alpha_m)P(Z;\alpha_n)Z^{\lambda}(1-Z)^{-\lambda}\,dZ = 0, \quad m \neq n \tag{4.2.28}$$

The steps to prove the orthogonal system can be found in Hjelmfelt and Lenau (1970).

a_m can be found from Equation (4.2.27) as follows:

From Equation (4.2.27)

$$\Rightarrow \quad \sum_{K=1}^{\infty} a_K P(Z;\alpha_K) Z^{\lambda}(1-Z)^{-\lambda} = M_{I0} Z^{\lambda}(1-Z)^{-\lambda} - \frac{B_2}{B_1}\left(\frac{A}{1-A}\right)^{\lambda} \quad (4.2.29)$$

Then, both sides of Equation (4.2.29) times $P(Z;\alpha_m)$ and then take integration from A to 1 to become:

$$\int_A^1 M_{I0} Z^{\lambda}(1-Z)^{-\lambda} P(Z;\alpha_m)dZ - \frac{B_2}{B_1}\left(\frac{A}{1-A}\right)^{\lambda} \int_A^1 P(Z;\alpha_m)dZ$$
$$= a_1 \int_A^1 Z^{\lambda}(1-Z)^{-\lambda} P(Z;\alpha_1)P(Z;\alpha_m)dZ + \cdots + a_m \int_A^1 Z^{\lambda}(1-Z)^{-\lambda} P^2(Z;\alpha_m)dZ + \cdots \quad (4.2.30)$$

Applying the Equation (4.2.28), then finally becomes:

$$a_m = \frac{\int_A^1 M_{I0} Z^{\lambda}(1-Z)^{-\lambda} P(Z;\alpha_m)dZ - \frac{B_2}{B_1}\left(\frac{A}{1-A}\right)^{\lambda} \int_A^1 P(Z;\alpha_m)dZ}{\int_A^1 Z^{\lambda}(1-Z)^{-\lambda} P^2(Z;\alpha_m)dZ} \quad (4.2.31)$$

The steps for calculating $\int_A^1 Z^{\lambda}(1-Z)^{-\lambda} P^2(Z;\alpha_m)dZ$ and $\int_A^1 P(Z;\alpha_m)dZ$ can be found in Hjelmfelt and Lenau (1970) and they are:

$$\int_A^1 Z^{\lambda}(1-Z)^{-\lambda} P^2(Z;\alpha_m)dZ = \frac{-A^{1+\lambda}(1-A)^{1-\lambda}}{2\alpha_m} \frac{\partial P(A;\alpha_m)}{\partial \alpha} \frac{\partial P(A;\alpha_m)}{\partial Z} \quad (4.2.32)$$

$$\int_A^1 P(Z;\alpha_m)dZ = \frac{A(1-A)}{(\alpha^2 - 0.25)} \frac{\partial P(A;\alpha_m)}{\partial Z} \quad (4.2.33)$$

The expressions for $\partial P/\partial \alpha$ and $\partial P/\partial Z$ can be found in Hjelmfelt and Lenau (1970). The expression of $\int_A^1 Z^{\lambda}(1-Z)^{-\lambda} P(Z;\alpha_m)dZ$ is as follows:

First, start from Equation (46) shown in Hjelmfelt and Lenau (1970, p1577):

$$\frac{\partial}{\partial Z}\left[\frac{\partial P}{\partial Z}(Z;\alpha_m) Z^{1+\lambda}(1-Z)^{1-\lambda}\right] + (\alpha_m{}^2 - \frac{1}{4}) P(Z,\alpha_m) Z^{\lambda}(1-Z)^{-\lambda} = 0 \quad (4.2.34)$$

$$\Rightarrow \quad \int_A^1 P(Z,\alpha_m)Z^{\lambda}(1-Z)^{-\lambda}\,dZ = \frac{-1}{\alpha_m{}^2-0.25}\int_A^1 \frac{\partial}{\partial Z}\left[\frac{\partial P}{\partial Z}(Z;\alpha_m)Z^{1+\lambda}(1-Z)^{1-\lambda}\right]dZ$$

$$\int_A^1 P(Z,\alpha_m)Z^{\lambda}(1-Z)^{-\lambda}\,dZ = \frac{-1}{\alpha_m{}^2-0.25}\frac{\partial P}{\partial Z}(Z;\alpha_m)Z^{1+\lambda}(1-Z)^{1-\lambda}\Big|_A^1 \qquad (4.2.35)$$

The expression of $\partial P/\partial Z$ is roughly as follows:

$$\frac{\partial P}{\partial Z}(Z,\alpha_m) = -\lambda(1-Z)^{-1+\lambda}F(\frac{1}{2}+\lambda+\alpha_m,\frac{1}{2}+\lambda-\alpha_m,1+\lambda,1-Z)+(1-Z)^{\lambda}(\cdots) \qquad (4.2.36)$$

$$\Rightarrow \quad (1-Z)^{1-\lambda}\frac{\partial P}{\partial Z}(Z,\alpha_m) = -\lambda F(\frac{1}{2}+\lambda+\alpha_m,\frac{1}{2}+\lambda-\alpha_m,1+\lambda,1-Z)+(1-Z)(\cdots)$$

At $Z = 1$, then becomes:

$$(1-Z)^{1-\lambda}\frac{\partial P}{\partial Z}(Z,\alpha_m)\Big|_{Z=1} = -\lambda F(\frac{1}{2}+\lambda+\alpha_m,\frac{1}{2}+\lambda-\alpha_m,1+\lambda,0)+(1-1)(\cdots) \qquad (4.2.37)$$

Based on the definition of F, the value of $F(0.5+\lambda+\alpha_m,0.5+\lambda-\alpha_m,1+\lambda,0)$ should be 1 and therefore the value of $\int_A^1 Z^{\lambda}(1-Z)^{-\lambda}P(Z;\alpha_m)dZ$ becomes:

$$= \frac{\lambda}{\alpha_m{}^2-0.25}+\frac{A^{1+\lambda}(1-A)^{1-\lambda}}{\alpha_m{}^2-0.25}\frac{\partial P}{\partial Z}(A;\alpha_m) \qquad (4.2.38)$$

Then, for M_0 is a constant value, a_m becomes:

$$a_m = \frac{2\alpha_m}{\left(\alpha_m^2-\frac{1}{4}\right)\frac{\partial P}{\partial \alpha}(A;\alpha_m)}\left[\frac{B_2}{B_1}-M_{I0}-\frac{M_{I0}\lambda}{A^{1+\lambda}(1-A)^{1-\lambda}\frac{\partial P}{\partial Z}(A;\alpha_m)}\right] \qquad (4.2.39)$$

And therefore, the solution of $M(Z,T)$, (Solution 1) is:

$$M = D\left(\frac{A}{1-A}\right)^{\lambda}\left(\frac{1-Z}{Z}\right)^{\lambda} + 2\sum_{K=1}^{\infty}\frac{\alpha_K P(Z;\alpha_K)e^{-T(\alpha_K^2-\frac{1}{4})}}{\left(\alpha_K^2-\frac{1}{4}\right)\frac{\partial P}{\partial \alpha}(A;\alpha_K)}\left[D - M_{I0} - \frac{M_{I0}\lambda}{A^{1+\lambda}(1-A)^{1-\lambda}\frac{\partial P}{\partial Z}(A;\alpha_K)}\right] \quad (4.2.40)$$

$$D = \frac{B_2}{B_1} = \frac{\gamma}{\phi}, \quad P(Z;\alpha_K) = (1-Z)^{\lambda}F(0.5+\lambda+\alpha_K, 0.5+\lambda-\alpha_K 1+\lambda, 1-Z)$$

if M_0 is a function of Z, a_m becomes:

$$a_m = \frac{2\alpha_m}{\frac{\partial P}{\partial \alpha}(A;\alpha_m)}\left[\frac{D}{(\alpha_m^2-\frac{1}{4})} - \frac{\int_A^1 M_{I0}Y^{\lambda}(1-Z)^{-\lambda}P(Z;\alpha_m)dZ}{A^{1+\lambda}(1-A)^{1-\lambda}\frac{\partial P}{\partial Z}(A;\alpha_m)}\right] \quad (4.2.41)$$

And therefore, the solution of $M(Z,T)$ for this case (Solution 2) is:

$$M = D\left(\frac{A(1-Z)}{(1-A)Z}\right)^{\lambda} + 2\sum_{K=1}^{\infty}\frac{\alpha_K P(Z;\alpha_K)e^{-T(\alpha_K^2-\frac{1}{4})}}{\frac{\partial P}{\partial \alpha}(A;\alpha_K)}\left[\frac{D}{(\alpha_k^2-\frac{1}{4})} - \frac{\int_A^1 M_{I0}Z^{\lambda}(1-Z)^{-\lambda}P(Z;\alpha_K)dZ}{A^{1+\lambda}(1-A)^{1-\lambda}\frac{\partial P}{\partial Z}(A;\alpha_K)}\right] \quad (4.2.42)$$

The integral term in the solution is solved by the numerical integration. The expressions for α_k, $\partial P/\partial \alpha$ and $\partial P/\partial Z$ can be found in Hjelmfelt and Lenau (1970).

4.3 General Analysis for Model 1

MATLAB program codes have been developed to generate computational results for the solutions of Model 1. An examination of the solution shows that the contaminant concentration is controlled by four

dimensionless factors, D, M_{l0}, A and λ, Each item is considered in the following paragraphs.

4.3.1 Effect of λ

In Model 1, λ is the ratio between the settling velocity, ω and $\beta_m \kappa u$. which controls the overall magnitude of the turbulent mixing coefficient. λ controls the ratio between the downward motion of contaminants (settling velocity) and the upward motion of contaminant (turbulent mixing coefficient) in the water column. Figure 2 shows the dimensionless averaged depth concentration average versus T for different λ values with $D = 1$, $M_{l0} = 0$ and $A = 0.05$. As λ increases, it implies an increase in the settling velocity or a decrease in the magnitude of turbulent mixing, the depth averaged concentration is decreased and the steady state is reached more rapidly. Conversely, the depth averaged concentration is increased and the steady state is approached less rapidly with a smaller λ, until the limiting case, $\lambda = 0$ is reached. The time required to approach a certain percentage of steady state concentration (e.g. 95%) decreases as λ increases. Therefore, the limiting case as $\lambda = 0$ requires the maximum time to achieve the steady state. The depth averaged concentration in the water column for smaller values of λ is larger than cases with larger values of λ at all times during the transport process, as a smaller λ represents a higher ratio of turbulent mixing to the settling velocity of the contaminant.

4.3.2 Effect of *A*

The parameter *A* in Model 1 represents a ratio between the reference level, *a*, and water depth, *H*. Based on the parabolic distribution of k_{mz}, since no flux is resuspended from the bottom sediment layer to the water column when *A=0*, *A* cannot be zero. Figure 3 shows the dimensionless averaged depth concentration profile versus *T* for different values of *A* with *D = 1*, M_{l0} *=0* and λ*=0.5*. As *A* is increased, the implication is that an increase in reference concentration level or an increase in the thickness of bed-load layer, the average concentration is increased and the steady state is reached less rapidly. Conversely, the dimensionless depth averaged concentration is decreased and the steady state is attained more rapidly, as *A* is decreased until the limiting case, *A* = 0 is reached (in this case, there is no contribution from the sediment bed layer). The time required to approach a certain percentage of steady state concentration (e.g. 95%) decreases as *A* decreases. Therefore, the limiting case with *A=1* requires the maximum time to approach the steady state. This is because when *A* is small, the value of k_{mz} at level *A* also decreases, meaning that the contribution of the shear force to the resuspension of sediment is decreased and therefore the contribution of sediment concentration from bottom to the water column, is smaller.

4.3.3 Effect of *D*

In the model, the parameter *D* is the ratio between the entrainment fluxes rate, γ_m, and the deposition flux rate of contaminant, ϕ_m, at the water-sediment interface. For some contaminants, such as sediment, the settling

velocity depends on the sediment concentration and usually the settling velocity at the water-sediment interface is smaller than the settling velocity in the water column. Figure 4 shows the dimensionless depth averaged concentration profile versus T for different values of D with $A = 0.05$, $M_{l0} = 0$ and $\lambda = 0.5$. The increase of D implies an increase in the entrainment fluxes rate or a decrease in deposition flux rate, the depth averaged concentration is increased and the equilibrium is reached less rapidly. Conversely, as D is decreased until the limiting case, $D = 0$ is reached (in this case, there is no contribution from the sediment bed), the dimensionless depth averaged concentration is decreased and steady state is approached more rapidly. The time required to approach a certain percentage of steady state concentration (e.g. 95%) decreases as D decreases and no time is required for the limiting case $D = 0$. This is because when D is small, the value of γ_m, which presents the magnitude of entrance flux at level A, also decreases. The contribution of the shear force to the resuspension of bed sediment is decreased and therefore the contribution of sediment concentration from the bottom to the water column is smaller.

4.3.4 Effect of M_{l0}

In the model, the parameter M_{l0} represents the ratio between the initial concentration, m_{l0} and the reference level concentration m_a. Figure 5 shows the dimensionless depth averaged concentration profile versus T for different values of M_{l0} with $A = 0.05$, $D = 1$ and $\lambda = 0.5$. The figure shows that, for all cases, the same depth averaged steady state concentration,

$\frac{1}{1-A} D \left(\frac{A}{1-A} \right)^{\lambda} \int_A^1 \left(\frac{1-Z}{Z} \right)^{\lambda} dZ$ is reached, and therefore the steady state concentration is independent of the value of the initial concentration m_{l0}. The required time increases as the difference between the depth averaged steady state concentration and M_{l0} increases.

Figure 2: Dimensionless depth averaged concentration profiles for different λ values

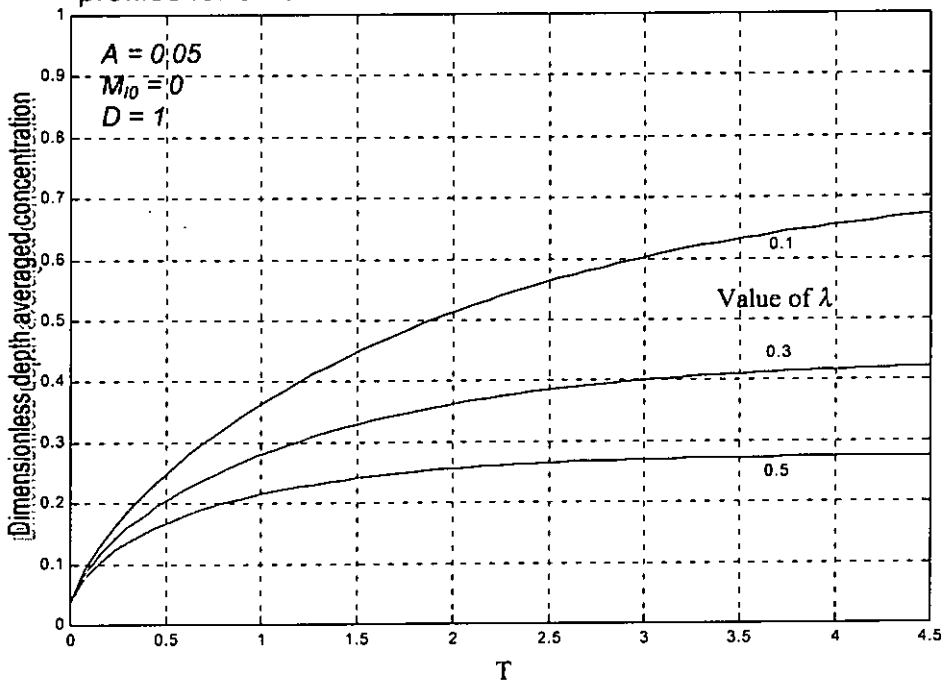

Figure 3: Dimensionless depth averaged concentration profiles for different A values

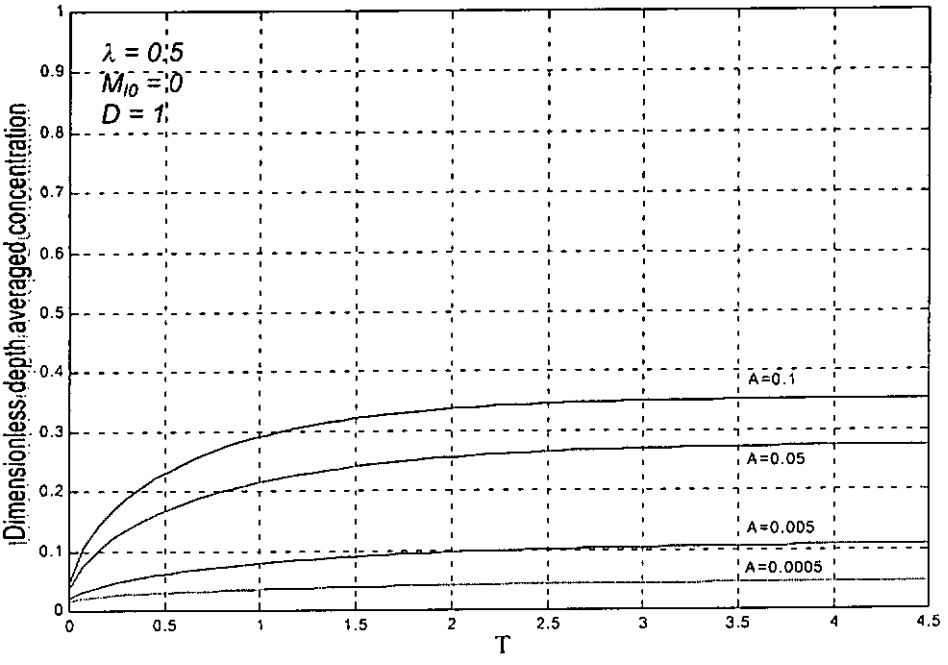

Figure 4: Dimensionless depth averaged concentration profiles for different D values

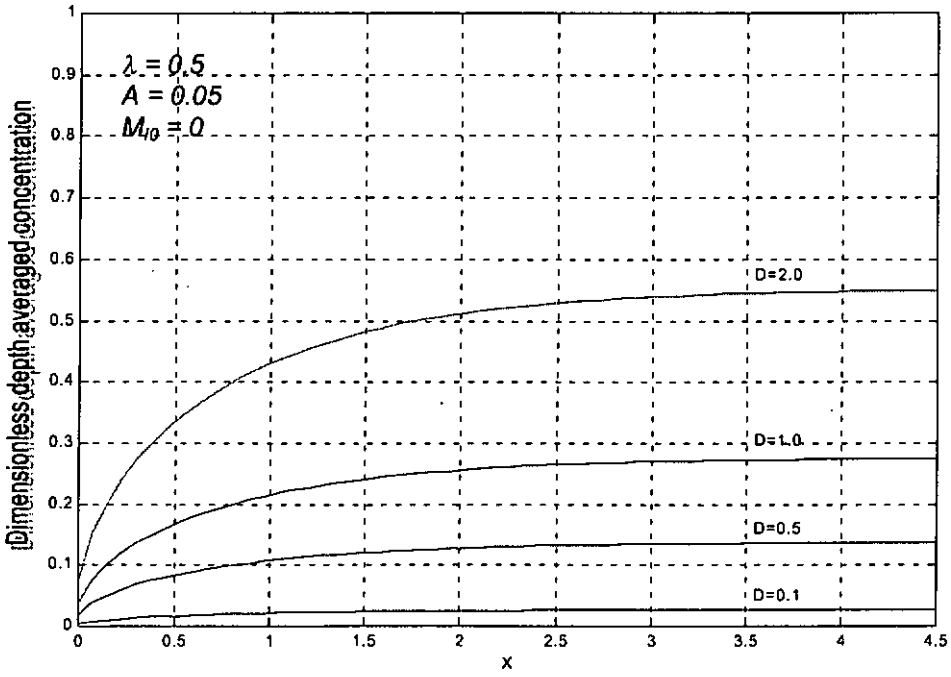

Figure 5: Dimensionless depth averaged concentration profiles for different M_{l0} values

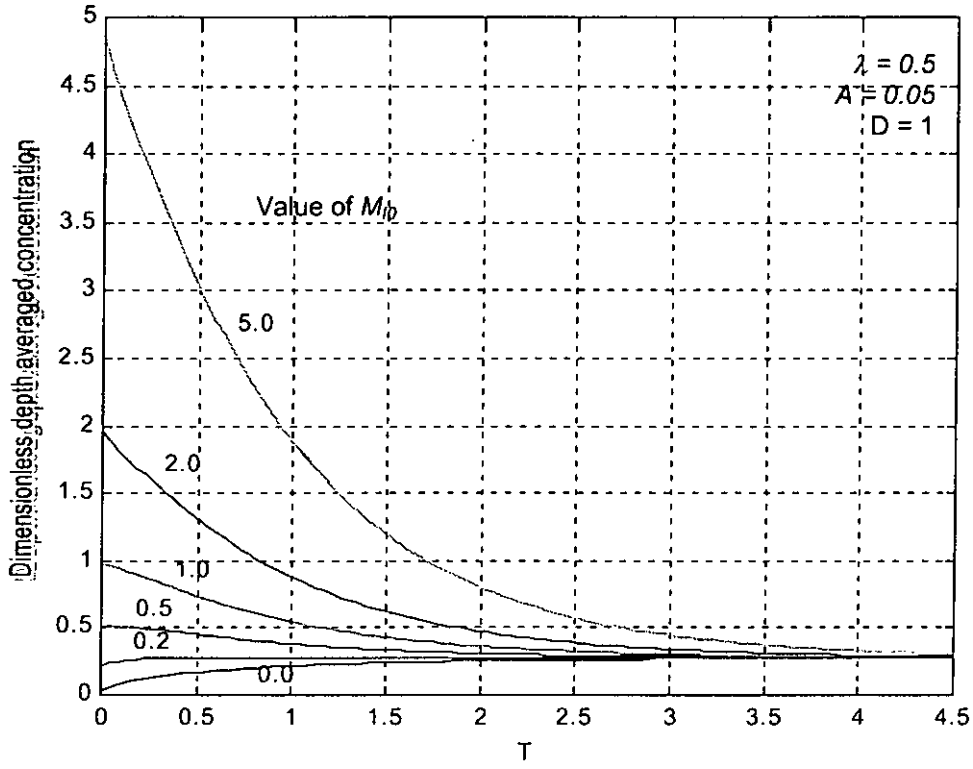

4.4 Governing system of Model 2

The second model, Model 2, is developed from the solution of Cheng (1984) by adding a first order source / sink term to the governing differential equation. Figure 6 shows the modeling environment of Model 2.

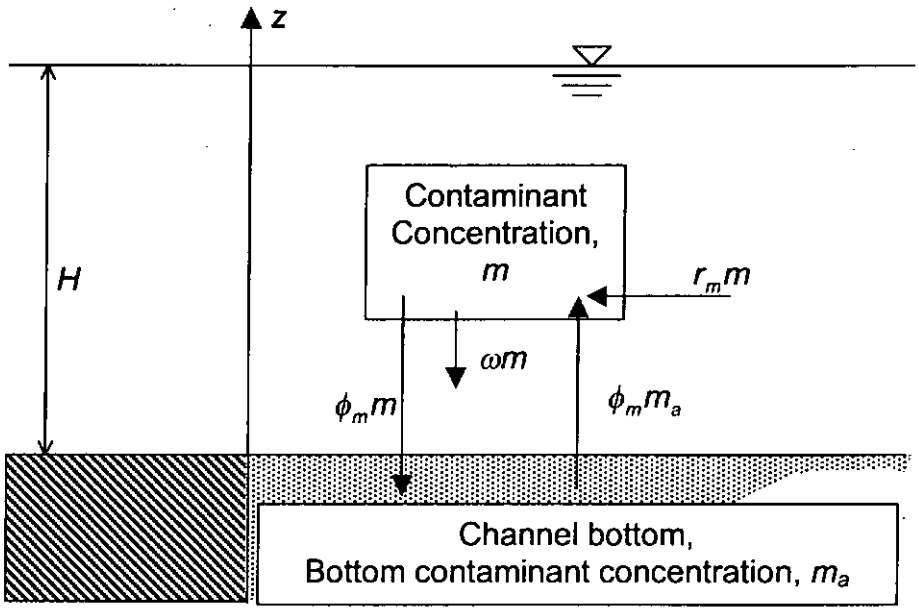

Figure 6: Problem Definition of Model 2

The governing equation, initial condition and boundary conditions are as follows:

Governing equation:

$$\frac{\partial M}{\partial T} = \frac{\partial M}{\partial Z} + K\frac{\partial^2 M}{\partial Z^2} + RM \tag{4.4.1}$$

Boundary conditions:

$$\left[K\frac{\partial M}{\partial Z} + M\right]_{Z=1} = 0 \tag{4.4.2}$$

$$\left[K\frac{\partial M}{\partial Z} + M\right]_{Z=0} = B(M - M_a)_{Z=0} \tag{4.4.3}$$

Initial condition:

$$M(Z,0) = 1 \tag{4.4.4}$$

Note that variables used in the above equations are dimensionless with:

$$M = \frac{m}{m_{I0}};\quad M_a = \frac{m_a}{m_{I0}};\quad Z = \frac{z}{H};\quad K = \frac{k_{mz}}{\omega H};\quad T = \frac{t\omega}{H};\quad B = \frac{\phi_m}{\omega};\quad R = \frac{Hr_m}{\omega}$$

in which m is contaminant concentration, m_{I0} is contaminant concentration at $t = 0$, m_a is contaminant concentration in the bed layer, H is the depth of flow, k_{mz} is the turbulent mixing coefficient, ω is the contaminant settling velocity, r_m is the coefficient for source/sink term, and ϕ_m is the contaminant settling velocity at the water-bed sediment interface. In this model, the resuspension velocity at the water-bed sediment interface is also equal to ϕ_m.

This is an unsteady one-dimensional (in the vertical direction) model. The model considers the settling of contaminant particles to the bottom of the water column. The model also takes into account the settling and resuspension exchange of sediment at the bottom boundary. The model assumes a constant rate of turbulent mixing along the water column. The growth/decay phenomenon of contaminants is considered by adding a first order source/sink term in the governing equation. The initial concentration is assumed to be a constant value along the water column.

4.5 Summary of solution steps of Model 2

Generally, the solution processes follow the steps in Cheng (1984). Detailed solution steps are shown as follows:

First, the concept of Laplace Transform as described in Section (2.5.2.1) is applied to the governing equation as follows:

The Laplace Transform of $M(Z,T)$ is $\tilde{M}(Z,q)$ and defines as follows:

$$\tilde{M}(Z,q) = \int_0^\infty e^{-qT} M(Z,T) dT \tag{4.5.1}$$

Then the governing equation becomes:

$$L\left\{\frac{\partial M}{\partial T}\right\} = L\left\{\frac{\partial M}{\partial Z}\right\} + L\left\{K\frac{\partial^2 M}{\partial Z^2}\right\} + L\{RM\} \tag{4.5.2}$$

$$q\tilde{M}(Z,q) - 1 - \frac{\partial \tilde{M}(Z,q)}{\partial Z} - K\frac{\partial^2 \tilde{M}(Z,q)}{\partial Z^2} - R\tilde{M}(Z,q) = 0 \tag{4.5.3}$$

$$\frac{d^2\tilde{M}(Z,q)}{dz^2} + \frac{1}{K}\frac{d\tilde{M}(Z,q)}{dz} - \frac{q-R}{K}\tilde{M}(Z,q) = \frac{-1}{K} \tag{4.5.4}$$

The governing equation is transformed to a second order ordinary differential equation with respect to z.

The solution of the above ordinary differential equation is:

$$\tilde{M}(Z,q) = C_1 e^{\theta Z} + C_2 e^{\phi Z} + {}^{1}\!/_{(q-R)} \tag{4.5.5}$$

$$\theta = \frac{-1+\sqrt{1+4(q-R)K}}{2K} \tag{4.5.6}$$

$$\phi = \frac{-1-\sqrt{1+4(q-R)K}}{2K} \tag{4.5.7}$$

in which C_1 and C_2 are arbitrary constants.

Applying Laplace Transform to the boundary conditions, they becomes:

$$L\left\{\left[K\frac{\partial M}{\partial Z} + M\right]_{Z=1}\right\} = L\{0\} \tag{4.5.8}$$

$$\Rightarrow \quad \left[K\frac{\partial \tilde{M}}{\partial Z}+\tilde{M}\right]_{Z=1}=0 \tag{4.5.9}$$

$$L\left[K\frac{\partial M}{\partial Z}+M\right]_{Z=0}=L\{B(M-M_a)\}_{Z=0} \tag{4.5.10}$$

$$\left[K\frac{\partial \tilde{M}}{\partial Z}+\tilde{M}\right]_{Z=0}=B\tilde{M}_{Z=0}-B\int_0^{\infty}e^{-qT}M_a dT$$

$$=B\tilde{M}_{Z=0}-BM_A\frac{e^{-qT}}{-q}\Big|_0^{\infty}$$

$$\left[K\frac{\partial \tilde{M}}{\partial Z}+\tilde{M}\right]_{Z=0}=\left[B\tilde{M}-BM_a/q\right]_{Z=0} \tag{4.5.11}$$

Solutions of C_1 and C_2 are found by substituting the solution of $\tilde{M}(Z,q)$ to the transformed boundary conditions. The solutions are as follows:

$$C_1=\frac{Bq-(1+K\phi)(q+e^{\phi}(Bq(1-M_a)-q+BM_aR))}{q(q-R)\left[(1+K\phi-B)(1+K\theta)e^{\theta}-(1+K\theta-B)(1+K\phi)e^{\phi}\right]} \tag{4.5.12}$$

$$C_2=\frac{(1+K\theta)(q+e^{\theta}(Bq(1-M_a)-q+BM_aR))-Bq}{q(q-R)\left[(1+K\phi-B)(1+K\theta)e^{\theta}-(1+K\theta-B)(1+K\phi)e^{\phi}\right]} \tag{4.5.13}$$

The solution of $\tilde{M}(Z,q)$ now becomes,

$$\tilde{M}=\frac{1}{(q-R)}+\frac{L\phi e^{\theta Z}+M\theta e^{\phi Z}}{q(q-R)\left[(1+K\phi-B)(1+K\theta)e^{\theta}-(1+K\theta-B)(1+K\phi)e^{\phi}\right]} \tag{4.5.14}$$

in which:

$$L\phi=Bq-(1+K\phi)(q+e^{\phi}(Bq(1-M_a)-q+BM_aR)) \tag{4.5.15}$$

$$M\theta=(1+K\theta)(q+e^{\theta}(Bq(1-M_a)-q+BM_aR))-Bq=-L\theta \tag{4.5.16}$$

Replacing q by q-$1/4k$, we have:

$$\theta = \frac{-1}{2K} + \sqrt{\frac{q-R}{K}} \tag{4.5.17}$$

$$\phi = \frac{-1}{2K} - \sqrt{\frac{q-R}{K}} \tag{4.5.18}$$

$q(q-R)\left((1+K\phi-B)(1+K\theta)e^{\theta} - (1+K\theta-B)(1+K\phi)e^{\phi}\right)$ becomes:

$$= (q-\frac{1}{4K})(q-R-\frac{1}{4K})e^{-1/2K}\begin{bmatrix} e^{\sqrt{(q-R)/K}} - e^{-\sqrt{(q-R)/K}} + K\phi(e^{\sqrt{(q-R)/K}} - e^{-\sqrt{(q-R)/K}}) \\ -B(e^{\sqrt{(q-R)/K}} - e^{-\sqrt{(q-R)/K}}) + K\theta(e^{\sqrt{(q-R)/K}} - e^{-\sqrt{(q-R)/K}}) \\ +K^2\theta\phi(e^{\sqrt{(q-R)/K}} - e^{-\sqrt{(q-R)/K}}) \\ -BK\theta e^{\sqrt{q-R/K}} + BK\phi e^{-\sqrt{q-R/K}} \end{bmatrix}$$

$$= (q-\frac{1}{4K})(q-R-\frac{1}{4K})e^{-1/2K}\begin{bmatrix} 2\sinh\sqrt{(q-R)/K} + 2K\phi\sinh\sqrt{(q-R)/K} \\ -2B\sinh\sqrt{(q-R)/K} \\ +2K\theta\sinh\sqrt{(q-R)/K} + 2K^2\theta\phi\sinh\sqrt{(q-R)/K} \\ -BKe^{\sqrt{(q-R)/K}}(-1/2K + \sqrt{(q-R)/K}) \\ +BKe^{-\sqrt{(q-R)/K}}(-1/2K - \sqrt{(q-R)/K}) \end{bmatrix}$$

$$= (q-\frac{1}{4K})(q-R-\frac{1}{4K})e^{-1/2K}\begin{bmatrix} -2(K(q-R)-1/4)\sinh\sqrt{\frac{q-R}{K}} - B\sinh\sqrt{\frac{q-R}{K}} \\ -2BK\sqrt{\frac{q-R}{K}}\cosh\sqrt{\frac{q-R}{K}} \end{bmatrix}$$

(4.5.19)

The solution of $\tilde{M}$ now becomes:

$$\tilde{M}(Z,q-1/4K)$$

$$= \frac{1}{q-R-\frac{1}{4K}} + \frac{L\phi e^{\theta Z} + M\theta e^{\phi Z}}{(q-\frac{1}{4K})e^{-1/2K}(q-R-\frac{1}{4K})\begin{bmatrix} -2(K(q-R)-1/4)\sinh\sqrt{\frac{q-R}{K}} \\ -B\sinh\sqrt{\frac{q-R}{K}} \\ -2BK\sqrt{\frac{q-R}{K}}\cosh\sqrt{\frac{q-R}{K}} \end{bmatrix}}$$

(4.5.20)

in which:

$$L\phi = B(q-1/4K) - (1+K\phi)(q-1/4K + e^{\phi}(B(q-1/4K)(1-M_a) - (q-1/4K) + BM_aR))$$

(4.5.21)

$$M\theta = (1+K\theta)(q-1/4K + e^{\theta}(B(q-1/4K)(1-M_a) - (q-1/4K) + BM_aR)) - B(q-1/4K)$$

(4.5.22)

Considering:

$$Q(q-\frac{1}{4K}) = (q-\frac{1}{4K})e^{-1/2K}(q-R-\frac{1}{4K})\begin{bmatrix} -2(K(q-R)-1/4)\sinh\sqrt{\frac{q-R}{K}} \\ -B\sinh\sqrt{\frac{q-R}{K}} \\ -2BK\sqrt{\frac{q-R}{K}}\cosh\sqrt{\frac{q-R}{K}} \end{bmatrix}$$

(4.5.23)

then $Q=0$ has roots at $q-1/4K=0$ or $q-R-1/4K=0$, i.e., $q=1/4K$ or $q=R+1/4K$ and the roots of the equation are given by

$$-2(K(q-R)-1/4)\sinh\sqrt{\frac{q-R}{K}} - B\sinh\sqrt{\frac{q-R}{K}} - 2BK\sqrt{\frac{q-R}{K}}\cosh\sqrt{\frac{q-R}{K}} = 0$$

(4.5.24)

or

$$\tanh\sqrt{\frac{q-R}{K}} = \frac{2BK\sqrt{(q-R)/K}}{0.5-2K(q-R)-B} \quad \text{for } q \text{ is real and larger than } R \qquad (4.5.25)$$

Based on the property that $\tanh(ix) = i\tan x(x)$ described in Section (2.5.3.3), then:

$$\tan\sqrt{\frac{-(q-R)}{K}} = \frac{2BK\sqrt{-(q-R)/K}}{0.5-2K(q-R)-B} \quad \text{for } q \text{ is real and less than R} \qquad (4.5.26)$$

In the Laplace transform, as described in Section (2.5.2.1), there is a property:

$$f(x) = \sum_{k=1}^{n} \frac{R(\lambda_k)}{Q'(\lambda_k)} \exp^{\lambda_k x} \qquad (2.5.2.1.7)$$

$$\text{for } Q(p) = \text{constant}^*(p-\lambda_1)\,(p-\lambda_2)\ldots(p-\lambda_n) \qquad (2.5.2.1.8)$$

$$\text{And } L[f(x)] = \frac{R(p)}{Q(p)} \qquad (2.5.2.1.9)$$

Applying the rule of the Inverse Laplace transform to $\tilde{M}(Z,q)$ with variable q-1/4K, we get:

$$M(Z,T) = e^{RT} + \sum_{q=\frac{1}{4K}}^{a_n} \frac{\left[L\phi e^{\theta Z} + M\theta e^{\phi Z}\right] e^{(q-1/4k)T}}{\frac{\partial}{\partial q}\left\{ e^{-1/2K}(q-R-\frac{1}{4K})(q-\frac{1}{4K}) \left[\begin{array}{l} -2(K(q-R)-1/4)\sinh\sqrt{\frac{q-R}{K}} \\ -B\sinh\sqrt{\frac{q-R}{K}} \\ -2BK\sqrt{\frac{q-R}{K}}\cosh\sqrt{\frac{q-R}{K}} \end{array} \right] \right\}} \qquad (4.5.27)$$

in which $q = a_i$ are roots of $\tanh\sqrt{\frac{q-R}{K}} = \frac{2BK\sqrt{(q-R)/K}}{0.5-2K(q-R)-B}$.

The contribution from the summation when $q = R + 1/(4K)$ can be calculated by direct substitution as follows:

$$\theta = \frac{-1+\sqrt{4K(R+1/4K-R)}}{2K} = 0 \tag{4.5.28}$$

$$\phi = \frac{-1-\sqrt{4K(R+1/4K-R)}}{2K} = -1/K \tag{4.5.29}$$

$$L\phi = B(R+\frac{1}{4K}-\frac{1}{4K})-(1+K(\frac{-1}{K}))(...) = BR \tag{4.5.30}$$

$$M\theta = 1^*(R+\frac{1}{4K}-\frac{1}{4K}+e^0(B(R+\frac{1}{4K}-\frac{1}{4K})(1-C.)-(R+\frac{1}{4K}-\frac{1}{4K})+BC.R) - B(R+\frac{1}{4K}-\frac{1}{4K}) = 0 \tag{4.5.31}$$

$$\frac{\partial}{\partial q}\left[(q-\frac{1}{4K})(q-R-\frac{1}{4K})\left((1+K\theta)(1+K\phi-B)e^{\theta}-(1+K\phi)(1+K\theta-B)e^{\phi}\right)\right]\Big|_{q=R+1/4K}$$
$$= (R+\frac{1}{4K}-\frac{1}{4K})\left[1^*(1+K(\frac{-1}{K})-B)e^0-(1+K(\frac{-1}{K}))(...)\right] = -RB \tag{4.5.32}$$

Thus, the contribution of the summation at q=R+1/4K is:

$$= \frac{BRe^{0^*Z}}{-BR}e^{(R+1/4K-1/4K)T} = -e^{RT} \tag{4.5.33}$$

when q is *1/4K*, we have:

$$\theta = \frac{-1+\sqrt{4K(1/4K-R)}}{2K} = \frac{-1+\sqrt{1-4KR}}{2K} = \theta_1 \tag{4.5.34}$$

$$\phi = \frac{-1-\sqrt{4K(1/4K-R)}}{2K} = \frac{-1-\sqrt{1-4KR}}{2K} = \phi_1 \tag{4.5.35}$$

$$L\phi_1 = B(\frac{1}{4K}-\frac{1}{4K})-(1+K\phi_1)\left[\frac{1}{4K}-\frac{1}{4K}+e^{\phi_1}\left(B(\frac{1}{4K}-\frac{1}{4K})(1-C.)-0+BC.R\right)\right]$$
$$= -(1+K\phi_1)e^{\phi_1}BC.R \tag{4.5.36}$$

$$M\theta_1 = (1+K\theta_1)e^{\theta_1} BC.R \tag{4.5.37}$$

$$\frac{\partial}{\partial q}\left[(q-\frac{1}{4K})(q-R-\frac{1}{4K})\left((1+K\theta)(1+K\phi-B)e^{\theta}-(1+K\phi)(1+K\theta-B)e^{\phi}\right)\right]_{q=1/4K}$$

$$=(\frac{1}{4K}-R-\frac{1}{4K})\left((1+K\theta_1)(1+K\phi_1-B)e^{\theta_1}-(1+K\phi_1)(1+K\theta_1-B)e^{\phi_1}\right)$$

$$=-R\left((1+K\theta_1)(1+K\phi_1-B)e^{\theta_1}-(1+K\phi_1)(1+K\theta_1-B)e^{\phi_1}\right) \tag{4.5.38}$$

Thus, the contribution from the summation term is:

$$=\frac{BM_a\left[(1+K\phi_1)e^{\phi_1}e^{\theta_1 Z}-(1+K\theta_1)e^{\theta_1}e^{\phi_1 Z}\right]}{a_1(\theta_1,\phi_1)} \tag{4.5.39}$$

in which:

$$a_1(\theta_1,\phi_1)=(1+K\theta_1)(1+K\phi_1-B)e^{\theta_1}-(1+K\phi_1)(1+K\theta_1-B)e^{\phi_1} \tag{4.5.40}$$

$$a_1(\theta_1,\phi_1)=(KR-B(1+K\theta_1))e^{\theta_1}-(KR-B(1+K\phi_1))e^{\phi_1}$$

$$=(KR-B/2)(e^{\theta_1}-e^{\phi_1})-B\sqrt{1-4KR}(e^{\theta_1}+e^{\phi_1})/2 \tag{4.5.41}$$

For *1 - 4KR > 0*, we have:

$$e^{\theta_1}-e^{\phi_1}=e^{-1/2K}(e^{\sqrt{1-4KR}/2K}-e^{-\sqrt{1-4KR}/2K})=2e^{-1/2K}\sinh(\sqrt{1-4KR}/2K) \tag{4.5.42}$$

$$e^{\theta_1}+e^{\phi_1}=2e^{-1/2K}\cosh(\sqrt{1-4KR}/2K) \tag{4.5.43}$$

While *1 - 4KR < 0*, we have:

$$e^{\theta_1}-e^{\phi_1}=e^{-1/2K}(e^{i\sqrt{4KR-1}/2K}-e^{-i\sqrt{4KR-1}/2K})=2ie^{-1/2K}\sin(\sqrt{1-4KR}/2K) \tag{4.5.44}$$

$$e^{\theta_1}+e^{\phi_1}=2e^{-1/2K}\cos(\sqrt{1-4KR}/2K) \tag{4.5.45}$$

Thus $a_1(\theta_1, \phi_1)$ become:

$$a_1(\theta_1,\phi_1)=e^{-1/2K}\left[(2KR-B)\sinh\frac{\sqrt{1-4KR}}{2K}-B\sqrt{1-4KR}\cosh\frac{\sqrt{1-4KR}}{2K}\right]$$

when 1 - 4KR > 0 (4.5.46)

$$a_1(\theta_1,\phi_1) = ie^{-1/2K}\left[(2KR-B)\sin\frac{\sqrt{4KR-1}}{2K} - B\sqrt{4KR-1}\cos\frac{\sqrt{4KR-1}}{2K}\right]$$

when 1 - 4KR < 0 (4.5.47)

Considering $(1+K\phi_1)e^{\phi_1}e^{\theta_1 Z} - (1+K\theta_1)e^{\theta_1}e^{\phi_1 Z}$:

$$= e^{\phi_1}e^{\theta_1 Z} - e^{\theta_1}e^{\phi_1 Z} + K(\phi_1 e^{\phi_1}e^{\theta_1 Z} - \theta_1 e^{\theta_1}e^{\phi_1 Z})$$

$$= \frac{1}{2}(e^{\phi_1}e^{\theta_1 Z} - e^{\theta_1}e^{\phi_1 Z}) - \frac{\sqrt{1-4KR}}{2}(e^{\phi_1}e^{\theta_1 Z} + e^{\theta_1}e^{\phi_1 Z}) \qquad (4.5.48)$$

For *1 - 4KR > 0*, we have:

$$e^{\phi_1}e^{\theta_1 Z} - e^{\theta_1}e^{\phi_1 Z} = \exp(\frac{-(1+Z)}{2K})\left(\exp(\frac{\sqrt{1-4KR}}{2K}(Z-1)) - \exp(\frac{-\sqrt{1-4KR}}{2K}(Z-1))\right)$$

$$= 2e^{\frac{(1+Z)}{2K}}\sinh\left(\frac{\sqrt{1-4KR}}{2K}(Z-1)\right) \qquad (4.5.49)$$

$$e^{\phi_1}e^{\theta_1 Z} + e^{\theta_1}e^{\phi_1 Z} = 2e^{\frac{(1+Z)}{2K}}\cosh\left(\frac{\sqrt{1-4KR}}{2K}(Z-1)\right) \qquad (4.5.50)$$

For *1 - 4KR < 0*, we have:

$$e^{\phi_1}e^{\theta_1 Z} - e^{\theta_1}e^{\phi_1 Z} = 2ie^{\frac{(1+Z)}{2K}}\sin\left(\frac{\sqrt{4KR-1}}{2K}(Z-1)\right) \qquad (4.5.51)$$

$$e^{\phi_1}e^{\theta_1 Z} + e^{\theta_1}e^{\phi_1 Z} = 2e^{\frac{(1+Z)}{2K}}\cos\left(\frac{\sqrt{4KR-1}}{2K}(Z-1)\right) \qquad (4.5.52)$$

Thus, $(1+K\phi_1)e^{\phi_1}e^{\theta_1 Z} - (1+K\theta_1)e^{\theta_1}e^{\phi_1 Z}$ become:

$$= e^{\frac{-(1+Z)}{2K}}\left[\sinh\left(\frac{\sqrt{1-4KR}}{2K}(Z-1)\right) - \sqrt{1-4KR}\cosh\left(\frac{\sqrt{1-4KR}}{2K}(Z-1)\right)\right]$$

when 1 - 4KR > 0 (4.5.53)

$$= ie^{\frac{-(1+Z)}{2K}}\left[\sin\left(\frac{\sqrt{4KR-1}}{2K}(Z-1)\right)-\sqrt{4KR-1}\cos\left(\frac{\sqrt{4KR-1}}{2K}(Z-1)\right)\right]$$

when 1 - 4KR < 0 (4.5.54)

When $q = a_i$, for *i=1, 2, ... n,* the value of

$$\frac{\partial}{\partial q}\left\{e^{-1/2k}(q-R-\frac{1}{4K})(q-\frac{1}{4K})\begin{bmatrix}-2(K(q-R)-1/4)\sinh\sqrt{\frac{q-R}{K}}-B\sinh\sqrt{\frac{q-R}{K}}\\-2BK\sqrt{\frac{q-R}{K}}\cosh\sqrt{\frac{q-R}{K}}\end{bmatrix}\right\}$$

becomes:

$$=\frac{\partial(q-1/4K)(q-R-1/4K)}{\partial q}e^{-1/2K}\begin{bmatrix}-2(K(q-R)-1/4)\sinh\sqrt{\frac{q-R}{K}}\\-B\sinh\sqrt{\frac{q-R}{K}}\\-2BK\sqrt{\frac{q-R}{K}}\cosh\sqrt{\frac{q-R}{K}}\end{bmatrix}$$

$$+(q-\frac{1}{4K})(q-R-\frac{1}{4K})e^{-1/2K}\frac{\partial}{\partial q}\begin{bmatrix}-2(K(q-R)-1/4)\sinh\sqrt{\frac{q-R}{K}}-B\sinh\sqrt{\frac{q-R}{K}}\\-2BK\sqrt{\frac{q-R}{K}}\cosh\sqrt{\frac{q-R}{K}}\end{bmatrix}$$

(4.5.55)

Note that at poles

$$-2(K(q-R)-\frac{1}{4})\sinh\sqrt{\frac{q-R}{K}}-B\sinh\sqrt{\frac{q-R}{K}}-2Bk\sqrt{\frac{q-R}{K}}\cosh\sqrt{\frac{q-R}{K}}=0,$$

and thus:

$$=(q-\frac{1}{4K})(q-R-\frac{1}{4K})e^{-1/2K}\frac{\partial}{\partial q}\begin{bmatrix}-2(K(q-R)-1/4)\sinh\sqrt{\frac{q-R}{K}}-B\sinh\sqrt{\frac{q-R}{K}}\\-2BK\sqrt{\frac{q-R}{K}}\cosh\sqrt{\frac{q-R}{K}}\end{bmatrix}$$

(4.5.56)

$$= (q - \frac{1}{4K})(q - R - \frac{1}{4K}) e^{-\frac{1}{2K}} \begin{bmatrix} -2(K(q-R) - \frac{1}{4})(\frac{1}{2\sqrt{K(q-R)}})\cosh\sqrt{\frac{q-R}{K}} \\ -2K\sinh\sqrt{\frac{q-R}{K}} - B(\frac{1}{2\sqrt{K(q-R)}})\cosh\sqrt{\frac{q-R}{K}} \\ -2BK(\frac{1}{2\sqrt{K(q-R)}})\cosh\sqrt{\frac{q-R}{K}} \\ -2BK(\frac{1}{2\sqrt{K(q-R)}})\sqrt{\frac{q-R}{K}}\sinh\sqrt{\frac{q-R}{K}} \end{bmatrix}$$

$$= (q - \frac{1}{4K})(q - R - \frac{1}{4K}) e^{-\frac{1}{2K}} \begin{bmatrix} (\frac{1}{2\sqrt{K(q-R)}})\begin{Bmatrix} -2(K(q-R) - \frac{1}{4}) \\ -B - 2Bk \end{Bmatrix}\cosh\sqrt{\frac{q-R}{K}} \\ -(2K+B)\sinh\sqrt{\frac{q-R}{K}} \end{bmatrix}$$

for q - R is positive (4.5.57)

Based on the properties of *sinh* and *cosh* described in Section (2.5.3.3), then:

$$= i(q - \frac{1}{4K})(q - R - \frac{1}{4K}) e^{-\frac{1}{2k}} \begin{bmatrix} \frac{2(K(q-R) - \frac{1}{4}) + B + 2Bk}{2\sqrt{K(R-q)}}\cos\sqrt{\frac{R-q}{K}} \\ -(2K+B)\sin\sqrt{\frac{R-q}{K}} \end{bmatrix}$$

for q - R is negative (4.5.58)

Consider $L\phi e^{\theta Z} + M\theta e^{\phi Z}$:

$$\begin{aligned} &= B(q - \frac{1}{4K})(e^{\theta Z} - e^{\phi Z}) - (q - \frac{1}{4K})\left[(1+K\phi)e^{\theta Z} - (1+K\theta)e^{\phi Z}\right] \\ &-\left[(q - \frac{1}{4K})(B - BC_* - 1) + BC_*R\right]\left[(1+K\phi)e^{\phi}e^{\theta Z} - (1+K\theta)e^{\theta}e^{\phi Z}\right] \end{aligned} \quad (4.5.59)$$

$$e^{\theta Z} - e^{\phi Z} = e^{-Z/2K}(e^{\sqrt{\frac{q-R}{K}}Z} - e^{-\sqrt{\frac{q-R}{K}}Z}) = 2e^{\frac{-Z}{2K}}\sinh\sqrt{\frac{q-R}{K}}Z \quad (4.5.60)$$

$$(1+K\phi)e^{\theta Z} - (1+K\theta)e^{\phi Z} = \frac{1}{2}(e^{\theta Z} - e^{\phi Z}) - \sqrt{K(q-R)}(e^{\theta Z} + e^{\phi Z})$$

$$= 2e^{\frac{-Z}{2K}}\left[\frac{1}{2}\sinh\sqrt{\frac{q-R}{K}}Z - \sqrt{K(q-R)}\cosh\sqrt{\frac{q-R}{K}}Z\right] \qquad (4.5.61)$$

$$(1+K\phi)e^{\phi}e^{\theta Z} - (1+K\theta)e^{\theta}e^{\phi Z}$$
$$= -2e^{\frac{-(1+Z)}{2K}}\left[\frac{1}{2}\sinh(\sqrt{\frac{q-R}{K}}(1-Z)) + \sqrt{K(q-R)}\cosh(\sqrt{\frac{q-R}{K}}(1-Z))\right] \qquad (4.5.62)$$

$L\phi e^{\theta Z} + M\theta e^{\phi Z}$ now becomes:

$$= 2e^{\frac{-Z}{2K}}\left\{\begin{array}{l}(q-\frac{1}{4K})\left[(B-\frac{1}{2})\sinh\sqrt{\frac{q-R}{K}}Z + \sqrt{K(q-R)}\cosh\sqrt{\frac{q-R}{K}}Z\right] \\ +e^{\frac{-1}{2K}}\left[(q-\frac{1}{4K})(B-BC_{\bullet}-1)+BC_{\bullet}R\right]\left[\begin{array}{l}\frac{1}{2}\sinh(\sqrt{\frac{q-R}{K}}(1-Z)) \\ +\sqrt{K(q-R)}\cosh(\sqrt{\frac{q-R}{K}}(1-Z))\end{array}\right]\end{array}\right\}$$
$$\text{for } q-R>0 \qquad (4.5.63)$$

Based on the properties that *sinh(ix) = isin(x)* and *cosh(ix) = cos(x)* as described in Section (2.5.3.3), $L\phi e^{\theta Z} + M\theta e^{\phi Z}$ for $q - R < 0$ becomes:

$$= e^{\frac{-Z}{2K}}\left\{\begin{array}{l}(q-\frac{1}{4K})\left[i\sqrt{K(R-q)}\cos(\sqrt{\frac{R-q}{K}}Z) + (B-\frac{1}{2})i\sin(\sqrt{\frac{R-q}{K}}Z)\right] \\ +e^{\frac{-1}{2K}}\left\{\begin{array}{l}\left[\begin{array}{l}(q-\frac{1}{4K})i\sqrt{K(R-q)}(B-BC_{\bullet}-1) \\ +i\sqrt{K(R-q)}BC_{\bullet}R\end{array}\right]\cos(\sqrt{\frac{R-q}{K}}(1-Z)) \\ +\left[\frac{1}{2}(q-\frac{1}{4K})(B-BC_{\bullet}-1)+\frac{BC_{\bullet}R}{2}\right]i\sin(\sqrt{\frac{R-q}{K}}(1-Z))\end{array}\right\}\end{array}\right\}$$

$$= ie^{\frac{-Z}{2K}}\left\{\begin{array}{l}(q-\frac{1}{4K})\left[\sqrt{K(R-q)}\cos(\sqrt{\frac{R-q}{K}}Z) + (B-\frac{1}{2})\sin(\sqrt{\frac{R-q}{K}}Z)\right] \\ +e^{\frac{-1}{2K}}\left[(q-\frac{1}{4K})(B-BC_{\bullet}-1)+BC_{\bullet}R\right]\left[\begin{array}{l}\sqrt{K(R-q)}\cos(\sqrt{\frac{R-q}{K}}(1-Z)) \\ +\frac{1}{2}\sin(\sqrt{\frac{R-q}{K}}(1-Z))\end{array}\right]\end{array}\right\}$$

for $q - R < 0$ (4.5.64)

Note: as q = R, since $\sqrt{K(R-q)}$, $sin(\sqrt{\frac{R-q}{K}}Z)$, and $sin(\sqrt{\frac{R-q}{K}}(1-Z))$ are all equal to zero. Thus Im[$L\phi e^{\theta Z}$] = 0 at q = R.

Finally, the solution of $M(Z,T)$ (Solution 3) is:

$$M(Z,T) = G(K,B,M_a,R,Z) + \sum_{q=a_i}^{a_n} \frac{2e^{\left[(q-\frac{1}{4K})T+\frac{1-Z}{2K}\right]} f(K,B,M_a,R,Z,q)}{(q-\frac{1}{4K})(q-R-\frac{1}{4K})h(K,B,R,Z,q)} \tag{4.5.65}$$

in which, a_i are the roots of $tanh\sqrt{\frac{q-R}{K}} = \frac{2BK\sqrt{(q-R)/K}}{0.5-2K(q-R)-B}$ for q larger than R, and

$$tan\sqrt{\frac{-(q-R)}{K}} = \frac{2BK\sqrt{-(q-R)/K}}{0.5-2K(q-R)-B} \text{ for } q \text{ less than } R, \tag{4.5.66}$$

where:

$$G(K,B,M_a,R,Z) = BM_a \frac{e^{\frac{-Z}{2K}}\left[sinh\left(\frac{\sqrt{1-4KR}}{2K}(Z-1)\right) - \sqrt{1-4KR}\,cosh\left(\frac{\sqrt{1-4KR}}{2K}(Z-1)\right)\right]}{\left[(2KR-B)sinh\frac{\sqrt{1-4KR}}{2K} - B\sqrt{1-4KR}\,cosh\frac{\sqrt{1-4KR}}{2K}\right]}$$

when 1 - 4KR > 0 (4.5.67)

$$G(K,B,M_a,R,Z) = BM_a \frac{e^{\frac{-Z}{2K}}\left[\begin{array}{l} \sin\left(\frac{\sqrt{4KR-1}}{2K}(Z-1)\right) \\ -\sqrt{4KR-1}\cos\left(\frac{\sqrt{4KR-1}}{2K}(Z-1)\right)\end{array}\right]}{\left[(2KR-B)\sin\frac{\sqrt{4KR-1}}{2K} - B\sqrt{4KR-1}\cos\frac{\sqrt{4KR-1}}{2K}\right]}$$

when $1 - 4KR < 0$ (4.5.68)

When q is larger than R:

$$h(K,B,R,q) = \frac{-2(K(q-R)-\frac{1}{4})-B-2BK}{2\sqrt{K(q-R)}}\cosh\sqrt{\frac{q-R}{K}} - (2K+B)\sinh\sqrt{\frac{q-R}{K}}$$

(4.5.69)

$$f(K,B,M_a,Z,R,q) = (q-\frac{1}{4K})\left[\sqrt{K(q-R)}\cosh(\sqrt{\frac{q-R}{K}}Z) + (B-\frac{1}{2})\sinh(\sqrt{\frac{q-R}{K}}Z)\right]$$

$$+ e^{\frac{-1}{2K}}\left[(q-\frac{1}{4K})(B-BM_a-1) + BM_aR\right]\left[\begin{array}{l}\sqrt{K(q-R)}\cosh(\sqrt{\frac{q-R}{K}}(1-Z)) \\ +\frac{1}{2}\sinh(\sqrt{\frac{q-R}{K}}(1-Z))\end{array}\right]$$

(4.5.70)

When q is less than R:

$$h(K,B,R,q) = \frac{2(K(q-R)-\frac{1}{4})+B+2BK}{2\sqrt{K(R-q)}}\cos\sqrt{\frac{R-q}{K}} - (2K+B)\sin\sqrt{\frac{R-q}{K}}$$

(4.5.71)

$$f(K,B,M_a,Z,R,q)=(q-\frac{1}{4K})\left[\sqrt{K(R-q)}cos(\sqrt{\frac{R-q}{K}}Z)+(B-\frac{1}{2})sin(\sqrt{\frac{R-q}{K}}Z)\right]$$

$$+e^{\frac{-1}{2K}}\left[(q-\frac{1}{4K})(B-BM_a-1)+BM_aR\right]\left[\begin{array}{l}\sqrt{K(R-q)}cos(\sqrt{\frac{R-q}{K}}(1-Z))\\+\frac{1}{2}sin(\sqrt{\frac{R-q}{K}}(1-Z))\end{array}\right]$$

(4.5.72)

The above model has a limitation of application in that the initial concentration m_{l0} cannot be set to zero. The model thus cannot simulate cases that start with initial contaminant free condition. However, a modified model allows for zero initial concentration. The initial and boundary conditions are changed as follows:

Boundary condition at bed layer level:

$$\left[K\frac{\partial M}{\partial Z}+M\right]_{Z=0}=B_1M-B_2\big|_{Z=0} \qquad (4.5.73)$$

Initial condition:

$$M(Z,0)=M_{l0} \qquad (4.5.74)$$

in which $M=\frac{m}{m_a}$ $M_{l0}=\frac{m_{l0}}{m_a}$ $B_1=\frac{\phi_m}{\omega}$ $B_2=\frac{\gamma_m}{\omega}$, ϕ_m and γ_m are the settling and resuspension velocity of the contaminant at the water-sediment interface, respectively.

The system is solved analytically with similar techniques and procedures as Model 2. The detailed solution is shown in Appendix 1 while the solution of $M(Z,T)$ (Solution 4) is as follows:

$$M(Z,T) = G(K,B_1,B_2,R,Z) + \sum_{q=a_1}^{a_n} \frac{2e^{\left[(q-\frac{1}{4K})T+\frac{1-Z}{2K}\right]} f(K,B_1,B_2,M_{I0},R,Z,q)}{(q-\frac{1}{4K})(q-R-\frac{1}{4K})h(K,B_1,R,Z,q)}$$

(4.5.75)

in which a_i are the roots of $\tanh\sqrt{\frac{q-R}{K}} = \frac{2B_1K\sqrt{(q-R)/K}}{0.5-2K(q-R)-B_1}$ for q larger than R, and

$$\tan\sqrt{\frac{-(q-R)}{K}} = \frac{2B_1K\sqrt{-(q-R)/K}}{0.5-2K(q-R)-B_1} \text{ for } q \text{ less than } R, \qquad (4.5.76)$$

where:

$$G(K,B_1,B_2,R,Z) = \frac{B_2\left[\sinh\left(\frac{(Z-1)\sqrt{1-4KR}}{2K}\right) - \sqrt{1-4KR}\cosh\left(\frac{(Z-1)\sqrt{1-4KR}}{2K}\right)\right]}{e^{\frac{Z}{2K}}\left[(2KR-B_1)\sinh\frac{\sqrt{1-4KR}}{2K} - B_1\sqrt{1-4KR}\cosh\frac{\sqrt{1-4KR}}{2K}\right]}$$

when $1 - 4KR > 0$ (4.5.77)

$$G(K,B_1,B_{2*},R,Z) = \frac{B_2\left[\sin\left(\frac{(Z-1)\sqrt{4KR-1}}{2K}\right) - \sqrt{4KR-1}\cos\left(\frac{(Z-1)\sqrt{4KR-1}}{2K}\right)\right]}{e^{\frac{Z}{2K}}\left[(2KR-B_1)\sin\frac{\sqrt{4KR-1}}{2K} - B_1\sqrt{4KR-1}\cos\frac{\sqrt{4KR-1}}{2K}\right]}$$

when $1 - 4KR < 0$ (4.5.78)

When q is larger than R:

$$h(K,B_1,R,q) = \frac{-2(K(q-R)-\frac{1}{4})-B_1-2B_1K}{2\sqrt{K(q-R)}}\cosh\sqrt{\frac{q-R}{K}} - (2K+B_1)\sinh\sqrt{\frac{q-R}{K}}$$

(4.5.79)

$$f(K,B_1,B_2,M_{I0},Z,R,q)$$
$$=(q-\frac{1}{4K})M_{I0}\left[(B_1-\frac{1}{2})sinh\sqrt{\frac{q-R}{K}}Z+\sqrt{K(q-R)}\,cosh\sqrt{\frac{q-R}{K}}Z\right]$$
$$+e^{\frac{-1}{2K}}\left[(q-\frac{1}{4K})(M_{I0}B_1-B_2-M_{I0})+B_2R\right]\left[\begin{array}{l}\frac{1}{2}sinh(\sqrt{\frac{q-R}{K}}(1-Z))\\+\sqrt{K(q-R)}\,cosh(\sqrt{\frac{q-R}{K}}(1-Z))\end{array}\right]$$

(4.5.80)

When q is less than R:

$$h(K,B_1,R,q)=\frac{2(K(q-R)-\frac{1}{4})+B_1+2B_1K}{2\sqrt{K(R-q)}}\cos\sqrt{\frac{R-q}{K}}-(2K+B_1)\sin\sqrt{\frac{R-q}{K}}$$

(4.5.81)

$$f(K,B_1,B_2,M_{I0},Z,R,q)$$
$$=M_{I0}(q-\frac{1}{4K})\left[\sqrt{K(R-q)}\cos(\sqrt{\frac{R-q}{K}}Z)+(B_1-\frac{1}{2})\sin(\sqrt{\frac{R-q}{K}}Z)\right]$$
$$+e^{\frac{-1}{2K}}\left[(q-\frac{1}{4K})(M_{I0}B_1-B_2-M_{I0})+B_2R\right]\left[\begin{array}{l}\sqrt{K(R-q)}\cos(\sqrt{\frac{R-q}{K}}(1-Z))\\+\frac{1}{2}\sin(\sqrt{\frac{R-q}{K}}(1-Z))\end{array}\right]$$

(4.5.82)

4.6 General Analysis for Model 2

Two forms solution, Solution 3 and Solution 4, have been developed for Model 2. MATLAB program codes have been developed for the solutions to generate computational results of the model. For Solution 4 of Model 2, the main input parameters are K, M_{I0}, R, B_1 and B_2. The contributions to fate of

the contaminant by changing above parameters are described in the following paragraphs.

4.6.1 Effect of *R*

In Model 2, the dimensionless term, *R*, is defined as follows:

$$R = Hr_m / \omega$$

and is a function of the water depth *(H)*, first order growth/decay term(r_m) and settling velocity(ω). The following analysis concerns the contribution by r_m to contaminant transport. The relationship between *R* and r_m is direct proportion with reference to the above expression of *R*. In general, r_m has been used to represent the growth or decay property of contaminants and a negative value of r_m represents a decay of the contaminant. In this model, since there is a continuous unlimited exchange of contaminants with the bottom boundary, a final steady concentration profile exists in most cases except when the contaminant has a sufficiently large growth rate. The condition of the existence of the steady state concentration profile is described in the following paragraphs.

4.6.2 Existence of steady state condition

Observing the Solution 4 of Model 2, the first term of the solution, $G(K,B_1,B_2,R,Z)$, in the model is independent of time and all other terms (the summation sequence) in the solution are time - dependent. In most cases, the magnitude of the summation sequence in the solution tends to become zero as time is large and the concentration profile approaches to equilibrium condition. Therefore, the first term represents the steady state concentration

distribution as time goes to infinity. Observing the solutions of Model 2, the term, $exp((q-1/4K)T)$, is the only part of the solution that depends on time (T) and it will tend to zero as $(q-1/4K)$ is negative. Thus, the existence of the steady state condition should satisfy the following condition:

$$R < 1/4K - q'_{max} \qquad (4.6.2.1)$$

and q'_{max} is the maximum value of q' found from the following equations

$$tanh\sqrt{\frac{q'}{K}} = \frac{2B_1K\sqrt{q'/K}}{0.5-2Kq'-B_1} \qquad \text{for q'>0} \qquad (4.6.2.2)$$

$$tan\sqrt{\frac{-q'}{K}} = \frac{2B_1K\sqrt{-q'/K}}{0.5-2Kq'-B_1} \qquad \text{for q'<0} \qquad (4.6.2.3)$$

Therefore, the existence of the steady state condition depends on B_1, K, and R, or depends on ω, ϕ_m, k_{mz} and H. Table 1 shows values of q'_{max} and $1/(4K)-q'_{max}$ with different inputs of K and B_1. Generally, q'_{max} decreases as K or B_1 increases but $1/(4K)$ decreases as K increases. In conclusion, the condition for the existence of the steady state condition is that $1/(4K)-q'_{max}$ decreases as K increases and increases as B_1 increases. A larger value of $1/(4K)-q'_{max}$ means that a larger value of R can be inputted to the system, which still maintains the existence of the steady state .

Two sets of figures have been generated using Solution 3 of Model 2. Figure 7 shows the concentration profiles for different R with $K=0.35$, $B=1$ and $M_a = 2$. All cases show the steady state condition. $G(K,B,M_a,R,Z)$, indicated by dotted lines, are the steady state profiles. Figure 7 shows that the overall magnitude of the steady state profile, $G(K,B,M_a,R,Z)$, increases as R increases. Figure 8 shows the concentration profiles of some cases

without a steady state for $K=0.35$ and $B=1$. Sufficient large values of R have been chosen in each of the cases shown in Figure 8. The large values of R mean the growth of the contaminant concentration in the water column (entrainment flux from the bottom boundary) cannot be balanced by the deposition flux to the same boundary. Thus the overall magnitudes of the concentration profiles in Figure 8 continuously grow as time increases. These figures reveal that the effect on the concentration profile caused by changing the value of R is more significant than it would be by changing the value of M_a.

4.6.3 Effect of M_{I0}

In Solution 4 of Model 2, the dimensionless term, M_{I0}, is defined as follows:

$$M_{I0} = m_{I0} / m_a$$

Thus, M_{I0} is a ratio between the initial concentration and the reference level concentration of the contaminant. Some cases have been generated using Solution 4 of Model 2. In Figure 9, curves of constant concentration are shown for K = 0.35 or 1 and M_{I0} = 0 or 1. The first term of the solution, $G(K,B_1,B_2,R,Z)$, is not a function of the initial concentration and hence the magnitude of the initial concentration does not affect the final solution. Thus, comparing the results in Figures 9(a) and 9(b), a significant difference only occurs at the beginning. The difference decreases as time increases and finally both cases approach the same steady state concentration profile. The same phenomenon also occurs in Figures 9(c) and 9(d). The magnitude of

the initial concentrations only affects the required time to reach the steady state.

4.6.4 Effect of *K*

In Model 2, the dimensionless term, *K*, is defined as follows:

$$K = k_{mz} / \omega H$$

Thus, K is directly proportional to k_{mz} and is inversely proportional to ω. The general physical meaning of *K* can be described as the ratio between the turbulent mixing coefficient, k_{mz}, and the settling velocity, ω, of the contaminant.

The definition of the settling velocity is that matter travels downward to the bottom layer because of gravity. The definition of turbulent mixing is that matter is mixed by large scale eddies or whirls in natural waters. In the model, the turbulent mixing coefficient controls the magnitude of upward motion of contaminants from the bottom layer to the water column and thus *K* represents the ratio between upward and downward motion of the contaminant in the water column. Comparing between Figures 9(a) and 9(c), the figure with the greater value of *K* shows a higher concentration in both the initial and final distribution and the same are observed between 9(b) and 9(d).

4.6.5 Effect of B_1 and B_2

In Solution 4 of Model 2, the dimensionless term, B_1, is the ratio between the settling velocity of the contaminant at the water-sediment interface to the settling velocity of the contaminant in the water column. The

simplest assumption for the value of B_1 is 1. However, based on former works such as that by Richardson and Zaki (1954) and Oliver (1961), the magnitude of the settling velocity is affected by the sediment concentration in the water column. The value is smaller than the one calculated by some basic laws such as Strokes' Law, when the sediment concentration is large which often occurs near the bottom water-sediment interface. This is better to set B_1 at a value less than 1 in such cases whereas the value of B_2 can be set to 1 in all cases. In the model, even the resuspension rate of the contaminant at the bottom boundary is different from the settling velocity in the water column. The effect can be taken into account by the value of m_a, reference level concentration in the bottom sediment layer. In Figure 10, curves of constant concentration are shown with different values of B_1. Figure 10(a) and 10(b) show cases with B_1 equal to 0.7 and 0.5 respectively. The figures show that the dimensionless concentration, M, near the bottom boundary, is greater than 1 when time is sufficiently large. The phenomenon is more obvious when a smaller value of B_1 is applied. Figure 10(c) shows a case with B_1 equal to 1.2 and in this case, values of M are always less than 1 over the water column. This is different from the cases shown in Figure 10(a) and 10(b).

As discussed in Section (4.6.2), the allowed value of R inputs into the system, without removing the steady state condition, increases as B_1 increases. Figure 10(d) shows a case for $R=2$, $K=0.35$, which does not have a steady state condition for $B=1$ (shown in Figure 8(a)). It has a steady state condition for $B_1=5$ instead. However, the time required to reach the steady

state condition is greater than that for the cases shown in Figure 10(a) to 10(c).

Table 1: Value of q'_{max} and $(1/4K-q'_{max})$ with different values of K and B_1

B_1 \ K	0.35	0.5	1	2	4
0.5	-0.33129	-0.37009	-0.42676	-0.46098	-0.47984
	(1.04558)	(0.87009)	(0.67676)	(0.58598)	(0.54234)
0.7	-0.56288	-0.59659	-0.64309	-0.67003	-0.68460
	(1.27717)	(1.09659)	(0.89309)	(0.79503)	(0.74710)
1	-0.80147	-0.85353	-0.92196	-0.95969	-0.97951
	(1.51576)	(1.35353)	(1.17196)	(1.08469)	(1.04201)
1.2	-0.91338	-0.98467	-1.08225	-1.13822	-1.16833
	(1.62767)	(1.48467)	(1.33225)	(1.26322)	(1.23083)
2	-1.17216	-1.32140	-1.57235	-1.75329	-1.86632
	(1.88644)	(1.82140)	(1.82235)	(1.87829)	(1.92882)

Figure 7: Concentration profiles for different *R* with *K=0.35, B=1* and M_a=2

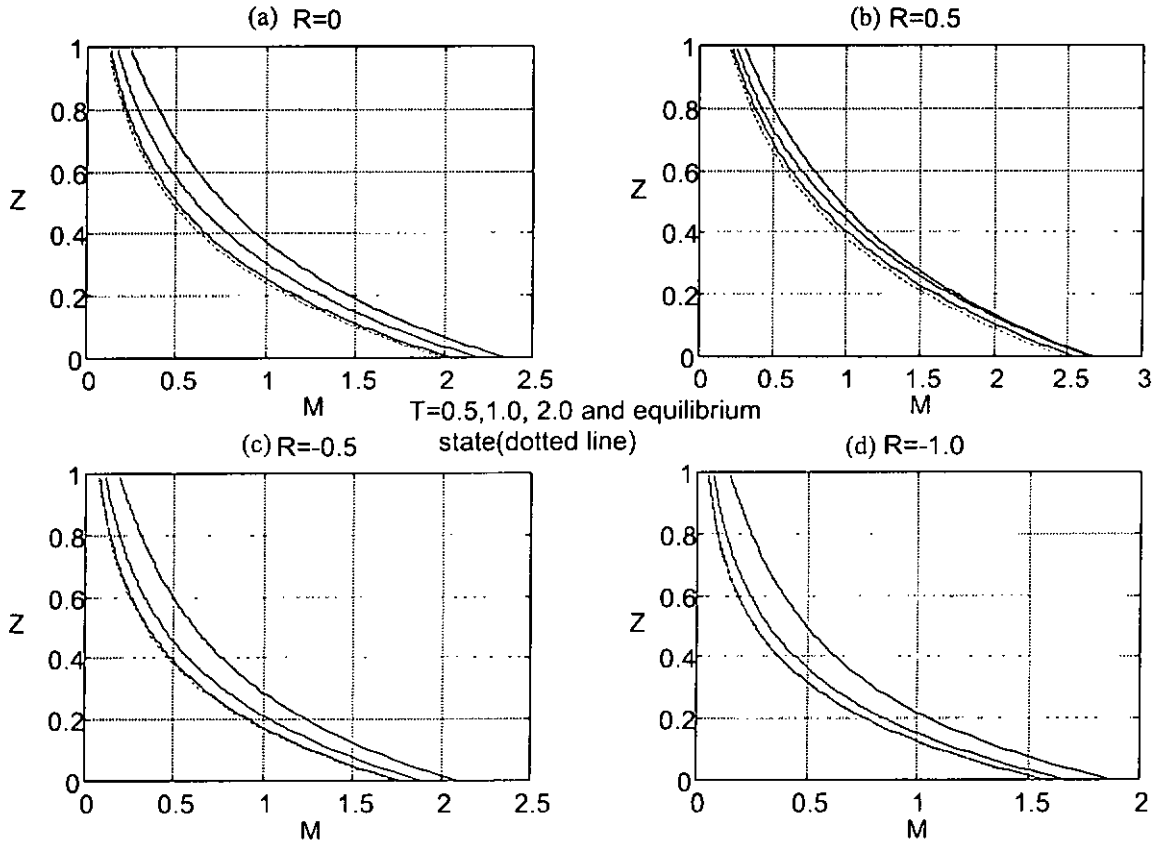

Figure 8: Concentration profiles for cases without steady state condition for different R with K=0.35, B=1

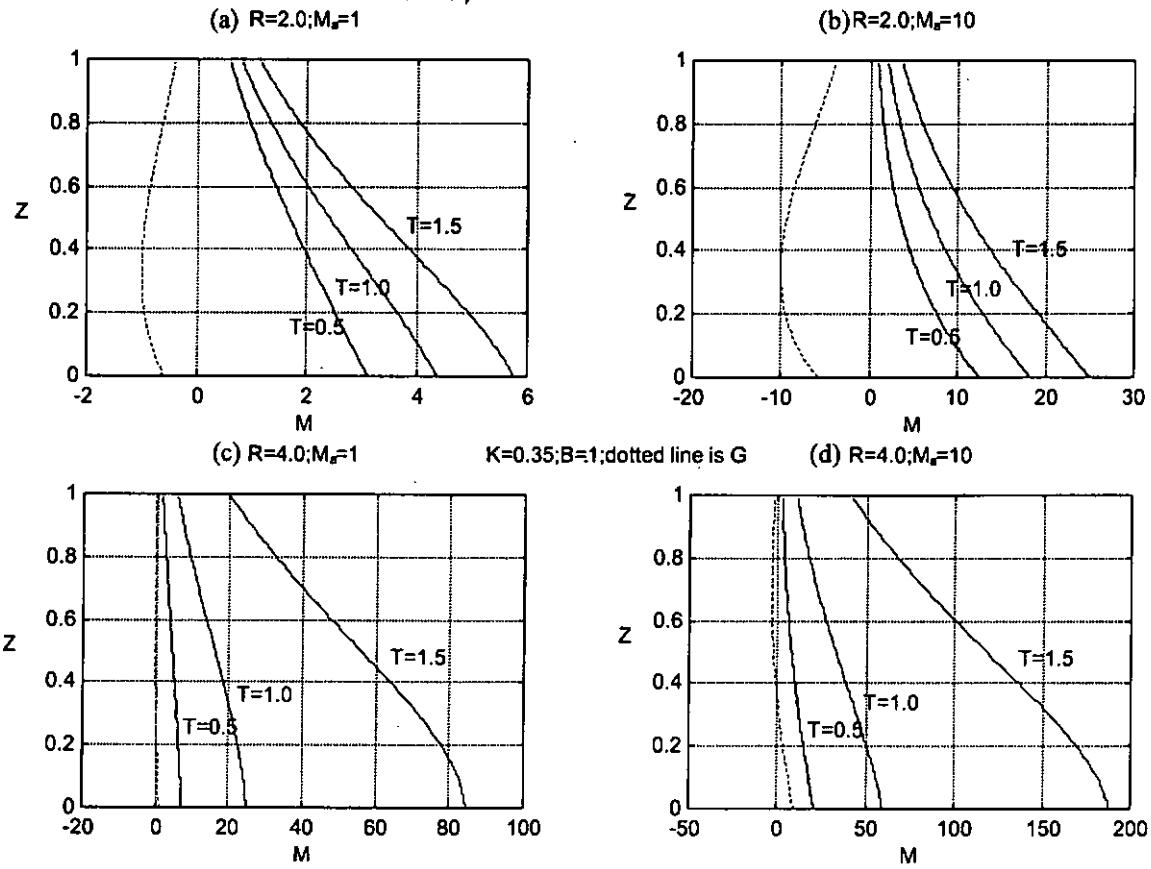

Figure 9: Concentration distributions with different values of input parameters

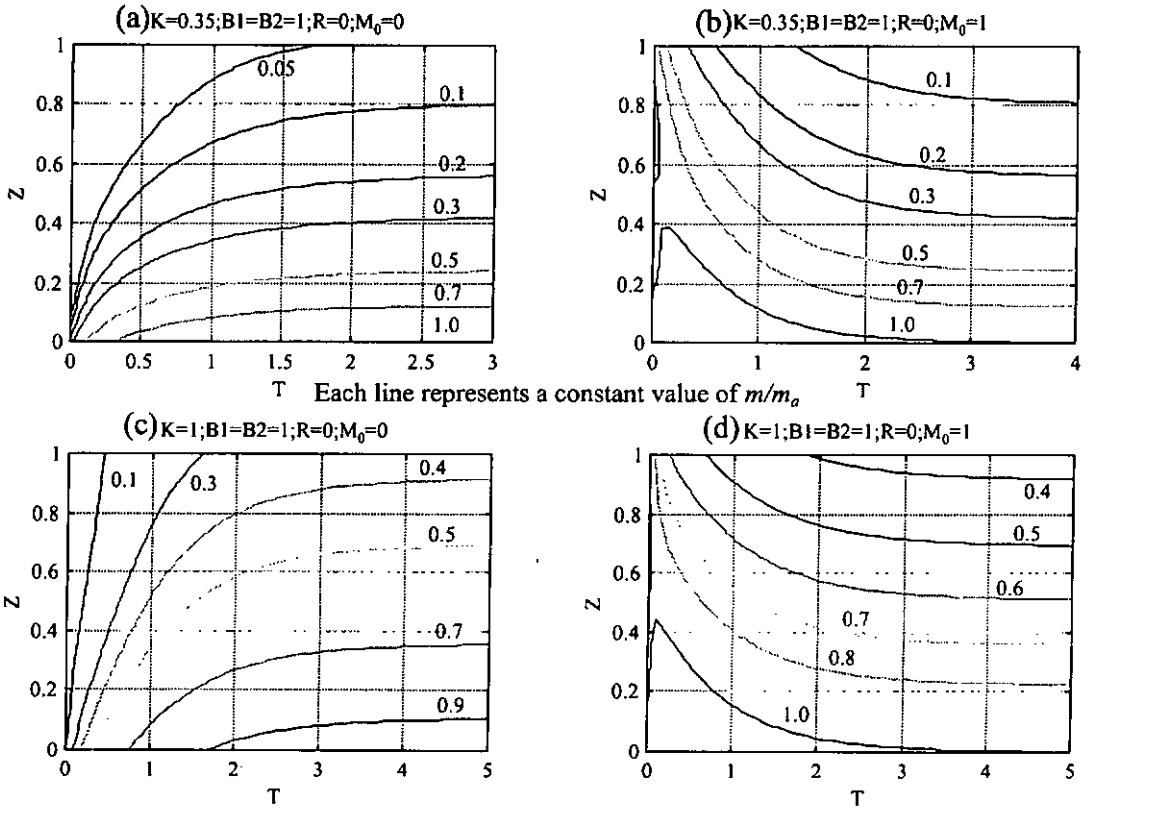

Figure 10: Concentration distribution with different values of B_1

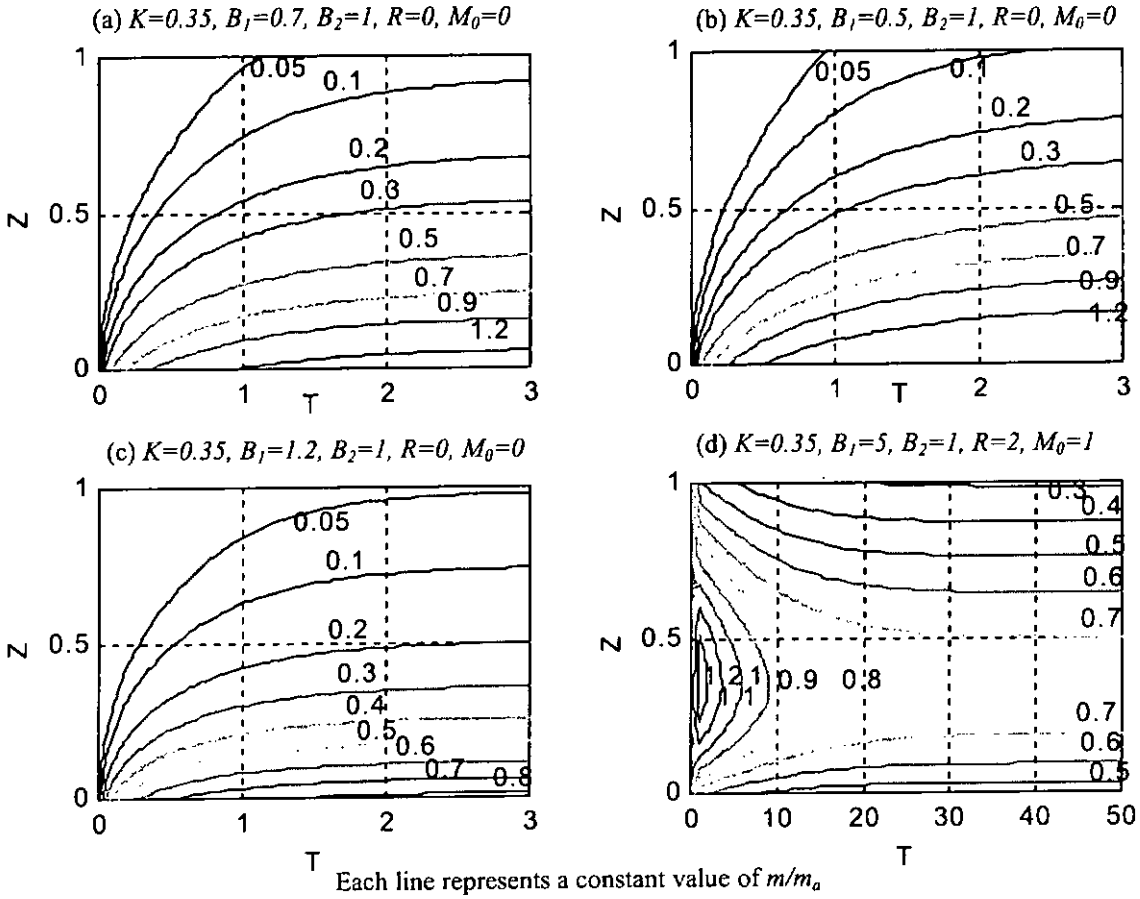

Each line represents a constant value of m/m_a

4.7 Governing system of Model 3

The third model, Model 3, is developed with reference to the analytical model given in Prakash (2000). It is also an upgraded Model 2. Model 3 considers diffusive exchanges of contaminants from both boundaries and allows input sources at the boundaries which grow/decay exponentially. Figure 11 shows the modeling environment of Model 3.

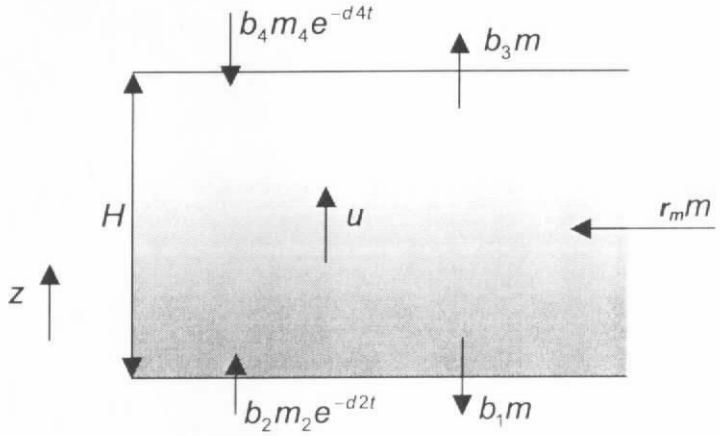

Figure 11: Problem Definition of Model 3

The governing equation and boundary conditions are as follows:

Governing equation:

$$\frac{\partial m}{\partial t} = -u\frac{\partial m}{\partial z} + k_{mz}\frac{\partial^2 m}{\partial z^2} + r_m m \tag{4.7.1}$$

Boundary condition:

$$\left[k_{mz}\frac{\partial m}{\partial z} - um\right]_{z=H} = b_4 m_4 \exp(-d_4 t) - b_3 m \tag{4.7.2}$$

$$\left[k_{mz}\frac{\partial m}{\partial z} - um\right]_{z=0} = b_1 m - b_2 m_2 \exp(-d_2 t) \tag{4.7.3}$$

Initial condition:

$$m(z,0) = m_{i0} \tag{4.7.4}$$

in which: m is the contaminant concentration. m_{I0} is the contaminant concentration at $t = 0$. m_2 is the reference contaminant concentration at $z = 0$. m_4 is the reference contaminant concentration at $z = H$. H is the depth of flow. k_{mz} is the turbulent mixing coefficient. u is the vertical contaminant flow velocity. r_m is the coefficient for the source/sink term. The terms b_1, b_2, b_3 *and* b_4 are coefficients for settling or resuspending contaminants at boundaries. The coefficients d_2 and d_4 are contaminant growth/decay rate input to the system from the boundaries.

Model 3 has the same governing equation of Model 2. This means constant settling velocity, a constant turbulent coefficient and first order source/sink term are considered in the model. Model 3 also assumes constant value of initial concentration along the water column. The main difference between Model 3 and Model 2 is the setting of boundary conditions. At the boundaries, the net contaminant flux is the difference between the incoming and outgoing contaminant fluxes. The model allows for an exponential growth/decay of input flux at the boundaries.

4.8 Summary of solution steps of Model 3

The major mathematical techniques involved to solve the govering system of Model 3 are Laplace transform and its inverse transform. A summary of the steps are shown as follows:

First, the governing equation is transformed into a second order ordinary differential equation with respect to z by applying Laplace Transform:

$$k_{mz}\frac{\partial^2\tilde{m}}{\partial z^2}-u\frac{\partial\tilde{m}}{\partial z}-(q-r_m)\tilde{m}=-m_{l0} \tag{4.8.1}$$

in which $\tilde{m}(z,q)$ is the Laplace Transform of $m(z,t)$.

The solution of $\tilde{m}$ is:

$$\tilde{m}=c_1e^{\theta z}+c_2e^{\phi z}+m_{l0}/(q-r_m) \tag{4.8.2}$$

in which $\theta;\phi=\frac{u}{2k_{mz}}\pm\frac{\sqrt{u^2+4k_{mz}(q-r_m)}}{2k_{mz}}$, c_1 ; c_2 are arbitrary constants.

Applying Laplace Transform to the boundary conditions, they becomes:

$$\left[k_{mz}\frac{\partial\tilde{m}}{\partial z}-u\tilde{m}\right]_{z=h}=\frac{b_4c_4}{q+d_4}-b_3\tilde{m} \tag{4.8.3}$$

$$\left[k_{mz}\frac{\partial\tilde{m}}{\partial z}-u\tilde{m}\right]_{z=0}=b_1\tilde{m}-\frac{b_2c_2}{q+d_2} \tag{4.8.4}$$

Solutions of c_1 and c_2 are found by substituting the solution of $\tilde{m}(z,q)$ to the transformed boundary conditions. The solutions are as follows:

$$c_1=\frac{\begin{Bmatrix}e^{\phi H}(k_{mz}\phi-u+b_3)(q+d_4)\left[(q+d_2)(u+b_1)m_{l0}-b_2m_2(q-r_m)\right]\\-(k_{mz}\phi-u-b_1)(q+d_2)\left[(q+d_4)(u-b_3)m_{l0}+b_4m_4(q-r_m)\right]\end{Bmatrix}}{(q-r_m)(q+d_2)(q+d_4)\begin{bmatrix}(k_{mz}\theta-u-b_1)(k_{mz}\phi-u+b_3)e^{\phi H}\\-(k_{mz}\phi-u-b_1)(k_{mz}\theta-u+b_3)e^{\theta H}\end{bmatrix}} \tag{4.8.5}$$

$$c_2=\frac{-\begin{Bmatrix}e^{\theta H}(k_{mz}\theta-u+b_3)(q+d_4)\left[(q+d_2)(u+b_1)m_{l0}-b_2m_2(q-r_m)\right]\\-(k_{mz}\theta-u-b_1)(q+d_2)\left[(q+d_4)(u-b_3)m_{l0}+b_4m_4(q-r_m)\right]\end{Bmatrix}}{(q-r_m)(q+d_2)(q+d_4)\begin{bmatrix}(k_{mz}\theta-u-b_1)(k_{mz}\phi-u+b_3)e^{\phi H}\\-(k_{mz}\phi-u-b_1)(k_{mz}\theta-u+b_3)e^{\theta H}\end{bmatrix}} \tag{4.8.6}$$

The solution of $\tilde{m}$ now becomes:

$$\tilde{m}=\frac{m_{l0}}{(q-r_m)}+\frac{L\phi e^{\theta z}+M\theta e^{\phi z}}{(q-r_m)(q+d_2)(q+d_4)Q(q)} \tag{4.8.7}$$

where:

$$L\phi = e^{\phi H}(k_{mz}\phi - u + b_3)(q + d_4)\left[(q + d_2)(u + b_1)m_{I0} - b_2 m_2(q - r_m)\right] - (k_{mz}\phi - u - b_1)(q + d_2)\left[(q + d_4)(u - b_3)m_{I0} + b_4 m_4(q - r_m)\right] \quad (4.8.8)$$

$$M\theta = -e^{\theta H}(k_{mz}\theta - u + b_3)(q + d_4)\left[(q + d_2)(u + b_1)m_{I0} - b_2 m_2(q - r_m)\right] + (k_{mz}\theta - u - b_1)(q + d_2)\left[(q + d_4)(u - b_3)m_{I0} + b_4 m_4(q - r)\right] \quad (4.8.9)$$

$$Q(q) = (k_{mz}\theta - u - b_1)(k_{mz}\phi - u + b_3)e^{\phi H} - (k_{mz}\phi - u - b_1)(k_{mz}\theta - u + b_3)e^{\theta H} \quad (4.8.10)$$

The term $Q(q)$ can be rearranged to as follows:

$$\begin{aligned} &= \left(\frac{u + \sqrt{u^2 + 4k_{mz}(q - r_m)}}{2} - u - b_1\right) \times \\ &\left(\frac{u - \sqrt{u^2 + 4k_{mz}(q - r_m)}}{2} - u + b_3\right) e^{\frac{uH}{2k_{mz}}} e^{\frac{-H\sqrt{u^2 + 4k_{mz}(q - r_m)}}{2k_{mz}}} \\ &- \left(\frac{u - \sqrt{u^2 + 4k_{mz}(q - r_m)}}{2} - u - b_1\right) \times \\ &\left(\frac{u + \sqrt{u^2 + 4k_{mz}(q - r_m)}}{2} - u + b_3\right) e^{\frac{uH}{2k_{mz}}} e^{\frac{H\sqrt{u^2 + 4k_{mz}(q - r_m)}}{2k_{mz}}} \end{aligned} \quad (4.8.11)$$

$$= e^{\frac{uH}{2k_{mz}}} \left\{ \begin{aligned} &\left(-k_{mz}(q - r_m) + \frac{u}{2}(b_1 - b_3) - b_1 b_3\right)\left(e^{\frac{-H\sqrt{u^2 + 4k_{mz}(q - r_m)}}{2k_{mz}}} - e^{\frac{H\sqrt{u^2 + 4k_{mz}(q - r_m)}}{2k_{mz}}}\right) \\ &+ \frac{\sqrt{u^2 + 4k_{mz}(q - r_m)}}{2}(b_1 + b_3)\left(e^{\frac{-H\sqrt{u^2 + 4k_{mz}(q - r_m)}}{2k_{mz}}} + e^{\frac{H\sqrt{u^2 + 4k_{mz}(q - r_m)}}{2k_{mz}}}\right) \end{aligned} \right\}$$

$$Q(q) = e^{\frac{uH}{2k_{mz}}} \left\{ \begin{aligned} &\left(2k_{mz}(q - r_m) + 2b_1 b_3 - u(b_1 - b_3)\right)\sinh\left(\frac{H\sqrt{u^2 + 4k_{mz}(q - r_m)}}{2k_{mz}}\right) \\ &+ (b_1 + b_3)\sqrt{u^2 + 4k_{mz}(q - r_m)}\cosh\left(\frac{H\sqrt{u^2 + 4k_{mz}(q - r_m)}}{2k_{mz}}\right) \end{aligned} \right\}$$

for $u^2 + 4k_{mz}(q - r_m) > 0$ (4.8.12)

For $u^2 + 4k_{mz}(q - r_m) < 0$, $Q(q)$ can be expressed by applying *sinh(ix) = isin(x)* and *cosh(ix) = cos(x)* as mentioned in Section (2.5.3.3) and becomes:

$$Q(q) = ie^{\frac{uH}{2k_{mz}}} \left\{ \begin{array}{l} \left(2k_z(q - r_m) + 2b_1b_3 - u(b_1 - b_3)\right)\sin\left(\dfrac{H\sqrt{-u^2 - 4k_{mz}(q - r_m)}}{2k_{mz}}\right) \\ +(b_1 + b_3)\sqrt{-u^2 - 4k_{mz}(q - r_m)}\cos\left(\dfrac{H\sqrt{-u^2 - 4k_{mz}(q - r_m)}}{2k_{mz}}\right) \end{array} \right\}$$

for $u^2 + 4k_{mz}(q - r_m) < 0$ (4.8.13)

Applying the inverse Laplace Transform with the rules described by Equation (2.5.2.1.7) to Equation (2.5.2.1.9) to $\tilde{m}(z,q)$, then it becomes:

$$m(z,t) = m_{10}e^{r_m t} + \sum_{q=\gamma_m}^{a_n} \frac{(L\phi e^{\theta z} + M\theta e^{\phi z})e^{qt}}{\dfrac{\partial}{\partial q}\{(q - r_m)(q + d_2)(q + d_4)Q(q)\}} \qquad (4.8.14)$$

where $q = r_m, d_2, d_4$ and $q = a_1, a_2, \cdots a_n$ are roots of the following equations:

$$\left(2k_z(q - r_m) + 2b_1b_3 - u(b_1 - b_3)\right)\sinh\left(\frac{H\sqrt{u^2 + 4k_{mz}(q - r_m)}}{2k_{mz}}\right)$$
$$+(b_1 + b_3)\sqrt{u^2 + 4k_{mz}(q - r_m)}\cosh\left(\frac{H\sqrt{u^2 + 4k_{mz}(q - r_m)}}{2k_{mz}}\right) = 0$$

for $u^2 + 4k_{mz}(q - r_m) > 0$ (4.8.15)

$$\left(2k_z(q - r_m) + 2b_1b_3 - u(b_1 - b_3)\right)\sin\left(\frac{H\sqrt{-u^2 - 4k_{mz}(q - r_m)}}{2k_{mz}}\right)$$
$$+(b_1 + b_3)\sqrt{-u^2 - 4k_{mz}(q - r_m)}\cos\left(\frac{H\sqrt{-u^2 - 4k_{mz}(q - r_m)}}{2k_{mz}}\right) = 0$$

for $u^2 + 4k_{mz}(q - r_m) < 0$ (4.8.16)

The term $L\phi e^{\theta z} + M\theta e^{\phi z}$ is rearranged to as follows:

$$= -(q+d_2)\left[(q+d_4)(u-b_3)c_0 + b_4c_4(q+r_m)\right]\left\{k_{mz}(e^{\theta z}\phi - e^{\phi z}\theta) - (u+b_1)(e^{\theta z} - e^{\phi z})\right\}$$
$$+(q+d_4)\left[(q+d_2)(u+b_1)c_0 - b_2c_2(q+r_m)\right]\begin{bmatrix} k_{mz}(e^{\phi H}e^{\theta z}\phi - e^{\theta H}e^{\phi z}\theta) \\ -(u-b_3)(e^{\phi H}e^{\theta z} - e^{\theta H}e^{\phi z}) \end{bmatrix} \tag{4.8.17}$$

$$e^{\theta z} - e^{\phi z} = 2e^{\frac{uz}{2k_{mz}}}\sinh\left[\frac{\sqrt{u^2 + 4k_{mz}(q-r_m)}}{2k_{mz}}z\right] \tag{4.8.18}$$

$$e^{\phi H}e^{\theta z} - e^{\theta H}e^{\phi z} = -2e^{\frac{u(H+z)}{2k_{mz}}}\sinh\left[\frac{\sqrt{u^2 + 4k_{mz}(q-r_m)}}{2k_{mz}}(H-z)\right] \tag{4.8.19}$$

$$e^{\theta z}\phi - e^{\phi z}\theta = \frac{e^{\frac{uz}{2k_{mz}}}}{k_{mz}}\begin{bmatrix} u\sinh\left[\frac{\sqrt{u^2 + 4k_{mz}(q-r_m)}}{2k_{mz}}z\right] \\ -\sqrt{u^2 + 4k_{mz}(q-r_m)}\cosh\left[\frac{\sqrt{u^2 + 4k_{mz}(q-r_m)}}{2k_{mz}}z\right] \end{bmatrix} \tag{4.8.20}$$

$e^{\phi H}e^{\theta z}\phi - e^{\theta H}e^{\phi z}\theta$ becomes:

$$= \frac{e^{\frac{u(H+z)}{2k_{mz}}}}{k_{mz}}\begin{bmatrix} u\sinh\left[\frac{\sqrt{u^2 + 4k_{mz}(q-r_m)}(z-H)}{2k_{mz}}\right] \\ -\sqrt{u^2 + 4k_{mz}(q-r_m)}\cosh\left[\frac{\sqrt{u^2 + 4k_{mz}(q-r_m)}(z-H)}{2k_{mz}}\right] \end{bmatrix} \tag{4.8.21}$$

Thus $L\phi e^{\theta z} + M\theta e^{\phi z}$ becomes:

$$= (q+d_4)\left[(q+d_2)(u+b_1)m_{l0} - b_2 m_2 (q-r_m)\right] e^{\frac{u(H+z)}{2k_z}} \times$$
$$\left[\begin{array}{l}(u-2b_3)\sinh\left[\left(\sqrt{u^2+4k_{mz}(q-r_m)}\right)(H-z)\right]/2k_{mz}\\ -\sqrt{u^2+4k_{mz}(q-r_m)}\cosh\left[\left(\sqrt{u^2+4k_{mz}(q-r_m)}\right)(H-z)\right]/2k_{mz}\end{array}\right] + (q+d_2)\times$$
$$\left[\begin{array}{l}(q+d_4)(u-b_3)m_{l0}\\ +b_4 m_4 (q-r_m)\end{array}\right] e^{\frac{uz}{2k_z}} \left[\begin{array}{l}(u+2b_1)\sinh\left[\dfrac{\sqrt{u^2+4k_{mz}(q-r_m)}}{2k_{mz}} z\right]\\ +\sqrt{u^2+4k_{mz}(q-r_m)}\cosh\left[\dfrac{\sqrt{u^2+4k_{mz}(q-r_m)}}{2k_{mz}} z\right]\end{array}\right]$$

for $u^2 + 4k_{mz}(q-r_m) > 0$ (4.8.22)

For $u^2 + 4k_{mz}(q-r_m) < 0$, $L\phi e^{\theta z} + M\theta e^{\phi z}$ can be expressed by applying *sinh(ix) = isin(x)* and *cosh(ix) = cos(x)* as mentioned in Section (2.5.3.3) and becomes:

$$= i(q+d_4)\left[(q+d_2)(u+b_1)m_{l0} - b_2 m_2 (q-r_m)\right] e^{\frac{u(H+z)}{2k_{mz}}} \times$$
$$\left[\begin{array}{l}(u-2b_3)\sin\left[\sqrt{-u^2-4k_{mz}(q-r_m)}(H-z)/2k_{mz}\right]\\ -\sqrt{-u^2-4k_{mz}(q-r_m)}\cos\left[\sqrt{-u^2-4k_{mz}(q-r_m)}(H-z)/2k_{mz}\right]\end{array}\right]$$
$$+ i(q+d_2)\left[\begin{array}{l}(q+d_4)(u-b_3)m_{l0}\\ +b_4 c_4 (q-r_m)\end{array}\right] e^{\frac{uz}{2k_{mz}}} \left(\begin{array}{l}(u+2b_1)\sin\left[z\sqrt{-u^2-4k_{mz}(q-r_m)}/2k_{mz}\right]\\ +\sqrt{-u^2-4k_{mz}(q-r_m)}\times\\ \cosh\left[z\sqrt{-u^2-4k_{mz}(q-r_m)}/2k_{mz}\right]\end{array}\right)$$

for $u^2 + 4k_{mz}(q-r_m) < 0$ (4.8.23)

The contribution of the summation sequence when $q = r_m$ can be calculated by direct substitution as follows:

$$\theta = \frac{u+\sqrt{u^2+4k_{mz}(r_m-r_m)}}{2k_{mz}} = \frac{u}{k_{mz}}; \quad \phi = 0 \qquad (4.8.24)$$

Substituting to the summation sequence, then:

$$L\phi = 0 \tag{4.8.25}$$

$$M\theta = (r_m + d_2)(r_m + d_4)m_{I0}\left[-b_1(u-b_3) - e^{\frac{uH}{k_{mz}}}b_3(u+b_1)\right] \tag{4.8.26}$$

$\frac{\partial}{\partial q}\{(q-r_m)(q+d_2)(q+d_4)Q(q)\}$ becomes:

$$= (r_m + d_2)(r_m + d_4)\left[b_1(u-b_3) + e^{\frac{uH}{k_{mz}}}b_3(u+b_1)\right] \tag{4.8.27}$$

Thus the contribution is:

$$= -m_{I0}\exp(r_m t) \tag{4.8.28}$$

The contribution of the summation sequence when $q = -d_2$ can be calculated as follows:

$L\phi e^{\theta z} + M\theta e^{\phi z}$ becomes:

$$= -(d_2 - d_4)b_2c_2(d_2 + r)[k_{mz}(e^{\phi H}e^{\theta z}\phi - e^{\theta H}e^{\phi z}\theta) - (u-b_3)(e^{\phi H}e^{\theta z} - e^{\theta H}e^{\phi z})] \tag{4.8.29}$$

$$e^{\phi H}e^{\theta z}\phi - e^{\theta H}e^{\phi z}\theta = \frac{-e^{\frac{u(H+z)}{2k_{mz}}}}{k_{mz}}\left\{\begin{array}{l} u\sinh\left[\frac{\sqrt{u^2 - 4k_{mz}(d_2 + r_m)}(H-z)}{2k_{mz}}\right] \\ +\sqrt{u^2 - 4k_{mz}(d_2 + r_m)}\cosh\left[\frac{\sqrt{u^2 - 4k_{mz}(d_2 + r_{mz})}(H-z)}{2k_{mz}}\right] \end{array}\right\} \tag{4.8.30}$$

$$e^{\phi H}e^{\theta z} - e^{\theta H}e^{\phi z} = -2e^{\frac{u(H+z)}{2k_{mz}}}\sinh\left[\frac{\sqrt{u^2 - 4k_{mz}(d_2 + r_m)}(H-z)}{2k_{mz}}\right] \tag{4.8.31}$$

Thus becomes:

$$= e^{\frac{u(H+z)}{2k_{mz}}}(d_2 - d_4)b_2c_2(d_2 + r_m)\left[\begin{array}{l}\sqrt{u^2 - 4k_{mz}(d_2 + r_m)}\times \\ \cosh\left[\dfrac{\sqrt{u^2 - 4k_{mz}(d_2 + r_m)}(H-z)}{2k_{mz}}\right] \\ -(u - 2b_3)\sinh\left[\dfrac{\sqrt{u^2 - 4k_{mz}(d_2 + r_m)}(H-z)}{2k_{mz}}\right]\end{array}\right] \tag{4.8.32}$$

$\frac{\partial}{\partial q}\{(q - r_m)(q + d_2)(q + d_4)Q(q)\}$ becomes:

$$= (d_2 - d_4)(d_2 + r)e^{\frac{uH}{2k_{mz}}}\times$$
$$\left[\begin{array}{l}(b_1 + b_3)\sqrt{u^2 - 4k_{mz}(d_2 + r_m)}\cosh\left(\dfrac{H\sqrt{u^2 - 4k_{mz}(d_2 + r_m)}}{2k_{mz}}\right) \\ -\left(2k_m(d_2 + r_m) - 2b_1b_3 + u(b_1 - b_3)\right)\sinh\left(\dfrac{H\sqrt{u^2 - 4k_{mz}(d_2 + r_m)}}{2k_m}\right)\end{array}\right] \tag{4.8.33}$$

Thus the contribution of the summation sequence when $q = -d_2$ is:

$$= \frac{e^{\frac{uz}{2k_{mz}} - d_2t}b_2m_2\left[\begin{array}{l}\sqrt{u^2 - 4k_{mz}(d_2 + r_m)}\cosh\left(\sqrt{u^2 - 4k_{mz}(d_2 + r_m)}(z-H)/2k_{mz}\right) \\ +(u - 2b_3)\sinh\left(\sqrt{u^2 - 4k_{mz}(d_2 + r_m)}(z-H)/2k_{mz}\right)\end{array}\right]}{\left[\begin{array}{l}(b_1 + b_3)\sqrt{u^2 - 4k_{mz}(d_2 + r_m)}\cosh\left(H\sqrt{u^2 - 4k_{mz}(d_2 + r_m)}/2k_{mz}\right) \\ -\left(2k_{mz}(d_2 + r_m) - 2b_1b_3 + u(b_1 - b_3)\right)\sinh\left(H\sqrt{u^2 - 4k_{mz}(d_2 + r_m)}/2k_{mz}\right)\end{array}\right]}$$

$$\text{when } u^2 - 4k_{mz}(d_2 + r_m) > 0 \tag{4.8.34}$$

For $u^2 + 4k_{mz}(d_2 - r_m) < 0$, the contribution of the summation sequence can be expressed by applying *sinh(ix) = isin(x)* and *cosh(ix) = cos(x)* as mentioned in Section (2.5.3.3) and becomes:

$$e^{\frac{uz}{2k_{mz}}-d_2 t} b_2 m_2 \left[\begin{array}{l} \sqrt{4k_{mz}(d_2+r_m)-u^2}\cos\left(\dfrac{\sqrt{4k_{mz}(d_2+r_m)-u^2}(z-H)}{2k_{mz}}\right) \\ +(u-2b_3)\sin\left(\dfrac{\sqrt{4k_{mz}(d_2+r_m)-u^2}(z-H)}{2k_{mz}}\right) \end{array}\right]$$

$$= \frac{\left[\begin{array}{l} (b_1+b_3)\sqrt{4k_{mz}(d_2+r_m)-u^2}\cos\left(\dfrac{H\sqrt{4k_{mz}(d_2+r_m)-u^2}}{2k_{mz}}\right) \\ -\left(2k_{mz}(d_2+r_m)-2b_1b_3+u(b_1-b_3)\right)\sin\left(\dfrac{H\sqrt{4k_{mz}(d_2+r_m)-u^2}}{2k_{mz}}\right) \end{array}\right]}{}$$

$$\text{when } u^2-4k_{mz}(d_2+r_m)<0 \qquad (4.8.35)$$

Similarly, the contribution of the summation sequence when $q=-d_4$ can be expressed by direct substitution and the contribution is:

$$e^{\frac{u(z-H)}{2k_{mz}}-d_4 t} b_4 m_4 \left[\begin{array}{l} \sqrt{u^2-4k_{mz}(d_4+r_m)}\cosh\left(\dfrac{\sqrt{u^2-4k_{mz}(d_4+r_m)}}{2k_z}z\right) \\ +(u+2b_1)\sinh\left(\dfrac{\sqrt{u^2-4k_{mz}(d_4+r_m)}}{2k_{mz}}z\right) \end{array}\right]$$

$$= \frac{\left[\begin{array}{l} (b_1+b_3)\sqrt{u^2-4k_{mz}(d_4+r_m)}\cosh\left(\dfrac{H\sqrt{u^2-4k_{mz}(d_4+r_m)}}{2k_{mz}}\right) \\ -\left(2k_z(d_4+r_m)-2b_1b_3+u(b_1-b_3)\right)\sinh\left(\dfrac{H\sqrt{u^2-4k_{mz}(d_4+r_m)}}{2k_{mz}}\right) \end{array}\right]}{}$$

$$\text{when } u^2-4k_{mz}(d_4+r_m)>0 \qquad (4.8.36)$$

$$= \frac{e^{\frac{uz}{2k_{mz}}-d_4 t} b_4 c_4 \left[\begin{array}{l} \sqrt{4k_{mz}(d_4+r_m)-u^2}\cos\left(\dfrac{\sqrt{4k_{mz}(d_4+r_m)-u^2}}{2k_{mz}}z\right) \\ +(u+2b_1)\sin\left(\dfrac{\sqrt{4k_{mz}(d_4+r_m)-u^2}}{2k_{mz}}z\right) \end{array} \right]}{\left[\begin{array}{l} (b_1+b_3)\sqrt{4k_{mz}(d_4+r_m)-u^2}\cos\left(\dfrac{H\sqrt{4k_{mz}(d_4+r_m)-u^2}}{2k_{mz}}\right) \\ -\left(2k_{mz}(d_4+r_m)-2b_1b_3+u(b_1-b_3)\right)\sin\left(\dfrac{H\sqrt{4k_{mz}(d_4+r_m)-u^2}}{2k_{mz}}\right) \end{array} \right]}$$

$$\text{when } u^2-4k_{mz}(d_4+r_m)<0 \qquad (4.8.37)$$

The expression of $\frac{\partial Q(q)}{\partial q}$ at $q=a_1,a_2,\cdots a_n$ become:

$$= e^{\frac{uH}{2k_{mz}}} \left\{ \begin{array}{l} (2k_{mz}(q-r_m)+2b_1b_3-u(b_1-b_3))\cosh\left[\dfrac{H\sqrt{u^2+4k_{mz}(q-r_m)}}{2k_{mz}}\right]\times \\ \dfrac{\partial}{\partial q}\left(\dfrac{H\sqrt{u^2+4k_{mz}(q-r_m)}}{2k_{mz}}\right)+2k_{mz}\sinh\left[\dfrac{H\sqrt{u^2+4k_{mz}(q-r_m)}}{2k_{mz}}\right] \\ +(b_1+b_3)\dfrac{\partial\sqrt{u^2+4k_{mz}(q-r_m)}}{\partial q}\cosh\left[\dfrac{H\sqrt{u^2+4k_{mz}(q-r_m)}}{2k_{mz}}\right] \\ +(b_1+b_3)\sqrt{u^2+4k_{mz}(q-r_m)}\sinh\left[\dfrac{H\sqrt{u^2+4k_{mz}(q-r_m)}}{2k_{mz}}\right]\times \\ \dfrac{\partial}{\partial q}\left(\dfrac{H\sqrt{u^2+4k_{mz}(q-r_m)}}{2k_{mz}}\right) \end{array} \right\}$$

$$= e^{\frac{uH}{2k_{mz}}} \left\{ \begin{array}{l} (2k_z+H(b_1+b_3))\sinh\left[\dfrac{H\sqrt{u^2+4k_{mz}(q-r_m)}}{2k_{mz}}\right] \\ +\dfrac{\left[\begin{array}{l}2k_{mz}H(q-r_m)+2b_1b_3H \\ -uH(b_1-b_3)+2k_{mz}(b_1+b_3)\end{array}\right]}{\sqrt{u^2+4k_{mz}(q-r_m)}}\cosh\left[\dfrac{H\sqrt{u^2+4k_{mz}(q-r_m)}}{2k_{mz}}\right] \end{array} \right\}$$

$$\text{for } u^2+4k_{mz}(q-r_m)>0 \qquad (4.8.38)$$

For $u^2 + 4k_{mz}(q - r_m) < 0$, the contribution of the summation sequence can be expressed by applying *sinh(ix) = isin(x)* and *cosh(ix) = cos(x)* as mentioned in Section (2.5.3.3) and becomes:

$$= ie^{\frac{uH}{2k_{mz}}} \left\{ \begin{array}{l} (2k_z + H(b_1 + b_3)) \sin\left[\dfrac{H\sqrt{-u^2 - 4k_{mz}(q - r_m)}}{2k_{mz}} \right] \\ - \dfrac{\left[\begin{array}{l} 2k_{mz}H(q - r_m) + 2b_1b_3H \\ - uH(b_1 - b_3) + 2k_{mz}(b_1 + b_3) \end{array} \right]}{\sqrt{-u^2 - 4k_{mz}(q - r_m)}} \cos\left[\dfrac{H\sqrt{-u^2 - 4k_{mz}(q - r_m)}}{2k_{mz}} \right] \end{array} \right\}$$

$$\text{for } u^2 + 4k_{mz}(q - r_m) < 0 \qquad (4.8.39)$$

Finally, the solution of $m(z,t)$, (Solution 5) is as follows:

$$\begin{aligned} &= \frac{e^{\frac{uz}{2k_{mz}} - d_2 t} D_h(z - H, d_2, b_2, m_2, -b_3)}{D_l(d_2)} + \frac{e^{\frac{u(z-H)}{2k_{mz}} - d_4 t} D_h(z, d_4, b_4, m_4, b_1)}{D_l(d_4)} \\ &+ \sum_{q=a_1}^{a_n} \frac{e^{qt + \frac{u(z-H)}{2k_{mz}}} \left\{ \begin{array}{l} P_f(q, b_4, m_4, -b_3, d_2) P_b(z, q, b_1) \\ - e^{\frac{uH}{2k_{mz}}} P_f(q, -b_2, m_2, b_1, d_4) P_b(z - H, q, -b_3) \end{array} \right\}}{(q - r_m)(q + d_2)(q + d_4) W(q)} \end{aligned} \qquad (4.8.40)$$

where $q = a_1, a_2, \cdots a_n$ are roots of the following equations:

$$\begin{aligned} &\left(2k_{mz}(q - r_m) + 2b_1b_3 - u(b_1 - b_3)\right) \sinh\left(\frac{H\sqrt{u^2 + 4k_{mz}(q - r_m)}}{2k_{mz}} \right) \\ &+ (b_1 + b_3)\sqrt{u^2 + 4k_{mz}(q - r_m)} \cosh\left(\frac{H\sqrt{u^2 + 4k_{mz}(q - r_m)}}{2k_{mz}} \right) = 0 \end{aligned} \qquad (4.8.41)$$

or

$$\tanh\left(\frac{H\sqrt{u^2 + 4k_{mz}(q - r_m)}}{2k_{mz}} \right) = \frac{(b_1 + b_3)\sqrt{u^2 + 4k_{mz}(q - r_m)}}{\left(u(b_1 - b_3) - 2b_1b_3 - 2k_{mz}(q - r_m)\right)}$$

$$\text{for } u^2 + 4k_{mz}(q - r_m) > 0 \qquad (4.8.42)$$

$$\left(2k_z(q-r_m)+2b_1b_3-u(b_1-b_3)\right)\sin\left(\frac{H\sqrt{-u^2-4k_{mz}(q-r_m)}}{2k_{mz}}\right)$$
$$+(b_1+b_3)\sqrt{-u^2-4k_{mz}(q-r)}\cos\left(\frac{H\sqrt{-u^2-4k_{mz}(q-r_m)}}{2k_{mz}}\right)=0$$

(4.8.43)

or

$$\tan\left(\frac{H\sqrt{-u^2-4k_{mz}(q-r_m)}}{2k_{mz}}\right)=\frac{(b_1+b_3)\sqrt{-u^2-4k_{mz}(q-r_m)}}{\left(u(b_1-b_3)-2b_1b_3-2k_{mz}(q-r_m)\right)}$$

$$\text{for } u^2+4k_{mz}(q-r_m)<0 \qquad (4.8.44)$$

$$D_h(z,d_4,b_4,m_4,b_1)=b_4m_4\left[\begin{array}{l}\sqrt{u^2-4k_{mz}(d_4+r_m)}\cosh\left(\frac{\sqrt{u^2-4k_{mz}(d_4+r_m)}}{2k_{mz}}z\right)\\+(u+2b_1)\sinh\left(\frac{\sqrt{u^2-4k_{mz}(d_4+r_m)}}{2k_{mz}}z\right)\end{array}\right]$$

$$\text{for } u^2-4k_{mz}(d_4+r_m)>0 \qquad (4.8.45)$$

$$D_l(d_4)=(b_1+b_3)\sqrt{u^2-4k_{mz}(d_4+r_m)}\cosh\left(\frac{H\sqrt{u^2-4k_{mz}(d_4+r_m)}}{2k_{mz}}\right)$$
$$-\left(2k_{mz}(d_4+r_m)-2b_1b_3+u(b_1-b_3)\right)\sinh\left(\frac{H\sqrt{u^2-4k_{mz}(d_4+r_m)}}{2k_{mz}}\right)$$

$$\text{for } u^2-4k_{mz}(d_4+r_m)>0 \qquad (4.8.46)$$

$$D_h(z,d_4,b_4,m_4,b_1)=b_4m_4\left[\begin{array}{l}\sqrt{4k_{mz}(d_4+r_m)-u^2}\cos\left(z\sqrt{4k_{mz}(d_4+r_m)-u^2}/2k_{mz}\right)\\+(u+2b_1)\sin\left(z\sqrt{4k_{mz}(d_4+r_m)-u^2}/2k_{mz}\right)\end{array}\right]$$

$$\text{for } u^2-4k_{mz}(d_4+r_m)<0 \qquad (4.8.47)$$

$$D_f(d_4) = (b_1 + b_3)\sqrt{4k_{mz}(d_4 + r_m) - u^2}\cos\left(\frac{H\sqrt{4k_{mz}(d_4 + r_m) - u^2}}{2k_{mz}}\right)$$
$$-\left(2k_{mz}(d_4 + r_m) - 2b_1b_3 + u(b_1 - b_3)\right)\sin\left(\frac{H\sqrt{4k_{mz}(d_4 + r_m) - u^2}}{2k_{mz}}\right)$$

$$\text{for } u^2 - 4k_{mz}(d_4 + r_m) < 0 \qquad (4.8.48)$$

$$P_f(q, b_4, c_4, -b_3, d^*) = (q + d_2)(q + d_4)(u - b_3)m_{j0} + b_4c_4(q - r)(q + d^*) \qquad (4.8.49)$$

$$P_b(z, q, b_1) = (u + 2b_1)\sinh\left[\frac{\sqrt{u^2 + 4k_{mz}(q - r_m)}}{2k_{mz}}z\right]$$
$$+\sqrt{u^2 + 4k_{mz}(q - r_m)}\cosh\left[\frac{\sqrt{u^2 + 4k_{mz}(q - r_m)}}{2k_{mz}}z\right]$$

$$\text{for } u^2 + 4k_{mz}(q - r_m) > 0 \qquad (4.8.50)$$

$$W(q) = (2k_{mz} + H(b_1 + b_3))\sinh\left[\frac{H\sqrt{u^2 + 4k_{mz}(q - r_m)}}{2k_{mz}}\right]$$
$$+\frac{2k_{mz}H(q - r_m) + 2b_1b_3H - uH(b_1 - b_3) + 2k_{mz}(b_1 + b_3)}{\sqrt{u^2 + 4k_{mz}(q - r_m)}}\cosh\left[\frac{H\sqrt{u^2 + 4k_{mz}(q - r_m)}}{2k_{mz}}\right]$$

$$\text{for } u^2 + 4k_{mz}(q - r_m) > 0 \qquad (4.8.51)$$

$$P_b(z, q, b_1) = (u + 2b_1)\sin\left[\frac{\sqrt{-u^2 - 4k_{mz}(q - r_m)}}{2k_{mz}}z\right]$$
$$+\sqrt{-u^2 - 4k_{mz}(q - r_m)}\cos\left[\frac{\sqrt{-u^2 - 4k_{mz}(q - r_m)}}{2k_{mz}}z\right]$$

$$\text{for } u^2 + 4k_{mz}(q - r_m) > 0 \qquad (4.8.52)$$

$$W(q) = (2k_{mz} + H(b_1 + b_3))\sin\left(H\sqrt{-u^2 - 4k_{mz}(q - r_m)}/2k_{mz}\right)$$
$$-\frac{2k_{mz}H(q - r_m) + 2b_1b_3H - uH(b_1 - b_3) + 2k_{mz}(b_1 + b_3)}{\sqrt{-u^2 - 4k_{mz}(q - r_m)}}\cos\left[\frac{H\sqrt{-u^2 - 4k_{mz}(q - r_m)}}{2k_{mz}}\right]$$

$$\text{for } u^2 + 4k_z(q - r_m) < 0 \qquad (4.8.53)$$

4.9 General analysis of Model 3

Model 3 is an upgraded version of Model 2. The contributions to contaminant transport by parameters that occur in both Model 2 and Model 3 have been already described in the Section (4.6). In Model 3, parameter u is the same as ω_s in Model 2, b_3 is the same as β_1 and b_4 is the same as β_2 in Solution 2 of Model 2. Effects on the transport by other parameters in the model are discussed in this section.

4.9.1 Existence of steady state condition

Based on the formulation and solution of Model 3, more necessary conditions should be met for the existence of a steady state condition than have been met in Model 2. In the solution, there are a total of three terms dependent on time t. The three terms are $exp(-d_2t)$ when $q = -d_2$, $exp(-d_4t)$ when $q = -d_4$, and $exp(qt)$ in the summation sequence. The steady state condition exists only if all tend to zero when time tends to infinity. Thus, the conditions for the existence of steady state condition are as follows:

$$\begin{cases} d_2 \geq 0 \\ d_4 \geq 0 \\ r_m \leq \dfrac{u^2 - q'_{max}}{4k_{mz}} \end{cases}$$

and q'_{max} is the maximum value of q' found from the following equations

$$\left(\frac{1}{2}(q'-u^2) + 2b_1b_3 - u(b_1 - b_3)\right)\sinh\left(\frac{H\sqrt{q'}}{2k_{mz}}\right) + (b_1 + b_3)\sqrt{q'}\cosh\left(\frac{H\sqrt{q'}}{2k_{mz}}\right) = 0$$

$$\text{for } q' > 0 \qquad (4.9.1.1)$$

$$\left(\frac{1}{2}(q-u^2)+2b_1b_3-u(b_1-b_3)\right)\sin\left(\frac{H\sqrt{-q'}}{2k_{mz}}\right)+(b_1+b_3)\sqrt{-q'}\cos\left(\frac{H\sqrt{-q'}}{2k_{mz}}\right)=0$$

for $q'<0$ (4.9.1.2)

Therefore, the existence of the steady state condition depends on u, k_{mz}, r_m, H, b_1, b_3, d_2 and d_4. Effects on the maximum allowed value of r_m with the existence of the steady state of u (u is equivalent to ω_s in Model 2), k_{mz} and b_3 (b_3 is equivalent to β_1 in Model 2) are generally described in Section (4.6). In addition, the value of $(u^2-q'_{max})/4k_{mz}$ decreases as k_{mz} increases and increases as b_1 or u increases.

4.9.2 Effect of d_4

The purpose of adding exponential growth/decay parameters, d_2 and d_4 at the boundaries is to simulate the changes of contaminant input from the boundaries. The coefficients d_2 and d_4 are commonly used to represent the first order growth/decay properties of the contaminant input from boundaries. In Figure 12, curves of constant concentration are shown for different values of d_4 and m_{l0}. Because of the different directions between u in Model 3 and ω_s in Model 2, the vertical direction *(H-z)/H* is equivalent to Z in Model 2. In all cases shown in Figure 12, the concentration profiles tend to zero, as time tends to infinity. All cases in Figure 12 assume zero net flux at the boundary, *z=0*, and thus there is no contaminant input from this boundary. Positive values of d_4 imply contaminant input from another boundary will decay through time and tends to zero as time tend to infinity. In long term, there will be no contaminant input from boundaries to the water column. In addition, all

contaminants, originally in the water column will settle to the bottom boundary. The water column will then be finally free from contaminants. For input parameters satisfying the requirements for the existence of the steady state condition and m_2, m_4 is not zero, a zero steady state concentration profile result if both d_2 and d_4 are positive values. For the case when d_2, d_4, b_1, b_2 and m_2 are all zero, Model 3 reduces to Solution 4 of Model 2. Examples of contaminant transport in different cases are given in Figure 9 where the final steady state concentration profiles in different cases are presented.

Generally, a larger d_4 represents a faster decay of the supporting source and the concentration profile approaches zero more rapidly. The phenomenon is already shown when comparing Figure 12(a) with Figure 12(c) or Figure 12(b) and Figure 12(d).

As in Model 2, the magnitude of m_{l0} only affects the concentration profiles at the initial states and the concentration profile is the same if time is sufficiently long. This is seen when comparing with Figure 12(a) with Figure 12(b) or Figure 12(c) with Figure 12(d).

Figure 13 shows cases with negative values of d_4 and these cases have no steady state conditions. Generally, as d_4 is less than zero, the concentration profiles increase without limit as time increase. This is reflected in all cases in Figure 13. In Figure 13(b) and Figure 13(d), the concentration decreases over the water column at initial states and then increases. The decrease in concentration at initial states are due to the settling of contaminants while the resuspension from the bottom boundary is not

significant at these states. As time increases, the fate of the contaminant will be totally controlled by resuspension from the bottom boundary and the concentration will then increase without limit. From the mathematical point of view, the settling and resuspension of the contaminant from the boundaries can be separated into two independent motions. The settling period of the contaminant is from $t=0$ to the time at which minimum concentration profile is reached. The time is around 2.3 for the case shown in Figure 13(b) and Figure 13(d). In other words, the concentration profile will be close to zero at the same time for the above cases, if there is no input from the boundaries, i.e. b_4, m_4 and d_4 are all zero.

4.9.3 Effect of d_2

Generally, the contribution to contaminant transport by d_2 is similar to that by d_4. In this section, the contribution to contaminant transport is investigated when both d_2 and d_4 are non zero.

If u=0, $d_2=d_4$, $b_2=b_4$, $m_2=m_4$ and $b_1=b_2$, the system becomes symmetric about $z=0.5H$. Thus, the concentration profile in this case becomes symmetrically distributed about the mid level. The direction of u is towards the boundary $z=1$ or to the input source $b_4 m_4 \exp(-d_4 t)$, thus, contaminant concentrates are at that side, even when $d_2=d_4$ and this case is shown in Figure 14(a). For cases where d_2 is larger than d_4, the contribution of the sources at the boundary $z=0$ decreases more rapidly than on the opposite side .In the case with $d_2=d_4$, the contribution of the sources at the boundary $z=0$ decreases at the same rate as the opposite side. Figure 14(b) shows a case with d_2=0.5 while d_4=0.25. When comparing Figure 12(b) with

Figure 14(b), it can be seen that significant differences only occur at positions where z is relatively close to *0* and t is small. There is no difference in the concentration profiles when z is equal to 1 or t is large. In all cases shown in Figures 12(a), 14(a) and 14(b), the concentration profiles will become zero as time tends to infinity.

Figure 14(c) shows a case for d_2=0. In this case, the final steady state concentration, is the same as the case setting all input parameters on another boundary (i.e. b_3, b_4, m_4 and d_4) to zero. The setting of such parameters to zero implies a zero net flux at the boundary *z=1*. In that case, since d_4 is positive and the source at the boundary decays to zero as time increases, the final steady state concentration profile is thus only contributed by the source at the boundary *z=0*. From the figure, the shape of the steady state concentration profile is seen to be nearly constant over the water column.

Figure 14(d) shows a case for a negative value of d_2. Similar to the effect of d_4, the concentration profile grows without limit as time increases. Generally, when time is large, the concentration profile is independent of the value of d_4. Therefore, in agreement with thus the concentration distribution is almost a constant value along the water column.

Figure 12: Concentration distribution of $m(z,t)$, with steady state condition for different values of d_4 and m_0.
($k_{mz}=0.35$, $u=1$, $r_m = b_1=b_2=m_2=d_2=0$, $H=b_3=b_4=m_4=1$)

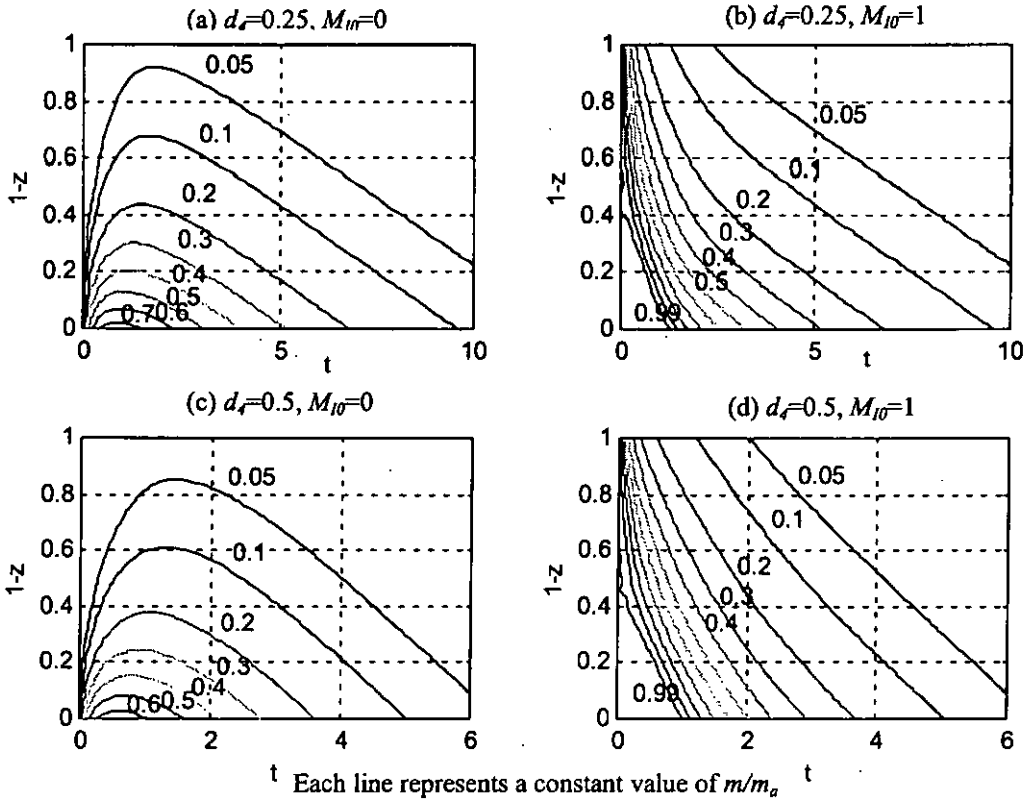

Figure 13: Concentration distribution of $m(z,t)$, without steady state condition for different values of d_4 and m_0.
($k_{mz}=0.35$, $u=1$, $r_m = b_1=b_2=m_2=d_2=0$, $H=b_3=b_4=m_4=1$)

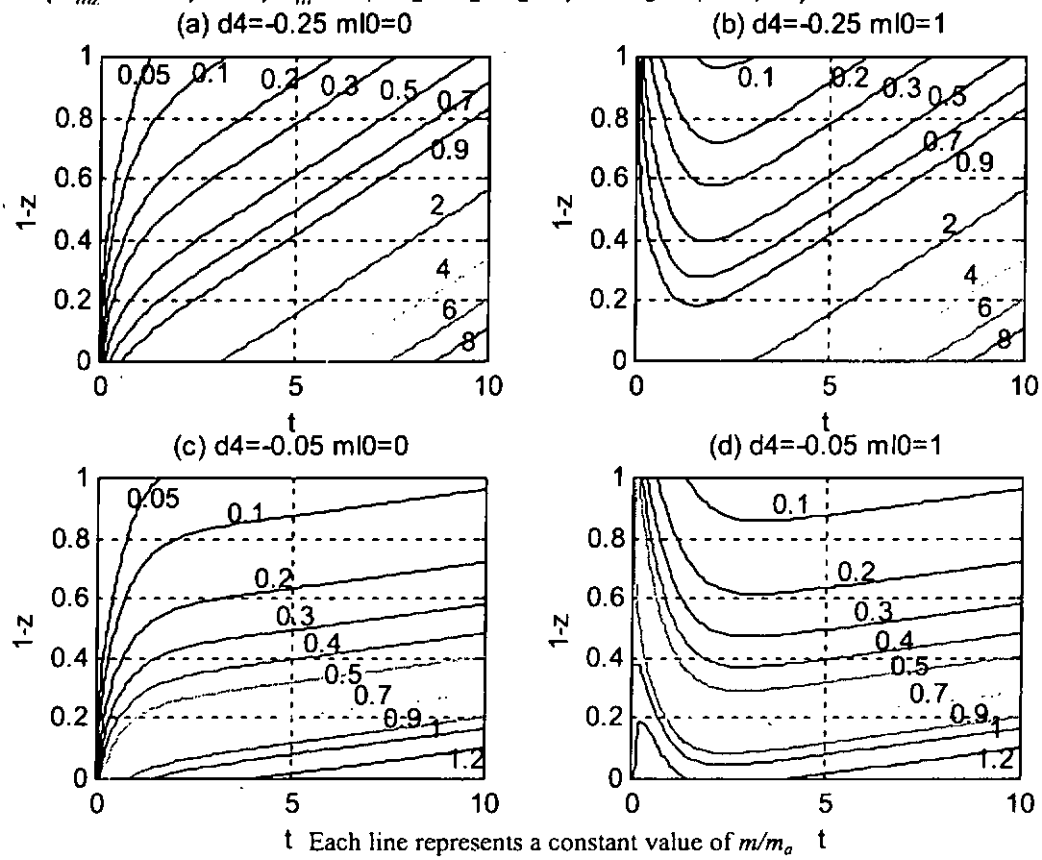

Figure 14: Concentration distribution of $m(z,t)$, for different values of d_2 (k_{mz} =0.35, u=1, r_m =0, H= b_1=b_2=b_3=b_4= m_2=m_4=1)

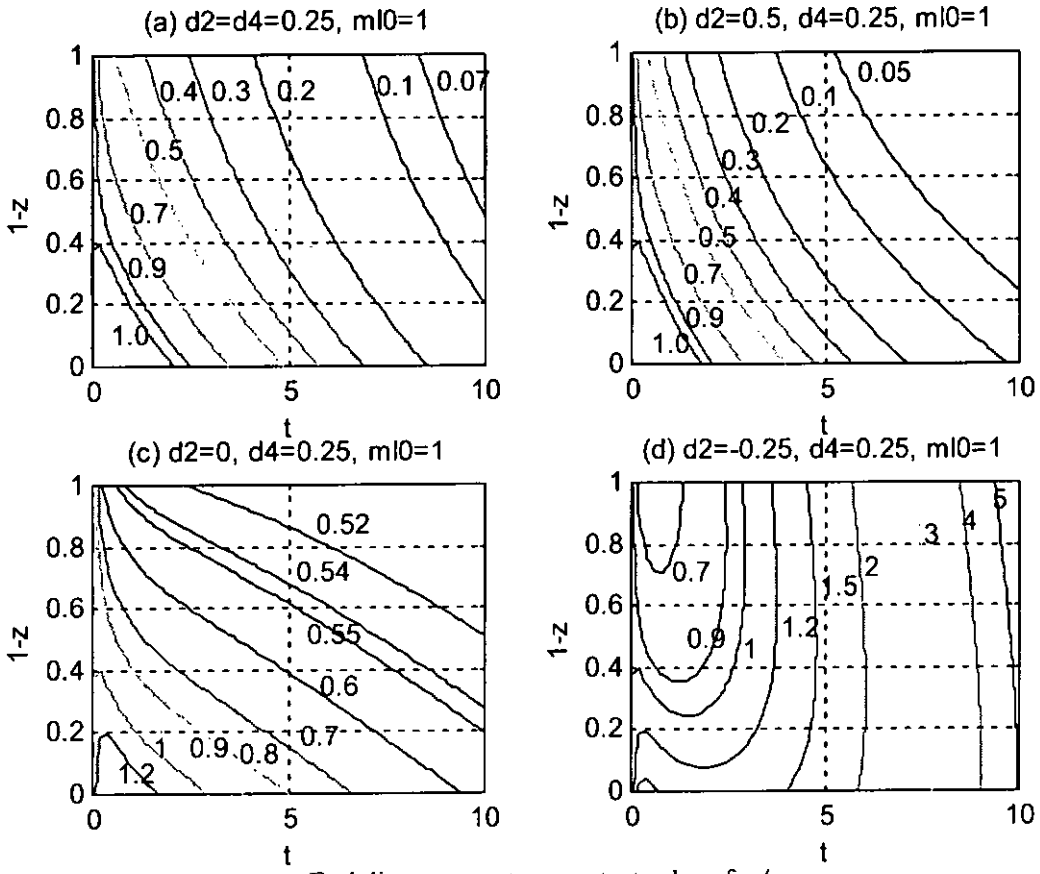

Each line represents a constant value of m/m_a

Chapter 5: Analysis of the physical and mathematical parameters in the governing system

The governing system for the transport of toxic substances is developed in Chapter 3 with some assumptions and simplifications. The developed governing system, however, is still too difficult to be solved analytically and three relatively simple models are developed in Chapter 4. The developed models do not always present an adequate representation of the governing system. In this chapter, physical and mathematical parameters shown in Chapter 3 are analyzed to investigate the ranges of parameters, which will render the developed models in Chapter 4 useful for the prediction of the transport of toxic substances.

5.1 Reviews of the range of parameters in the natural environment

The developed models in Chapter 4 are generally useful without any limitation on the ranges of input parameters. However, in order for solutions to be realistic, the range of magnitude of each parameter appearing in the natural environment should be studied. The studies are useful to check the conclusions made in later sections. They are obtained by mathematical and physical means and they are reasonable and useful from the physical point of view.

5.1.1 Range of sediment settling velocity (ω_s) in natural environment

As described in the Literature Review, the magnitude of the settling velocity of a sediment particle is highly dependent on its size. Table 2 shows

the ranges of settling velocity with different particle sizes calculated by Equations (2.1.2.3a) to (2.1.2.3c). The range lies between 10^{-6} and 0.4 m/s.

5.1.2 Range of water depth (*H*) in natural environment

In the natural environment, water depth ranges from the order of 0.1m for streams to the order of hundred meters for lakes and estuaries. Schnoor (1996, p58-61) listed the water depth for some streams and lakes in the world. The developed model can also be applied to some experimental cases, which have water depths from several centimeters to several meters.

5.1.3 Range of vertical mixing coefficients, k_z and k_{sz}, in natural environment

The magnitudes of vertical mixing coefficients depend on the transport environment and are different for different coastal environments. Eddy diffusivity is often used to describe the turbulent diffusion coefficient for dissolved substances in lakes. The mixing coefficient in this case is usually assumed to be constant and ranges from 10^{-2} to 10 cm^2/s. Schnoor (1996, p57) mentioned that the vertical diffusion coefficient can be correlated with the mean depth of the lake as follows:

$$k_z = 0.0142H^{1.49} \qquad (5.1.3.1)$$

in which k_z = vertical eddy diffusivity, m^2/d and H = mean depth, m.

In rivers, Jobson and Sayre (1970) reported that the vertical dispersion coefficient can be in a parabolic form. The range lies between 10 to 1000 cm^2/s. It should also be noted that k_z and k_{sz} are generally in the same order of magnitude. From Equation (2.1.3.1), the depth averaged value of k_{sz}, $\bar{k}_{sz}$, is $\beta\kappa u_* H/6$ and therefore

$$\beta\kappa u_* = 6\bar{k}_{sz} / H \qquad (5.1.3.2)$$

in which κ is the von Karman coefficient (= 0.4 for clear water), β is the ratio of sediment mixing coefficient to the momentum diffusion coefficient (can simply be assumed to be unity) and u_* is the shear velocity.

The range of β in k_{sz} (Equation (2.1.3.1)), can be found from Equation (2.1.3.5) to Equation (2.1.3.7). The value of β_s shown in Equation (2.1.3.6) lies between 1 and 2. The value of ϕ_s shown in Equation (2.1.3.7) lies between 0 and 1. Generally β lies between 0 and 2 from $\beta = \beta_s \phi_s$. However, by limiting the range of suspended solids between 10 mg/L and 100000 mg/L (O'Connor (1988)), ϕ_s lies between 0.4 and 1 and β lies between 0.4 and 2.

5.1.4 Range of suspended sediment concentration (*s*) in natural environment

Chapra (1997, p.700) reported that suspended solid concentrations range from approximately 1 mg/L for clear lakes to 100 mg/L for turbid rivers. O'Connor (1988) mentioned that the concentration range of suspended solids lies from less than 10 mg/L in clear water to larger than 100000 mg/L in stable beds. The concentration of suspended sediment should not exceed the value of the maximum volume concentration, which is 0.65β or 1722 kg/m^3 for sediment density of 2650 kg/m^3.

The range of reference level sediment concentration (s_a) is calculated by Equation (2.1.6.8). Using Equation (2.1.6.8) and by substituting known values of parameters to the equation:

$$s_a = \frac{0.295\overline{u}^{2.76}}{(H\omega_s)^{0.92}} \qquad (5.1.4.1)$$

As described in Sections 5.1.1 and 5.1.2, ω_s ranges from 10^{-6} to 0.4 m/s and H ranges from 0.1 to 100m. The range of $\omega_s H$ lies between 10^{-7} to 40 m^2/s. The range of $(H\omega_s)^{-0.92}$ lies between 0.036 and 2.75×10^6. Assuming the depth averaged flow velocity, $\overline{u}$, lying between 0 and 10 m/s, $\overline{u}^{2.76}$ then lies between 0 and 575. Therefore, s_a ranges from 0 to 5×10^8 kg/m^3.

5.1.5 Range of partition coefficient (k_d) in natural environment

The value of the sorption partition coefficient (k_d) is mainly dependent on the type of the toxic substance. Wu and Gschwend (1986) have found that for a number of natural bed sediment, the sorption partition coefficient can be as high as 4700 L/kg where the sorbates are chlorobenzenes. Heavy metals and polychorinated biphenyls also have very high values of k_d, in the order of 10^4 – 10^6 L/kg. Schnoor (1996, p.427) has calculated the value of f_p, which can exceed 0.5 at pH 7 or above in a lake where the suspended solid concentration is only 10^{-6} kg/L. O'Connor (1988) considered that the partition coefficient varies from approximately 500 to 500000 L/kg. Chapra (1997, p700) mentioned that the range of partition coefficients is from 100 L/kg to 10^7 L/kg. The values for several radionuclides which vary from 200 L/kg for ^{90}Sr to 10^7 L/kg for ^{210}Pb (p.760) are also listed. Carroll and Harms (1999) investigated the most likely value of k_d for some common radionuclides. The range lies between 10 L/kg for Strontium and 10^6 L/kg for Americium.

5.1.6 Range of deposition velocity (ϕ) and resuspension velocity (γ) of sediment at the water-sediment interface

The simplest and most common approach for estimating the value of ϕ and γ is to assume both values equal to the settling velocity (ω_s). However, for situations with high sediment concentration at positions near the sediment–water interface based on some former research and formulae, the effective settling velocity is usually smaller than ω_s. Based on Equation (2.1.2.5), range of ϕ lies between $0.95\omega_s$ and $0.68\omega_s$ for s between 1 and 100 kg/m^3. γ can be always assumed to be the same as ω_s. Significantly, the parameters s_a and γ always appear together in the solutions of the developed models. From the physical point of view, the term γs_a represents the entrainment flux from the bed sediment layer to the water column and hence should be considered as a whole. Thus, all contributions from hydraulic transport and chemical reaction phenomena can be considered in the estimation of s_a. In conclusion, the ratio of γ to ϕ lies between 1 and 1.47 for s lying between 0 and 100 kg/m^3.

5.1.7 Range of the first order decay rate of dissolved toxicant (k_{dc}) and particulate toxicant (k_{dp})

For toxic substances that do not decay naturally, such as heavy metals, k_{dc} and k_{dp} are simply equal to zero. In general, it is assumed that the values of k_{dc} and k_{dp} are the same. However, more research is needed to investigate the difference between them. For radionuclides, the following equation is given in Chapra (1997 p.760):

$$k_{dc} = k_{dp} = 0.693 / t_{50} \qquad (5.1.7.1)$$

in which t_{50} is the half-life of the radionuclide,

For example, the value of t_{50} of Cesium-137 (^{137}Cs), Strontium-90 (^{90}Sr) and Lead-210 (^{210}Pb) given by Chapra (1997 p.760) are 30, 28.8 and 22.3 years respectively and thus values of k_{dc} are 0.0231, 0.024 and 0.031 yr^{-1}, respectively.

For toxic organic chemicals, such as PCBs and DDT, the decay terms k_{dc} and k_{dp} are contributed by biological transformations, chemical hydrolysis, photodegradation and oxidation reaction. The range of the decay terms lies between 0.001 d^{-1} for Benzidine and 135 d^{-1} for $C_6H_5CHCl_2$.

5.2 Analysis of physical parameters in the governing system

5.2.1 Effect of suspended sediment distribution on the governing system

Based on the two equilibrium suspended sediment concentration profiles (Equations (3.4.6.1.1) and (3.4.6.2.1)) described in Chapter 3, the change of the suspended sediment concentration over the water column is mainly dependent on the sediment settling velocity (ω_s) and sediment vertical mixing coefficient (k_{sz}).

5.2.1.1 Sediment equilibrium distribution in the form of exponential function

The exponential function, Equation (3.4.6.1.1), is presented in Figure 15. The distribution of sediment concentration along the water column for

different values of $\omega_s H / k_{sz}$ is clearly shown. The figure shows that the distribution of sediment is almost uniform along the water column for $\omega_s H / k_{sz}$ less than 0.1. Most suspended sediment concentrates is located at the bottom part (z=0 to 0.1*H*) of the water column for $\omega_s H / k_{sz}$ greater than 20, and it can be assumed that the toxic substance transport in the water column is independent of the suspended sediment. The term $\omega_s H / k_{sz}$ is known as the Peclet (P_e) number.

$$P_e = \omega_s H / k_{sz} \qquad (5.2.1.1.1)$$

For the above two extreme cases, it can be assumed that the sediment concentration distribution is uniform over the water column and hence f_d and f_p are constant. The derivatives of s are thus zero. The coefficients $\overline{A}_e$, $\overline{B}_e$ and $\overline{C}_e$ in Equation (3.4.6.1.7) become constants and Model 2 and Model 3 developed by the author match perfectly with such cases. For a case where P_e is larger than 20, f_p becomes zero since the sediment concentration s is assumed to be zero over the entire depth. Coefficients $\overline{A}_e$, $\overline{B}_e$ and $\overline{C}_e$ can be further simplified to:

$$\overline{A}_e = f_d k_z \qquad (5.2.1.1.2)$$

$$\overline{B}_e = 0 \qquad (5.2.1.1.3)$$

$$\overline{C}_e = k_{dp} f_p + k_{dc} f_d \qquad (5.2.1.1.4)$$

The Governing Equation (3.4.6.1.7) reduces to a second order diffusion equation with a first order decay term. Based on the above estimation, the

distributions of coefficients $\overline{A}_e$, $\overline{B}_e$ and $\overline{C}_e$ can be considered as functions of z for P_e between 0.1 and 20. Based on the ranges of ω_s, H and k_{sz} (described in Section 5.1) the range of P_e is from 10^{-6} to 4×10^{7}. Therefore, it is possible to have real case applications even when the value of P_e is outside the range from 0.1 to 20. All analyses done in later sections will consider P_e only in the range from 0.1 to 20.

5.2.1.2 Sediment equilibrium distribution in the form of Rouse profile

Figure 16 shows the distribution of sediment concentration in from of Rouse profile by Equation (3.4.6.2.1) along the water column for different values of $\omega_s / \beta\kappa u_*$ and a = 0.1. The figure shows that the distribution of sediment is almost uniform along the water column for values of $\omega_s / \beta\kappa u_*$ less than 0.02. For $\omega_s / \beta\kappa u_*$ greater than 5, most suspended sediment concentrates is located at the bottom part ($z = a$ to $0.1H$) of the water column and it can be assumed that the toxic substance transport in the water column is independent of the suspended sediment. For the above two extreme cases, the sediment concentration distribution can be assumed to be uniform over the water column and hence in, f_d and f_p, are constants. The derivatives of s are zero. Thus coefficients $\overline{A}_R$, $\overline{B}_R$ and $\overline{C}_R$ shown in Chapter 3 become:

$$\overline{A}_R = k_z(f_d + \beta f_p)$$

$$\overline{A}_R = (f_d + \beta f_p)\kappa u_* z(1 - z/H) \qquad (5.2.1.2.1)$$

$$\overline{B}_R = \omega_s f_p + (f_d + \beta f_p)\partial k_z / \partial z$$

$$\overline{B}_R = \omega_s f_p + (f_d + \beta f_p)\kappa u_*(1 - 2z/H) \qquad (5.2.1.2.2)$$

$$\overline{C}_R = -(k_{dp} f_p + k_{dc} f_d) \qquad (5.2.1.2.3)$$

the term f_p tends to zero as $\omega_s / \beta\kappa u_*$ greater than 5 since the sediment concentration s is assumed to be zero over the entire depth. Coefficient $\overline{A}_R$ and $\overline{B}_R$ can be further simplified to:

$$\overline{A}_R = f_d k_z = f_d \kappa u_* z(1 - z/H) \qquad (5.2.1.2.4)$$

$$\overline{B}_R = f_d \kappa u_* (1 - 2z/H) \qquad (5.2.1.2.5)$$

For conservative toxic substances such as heavy metals, k_{dp} and k_{dc} are zero and $\overline{C}_R$ also becomes zero. In this way, Model 1 developed in Chapter 4 matches perfectly with the above extreme cases. Based on the above estimations, all analyses done in later sections will only consider $\omega_s / \beta\kappa u_*$ with a range from 0.02 to 5.

5.2.2 Effect of the values of partition coefficient and sediment distribution on the distribution of f_d and f_p

The range of f_d and f_p should lie between 0 and 1 by the definition of partition fractions,. The shapes of f_d and f_p depend on the distributions of the suspended sediment and the magnitude of the partition coefficient (k_d). The effects of f_d and f_p based on the two equilibrium suspended sediment profiles (Equations (3.4.6.1.1) and (3.4.6.2.1)) is studied in the following sections. The author focuses on the ranges of input parameters, which the distribution of f_d or f_p tends to uniform distribution along the water column.

5.2.2.1 Sediment equilibrium distribution in the form of exponential function

Figure 17 shows the distribution of f_p with different values of $\gamma k_d s_a/\phi$ and $\omega_s H/k_{sz}$ by Equation (3.4.6.1.1). Firstly, it should be noted that $f_d = 1 - f_p$ (Equation (2.4.4.1.3)) and thus Figure 17 also represents the distribution of f_d. From the definition of f_p and Figure 17, the overall magnitude of f_p increases as $\gamma k_d s_a/\phi$ increases. For a particular value of $\gamma k_d s_a/\phi$, the difference of f_p between the bottom and the water surface increases with increasing $\omega_s H/k_{sz}$. The figure shows that the values of f_p at the bottom (z/H = *0*) with different values of $\gamma k_d s_a/\phi$ are independent of the value of $\omega_s H/k_{sz}$. In fact, by substituting z = 0 into Equation (3.4.6.1.2a), f_p becomes:

$$f_p = \frac{\gamma k_d s_a}{\phi} \Bigg/ \left(\frac{\gamma k_d s_a}{\phi} + 1 \right) \qquad (5.2.2.1.1)$$

which is independent of the value of $\omega_s H/k_{sz}$. The author focuses on the range of values of $\gamma k_d s_a/\phi$, which the distribution of f_d or f_p tends to uniform along the water column. A tolerance value, T_{ed}, which represents the difference between the value of f_d at the bottom (z = *0*) and f_d at the top (z = *H*) is defined as follows:

$$f_d\big|_{z=0} \Big/ f_d\big|_{z=H} = T_{ed} \qquad (5.2.2.1.2)$$

$$T_{ed} = \frac{1}{k_d \dfrac{\gamma s_a}{\phi} + 1} \Bigg/ \frac{e^{H\omega_z/k_{sz}}}{k_d \dfrac{\gamma s_a}{\phi} + e^{H\omega_z/k_{sz}}}$$

$$k_d \frac{\gamma s_a}{\phi} = \frac{e^{H\omega_z/k_{sz}}(1 - T_{ed})}{T_{ed} e^{H\omega_z/k_{sz}} - 1} \qquad (5.2.2.1.3)$$

Similarly, another tolerance value, T_{ep}, is defined as follows:

$$f_p\big|_{z=H} \Big/ f_p\big|_{z=0} = T_{ep} \qquad (5.2.2.1.4)$$

$$\Rightarrow k_d \frac{\gamma s_a}{\phi} = \frac{T_{ep} e^{H\omega_z / k_{sz}} - 1}{1 - T_{ep}} \qquad (5.2.2.1.5)$$

Figure 18 shows the values of $k_d \gamma s_a / \phi$ with $\omega_s H/k_{sz}$ by substituting different values of T_{ed} in Equation (5.2.2.1.3). Each line in the figure represents the value of $k_d \gamma s_a / \phi$ required to achieve a particular tolerance, T_{ed}, for different values of $\omega_s H/k_{sz}$. Lines in the figure rapidly tend to a constant value of $k_d \gamma s_a / \phi$ as $\omega_s H/k_{sz}$ increases. The constant values of $k_d \gamma s_a / \phi$ for the five lines in Figure (18) are 0.0101, 0.0527, 0.1112, 0.1766 and 0.2502 for Ted values at 0.99, 0.95, 0.9, 0.85 and 0.8., respectively. Therefore, f_d can be considered as a constant when the value of $k_d \gamma s_a / \phi$ is smaller than the corresponding value mentioned in the above sentence. From the physical point of view, a small value of $k_d \gamma s_a / \phi$ means either the sorptive effect between the toxic substance and sediment particles is very small (i.e. k_d is very small) or the overall magnitude of suspended sediment concentration in the water column is likewise small (i.e. s_a is very small). In both situations, the toxic substance will mainly transports in dissolved form and the particulate form can be neglected.

From Equation (5.2.2.1.5), it is difficult to find a value of $k_d \gamma s_a / \phi$ to achieve a particular tolerance limit, T_{ep} for different values of $\omega_s H/k_{sz}$. In general, when $\omega_s H/k_{sz}$ is large enough, Equation (5.2.2.1.5) tends to be a simple exponential function. The required value of $k_d \gamma s_a / \phi$ to achieve the

required tolerance limit thus can only be found case by case. A large value of $k_d \gamma s_a / \phi$ represents a large sorptive capacity of the toxic substances (k_d is very large) or a high concentration of the suspended sediment. In both cases, most of the toxic substances travel in particular forms and dissolved forms can be neglected. In conclusion, the distributions of f_d and f_p should be considered when the value of $k_d \gamma s_a / \phi$ is greater than 0.1, assuming T_{ed} to be 0.9. As described in Section (5.2.1.1), the coefficients $\overline{A}_e$, $\overline{B}_e$ and $\overline{C}_e$ in Equation (3.4.6.1.7) become constant for constant values of f_d and f_p. Models 2 and 3 developed by the author thus provide perfect matches with cases when $k_d \gamma s_a / \phi$ is smaller than 0.1. Based on the ranges of k_d, γ / ϕ and s_a described in Section 5.1, the range of $k_d \gamma s_a / \phi$ lies from 10^{-4} to 1.47×10^6 and therefore it is possible to have real case applications even when the value of $k_d \gamma s_a / \phi$ is smaller than 0.1. In accordance with the above conclusion, all analyse done in later sections will only consider $k_d \gamma s_a / \phi$ above 0.1.

5.2.2.2 Sediment equilibrium distribution in the Rouse profile

For the Rouse profile given by Equation (3.4.6.2.1), Figure 19 shows the distributions of f_p with different values of $\gamma k_d s_a / \phi$ and $\omega_s / \beta \kappa u_*$. All the curves in the figure have zero value at position $z = H$, because the sediment concentration at this position is zero in the Rouse profile. Generally, the effects on f_p of $\omega_s / \beta \kappa u_*$ and $\gamma k_d s_a / \phi$ are that the overall magnitude of f_p increases as $\gamma k_d s_a / \phi$ increases and the difference of f_p between the bottom

and water surface increases as $\omega_s/\beta\kappa u_*$ increases. Based on the definition of T_{ed} (Equation (5.2.2.1.2)) given in the last section and substitution of s by Equation (3.4.6.2.1), the equation for finding the necessary magnitude of $\gamma k_d s_a/\phi$ to achieve the tolerance T_{ed} is:

$$f_d|_{z=a} / f_d|_{z=H} = T_{ed} \tag{5.2.2.2.1}$$

$$T_{ed} = \frac{1}{k_d \dfrac{\gamma s_a}{\phi} + 1}$$

$$k_d \frac{\gamma s_a}{\phi} = \frac{1 - T_{ed}}{T_{ed}} \tag{5.2.2.2.2}$$

Equation (5.2.2.2.2) is independent of $\omega_s/\beta\kappa u_*$. For T_{ed} = 0.9, the required value of $\gamma k_d s_a/\phi$ is 0.111 and in this case, f_d and f_p can be assumed as constants for $\gamma k_d s_a/\phi$ less than 0.111. Another tolerance T_{ep} is also defined for the case of the Rouse profile. However, since the value of s is always zero at $z = H$. The definition of T_{ep} is changed as follows:

$$f_p|_{z=0.9H} / f_p|_{z=a} = T_{ep} \tag{5.2.2.2.3}$$

$$\Rightarrow k_d \frac{\gamma s_a}{\phi} = \frac{1}{1 - T_{ep}} \left[T_{ep} \left(\frac{0.1a}{0.9(H-a)} \right)^{\frac{-\omega_s}{\beta\kappa u_*}} - 1 \right] \tag{5.2.2.2.4}$$

As with the Equation (5.2.2.1.5) described in the last section, it is difficult to fine a value of $k_d \gamma s_a / \phi$ to achieve a particular tolerance limit, T_{ep} for different values of $\omega_s/\beta\kappa u_*$. Thus, the required value of $k_d \gamma s_a / \phi$ can only be found case by case. In conclusion, the distribution of f_d and f_p should be

considered when the value of $k_d \gamma s_a / \phi$ greater than 0.1, assuming T_{ed} to be 0.9.

If f_d and f_p are constant and their derivatives become zero, the terms shown in Equation (3.4.5.3) become:

$$\frac{\partial \omega_s f_p c_T}{\partial z} = \omega_s f_p \frac{\partial c_T}{\partial z} \qquad (5.2.2.2.5)$$

$$\frac{\partial}{\partial z}\left((k_{sz} - k_z)\frac{\partial f_p c_T}{\partial z}\right) = f_p(\beta - 1)\left(\frac{\partial k_z}{\partial z}\frac{\partial c_T}{\partial z} + k_z \frac{\partial^2 c_T}{\partial z^2}\right) \qquad (5.2.2.2.6)$$

Combining the expressions of k_z and its derivative shown in Equations (3.4.6.2.5) and (3.4.6.2.7), can prove that the coefficients of the Governing Equation (3.4.5.3) are the same as $\overline{A}_R$, $\overline{B}_R$ and $\overline{C}_R$ in Equations (5.2.1.2.1) to (5.2.1.2.3). Therefore, Model 1 matches perfectly the above extreme cases for conservative toxic substances such as heavy metals, for further assuming k_{dp} and k_{dc} as zero and then $\overline{C}_R$ becomes zero too.

5.3 Analysis of mathematical coefficient $\overline{A}$ in Equation (3.4.5.8)

In Chapter 3, Equation (3.4.5.8) represents the transport of toxic substances by assuming instantaneous equilibrium of sorptive mechanics. The equation is further developed by assuming different sediment distribution functions in Section (3.4.6.1) and (3.4.6.2). The coefficients $\overline{A}$, $\overline{B}$ and $\overline{C}$ in the governing equation are different from coefficients in the governing equations in the developed models in Chapter 4 and they are more complex in shape. However, some analyses have been carried out in the following

sections for each coefficient, to identify cases where the coefficients can be simplified to have the same value as the corresponding coefficient value in the developed models. Coefficient $\overline{A}$ is estimated by Equation (3.4.5.9), which is dependent on the vertical dimension z and can be rewritten as follows:

$$\overline{A} = k_z\left(1+(\beta-1)f_p\right) \tag{5.3.1}$$

Since f_p depends on k_d and s, the coefficient $\overline{A}$ depends on k_z, β, k_d and s. In general, the magnitude of $\overline{A}$ is controlled by the turbulent mixing coefficients of water and sediment. $\overline{A}$ should always be positive for β lying between 0 and 2. The author assumes that the contribution to the variation of coefficient $\overline{A}$ by the term $(\beta-1)f_p$ can be neglected and can be replaced by the depth averaged of $(\beta-1)f_p$, if the maximum magnitude of $(\beta-1)f_p$ along the water depth is smaller than 0.1. This means the contribution to $\overline{A}$ by the term $(\beta-1)f_p k_z$ is less than ten percent of k_z. Since f_p must be less than 1, the magnitude of $(\beta-1)f_p$ must be smaller than 0.1 for β lying between 0.9 and 1.1. The maximum value of f_p must occur at the reference level (a). In this way, the inequality that defines the condition for the negligible contribution of $(\beta-1)f_p$ is as follows:

$$\left|(\beta-1)f_p\right|_{z=a}\Big| < 0.1 \tag{5.3.2}$$

As described in Section (5.1.3), β lies between 0 and 2. The maximum value of f_p is equal to $(\gamma k_d s_a/\phi)/(1+\gamma k_d s_a/\phi)$ for both sediment

equilibrium distributions in the form of the exponential function and Rouse profile. Thus, Equation (5.3.2) becomes:

$$\frac{|(\beta-1)|\gamma k_d s_a/\phi}{\gamma k_d s_a/\phi+1}<0.1$$

$$\Rightarrow \begin{cases}\gamma k_d s_a/\phi<1/(10\beta-11) & for \quad 1.1<\beta\le 2\\ \gamma k_d s_a/\phi<1/(9-10\beta) & for \quad 0\le\beta<0.9\end{cases} \tag{5.3.3}$$

The maximum value of $(10\beta-11)$ or $(9-10\beta)$ is 9 and thus the inequality (5.3.3) must satisfy the following inequality:

$$\gamma k_d s_a/\phi<1/9 \tag{5.3.4}$$

This result is generally the same as the results concluded in Sections (5.2.2.1) and (5.2.2.2), respectively.

Another approach to estimate the ranges of parameters that render the distribution of $\overline{A}$ to be uniform, is to calculate the depth averaged value of the difference between $\overline{A}$ and its depth averaged value in the region above the reference level. The relative different function, *DA*, is defined as follows:

$$DA=\frac{1}{H}\int_0^H\left|\left(\overline{A}-\overline{A}_{ave}\right)/\overline{A}_{ave}\right|dz \tag{5.3.5}$$

$$\overline{A}_{ave}=\frac{1}{(H-a)}\int_a^H\overline{A}\,dz \tag{5.3.6}$$

The author assumes that the depth variation of $\overline{A}$ for a particular case study can be neglected, if *DA* is less than a particular value, for example, 0.1 (10% difference). In the following section, the distributions of $\overline{A}_{ave}$ and *DA* are investigated for different values of the input parameters.

5.3.1 Sediment equilibrium distribution in the form of exponential function

Coefficient $\overline{A}_e$ estimated by Equation (3.4.6.1.8) depends on the vertical dimension z and it can be rewritten as follows:

$$\overline{A}_e = k_z\left[1+(\beta-1)\left(\frac{k_d\gamma s_a/\phi}{k_d\gamma s_a/\phi + e^{z\omega_s/H}}\right)\right] \qquad (5.3.1.1)$$

From Equation (5.3.1.1), β, k_z, k_d, and the sediment distribution are the main physical parameters that control the magnitude of $\overline{A}_e$. The author considers the Equation (5.3.1.1) as a function of β, $\gamma k_d s_a/\phi$ and $\omega_s H/k_{sz}$. A set of MatLab computer codes for Equations (5.3.5) and (5.3.6) has been developed after substituting Equation (5.3.1.1). Figure 20 shows the distributions of $\overline{A}_{ave}/k_z$ and *DA* by assuming the sediment concentration distribution in exponential form for different values of β, $\omega_s H/k_{sz}$ and $\gamma k_d s_a/\phi$. From Figures 20(a) and 20(c), for cases that β is less than 1, the overall magnitude of $\overline{A}_{ave}/k_z$ increases as $\omega_s H/k_{sz}$ increases and its overall magnitude decreases as $\gamma k_d s_a/\phi$ increases. From Figures 20(e) and 20(f), for cases that β is larger than 1, the overall magnitude of $\overline{A}_{ave}/k_z$ decreases as $\omega_s H/k_{sz}$ increases and its overall magnitude of $\overline{A}_{ave}/k_z$ increases as $\gamma k_d s_a/\phi$ increases. In general the magnitude of $\overline{A}_{ave}/k_z$ increases as β increases. For cases where β is less than 1, the minimum value of $\overline{A}_{ave}/k_z$ is equal to the value of β. For cases where β is larger than 1, the maximum value of $\overline{A}_{ave}/k_z$ is equal to the value of β.

Figures 21(b), (d), (f) and (h) show the distribution of the relative difference function *DA*. The value of *DA* decreases if the value of β is closer to 1 and *DA* should be zero for β = 1. For particular values of β and $\gamma k_d s_a/\phi$, the value of *DA* increases rapidly as $\omega_s H/k_{sz}$ increases until it reaches a maximum point and then decreases gradually as $\omega_s H/k_{sz}$ further increases when the value of $\gamma k_d s_a/\phi$ is sufficiently large, the value of DA decreases as $\gamma k_d s_a/\phi$ increases. In general, the range of *DA* lies between 0 to 0.3. For β lying between 1 and 2, the value of *DA* is maximum at β = 2 for the particular values of $\gamma k_d s_a/\phi$ and $\omega_s H/k_{sz}$.

5.4 Analysis of mathematical coefficient $\overline{B}$ in Equation (3.4.5.8)

In order to estimate the ranges of parameters that render the distribution of $\overline{B}$ to be uniform, the relative difference function, *DB*, denoting the depth averaged value of the difference between magnitude of $\overline{B}$ along the water depth and its depth averaged value, $\overline{B}_{ave}$ in the region above the reference level, is defined as follows:

$$DB = \frac{1}{H}\int_0^H \left|\left(\overline{B} - \overline{B}_{ave}\right)/\overline{B}_{ave}\right| dz \qquad (5.4.1)$$

$$\overline{B}_{ave} = \frac{1}{(H-a)}\int_a^H \overline{B}\, dz \qquad (5.4.2)$$

The author assumes that the distribution of $\overline{B}$ for a particular case study can be assumed uniform if *DB* is less than a particular value, for example, 0.1. In

the following section, distributions of $\overline{B}_{ave}$ and *DB* are investigated for different values of the input parameters.

5.4.1 Sediment equilibrium distribution in the form of exponential function

Coefficient $\overline{B}_e$ estimated by Equation (3.4.6.1.9) depends on the vertical dimension z and it can be rewritten as follows:

$$\overline{B}_e = \left(2 - \beta + 2(\beta - 1)f_p\right)f_p \frac{\omega_s}{\beta} \qquad (5.4.1.1)$$

From Equation (5.4.1.1) the settling velocity ω_s is the main physical parameter that controls the magnitude of $\overline{B}_e$. Firstly, by the following analysis, the author proves that $\overline{B}_e$ is always positive. From Equation (5.4.1.1), $\overline{B}_e$ may be negative if

$$2 - \beta + 2(\beta - 1)f_p < 0$$

For β lying between 1 and 2, the inequality can not be satisfied for all values of f_p. For β lying between 0 and 1, Equation (5.4.1.3) becomes:

$$\Rightarrow f_p > (2 - \beta)/(2(1 - \beta))$$

Since f_p must lie between 0 and 1, the condition that the above inequality can satisfy is:

$$(2 - \beta) < 2(1 - \beta)$$

$$\Rightarrow \quad \beta < 0$$

Therefore, the value of $\overline{B}_e$ must be positive for β lying between 0 and 2.

Substituting the expression of f_p (Equation (3.4.6.1.2a)), Equation (5.4.1.1) becomes:

$$\overline{B}_e = \frac{k_d \frac{\gamma s_a}{\phi}}{k_d \frac{\gamma s_a}{\phi} + e^{z\omega_z / k_{sz}}} \left[2 - \beta + \frac{2(\beta - 1) k_d \frac{\gamma s_a}{\phi}}{k_d \frac{\gamma s_a}{\phi} + e^{z\omega_z / k_{sz}}} \right] \qquad (5.4.1.2)$$

The author considers Equation (5.4.1.2) as a function of β, $\gamma k_d s_a / \phi$ and $\omega_s H / k_{sz}$. A set of MatLab computer codes for Equations (5.4.1) and (5.4.2) has been developed after substituting Equation (5.4.1.2). Figure 21 shows the distributions of $\overline{B}_{ave}$ and *DB* by assuming the sediment concentration distribution in the exponential form for different values of β, $\omega_s H/k_{sz}$ and $\gamma k_d s_a/\phi$. From Figures 21(c), 21(e) and 21(g), the overall magnitude of $\overline{B}_{ave} / \omega_s$ decreases as $\omega_s H/k_{sz}$ increases and its overall magnitude increases as $\gamma k_d s_a/\phi$ increases. The magnitudes and shapes of the distribution of $\overline{B}_{ave} / \omega_s$ shown in Figures 21(c), 21(e) and 21(g) are similar but the magnitude of $\overline{B}_{ave} / \omega_s$ decreases slightly with increasing β. Since there is no significant difference in the magnitude of $\overline{B}_{ave} / \omega_s$ between different values of β, it is clear that $\overline{B}_{ave} / \omega_s$ mainly depends on the value of ω_s and the effect of β is relatively small for β larger than 1.

Figures 21(b), 21(d), 21(f) and 21(h) show the distribution of the relative difference function *DB*. In general, *DB* decreases as $\gamma k_d s_a/\phi$ increases and increases as $\omega_s H/k_{sz}$ increases. From Figure 21(d), (f) and (h), the magnitudes and shapes for the distribution of *DB* are similar but the magnitude increases slightly with increasing β. Therefore, with β ranging from 1 to 2, the value of *DB* for particular values of $\gamma k_d s_a/\phi$ and $\omega_s H/k_{sz}$

increases gradually, and its value is the maximum at β = 2. The author assumes that the distribution of $\overline{B}_e$ is uniform for *DB* less than 0.1. For example, *DB* should not exceed 0.1 for $\omega_s H/k_{sz}$ less than 5.5 when $\gamma k_d s_a/\phi$ = 1000 and β lies between 1 and 2.

5.5 Analysis of mathematical coefficient $\overline{C}$ in Equation (3.4.5.8)

For finding the condition that the coefficient, $\overline{C}$, can be assumed as constant. A relative difference function, *DC*, denoting the depth averaged value of difference between the magnitude of $\overline{C}$ along the water depth and its depth averaged value, $\overline{C}_{ave}$, in the region above the reference level, is defined as follows:

$$DC = \frac{1}{H}\int_0^H \left|(\overline{C} - \overline{C}_{ave})/\overline{C}_{ave}\right| dz \qquad (5.5.1)$$

$$\overline{C}_{ave} = \frac{1}{(H-a)}\int_a^H \overline{C} dz \qquad (5.5.2)$$

Similar to the approach in Section (5.4), the distribution of $\overline{C}$ can be replaced by a constant value $\overline{C}_{ave}$ for a particular case study if *DC* is less than a particular value, for example, 0.1. In the following section, distributions of $\overline{C}_{ave}$ and *DC* are investigated for different values of the input parameters.

5.5.1 Sediment equilibrium distribution in the form of exponential function

Coefficient $\overline{C}_e$ estimated by Equation (3.4.6.1.10) is depended on the vertical dimension z and it can be rewritten as follows:

$$\overline{C}_e = \omega_s P_e \left(1-2(1-\beta)f_p\right) f_p f_d / (\beta H) + (k_{dc} f_p + k_{dc} f_d) \qquad (5.5.1.1)$$

The forms of f_p and f_d are shown in Equation (3.4.6.1.2). The water mixing coefficient, sediment mixing coefficient, settling velocity, decay rate of contaminant, and partition coefficient are the main parameters that affect the magnitude of $\overline{C}_e$. Generally, it is assumed that k_{dc} = k_{dp} and the term $k_{dc} f_p + k_{dc} f_d$ becomes k_{dc}, which is constant. Under this assumption, Equation (5.5.2) becomes:

$$\overline{C}_{ave} = \overline{C}_{ave}\Big|_{k_{dc}=0} + k_{dc} \qquad (5.5.1.2)$$

$\overline{C}_{ave}\Big|_{k_{dc}=0}$ is the depth averaged value of $\overline{C}$ when k_{dc} is zero. Thus, the contribution to $\overline{C}_{ave}$ by k_{dc} is linear. In these cases, most toxic substances can be considered to have no decay or with decay property and k_{dc} is zero or positive. In this respect, the value of *DC* is maximum for the case that k_{dc} is zero and the analysis for $\overline{C}_{ave}$ and *DC* at k_{dc} = 0 is shown in the following paragraphs.

A set of MatLab computer codes for Equations (5.5.1) and (5.5.2) has been developed after substituting Equation (5.5.1.1). Figure 22 shows the distributions of $\overline{C}_{ave} H / \omega_s$ and *DC* by assuming the sediment concentration distribution in the exponential form and k_{dc} = 0 for different values of β, $\omega_s H/k_{sz}$ and $\gamma k_d s_a/\phi$. From Figure 22(c), 22(e) and 22(g), the overall

magnitude of $\overline{C}_{ave}H/\omega_s$ increases as $\omega_s H/k_{sz}$ increases. From the figures, for $\gamma k_d s_a/\phi$ lying between 0.2 to 10, $\overline{C}_{ave}H/\omega_s$ increases as $\gamma k_d s_a/\phi$ increases for $\omega_s H/k_{sz}$ greater than 5. For $\gamma k_d s_a/\phi$ greater than 100, $\overline{C}_{ave}H/\omega_s$ decreases as $\gamma k_d s_a/\phi$ increases for $\omega_s H/k_{sz}$ less than 10. The magnitudes and shapes of the distribution of $\overline{C}_{ave}H/\omega_s$ shown in Figure 22(c), 22(e) and 22(g) are similar. For $\gamma k_d s_a/\phi$ lying between 0.2 to 10, the magnitude of $\overline{C}_{ave}H/\omega_s$ decreases slightly with increasing β. For $\gamma k_d s_a/\phi$ greater than 100, the magnitude of $\overline{C}_{ave}H/\omega_s$ increases slightly with increasing β. Since there is no significant difference in magnitude of $\overline{C}_{ave}H/\omega_s$ between different values of β, its magnitude mainly depends on the value of ω_s and H. Figure 22(a) shows that the value of $\overline{C}_{ave}$ can be negative for cases that β = 0.3. From Equation (5.5.1.1), the value of $\overline{C}$ can be negative if $1-2(1-\beta)f_p$ is less than zero and it is only possible for β less than 0.5. The range of the value of $\omega_s H/k_{sz}$, with negative value of $\overline{C}_{ave}$ increases as $\gamma k_d s_a/\phi$ increases.

Figure 22(b), (d), (f) and (g) show the distributions of *DC* for different values of the input parameters. Most of the values of *DC* shown in the figures are greater than 0.1 and thus the distribution of $\overline{C}$ should be considered.

5.6 Comparisons of magnitudes of coefficients $\overline{A}$, $\overline{B}$, and $\overline{C}$

In order to compare the magnitude of $\overline{A}$, $\overline{B}$, and $\overline{C}$, the author defines three dimensionless numbers that can reasonably compare the magnitudes. They are as follows:

$$N_{o1} = \overline{B}H / \overline{A} \tag{5.6.1}$$

$$N_{o2} = \overline{C}H^2 / \overline{A} \tag{5.6.2}$$

$$N_{o3} = \overline{C}H / \overline{B} \tag{5.6.3}$$

The first number (N_{o1}) is developed based on the concept of the Peclet number (Equation (5.2.1.1.1)) and is used to compare the magnitudes of $\overline{A}$ and $\overline{B}$. Number N_{o2} and N_{o3} are developed to compare the magnitudes of $\overline{A}$ and $\overline{C}$ and of $\overline{B}$ and $\overline{C}$, respectively. If the difference between two coefficients is significantly large, the distribution of the coefficient with smaller magnitude can be neglected. It can then be assumed a constant by taking the depth averaged value, or even assumed to be zero. The author assumes that one of the coefficients shown in the dimensionless numbers can be assumed as constant if the values of a dimensionless number is smaller than 0.1 or larger than 10.

5.6.1 Comparison between coefficients in Equation (3.4.6.1.11)

Equation (3.4.6.1.11) is a special case of Equation (3.4.6.1.7) by setting β = 1 described in Section (3.4.6.1). The forms of the coefficients $\overline{A}_e$, $\overline{B}_e$ and $\overline{C}_e$ in this case are:

$$\overline{A}_e = k_z \tag{5.6.1.1}$$

$$\overline{B}_e = \omega_s f_p \tag{5.6.1.2}$$

$$\overline{C}_e = \frac{\omega_s{}^2 f_d f_p}{k_z} + k_{dc} f_d + k_{dp} f_p \qquad (5.6.1.3)$$

All the above three coefficients are always positive and the forms of the three numbers are:

$$N_{o1} = \frac{\omega_s f_p H}{k_z} = P_e f_p \qquad (5.6.1.4)$$

$$N_{o2} = \frac{\omega_s{}^2 f_d f_p H^2}{k_z{}^2} + \frac{(k_{dc} f_d + k_{dp} f_p) H^2}{k_z} \qquad (5.6.1.5)$$

$$N_{o3} = P_e f_d + \frac{(k_{dc} f_d + k_{dp} f_p) H}{\omega_s f_p} \qquad (5.6.1.6)$$

in which P_e is the Peclet number mentioned in Equation (5.2.1.1.1). By assuming $k_{dc} = k_{dp}$, N_{o2} and N_{o3} become:

$$N_{o2} = P_e{}^2 f_d f_p + \frac{k_{dc} H^2}{k_z} \qquad (5.6.1.7)$$

$$N_{o3} = P_e f_d + \frac{k_{dc} H}{\omega_s f_p} \qquad (5.6.1.8)$$

Since k_z is assumed to be a constant value in Section (3.4.6.1), coefficient $\overline{A}_e$ is always constant. Hence, it is only necessary to determine the situations where the magnitudes of $\overline{B}_e$ and $\overline{C}_e$ are both much smaller than $\overline{A}_e$. All the coefficients can then be assumed to be constant. The corresponding condition to achieve the goal is to set both N_{o1} and N_{o2} less than 0.1.

From Equation (5.6.1.7), the term $k_{dc} H^2 / k_z$ is always constant and therefore the distribution of $\overline{C}_e$ can be taken as uniform, if $P_e{}^2 f_d f_p$ is less than

0.1. Based on $f_d = 1 - f_p$, it is easy to prove that the maximum value of $f_d f_p$ is 0.25. Finally, it can be found that P_e should be less than 0.632 in order to take the distribution of $\overline{C}_e$ as uniform.

The maximum value of f_p is reached at the position z = 0 and is equal to $(k_d \gamma s_a / \phi)/((k_d \gamma s_a / \phi)+1)$. Based on the conclusions made in Section (5.2.2.1), the author considers only $k_d \gamma s_a / \phi$ greater than 0.1, therefore, the minimum value of f_p at z = 0 is 1/11. By setting $N_{o1} = P_e f_p$ less than 0.1, it can be concluded that it is possible to meet the condition for P_e less than 1.1 and therefore the condition mentioned in the above paragraph is possible to meet in real life situations. A summary of the conclusions made in this section is that P_e should be less than 0.632 and the product of P_e and f_p at z = 0 should be less than 0.1.

5.6.2 Comparison of coefficients in Equation (3.4.6.1.7)

Coefficients $\overline{A}_e$, $\overline{B}_e$ and $\overline{C}_e$ shown in Equation (3.4.6.1.7) are functions of the vertical dimension z. Thus their depth averaged values are used for the estimation of the numbers N_{o1}, N_{o2} and N_{o3}. For each parameter, the author focuses on the range of parameters that the values of the numbers are less than 0.1 or greater than 10. Figure 23 shows the distributions of N_{o1} with the sediment concentration distribution in the exponential form for different values of β, $\omega_s H/k_{sz}$ and $\gamma k_d s_a/\phi$. Coefficient N_{o1} is used to compare the magnitudes of $\overline{A}_e$ and $\overline{B}_e$. The distribution of $\overline{B}_e$ can be taken as uniform for N_{o1} less than 0.1, while the distribution of $\overline{A}_e$ can be

taken as uniform for N_{o1} greater than 10. For the ranges of most input parameters, the value of N_{o1} is greater than 0.1 and the author focus on the ranges of parameters that N_{o1} is greater than 10. From the figure, the value of N_{o1} increases as $\gamma k_d s_a/\phi$ increases. From Figure 23(b), 23(c) and 23(d), N_{o1} increases as $\omega_s H/k_{sz}$ increases. It is possible that N_{o1} is larger than 10 if the value of $\gamma k_d s_a/\phi$ is sufficiently large. The minimum required value of $\gamma k_d s_a/\phi$ for N_{o1} larger than 10 decreases as β increases. From Figure 23, it can be concluded that the value of $\omega_s H/k_{sz}$ that can make N_{o1} larger than 10, must be larger than 10 for any values of $\gamma k_d s_a/\phi$ and β.

As described in Section (5.5.1), the distribution of $\overline{C}_e$ must be considered for most of input parameters. The author thus only focuses on the range of parameters that can make the value of N_{o2} and N_{o3} less than 0.1. Figure 24 shows the distributions of N_{o2} assuming the sediment concentration distribution in the exponential form and k_{dc} = 0 for different values of β, $\omega_s H/k_{sz}$ and $\gamma k_d s_a/\phi$. Coefficient N_{o2}, is used to compare the magnitudes of $\overline{A}_e$ and $\overline{C}_e$. The distribution of $\overline{C}_e$ can be taken as uniform for N_{o2} less than 0.1. From Figures 24(b), 24(c) and 24(d), N_{o2} increases as $\omega_s H/k_{sz}$ increases and decreases as $\gamma k_d s_a/\phi$ increases for β greater than 1. From Figures 24(b), (c) and (d), it can be seen that the magnitudes and shapes of the distribution of N_{o2} are similar but the magnitude increases slightly with increasing β. Therefore, with β ranging from 1 to 2, the value of

N_{o2} for particular values of $\gamma k_d s_a/\phi$ and $\omega_s H/k_{sz}$ should increase gradually, and the value of N_{o2} will be maximum at $\beta = 2$.

Figure 25 shows the distributions of N_{o3} for assuming the sediment concentration distribution in the exponential form and $k_{dc} = 0$ for different values of β, $\omega_s H/k_{sz}$ and $\gamma k_d s_a/\phi$. N_{o3} is used to compare the magnitude of $\overline{B}_e$ and $\overline{C}_e$. The distribution of $\overline{C}_e$ can be taken as uniform for N_{o3} less than 0.1. From Figures 25(b), 25(c) and 25(d), Coefficient N_{o3} increases as $\omega_s H/k_{sz}$ increases and decreases as $\gamma k_d s_a/\phi$ increases for β greater than 1. From Figures 25(b), (c) and (d), the magnitudes and shapes of the distribution of N_{o3} are similar but the magnitude increases slightly with increasing β. Therefore, with β ranging from 1 to 2, the value of N_{o3} for particular values of $\gamma k_d s_a/\phi$ and $\omega_s H/k_{sz}$ should increase gradually, and the value of N_{o3} will be maximum at $\beta = 2$.

By comparing Figures 24 and 25, it is seen that the value of N_{o2} is larger than that of N_{o3} for particular values of the input parameters and β larger than 1. Therefore, with β larger than 1, the value of N_{o3} should be smaller than 0.1 if N_{o2} is smaller than 0.1. Coefficient N_{o2} only needs to be considered for β larger than 1.

5.7 Summary of the requirements on the parameters that can simplify the governing system

In Sections (5.2) to (5.6), analysis has been done using different mathematical and physical means to ascertain the parameters requirements,

so that coefficients $\overline{A}$, $\overline{B}$ and $\overline{C}$ in the Governing Equation (3.4.5.8) can be simplified. In this section, the conclusions made in the previous sections are re-inforced.

In Section (5.2.1), the distribution of suspended sediment concentrations has been studied. It is concluded that the distribution of the suspended sediment concentration, given by Equation (3.4.6.1.1), can be assumed to be a uniform distribution if $\omega_s H / k_{sz}$ is less than 0.1 or greater than 20. The coefficients $\overline{A}_e$, $\overline{B}_e$ and $\overline{C}_e$ in Equation (3.4.6.1.7) then become constant. Therefore, Models 2 and 3 developed by the author in Chapter 4 are perfect matches with such cases. The sediment concentration distribution in the form of the Rouse profile given by Equation (3.4.6.2.1) can also be assumed to be a uniform distribution if $\omega_s / \beta \kappa u_*$ is less than 0.02 or greater than 5. Hence, Model 1 developed by the author in Chapter 4 is a perfect match for conservative toxic substance cases ($k_{dc} = k_{dc} = 0$).

In Section (5.2.2), the distributions of the partition fractions have been studied. It is concluded that the distribution of f_d and f_p can be assumed to be constant for $k_d \gamma s_a / \phi$ less than 0.1 and $T_{ed} = 0.9$. For sediment concentration distribution in the exponential form shown in Equation (3.4.6.1.1), f_d and f_p can be assumed as constants for $k_d \gamma s_a / \phi$ larger than $(T_{ep} e^{H\omega_z / k_{sz}} - 1)/(1 - T_{ep})$ (Equation (5.2.2.1.5)). For sediment concentration distribution in the form of the Rouse profile shown in Equation (3.4.6.2.1), f_d and f_p can be assumed to be constants for $k_d \gamma s_a / \phi$ larger than the value of

$k_d \gamma s_a / \phi$ calculated by Equation (5.2.2.2.4). The value of T_{ep} can be assumed to be 0.9. Hence, coefficients $\overline{A}_e$, $\overline{B}_e$ and $\overline{C}_e$ in Equation (3.4.6.1.7) become constant and Models 2 and 3 match with such cases perfectly.

In Section (5.3), the distribution of the coefficient $\overline{A}$ has been studied. $\overline{A}$ can be taken as constant for β lying between 0.9 and 1.1. $\overline{A}$ can also be assumed constant for $k_d \gamma s_a / \phi$ satisfying the inequality (5.3.3). In Section (5.3.1), the estimation for coefficient $\overline{A}_e$ by Equation (3.4.6.1.8) is done using the relative difference function *DA* (Equation (5.3.5)). $\overline{A}_e$ can be assumed constant for *DA* less than 0.1. For β lying between 1 and 2, the value of *DA* is maximum at the case β = 2 for particular values of $\gamma k_d s_a/\phi$ and $\omega_s H/k_{sz}$ and Figure 20(h) shows the distribution of *DA* for β = 2.

In Section (5.4), the distributions of the coefficients $\overline{B}$ and $\overline{B}_e$ defined by Equation (3.4.6.1.9) are estimated by the relative difference function *DB* (Equation (5.4.1). Therefore, with β ranging from 1 to 2, the value of *DB* for particular values of $\gamma k_d s_a/\phi$ and $\omega_s H/k_{sz}$ should increase gradually, Figure 21(h) shows that the value of *DB* will be the maximum for β = 2.

In Section (5.5), the distributions of the coefficient $\overline{C}$ and $\overline{C}_e$ defined by Equation (3.4.6.1.10) are estimated by the relative difference function *DC* (Equation (5.5.1). However, no range of the parameters can be found that makes *DC* less than 0.1.

In Section (5.6), comparisons between the magnitudes of coefficients $\overline{A}$, $\overline{B}$ and $\overline{C}$ are made at the case that β=1. In conclusion, coefficients in

Equation (3.4.6.1.11) can be taken as constants if the value of P_e is less than 0.632 and the product of P_e and f_p at $z = 0$ less than 0.1.

In Section (5.6.2), the magnitudes of coefficients $\overline{A}_e$, $\overline{B}_e$ and $\overline{C}_e$ in Equation (3.4.6.1.7) are compared by the analysis of three numbers, N_{o1}, N_{o2} and N_{o3} (Equation (5.6.1), (5.6.2) and (5.6.2)). Figure 23 shows that it is possible for N_{o1} to be larger than 10 for $\omega_s H/k_{sz}$ equal to 10 or above and $\overline{A}_e$ can be taken as constant for N_{o1} larger than 10. After analyzing numbers N_{o2} and N_{o3} with β larger than 1, the value of N_{o3} should be smaller than 0.1 if N_{o2} is smaller than 0.1. It is only necessary to consider N_{o2} for β larger than 1 and $\overline{C}_e$ can be considered as constant for N_{o2} larger than 10.

Since the analysis in Section (5.6.2) only shows situations where coefficients $\overline{A}_e$ and $\overline{C}_e$ can be assumed to be constants. The analysis of $\overline{B}_e$ in Section (5.4.1) should also be applied at the same time in order to assuming all coefficients in constant values in the Governing Equation (3.4.6.1.7).

5.8 Relations between parameters in the governing system and in the developed models

In the previous sections, analysis has been done to identify the range of parameters such that the governing system can be further simplified. The developed models in chapter 4 can then be used to simulate the transport of toxic substances. In this section, the relationship of parameters and coefficients in the governing system and developed models are studied. The

contribution to the transport of toxic substances of a particular physical or chemical parameter is investigated based on the analyses shown in Chapter 4 and Chapter 5.

5.8.1 Relations between coefficients in governing Equation (3.4.6.1.7) and coefficients in Model 2

The coefficients of the governing Equation (3.4.6.1.7) and that of governing equation of Model 2 are compared. The relationship between coefficients in Equation (3.4.6.1.7) are $m = c_T$, $k_{mz} = \overline{A}_e$, $\omega = \overline{B}_e$ and $r_m = -\overline{C}_e$. Therefore, the following dimensionless variables in Model 2 become:

$$K = \overline{A}_e / \overline{B}_e H = 1/N_{o1} \tag{5.8.1}$$

$$R = -H\overline{C}_e / \overline{B}_e = -N_{o3} \tag{5.8.2}$$

Based on the sensitivity analysis described in Section (4.6.4), the overall toxic substance concentration increases as K increases in both the initial and final states of the distribution. Therefore, the overall toxic substance concentration decreases as N_{o1} increases. Based on the analysis in Section (5.6.2), the value of N_{o1} increases as $\gamma k_d s_a/\phi$ increases (Figure 23) and the overall toxic substance concentration decreases as $\gamma k_d s_a/\phi$ increases. In conclusion, the toxic substance concentration decreases as the value of the partition coefficient (k_d) increases. A larger value of k_d means that toxic substances are being sorbed more easily onto the sediment particles. The settling phenomenon of sediment particles makes the particulate toxic substance settles to the bottom layer of the water column at a faster rate than the dissolved component. Therefore, the overall transportation rate of toxic

substances from the water column to the bottom layer is faster for cases with a larger value of k_d and the overall concentration of toxic substances is smaller. From Figures 23(b), 23(c) and 23(d), N_{o1} increases as $\omega_s H/k_{sz}$ increases for β larger than 1. In this way, the concentration of toxic substances decreases as the value of the sediment settling velocity (ω_s) increases or the value of the sediment mixing coefficient (k_{sz}) decreases for β larger than 1. A larger value of ω_s represents the fact that the particulate toxic substance settles to the bottom layer at a faster rate. This makes the overall concentration of toxic substance decreases at a faster rate. A larger value of the turbulent mixing coefficient represents a rapider contaminant mixing in the water column and helps toxic substances to be maintained in the water column instead of settling on the bottom layer. Therefore, the overall concentration increases with the increase in the turbulent mixing coefficient.

Based on the sensitivity analysis described in Section (4.6.1), the overall concentration of toxic substances decreases with time for a negative value of R and increases with time for a positive value of R. In Section (5.4.1), it has been shown that $\overline{B}_e$ is always positive. Figure (22) shows that the depth averaged value of $\overline{C}_e$ is positive in most situations. Therefore, the value of R is negative in most situations considered in the analysis. From analysis described in Section (5.6.2), N_{o3} increases as $\omega_s H/k_{sz}$ increases and decreases as $\gamma k_d s_a/\phi$ increases for β greater than 1. Hence, the concentration of toxic substance decreases at a faster rate as the value of

the sediment settling velocity (ω_s) increases or the value of the sediment mixing coefficient (k_{sz}) decreases for β larger than 1. The concentration of toxic substances decreases at a faster rate as the value of the partition coefficient or reference level concentration increases. The value of N_{o3} increases slightly with increasing β for β larger than 1 and therefore the concentration of toxic substances decreases at a faster rate as β increases. It is obvious that the value of R decreases as the decay terms k_{dc} and k_{dp} increases. Thus, the concentration of toxic substances decreases more rapidly as k_{dc} and k_{dp} increases.

5.8.2 Relations between coefficients in the boundary condition of Equation (3.4.7.5) and coefficients in the boundary condition of Model 3 at the sediment water interface

The coefficients in the boundary condition (Equation (3.4.7.5)) and those in the boundary condition at $z = 0$ of Model 3 are compared. However, a comparison between coefficients in the governing Equation (3.4.6.1.7) and those in the governing equation of Model 3 is also needed. The relationship between some parameters are $m = c_T$, $k_{mz} = \overline{A}_e$, $r_m = -\overline{C}_e$ and $u = -\overline{B}_e$. In this way, b_1 should be equal to $\upsilon_f f_d + \phi f_p + 2\frac{1-\beta}{\beta} f_d f_p \omega_s$. If it is assumed $\gamma_{cb} = \gamma_{pb}$, then $d_2 = \gamma_{cb}$ and $b_2 = \upsilon_f c_a + \gamma p_a$. From the analysis of d_2 in Section (4.9.3), the toxic substance input from the boundary decreases as time increases and is close to zero for a significantly large value of time if a positive value of $d_2 = \gamma_{cb}$ is applied. The concentration decreases more

rapidly when a larger γ_{cb} is used. From the physical point of view, a positive γ_{cb} means that the toxic substance input from the boundary will decay with time and the entrainment flux from the boundary decreases with time. In general, the overall concentration at a particular time is smaller for cases with a larger value of γ_{cb}.

Table 2: Settling velocity for different particle sizes

Class Name	Size Range (mm)	Settling velocity range (cm/s)
Clay	0.002-0.006	0.00036 ~ 0.0032
Fine Silt	0.006-0.02	0.0032 ~ 0.034
Coarse Silt	0.02-0.06	0.034 ~ 0.3
Fine Sand	0.06-0.2	0.3 ~ 2.5
Medium Sand	0.2-0.6	2.5 ~ 8.5
Coarse Sand	0.6-2	8.5 ~ 20
Fine Gravel	2-6	20 ~ 35

Figure 15: Distribution of sediment by Equation (3.4.6.1.1) with different values of $\omega_s H / k_{sz}$

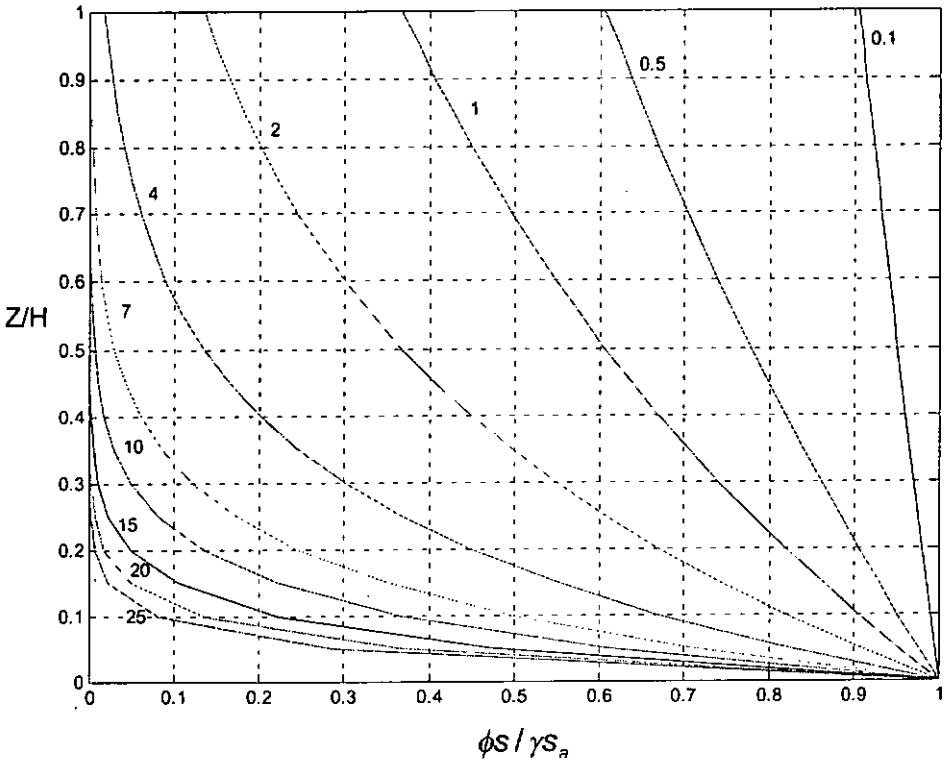

Figure 16: Distribution of sediment by Equation (3.4.6.2.1.) for different values of $\omega_s / \beta\kappa u_*$ and $a = 0.1$

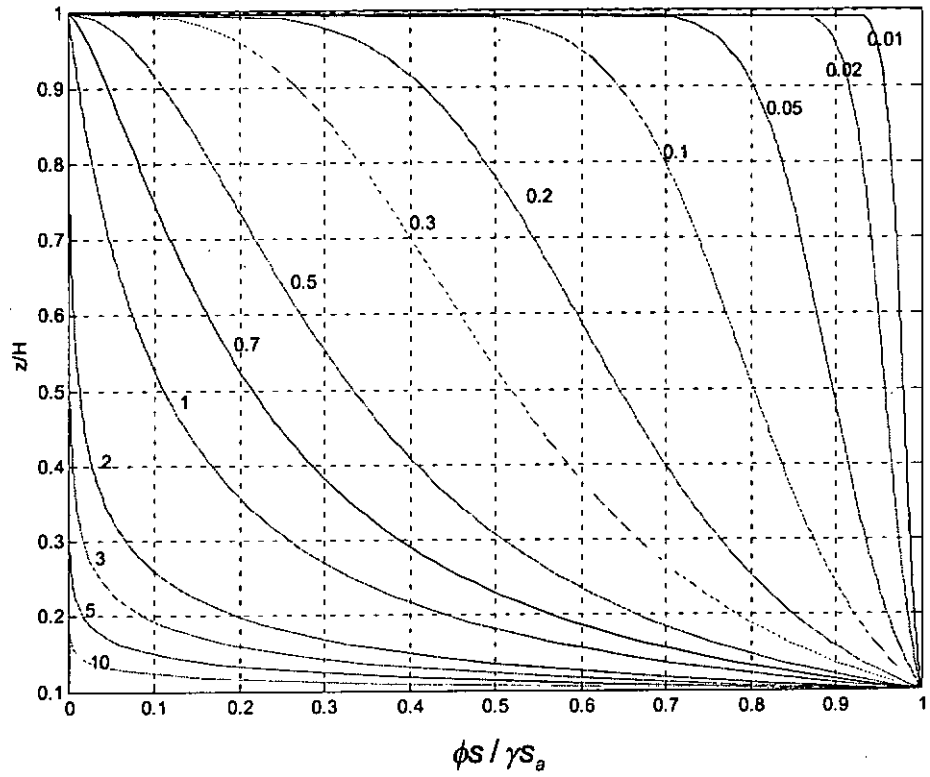

Figure 17: Distribution of f_p with different values of $\gamma k_d s_a/\phi$ and $\omega_s H/k_{sz}$ and with sediment distribution in exponential form Equation (3.4.6.1.1)

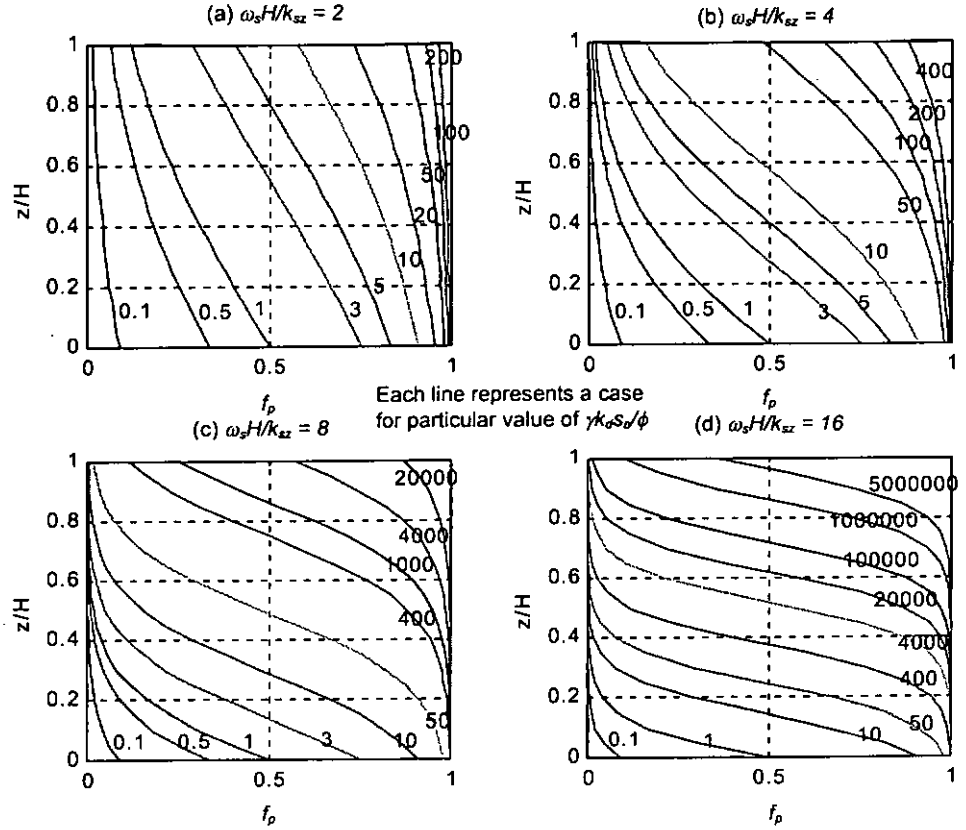

Figure 18: Variation of the values of $k_d \gamma s_e / \phi$ with $\omega_s H/k_{sz}$ by substituting different values of T_{ed} in Equation (5.2.2.1.3)

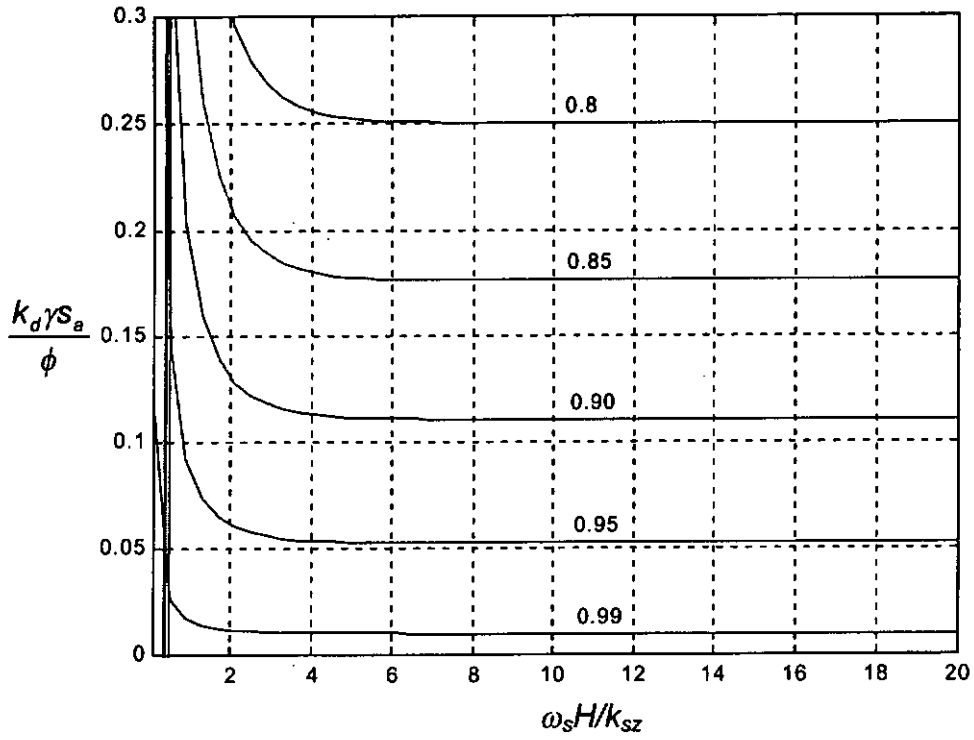

Figure 19: Variation of the distribution of f_p with different values of $\gamma k_d s_e/\phi$ and $\omega_s/\beta\kappa u_*$ with sediment distribution in Rouse profile (3.4.6.2.1)

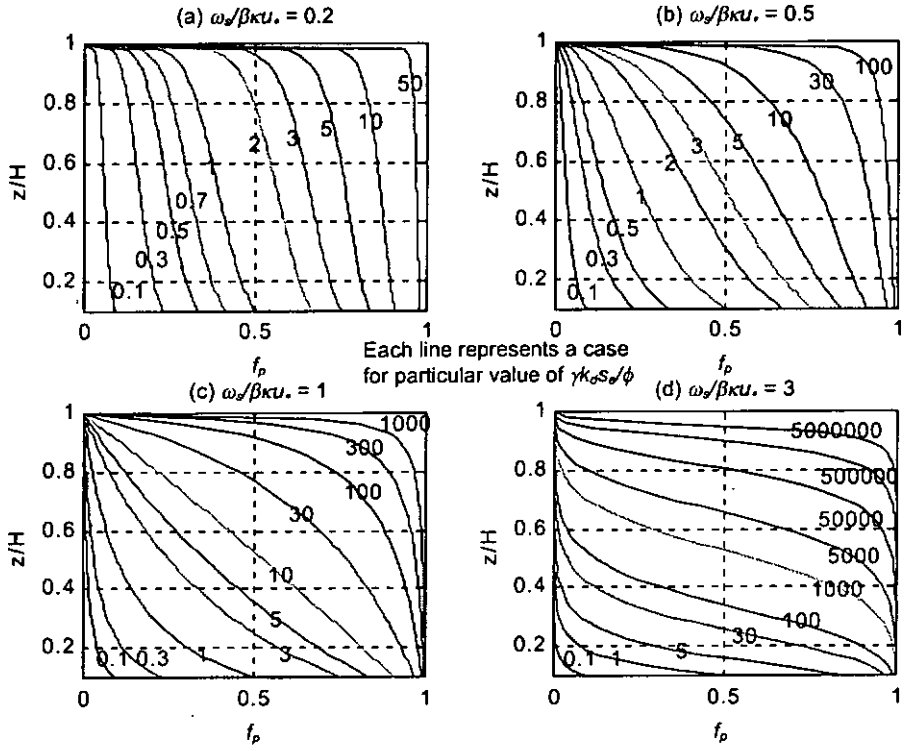

Figure 20: Distributions of $\overline{A}_{ave}/k_z$ and DA assuming sediment concentration distribution in exponential form for different values of β, $\omega_s H/k_{sz}$ and $\gamma k_d S_a/\phi$.

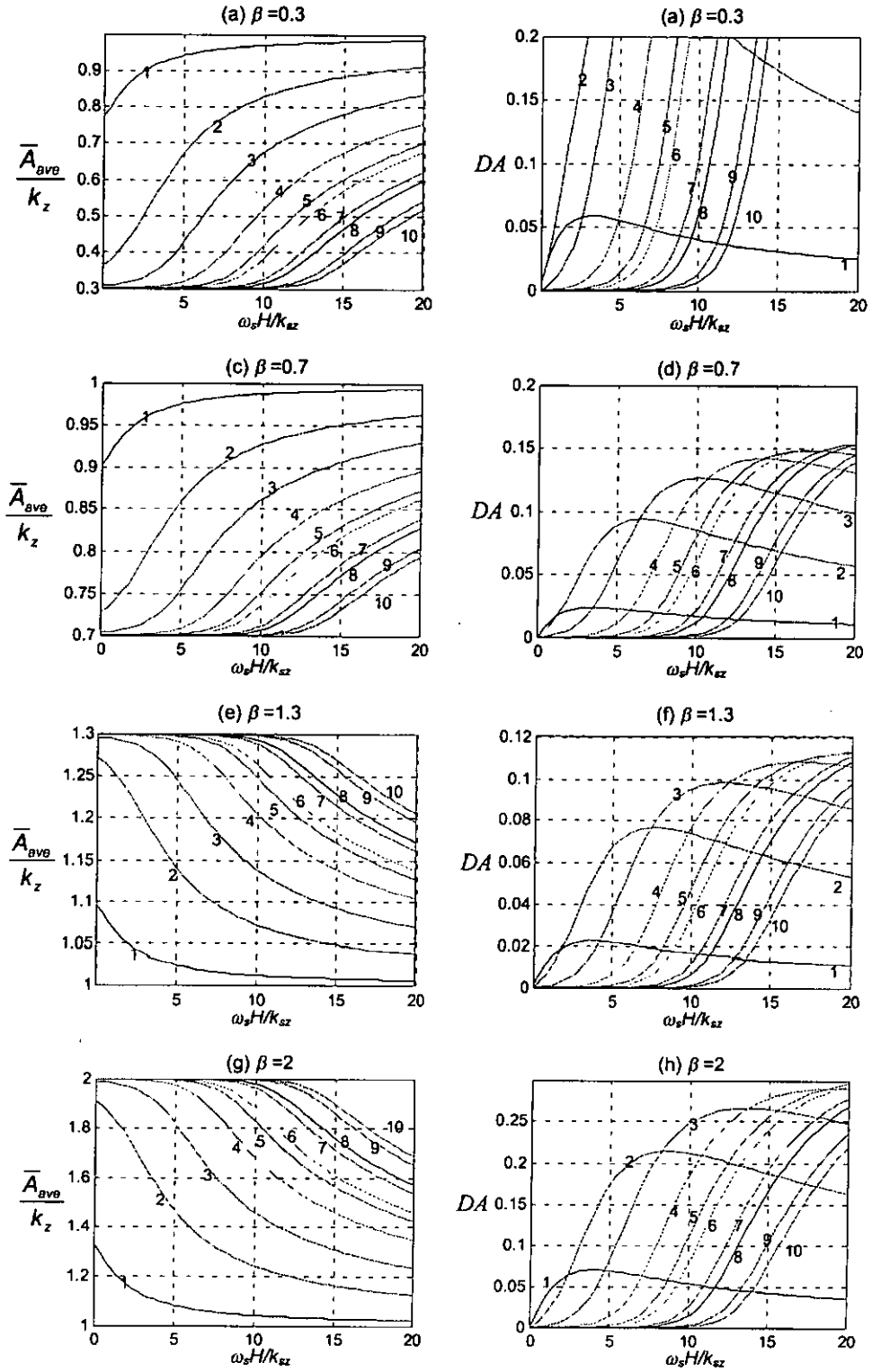

Lines with numbers from 1 to 10 represent values of $\gamma k_d S_a/\phi$ = 0.5, 10, 100, 1000, 5000, 10000, 50000, 100000, 500000 and 1000000 respectively.

Figure 21: Distributions of $\overline{B}_{ave}/\omega_s$ and DB assuming sediment concentration distribution in exponential form for different values of β, $\omega_s H/k_{sz}$ and $\gamma k_\sigma s_a/\phi$.

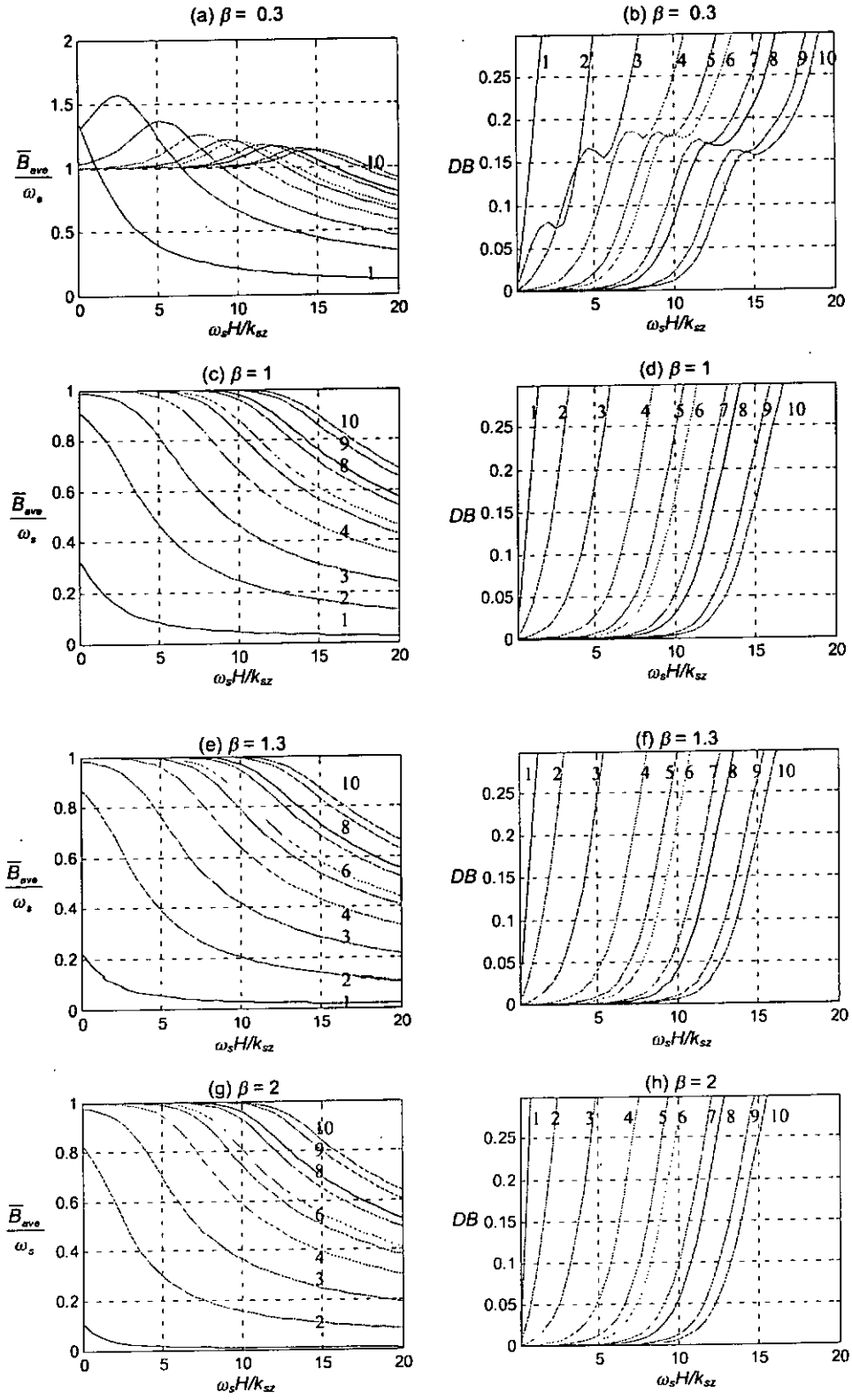

Lines with numbers from 1 to 10 represent values of $\gamma k_\sigma s_a/\phi$ = 0.5, 10, 100, 1000, 5000, 10000, 50000, 100000, 500000 and 1000000 respectively.

Figure 22: Distributions of $\overline{C}_{ave}H/\omega_s$ and DC assuming sediment concentration distribution in exponential form and k_{dc} = 0 for different values of β, $\omega_s H/k_{sz}$ and $\gamma k_d s_e/\phi$.

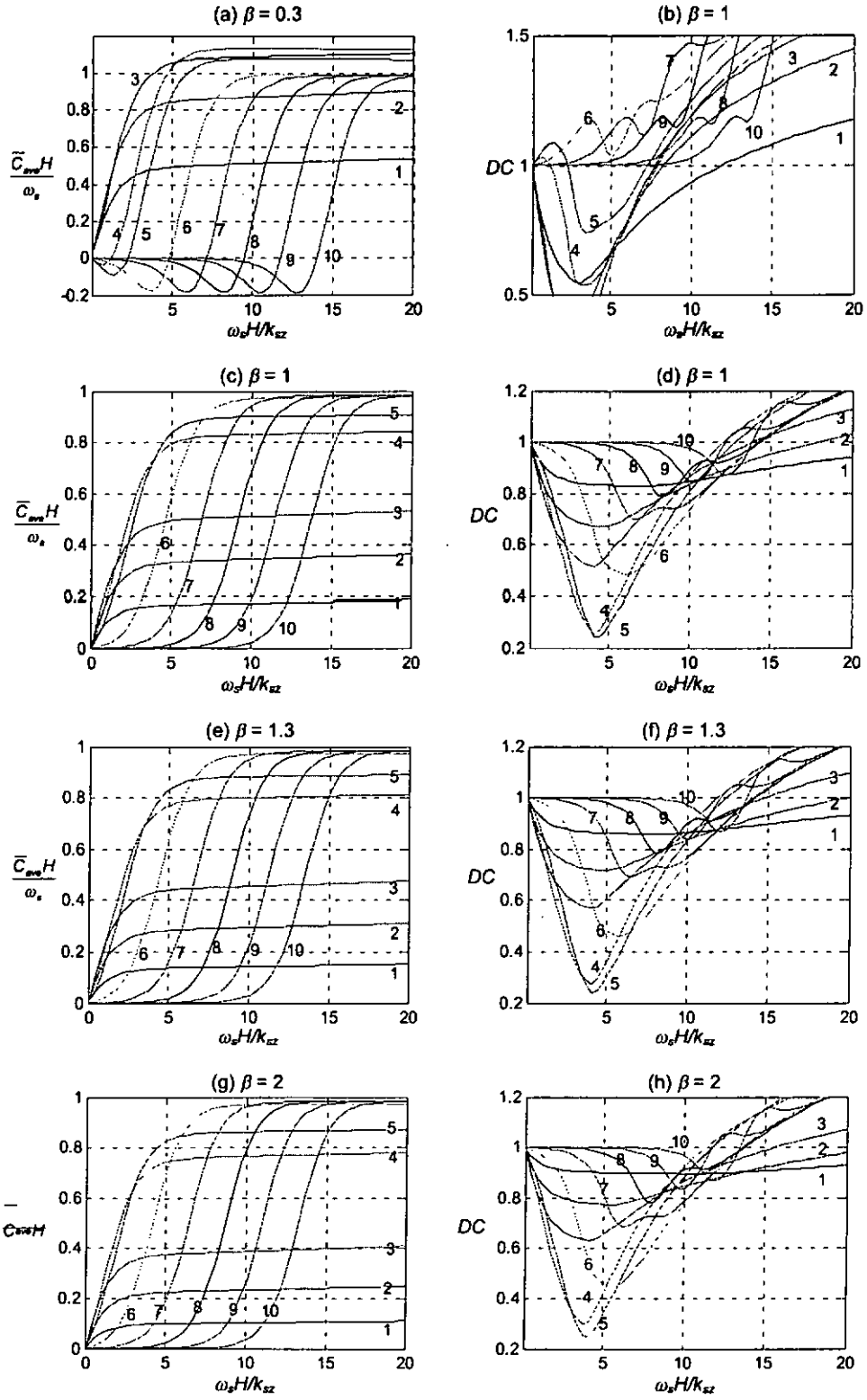

Lines with numbers from 1 to 10 represent values of $\gamma k_d s_e/\phi$ = 0.2, 0.5, 1, 5, 10, 100, 1000, 10000, 100000 and 1000000 respectively.

Figure 23: Distributions of N_{o1} for assuming sediment concentration distribution in exponential form for different values of β, $\omega_s H/k_{sz}$ and $\gamma k_d s_e/\phi$.

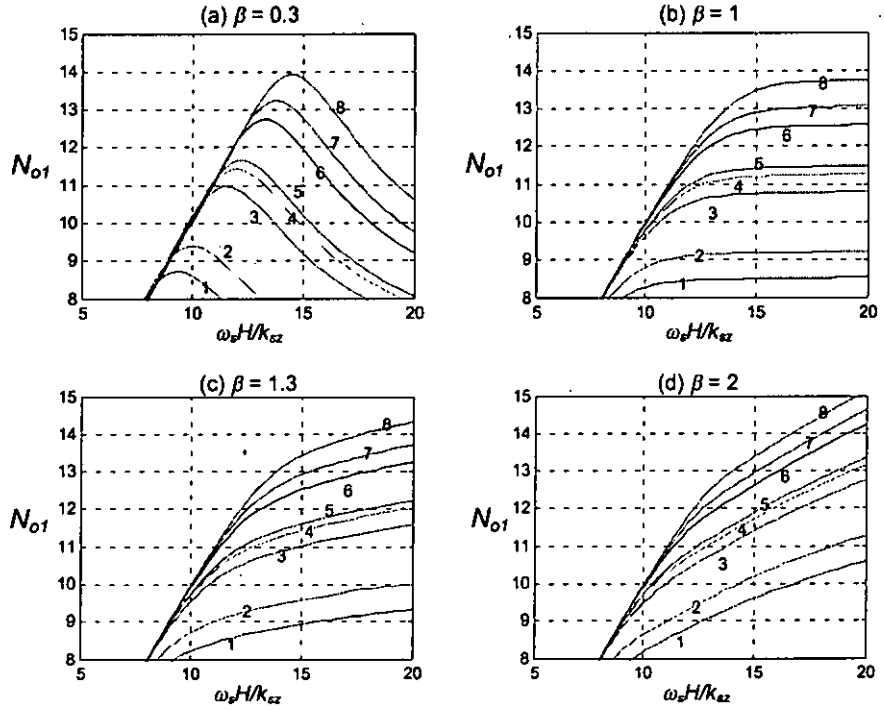

Lines with numbers from 1 to 8 represent values of $\gamma k_d s_e/\phi$ = 5000, 10000, 50000, 80000, 100000, 300000, 500000 and 1000000 respectively.

Figure 24: Distributions of N_{o2} for assuming sediment concentration distribution in exponential form and k_{dc} = 0 for different values of β, $\omega_s H/k_{sz}$ and $\gamma k_d s_e/\phi$.

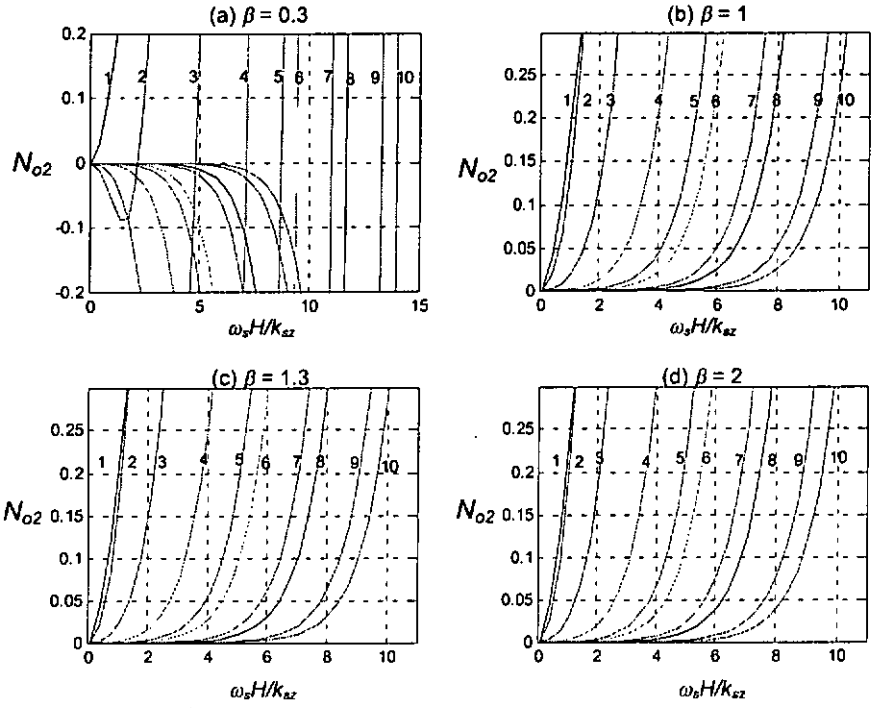

Lines with numbers from 1 to 10 represent values of $\gamma k_d s_e/\phi$ = 0.5, 10, 100, 1000, 5000, 10000, 50000, 100000, 500000 and 1000000 respectively.

Figure 25: Distributions of N_{o3} for assuming sediment concentration distribution in exponential form and $k_{dc} = 0$ for different values of β, $\omega_s H/k_{sz}$ and $\gamma k_d s_a/\phi$.

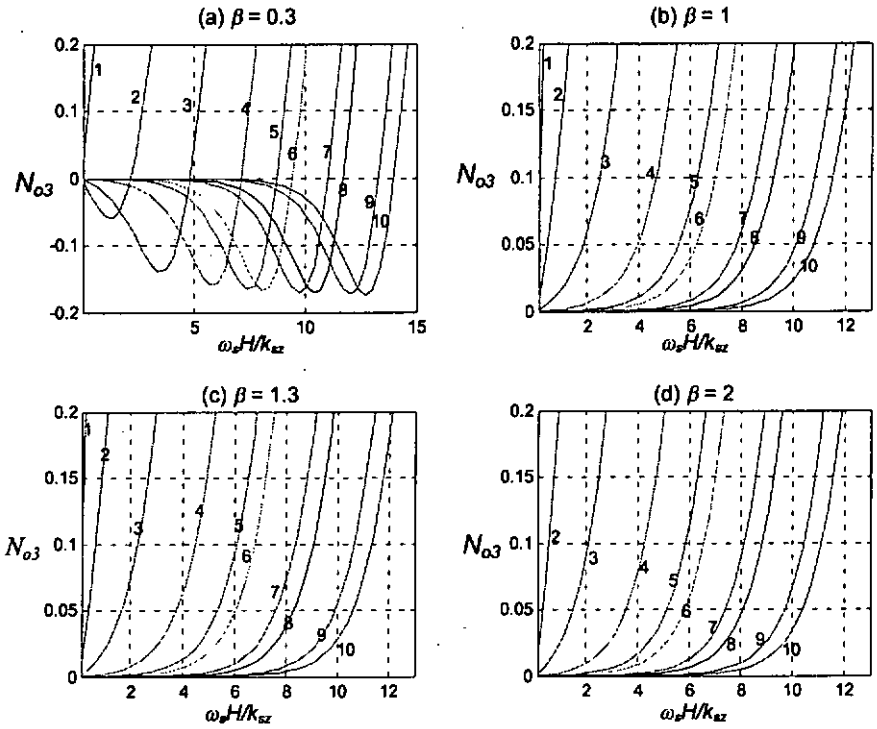

Lines with numbers from 1 to 10 represent values of $\gamma k_d s_a/\phi$ = 0.5, 10, 100, 1000, 5000, 10000, 50000, 100000, 500000 and 1000000 respectively.

Chapter 6: Case studies

The developed models in Chapter 4 are particular cases of the solutions of ADE. Therefore the developed models are not only useful for the simulation of the transport of toxic substances in the water column, they are also useful for the simulation of the sediment transport and other contaminants in different environments, such as in soil layers. In this chapter, the models are used to simulate the transport of sediment and chemicals in different environments to show the possible applications of the models.

6.1 Application of Model 1 to sediment transport

The solution form of Model 1, which allows the inputting of an arbitrary initial sediment concentration distribution, was used to simulate an experimental case (data set CS21) described in Jobson and Sayre (1970). In the experiment, coarse sediment particles were discharged continuously from a line source located near the water surface into a fully developed channel flow. The channel had a fixed bed covered with relatively large rectangular wooden cleats as roughness elements. Thus, there was no sediment source from the channel bed. The flow and sediment discharge rates were adjusted in such a way that, the deposition and resuspension of particles reaching the bed could be studied.

Some former research studies used numerical models to simulate the experimental case presented by Jobson and Sayre (1970), such as Celik and Rodi (1988) and Wai and Lu (1999). The model presented by Wai and Lu

(1999) was chosen to compare with the result generated by Model 1. Wai and Lu's (1999) model is a two-dimensional, time varying advection-dispersion model. It assumes a constant value of settling velocity (ω_s) and a parabolic distribution function of the vertical mixing coefficient (k_{sz}). The experiment, however, was a steady state transport of sediment particles and the numerical model was reduced to a two-dimensional steady state model. In order to simulate the rigid bottom that does not provide any sediment source used in the experiment, Wai and Lu's (1999) model used the following boundary condition:

$$k_{sz}\frac{\partial s}{\partial z}+\omega_s s\Big|_{z=0}=\begin{cases}\omega_s(s-s_a)\big|_{z=0} & \text{for } s\geq s_a\\ 0 & \text{for } s<s_a\end{cases} \qquad (6.1.1)$$

Model 1 is a one-dimensional, time varying model and thus it is necessary to transform the variable time, *T*, to horizontal distance, *X*. Using $x=\overline{u}t$, in which $\overline{u}$ is the depth averaged flow velocity in the *x* direction, the variable T in Model 1 is transformed to $X=\varepsilon x/H$ in which $\varepsilon=\beta\kappa u_*/\overline{u}$. Using the information provided by Wai and Lu (1999), the magnitudes of the input parameters chosen for this study are $\varepsilon=0.05376$, $\lambda=1.171875$, $A=0.05$ and $s_a=0.5645kg/m^3$. The initial distribution profile is a profile simulated by the numerical model of Wai and Lu (1999). The profile generated by the numerical model provided many more data points than the experimental one which consists of only seven data. In the simulation, the concentration profile taken from the numerical model of Wai and Lu (1999) at travelling distance $x/H=4$ is used as the input arbitrary initial sediment

distribution. This generates, in turn, concentration profiles at other travelling distances. Figure 26 plots the analytical solution, numerical results of Wai and Lu (1999) and the experimental data of Jobson and Sayre (1970). Calibrations of the physical parameter *D* for each traveling distance are required to obtain closer agreement between the analytical solutions and the experimental data. The reason for the need of the calibration process is the difference of the bottom boundary conditions between Model 1 and the model used in Wai and Lu's (1999) research. Wai and Lu (1999) assumed that there was no net sediment flux from bed layer until the concentration at the bed layer reached the value of the reference level concentration. However, Model 1 always assumes net sediment flux from bed layer. The boundary condition of Model 1 is ideal for simulating cases with a loose sediment layer on the channel bottom but not for a rigid bottom. In Model 1, the parameter *D* represents the ratio between the deposition velocity and the resuspension velocity of sediment at the water-sediment interface (reference level). Thus, choice of *D* as the tuning factor is the most satisfactory, in view of the physical difference between the two models. This indicates that the closed form solutions can reveal the unsteadiness of the exchange processes at the sediment-water interface.

6.2 Application of Model 3 to transport of organic compounds in soil layers

Model 3 is applied to simulate the modeling results given by Prakash (2000). In the paper, a model was developed to simulate the fate of

trichloroethylene, a volatile organic compound through vadose and saturated soil zones. Model 3 has been simplified by two different assumptions and Figure 27 shows the assumptions. It is first assumed that the soil properties in vadose (above water table) and saturated (below water table) zone are the same. The model is simplified to one in which contaminants are input from the ground level (z = $0m$). There is no net flux from the bottom layer. The total thickness of vadose and saturated soil zones is assumed to be twice the 9.14m depth where the water table is located. This assumption is close to the analytical model used in Prakash (2000) which simulated the fate of the contaminant in the vadose zone. The major difference between the two models is that the model used in Prakash (2000) assumes an infinity depth of soil, with a concentration of zero at the infinity level.

In assumption 2, different soil properties between the two zones are considered. Model 3 was used to generate the concentration profile in the vadose zone. At the water table, the net flux through the two zones was only contributed by contaminant transport from vadose to saturated zones.

Based on the above simplification, the input of b_1, b_4, m_4 and d_4 in Model 3 should be zero. Following Prakash (2000), the values of the following input parameters in Model 3 are the same under both assumptions:

$k_{mz} = (0.001426 m^2/day)/1.5$, $u = (0.00156 m/day)/1.5$, $r_m = -0.00112/d$
$b_2 = (0.00156 m/day)/1.5$, $m_2 = 1100 mg/L$, $d_2 = 0.000419/d$, $m_{l0} = 0$

In assumption 1, $H = 18.28m$ and $b_3 = 0$ while in assumption 2, $H = 9.14m$ and $b_3 = (0.00156 m/day)/1.5$.

Figure 1 in Prakash's (2000) paper shows the concentration with time at the level z = 9.14m. Model results have been generated under both assumptions and Figure 28 shows those comparisons of the results.

The modeling results have similar shapes to that of Prakash (2000) but are smaller in magnitude. This is in line with the boundary condition used by Prakash (2000):

$$m(0,t) = m_2 e^{-d2t} \qquad (6.2.1)$$

The model in Prakash (2000) assumes that the concentration at the boundary is initially equal to m_2 and decays with time. The concentration at the boundary in Model 3 starts from zero and its maximum value does not always reach the magnitude m_2. The contaminant input from the boundary in Prakash's model is larger than that from Model 3, resulting in higher concentrations. Figure 31 compares the concentration profiles at z=0 between the two models. The concentration profiles under the two different assumptions at the boundary are almost the same.

In order to reduce the difference between the two models, some calibration must be carried out. Minor adjustments of the overall decay coefficient at source (d_2) and retardation factor in Prakash's model are made for calibration. In this way, value of the retardation factor is changed thus affecting the input values of u, k_{mz}, b_2 and b_3 in the two assumptions for calibration. Both assumptions then give results that agree with those of Prakash (2000) as shown in Figure 32. The calibrated retardation factors for assumptions 1 and 2 are 1.35 and 1.45, respectively. The retardation factor

in the model represents the effect of contaminant sorption by soil. Generally, a larger retardation factor, which implies a higher sorption rate, has the effect of slowing down the entire process of pollutant migration. Thus smaller retardation factors are assumed to speed up the transport of the contaminant.

Figures 29 and 30 show the concentration profiles along the soil depth under the two assumptions. Generally, the differences between them are small and the concentration profiles under assumption 1 have a slightly higher magnitude. It can be observed from Figure 29 that the contaminant settles near the bottom level (depth close to 18.28m) because the model assumes that there is no contaminant flow throughout the bottom layer.

6.3 Application of Model 3 to contaminated mud dumping at East Sha Chau (ESC)

In East Sha Chau, there are several excavated pits, which are used for collecting contaminated mud produced from different construction projects. Mud contaminated by Lead, Copper and others pollutants is dredged from Rambler Channel due to the development of the Tsing Yi Container Terminal Port 9 (CT9). The contaminated mud is then dumped to the aforementioned pits. In this case study, Lead (Pb) is chosen as the toxic substance of interest and Model 3 is used to simulate the fate of the toxic substance due to the marine dumping.

When a hopper barge arrives at the ESC dumping pit, it will rapidly open the bottom door and dispose the dredged contaminated mud. Thus, a large amount of contaminated mud is discharged from the water surface into the

water column in a short period. Figure 33 shows the various processes involved.

As described in Chapter 3, the governing equation for the fate of Pb can be described by Equation (3.4.5.8). Also, Equation (3.4.7.4) is used to describe the boundary condition of the problem at the sediment-water interface. At the water surface, Equation (3.4.7.8) is used with an additional term representing the loading due to the marine dumping. Equation (2.4.4.1.1) is the expression for the partition fractions for toxic substances.

With reference to the Environmental Impact Assessment report for disposal of contaminated mud in ESC Marine Borrow Pit (Civil Engineering Department of HKSAR, 1997, p.19), the water depth (H) of the dumping pit can reach 17m at some area. In this case study, H is set to 15m. The report also (Civil Engineering Department of HKSAR, 1997, (p.20)) mentions that the magnitude of the depth averaged flow velocity ($\bar{u}$) is generally less than 0.4m/s but it can reach a maximum of 1.5m/s. In the study, three values of $\bar{u}$ (0.2, 0.6 and 1m/s) are used to calculate the toxic substance concentration profiles under different tidal conditions.

The Environmental Protection Department of HKSAR (EPD) regularly monitors the marine water and marine sediment qualities in different areas of Hong Kong. With reference to the raw data of marine sediment water quality gathered between 1997 and 2001, downloaded from the EPD website (www.info.gov.hk/epd/), the data collected at the two closest monitoring stations near ESC in the Rambler Channel, namely VS9 and V210, are used to determine some essential parameters in this case study. It is assumed that

the average values of the measured data at the two stations can adequately represent the corresponding conditions in the Rambler Channel. The average concentration of Pb in the contaminated mud from the EPD data is 67.9mg/kg. Since the total mass of heavy metal is conservative in the environment (Schnoor, 1996, p.382). The values of k_{dp}, k_{dc} and υ_v in Equation (3.4.5.11) and Equation (3.4.7.8) can be set to zero. As described in Section 5.1.5, the value of the partition coefficient (k_d) for Pb can be up to 10^7L/kg. In the study, a value of 10^6L/kg is assumed.

The data from EPD has provided the size fractions of sediments in each sediment sample, which generally consists of particles with sizes less than 63μm. The average size fraction of the sediments that have sizes less than 63μm is 90.15%. It is assumed that the distribution of sediment follows the Normal Distribution. The value in Standard Normal Distribution for 90.15% less than that value is 1.2903 and the following equation is formed:

$$-1.290377\sigma_d = 63\mu m - \bar{x} \qquad (6.3.1)$$

Hence, $\bar{x}$ and σ_d are the mean and the standard deviation of the sediment distribution. In order to find such values, it is also assumed that 0.1% of sediment is smaller than 0.001μm and the corresponding value in Standard Normal Distribution is –3.09024. Thus:

$$-3.09024\sigma_d = 0.001\mu m - \bar{x} \qquad (6.3.2)$$

After solving Equation (6.3.1) and Equation (6.3.2), $\bar{x}$ and σ_d are 44.4μm and 14.4μm, respectively. Finally, the value of the settling velocity (ω_s) calculated by Equation (2.1.2.3a) assuming $\gamma_s = 2.65\gamma_w$ and T_e = 20°C, is 0.001775m/s.

As described in Sections 2.1.4 and 2.1.5, the deposition velocity (ϕ) and entrainment velocity (γ) of sediment at the water-sediment interface can be set equal to the settling velocity, 0.001775m/s.

In this case study, a hopper barge 57m long and 13m wide is considered. It is assumed that the area for disposal of the hopper barge is 45m long and 10m wide. The maximum allowable loading of the hopper barge is 1280m^3 of water. From the information provided by the Civil Engineering Department of HKSAR, the maximum allowable volume of mud that the hopper barge can be loaded is only 943m^3. Assuming ρ_w = 1000kg/m^3, ρ_s = 2650kg/m^3, the following information is calculated:

Maximum loading weight of the hopper barge = 1280 x 1000kg

The maximum allowable volume fraction of sediment in the contaminated mud (f_s) can be calculated as follows:

$$1280 \times 1000\text{kg} = 943(1 - f_s)1000\text{kg/m}^3 + 943 \times 2650\text{kg/m}^3 f_s \quad (6.3.3)$$

$$\Rightarrow \qquad f_s = 0.2166$$

Thus, the total weight of sediment in the hopper barge = 943 x 2650kg x 0.22

= 541300kg

The total weight of Pb in the hopper barge = 541300kg x 67.9mg/kg

Model 3 cannot simulate the situation that there is a source input from a boundary for a finite duration. However, the term $b_2 m_2 e^{-d2t}$ in the boundary condition (Equation (4.7.3)) in Model 3 can represent a loading function from the boundary to the water column and the term can decay exponentially. The exponential decay function can be used to simulate the cases that most of the mud dumps into the water column during the first several seconds. If it is

assumed that 99.9% of sediment will get into the water column in the first 5 seconds, then, the value of d_2 can be calculated as follows:

$$0.999\int_0^{\infty} e^{-d_2 t}dt = \int_0^5 e^{-d_2 t}dt \qquad (6.3.4)$$

$$\Rightarrow \qquad d_2 = 1.3816/s$$

$$\Rightarrow \quad \int_0^5 e^{-d_2 t}dt = 0.7231s$$

Then the value of b_2m_2 can be calculated by the following equation:

$$0.999x541300x67.9mg = 10x45xb_2m_2\int_0^5 e^{-d_2 t}dt \qquad (6.3.5)$$

$$b_2m_2 = 112800 mg/m^2s$$

If the assumption is changed to 10 seconds, the values of d_2, $\int_0^{10} e^{-d_2 t}dt$, and b_2m_2 become 0.6908/s, 1.4461s and 56421 mg/m^{2}s, respectively. Figure 34 shows the changes of the function $b_2m_2e^{-d2t}$ with time for the above two assumptions.

The value of the water turbulent mixing coefficient k_z can be calculated by Equation (5.1.3.2) with the relationship $k_{sz} = \beta k_z$. The value of u_* in the equation can be calculated by Equation (2.1.3.2). The value of the effective bed-shear stress ($\tau_{b,c}$) in Equation (2.1.3.2) can be calculated by Equation (2.1.6.3a&b). The value of C" calculated by Equation (2.1.6.3b) is 107.6m$^{0.5}$/s with d_{90} = 63μm. Finally, the values of $\tau_{b,c}$, u_* and k_z for various $\bar{u}$ magnitudes (0.2, 0.6 and 1m/s) are shown in Table 3. Equation (2.1.3.6) and Equation (2.1.3.7) are formulae to calculate the value of β, which depends on the sediment concentration as shown in Equation (2.1.3.7). Since the marine dumping discharges large amount of sediment into the water column, the

value of ϕ_s calculated by Equation (2.1.3.7) is assumed as 0.7. The results of k_{sz} are shown in Table 3.

With reference to Equation (2.4.4.1.1) for the calculation of the partition fractions and $k_d = 10^6$ L/kg, it can be shown that the value of f_p is larger than 0.99 for sediment concentration (s) larger than 0.1kg/m^3. For this case study, the sediment concentration profiles have a magnitude larger than 0.1kg/m^3 in most of the time due to the extremely large input of sediment during the marine dumping activity. Thus, it is assumed that $f_p = 1$ and $f_d = 0$ in the study.

Equation (2.1.6.8) is used to calculate the value of the reference level sediment concentration s_a. The value of the reference level total toxic substance concentration (c_{Ta}), which is equal to the sum of c_a and p_a, is equal to 67.9 x s_a mg/m^3. Table 3 shows the results for different values of $\overline{u}$.

It is reasonable to assume that the Pb and the sediment distributions in the water column are in steady state before dumping. Thus, the steady state condition is used as the initial condition for this case study. Equation (3.4.6.1.1) calculates the steady state distribution profile of sediment. However, in Model 3, only constant initial concentration can be used as input to the model. Therefore, the initial Pb concentration is calculated using the product of Pb concentration in sediment (67.9mg/kg) and the depth averaged value of the sediment concentration calculated by Equation (3.4.6.1.1). The results are shown in Table 3.

The values of various input parameters in Model 3 are summarized below:

Input parameter	Input value
H	15m
u, b_2, b_3, b_4	ω_s = 0.001775m/s
r_m	0
b_1	0
d_4	0
$b_2 m_2$	57800 mg/m^{2}s (5 seconds) 28900 mg/m^{2}s (10 seconds)
d_2	1.382/s (5 seconds) 0.691/s (10 seconds)
m_4	c_{Ta}
k_{mz}	k_{sz}
m_{l0}	Initial Pb concentration (mg/m^3)

Figures 35 to 37 show the Pb concentration profiles at different points of time for different values of $\bar{u}$. Since the difference in concentration for different loading functions (5 sec or 10 sec) is very small. Only the concentration profiles for the loading function of 5 seconds are shown here.

Since, it is assumed that the initial Pb concentration profiles are in the steady state condition before the contaminated mud is dumped into the water column, the concentration profiles will return to the steady state again after a sufficient long time from the disposal. All the modeling results show that the required time for returning to the steady state are very long for various magnitudes of $\bar{u}$. The Pb concentration profiles do not seem to reach steady state even 8000 seconds (more than 2 hours) after the disposal. The main reason is that the average size of the sediment particles, 44μm, classified as coarse silt in Table 2, is relatively small. Thus, the settling velocity (ω_s) will be also very small and the time to settle all dumped sediment and toxic substances is long. This required extended period of time will limit the performance of collecting contaminated mud by the dumping pit. The

quantities of suspended toxic substances and sediment, which disperse to the area outside the designed dumping area, will increase due to the long settling period. Besides, the hopper barge and the tug boat when moving away from the dumping area will also disturb the flow and turbulent conditions. Such changes will increase the chance of the toxic materials to disperse out from the dumping pit area. Since the results show that large amount of the toxic substance still remains near the water surface even after 1000 seconds after the disposal, it is not economical for the hopper barge and tug boat to stay in the dumping area until the majority of the mud has settled to the bottom. It is suggested that the vessels should depart from the dumping area in slow speed to minimize the impact. Besides, it is also important to ensure that only one pair of vessels works in the area at any one time.

When comparing the concentration profiles computed under different values of $\overline{u}$, it can be found that the overall magnitude of the toxic substance decreases as $\overline{u}$ increases. This indicates that the speed for returning to the steady state condition increases as $\overline{u}$ increases. Table 3 shows that the value of k_{sz}, c_{Ta} and initial Pb concentration increases as $\overline{u}$ increases. A larger k_{sz} means that the toxic substance in the water column mixes more rapidly and thus the time to steady state will be shortened. However, for a sufficient long period of time, the overall concentration increases as $\overline{u}$ increases. This is because most settled toxic substances are re-entrained from the bed by the high velocity induced bottom shear back into the water column. As described in the pervious paragraph, the initial Pb concentration

used in Model 3 is the same as the depth averaged Pb concentration at steady state. Table 3 shows that when $\overline{u}$ increases 5 times from 0.2 to 1m/s, the initial Pb concentration increases over 265 times from 1.12 to 315 mg/m^3. Thus, the overall magnitude of the steady state concentration increases sharply as $\overline{u}$ increases. Nevertheless, the required time for the toxic substance to recover the steady state condition decreases as $\overline{u}$ increases due to the reason mentioned above and the larger steady state concentration profile.

The required times to achieve steady state as $\overline{u}$ = 0.2, 0.6 and 1m/s are around 60k, 60k and 55k seconds, respectively. The results generally agree with the discussion given in the last paragraph but the difference between the times approaching steady state is small. This is because the extremely large dumping quantity dominates the overall fate of the toxic substances. The magnitude of the steady state (or initial) concentration profile is very small when compares with the dumping quantity. The mud also settles in a low speed due to the small averaged sediment size. Therefore, the required time is mostly controlled by the deposition of the dumping materials, which mainly depends on the settling velocity, and the sediment turbulent mixing coefficient. In this case study, the same settling velocity is used for different $\overline{u}$ values and thus the difference of the time to steady state is small.

In the study, the value of partition coefficient (k_d) for Pb is assumed to be 10^6 L/kg and the required sediment concentration, for ensuring the value of f_p always larger than 0.99, is 0.1kg/m^3. If k_d is reduced to 10^5 and 10^4 L/kg, the required sediment concentration will be increased to 1 and 10kg/m^3,

respectively. Because of the extremely large amount of sediment dumped into the water, f_p can still maintain at a magnitude larger than 0.99 for most of the modeling period based on the aforementioned range of k_d which represents many kinds of heavy metals as described in Section 5.1.5. This has proven that Model 3 is adequate to simulate the fate of many different kinds of heavy metals in the water column due to marine dumping activities.

Figure 26: Sediment concentration profile generated by Model 1 for different distances with compared to (1) numerical modeling results by Wai and Lu (1999) and (2) experimental results by Jobson and Sayre (1970).

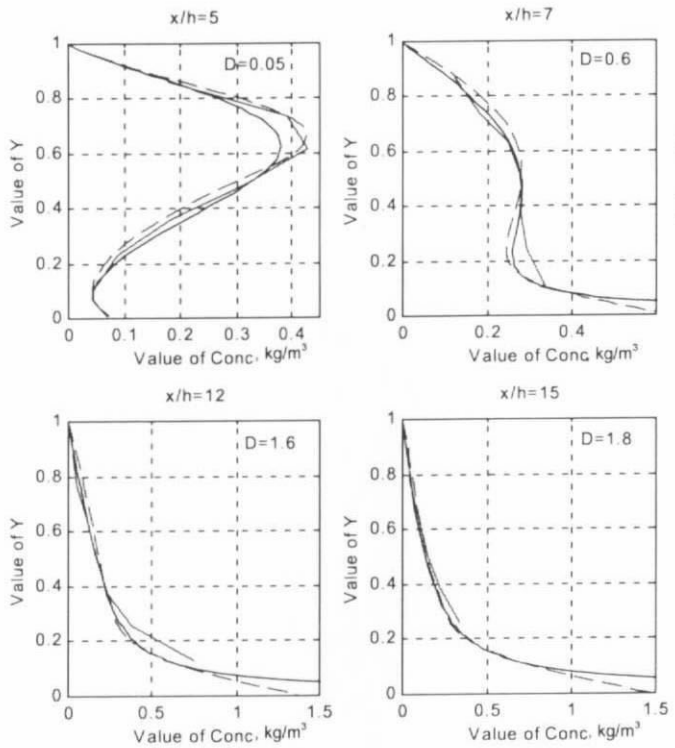

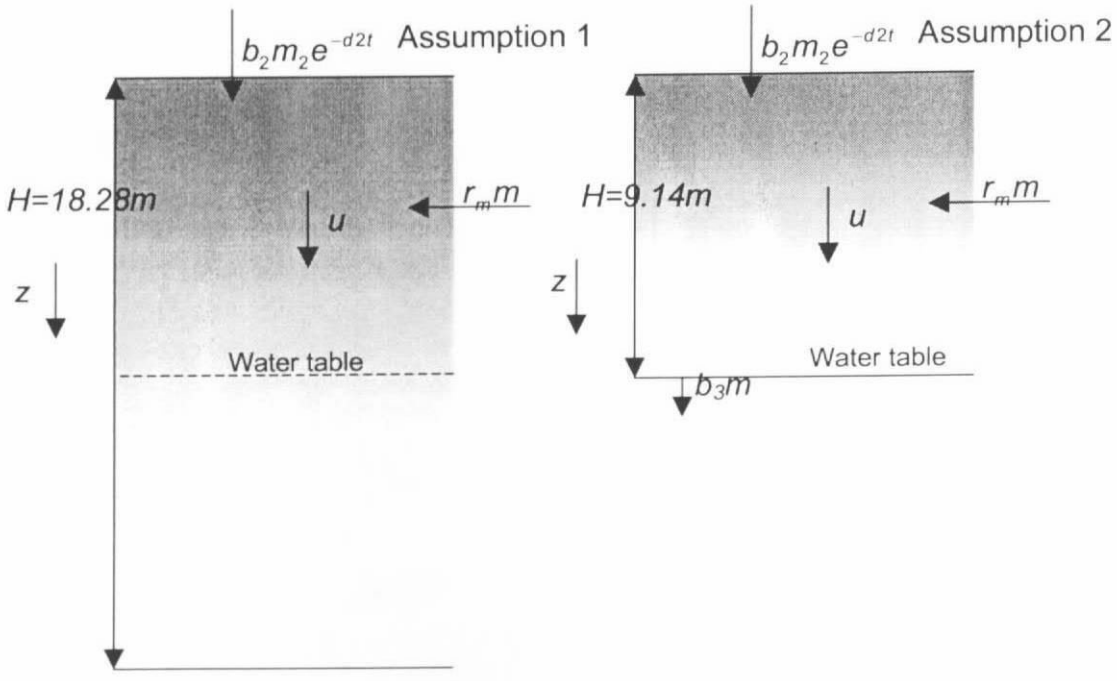

Figure 27: Simplification of Model 3 with two different assumptions for simulating the case shown in Prakash (2000)

Figure 28: Comparison of results of Prakash (2000) and of model pollutants reaching the water table

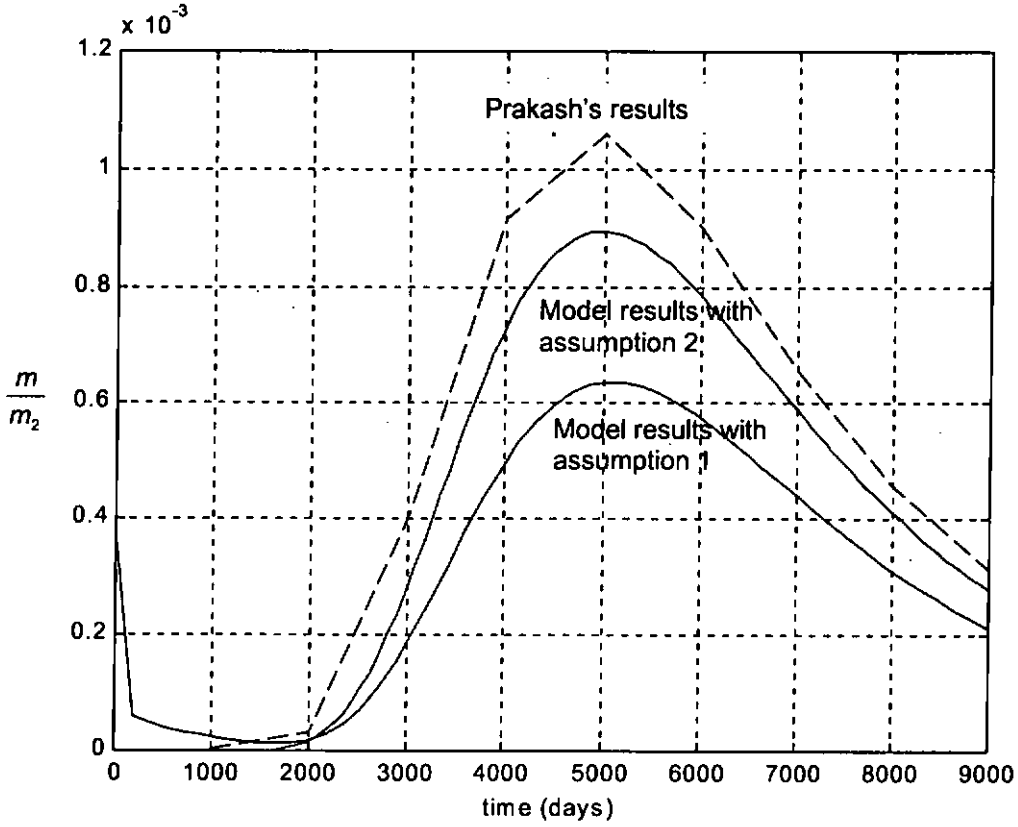

Figure 29: Concentration profiles along soil depth in different days with model assumption 1, retardation factor=1.35

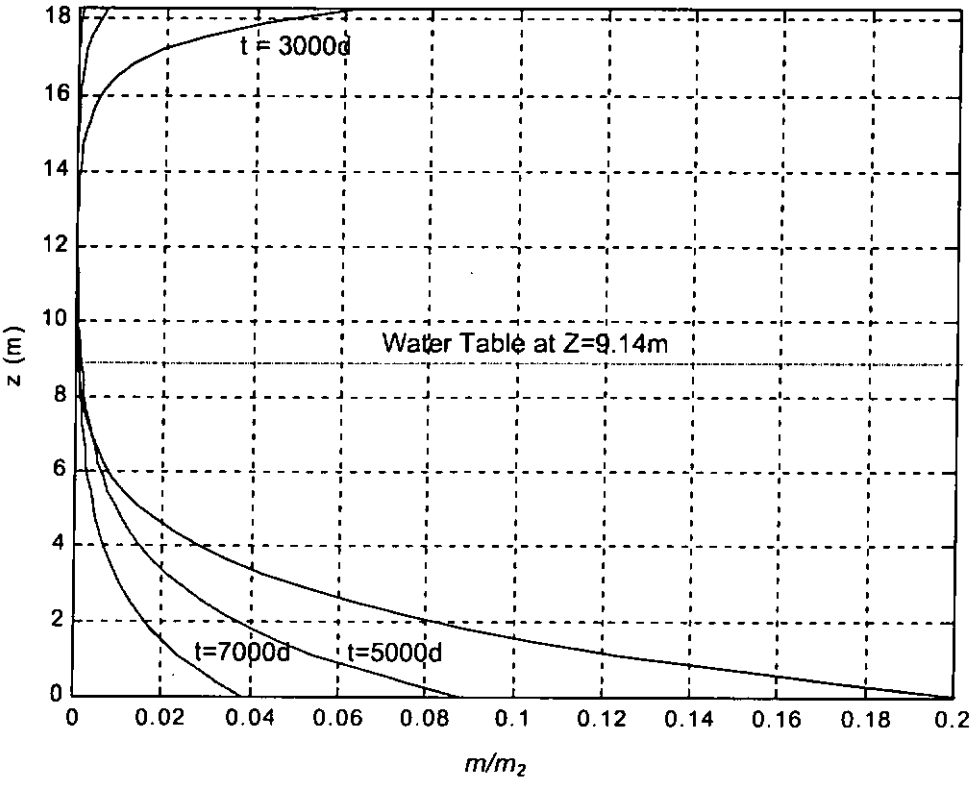

Figure 30: Concentration profiles along soil depth in different days with model assumption 2, retardation factor=1.45

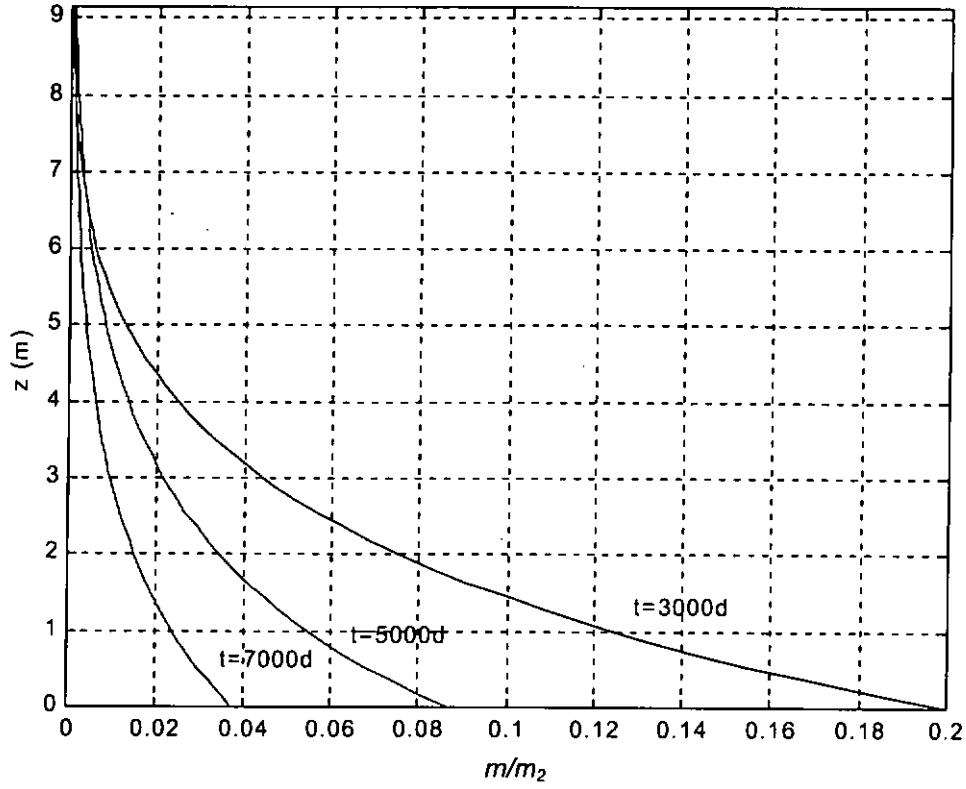

Figure 31: Concentration profiles at z=0 for model and Prakash's model

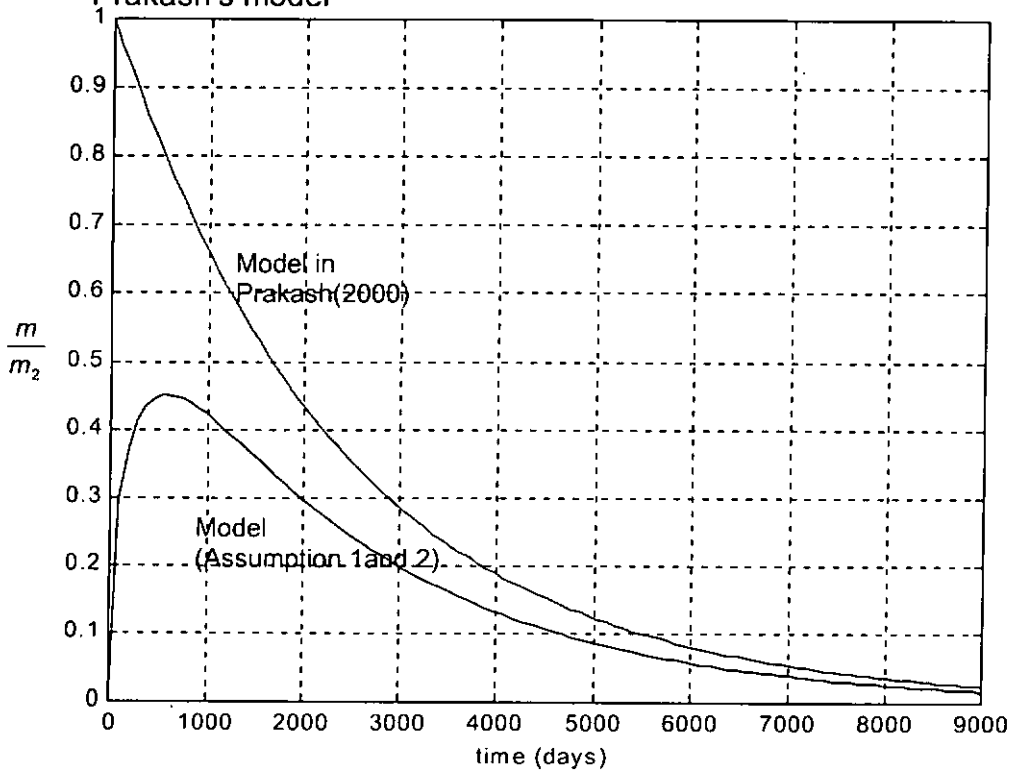

Figure 32: Concentration profiles at water table (z=9.14m) with adjustment of the retardation factor R_d

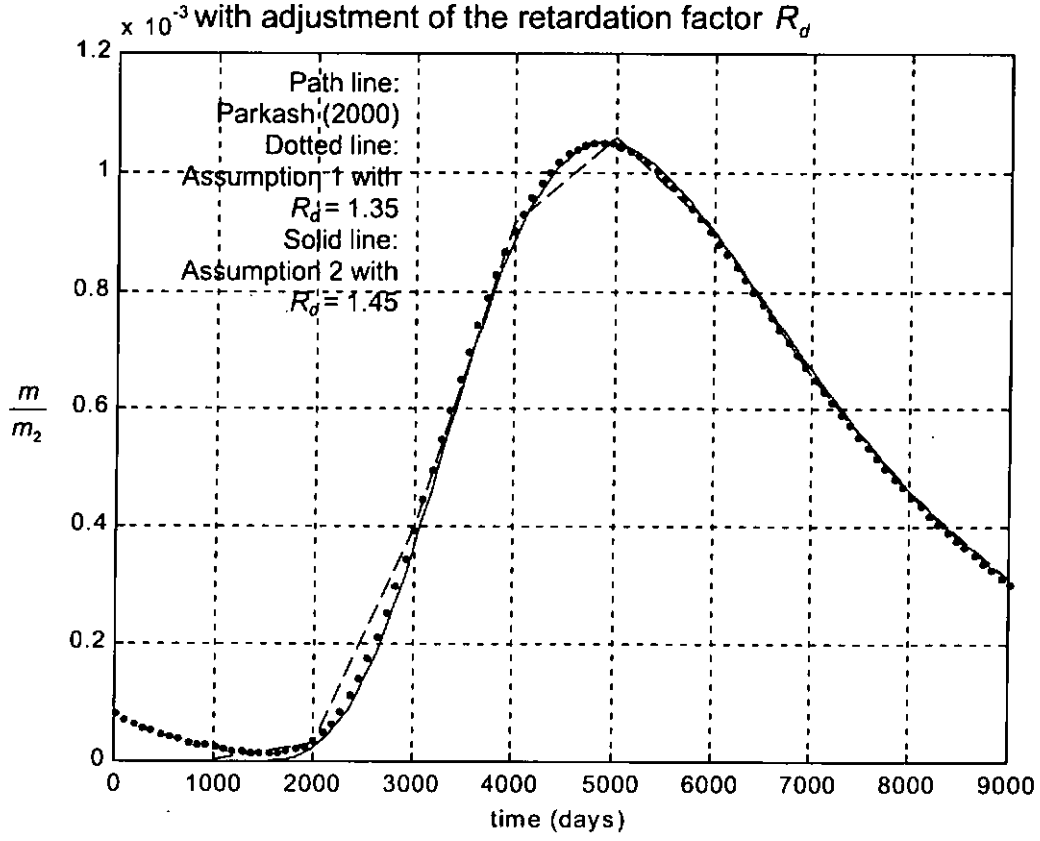

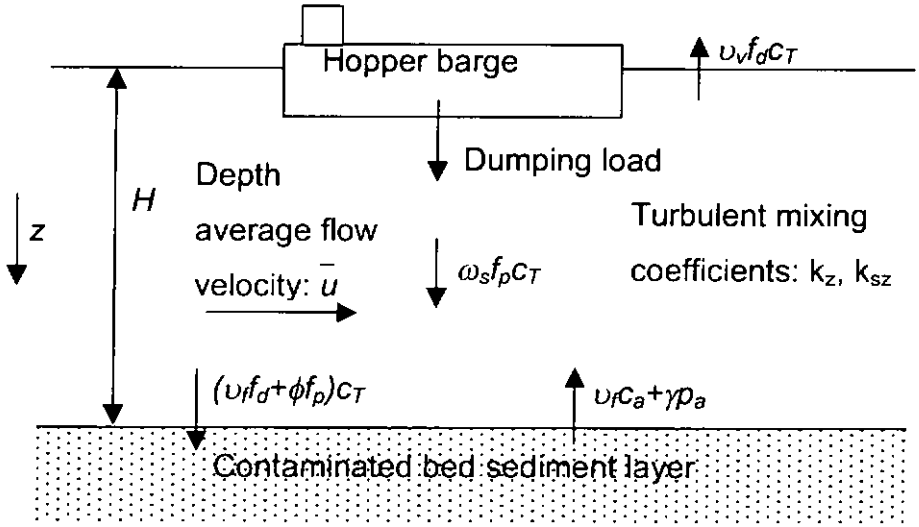

Figure 33: Contaminant transport processes in a dumping activity at ESC

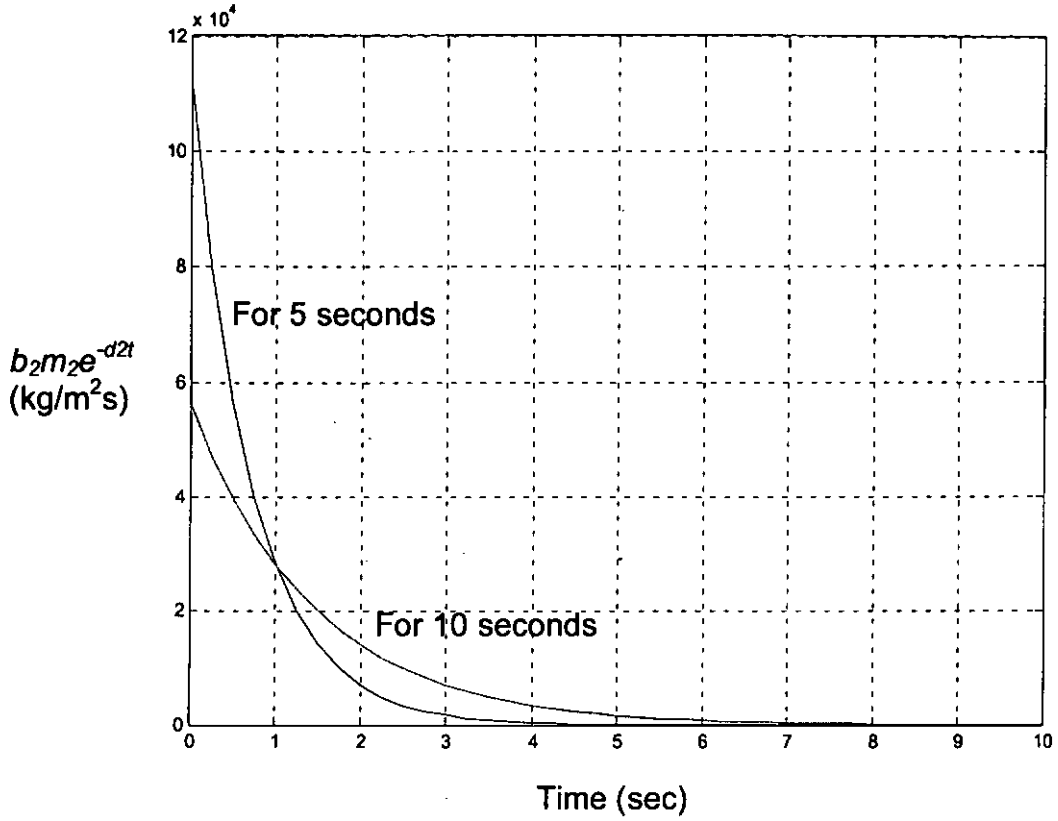

Figure 34: Loading functions ($b_2m_2e^{-d2t}$) for dumping action of hopper barge assuming: most material enters to the water column within 5 sec and 10 sec, respectively.

Table 3: Values of different physical/chemical parameters for different values of depth average flow velocity ($\bar{u}$)

$\bar{u}$ (m/s)	0.2	0.6	1
$\tau_{b,c}$ (N/m^2)	0.03388	0.3049	0.8470
u_* (m/s)	0.00582	0.01746	0.02910
k_z (m^2/s)	0.00582	0.01746	0.02910
k_{sz} (m^2/s)	0.00483	0.01248	0.02052
s_a (kg/m^3)	0.09758	2.02407	8.2895
c_{Ta} (mg/m^3)	6.6257	137.43	562.86
Initial Pb concentration (mg/m^3)	1.197	56.79	315.3

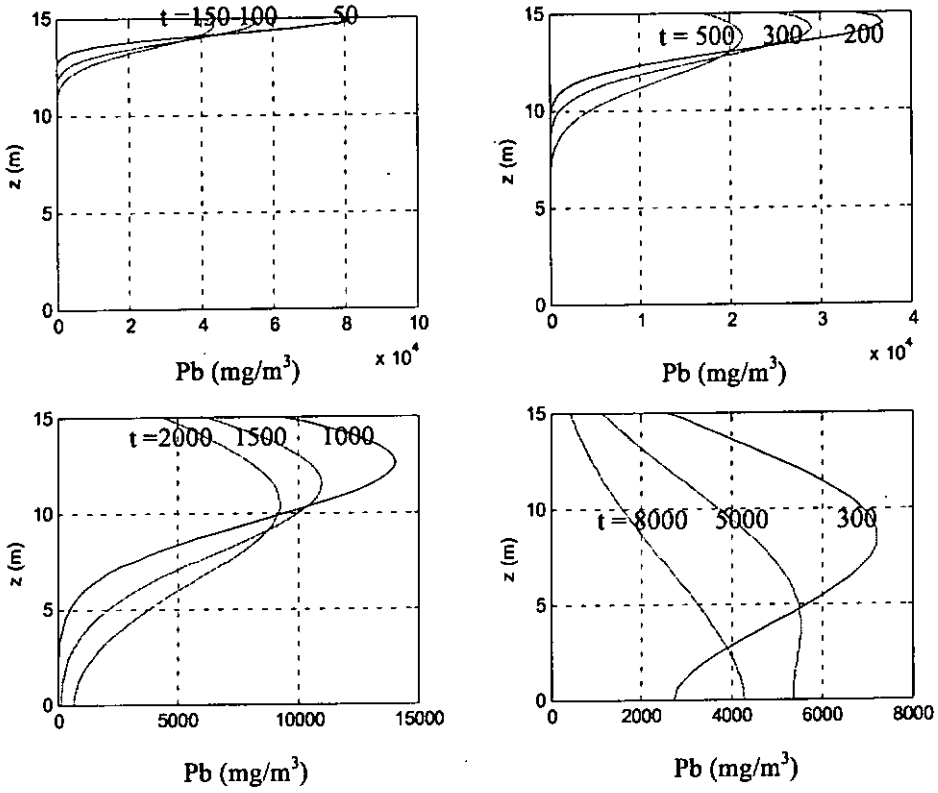

Figure 35: Concentration profiles of Pb at different points of time assuming $\overline{u}$ = 0.2m/s.

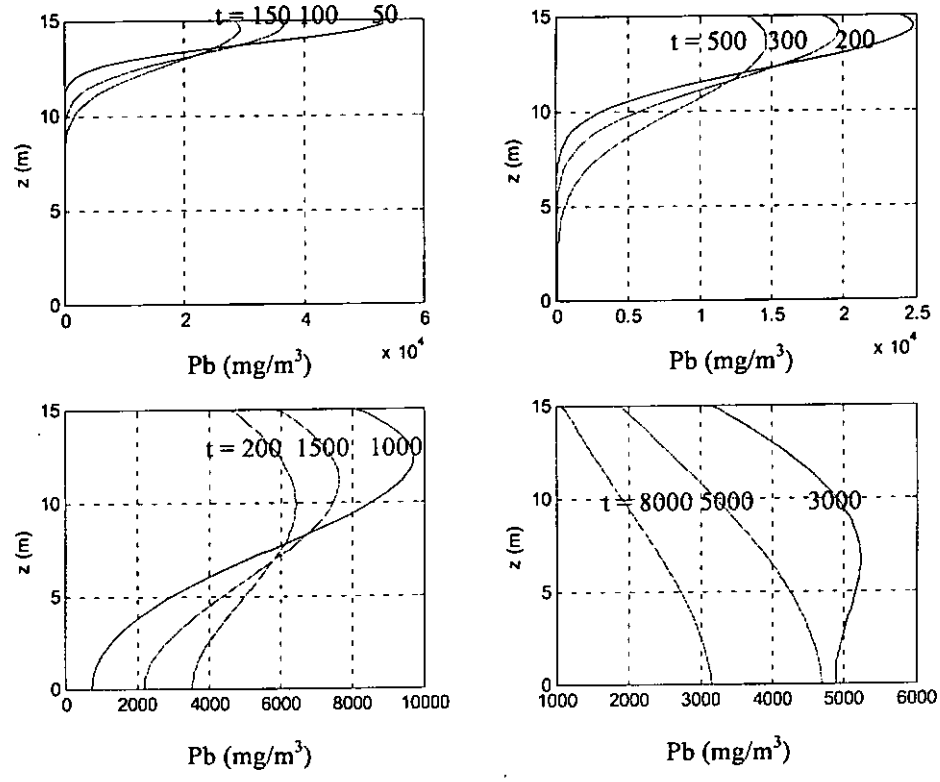

Figure 36: Concentration profiles of Pb at different points of time assuming $\overline{u}$ = 0.6m/s.

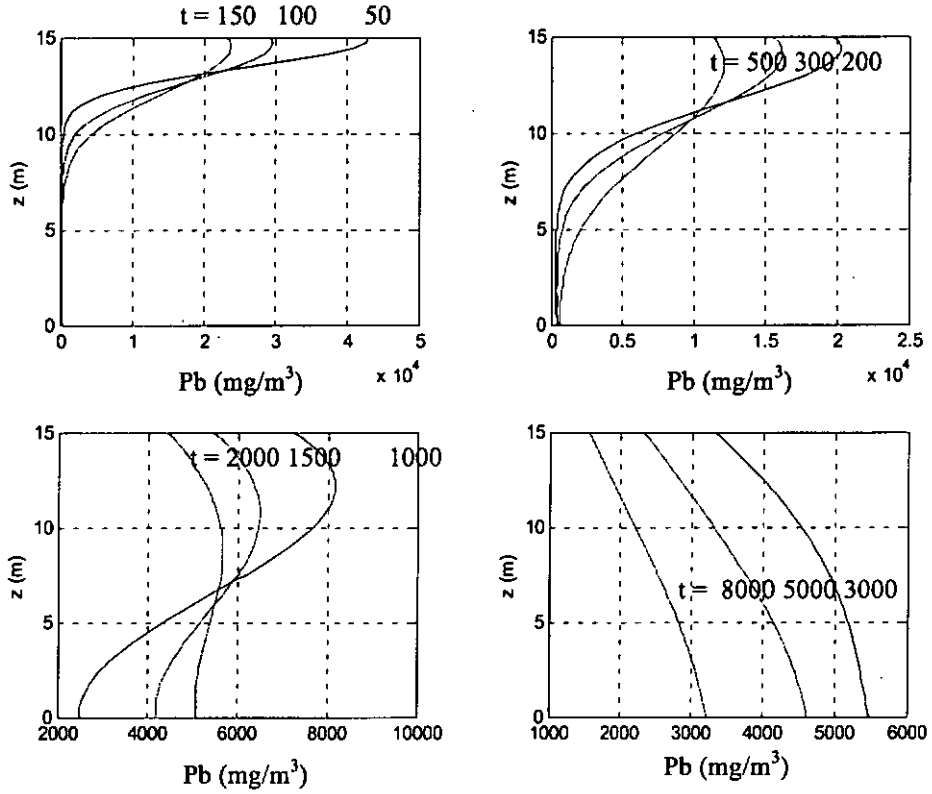

Figure 37: Concentration profiles of Pb at different points of time assuming $\bar{u}$ = 1m/s.

Chapter 7: Conclusions and recommendations

7.1 Conclusions

The governing system that describes the transport of toxic substances in the aquatic environment has been studied in this research. The system considers the most important physical and chemical transport phenomena of toxic substance transport in the aquatic environment. The fate of toxic substances is highly related to the distributions of suspended and bottom sediment in such environments. This is owing to the fact that toxic substances may sorb onto particles in the water body causing the contaminated sediment, to release the toxic chemicals back to the aquatic environment after being transported to other locations. Therefore, the interaction between toxic substances and sediment and the sediment transport should be considered in the governing system. From the physical point of view, the advection and dispersion transport processes, which always play the most important roles in the transport, should be considered. Other phenomena such as decay of toxic substances and losses due to other chemical and physical processes are also considered in the system. The toxic substance is considered to have two phases in the water body, (dissolved and particulate) and the first-order kinetics expression is used to describe the exchange process between these two phases. Two governing equations for dissolved and particulate toxic substances are then developed.

The generalised governing equations of the system are simplified in order to formulate a relatively simple system that can be solved analytically,

but still retain sufficient physics and chemistry to be realistic. In this research, the particle settling, the turbulence, toxic substance exchange processes between sediment and toxic substances in the water column and at the sediment water interface are the main phenomena considered. All these processes are vertical transport processes or vary along the vertical axis, thus even through only the vertical axis z is considered in the simplified governing equations, the system can still includes the most important processes involved in toxic substance transport.

Instantaneous equilibrium of sorption kinetics between dissolved and particulate components of a toxic substance is a common and most important assumption used in former research and is also used here. Following this assumption, the two governing equations of dissolved and particulate toxic substances can be combined into one governing equation in terms of the total concentration. The simplified governing equation (Equation (3.4.5.8)) is generally a one dimensional, time varying advection-dispersion equation (ADE) with linear coefficients that depend on the vertical coordinate z and sediment concentration (s).

The governing equation is further developed by studying two different specific flow conditions in aquatic environments. In both cases, the distribution of suspended sediment is assumed steady. The first case assumes a constant distribution of the mixing coefficient while the second case assumes a parabolic distribution. The coefficients in the governing equation for toxic substance transport are further specified under the two cases.

Boundary conditions for the governing systems are based on the concept of counting the net flux through the boundary surface. This includes exchange processes of contaminants at the interface. Settling and resuspension of contaminant sediment, exchange of dissolved toxic substances and decay property of toxic substance are considered at the sediment-water interface. At the water surface, the volatilisation loss of dissolved toxic substances is considered.

The coefficients in the simplified governing equations are complicated functions of the vertical coordinate z causing it to be impossible to solve the governing system analytically. Instead, three advection-dispersion models with governing equations having coefficients, either as constants or specific functions, are developed. In this way analytical simulations of the fate of toxic substances in different transport environments are provided. Analysis of the physical and mathematical parameters in the governing system has been carried out. The analysis has two focuses. The first is to identify the ranges of physical/chemical parameters that can further simplify the governing system but still be useful in the simulation of the transport of toxic substances in real life problems. The second focus is to find the effects of particular physical or chemical parameters on the fate of toxic substances.

Regarding the first focus, firstly, the developed models are useful when the distribution of suspended sediment is close to complete mixing in the water column or when most sediment remains at the bottom. In this way, Model 1 perfectly matches the cases for non-decay toxic substance with the value of $\omega_s / \beta \kappa u_*$ described in Section (3.4.6.2) which is less than 0.02 or

greater than 5. Model 2 and Model 3 perfectly match the cases where the value of $\omega_s H/k_{sz}$, denoted as P_e, (described in Section (3.4.6.1)) is less than 0.1 or greater than 20. Secondly it can be concluded that the developed models are useful for the cases where most toxic substances remain in dissolved forms or in particulate forms. In this approach, Model 1 is applicable to non-decay toxic substance, and the Models 2 and 3 are useful for situations where $k_d \gamma s_a / \phi$ less than 0.1 or greater than the value calculated by Equations (5.2.2.2.4) and (5.2.2.1.5), respectively.

For the ratio between the sediment mixing coefficient and the mixing coefficient of water equal to 1 (β =1), Models 2 and 3 are useful in matching the governing equation described in Section (3.4.6.1) for P_e less than 0.632 and the product of P_e and f_p at $z = 0$ less than 0.1.

For β not equal to 1, Models 2 and 3 match the governing system described in Section (3.4.6.1), providing coefficients $\overline{A}_e$, $\overline{B}_e$ and $\overline{C}_e$ in Equation (3.4.6.1.7) can be assumed as constant values. The requirements for assuming $\overline{B}_e$ as constant are described in Section (5.4.1). The requirement for assuming $\overline{C}_e$ to be constant is for the value of N_{o2}, introduced in Section 5.6, to be greater than 10. The requirements for assuming $\overline{A}_e$ to be constant, are described in Section (5.3.1) or the value of N_{o1}, introduced in Section 5.6, is greater than 10.

Thus, the developed models are capable of simulating the transport of toxic substances when the values of the input parameters lie in the particular ranges as described.

Regarding the second focus, the following conclusions have been made. Firstly, the contributions of the partition coefficient (k_d) to the transport of toxic substances are that the concentration of toxic substances in the water column decreases, as the value of the partition coefficient increases. Secondly, the concentration of toxic substances is smaller and decreases at a faster rate in cases where the value of the sediment settling velocity (ω_s) increases or the value of the sediment mixing coefficient (k_{sz}) decreases for β larger than 1. The concentration of toxic substances decreases at a faster rate as β , k_{dc} and k_{dp} increase. Lastly, the overall concentration at a particular time is smaller for cases where larger values of γ_{cb} and γ_{pb} (decay coefficients of toxic substance at the sediment-water interface) are used.

The governing equations in the developed models are in the form of the advection-dispersion equation (ADE). In this research, the author applies the models to simulate the transport of toxic substances due to marine dumping. Besides the author also use the models for suspended sediment transport in the water column and transport of chemicals in soil layers to show the possible areas of application of the models other than toxic substance modelling.

In conclusion, three analytical models have been developed to provide useful tools for environmental engineers and scientists to aid the prediction of the fate of toxic substances with specific ranges of physical and chemical parameters in specific aquatic environments. Based on the developed governing system and models, the contributions to toxic substance transport

of particular parameters are identified. The models are not only useful for toxic substance transport but also for simulating the transport of sediment and chemicals in aquatic or other areas such as in soil layers.

7.2 Recommendations

In this research, the governing system has been developed to describe the transport of toxic substances and three models have been built to simulate the transport in different situations based on the governing system. However, the three models can only be used for cases where some of the input parameters lie in particular ranges as described in Chapter 5. Because the developed models have coefficients that are either constants (Model 2 and Model 3) or specific functions (Model 1), they may not always be adequate to represent coefficients $\overline{A}$, $\overline{B}$ and $\overline{C}$ in the governing Equation (3.4.5.8). These coefficients are originally complicated functions of z.

In order to find methods that can effectively describe the coefficients and solve the system analytically, the author advises the development of a model based on the multi-layer approach idea. The governing system can be divided into several subsystems along the z-axis by using this approach, each of them having constant coefficients in the corresponding layer. Coefficients $\overline{A}$, $\overline{B}$ and $\overline{C}$ can then be effectively described because each layer is then responsible for only part of the water column with corresponding constant coefficients. A whole picture can be obtained by combining the

effects of the coefficients of different layers. The multi-layer system can effectively represent the transport of toxic substances if the number of layers is sufficient. Section 2.3 reviews the existing analytical solutions for contaminant transport in multi-layer medias. Liu et al. (1998) developed an analytical solution to the one-dimensional solute advection-dispersion equation in a multi-layer porous media and it is a useful reference for the development of the new model. However the changing of boundary conditions to examine the exchange effects of toxic substances at the bottom layer must be considered.

One of the advantages of analytical models is that they can provide fundamental insight into the effects on the transport contributed by particular parameters of the transport process. Sometimes, mathematical equations that describe effects on the transport or requirements to achieve some specific conditions, such as an equilibrium state, can be derived from the analytical solutions. In this research, general contributions to transport by most parameters have been discussed in Chapter 5. In Section (4.6.2), requirements for the existence of steady state has been defined in Solution 4 of Model 2 and shows the advantages of analytical models. In addition an analysis of physical and chemical parameters has been conducted based on the developed governing system and models. Further analyses, such as comparisons between the contributions of different parameters or identifications for the usages of the requirements for steady states described in Section (4.6.2), is strongly recommended by the author.

A case study for the toxic substance transport in the water column due to marine dumping is conducted by Model 3 in this research. However, the accuracy of the results cannot identify due to the lack of the corresponding monitoring data. The author expects that such monitoring will be performed in the future for verifying the modeling results and improving the applicability to predict the developed models in the transport of toxic substances.

In this research, the developed models are applied to two real cases in different areas to demonstrate their usage in areas other than toxic substance transport. As advection-dispersion models are also useful in other areas, such as simulation of transport of BOD. The corresponding investigations and case studies should be carried out in order to further realize the applicability of these developed models.

In conclusion the current research provides a firm base for the conduct of further investigation into the transport of toxic substances by analytical solutions.

Appendix 1
Detailed solutions of model 2 (Solution 4)

Governing equation:

$$\frac{\partial M}{\partial T} = \frac{\partial M}{\partial Z} + K\frac{\partial^2 M}{\partial Z^2} + RM$$

Boundary conditions:

$$\left[K\frac{\partial M}{\partial Z} + M\right]_{Z=1} = 0$$

$$\left[K\frac{\partial M}{\partial Z} + M\right]_{Z=0} = B_1 M - B_2\Big|_{Z=0}$$

Initial condition:

$$M(Z,0) = M_{I0}$$

Note that variables used in the above equations are dimensionless with:

$$M = \frac{m}{m_a} \quad M_{I0} = \frac{m_{I0}}{m_a}; \quad Z = \frac{z}{H}; \quad K = \frac{k_{mz}}{\omega H}; \quad T = \frac{t\omega}{H}; \quad B_1 = \frac{\phi_m}{\omega} \quad B_2 = \frac{\gamma_m}{\omega}; \quad R = \frac{Hr_m}{\omega}$$

in which m is contaminant concentration, m_{I0} is contaminant concentration at $t = 0$, m_a is contaminant concentration in bed layer, H is the water depth, k_{mz} is the turbulent mixing coefficient, ω is the settling velocity of contaminant, r_m is the coefficient for source/sink term, and ϕ_m and γ_m are settling and resuspension velocity of contaminant at water-sediment interface respectively.

Definition and Properties of Laplace Transform :

The Laplace Transform of $M(Z,T)$ is $\tilde{M}(Z,q)$ and defines as follows:

$$\tilde{M}(Z,q) = \int_0^\infty e^{-qT} M(Z,T)dT$$

Laplace transform of derivatives and integrals:

$$L\{\frac{\partial^n M}{\partial T^n}\} = q^n\tilde{M}(Z,q) - q^{n-1}M(Z,0) - q^{n-2}M'(Z,0) - \ldots - M^{n-1}(Z,0)$$

$$L\left\{a\frac{\partial^2 M}{\partial Z^2}\right\} = a\frac{\partial^2}{\partial Z^2}L\{M\} = a\frac{\partial^2\tilde{M}(Z,q)}{\partial Z^2}$$

Thus:

$$L\left\{\frac{\partial M}{\partial T}\right\} = q\tilde{M}(Z,q) - M(Z,0)$$

$$= q\tilde{M}(Z,q) - M_{I0}$$

Define:

$$\frac{\partial\tilde{M}(Z,q)}{\partial Z} = \tilde{M}_Z(Z,q)$$

$$\frac{\partial^2\tilde{M}(Z,q)}{\partial Z^2} = \tilde{M}_{ZZ}(Z,q)$$

From:

$$\frac{\partial M}{\partial T} = \frac{\partial M}{\partial Z} + K\frac{\partial^2 M}{\partial Z^2} + RM$$

$$q\tilde{M}(Z,q) - M_0 - \tilde{M}_Z(Z,q) - K\tilde{M}_{ZZ}(Z,q) - R\tilde{M}(Z,q) = 0$$

$$\tilde{M}_{ZZ}(Z,q) + \frac{1}{K}\tilde{M}_Z(Z,q) - \frac{q-R}{K}\tilde{M}(Z,q) = \frac{-M_{I0}}{K}$$

which is a second order ODE with respect to Z:

Consider:

$$\tilde{M}_{ZZ}(Z,q) + \frac{1}{K}\tilde{M}_Z(Z,q) - \frac{q-R}{K}\tilde{M}(Z,q) = 0$$

Put:

$$\tilde{M}(Z,q) = e^{\lambda Z}$$

$$\tilde{M}_Z(Z,q) = \lambda e^{\lambda Z}$$

$$\tilde{M}_{ZZ}(Z,q) = \lambda^2 e^{\lambda Z}$$

$$\Rightarrow e^{\lambda Z}(\lambda^2 + \frac{1}{K}\lambda - \frac{q-R}{K}) = 0$$

$$\lambda^2 + \frac{1}{K}\lambda - \frac{q-R}{K} = 0$$

$$\Rightarrow \lambda = \frac{-1 \pm \sqrt{1+4K(q-R)}}{2K}$$

Thus, the general solution is:

$$= C_1 e^{\theta Z} + C_2 e^{\phi Z}$$

where:

$$\theta = \frac{-1+\sqrt{1+4(q-R)K}}{2K}$$

$$\phi = \frac{-1-\sqrt{1+4(q-R)K}}{2K}$$

Try a particular solution as:

$$\tilde{M}(Z,q) = A$$

$$\Rightarrow 0 + 0 - \frac{q-R}{K}A = \frac{-M_{I0}}{K}$$

$$A = C_0/(q-R)$$

Therefore:

$$\tilde{M}(Z,q) = C_1 e^{\theta Z} + C_2 e^{\phi Z} + {}^{M_{I0}}\!/_{(q-R)}$$

From Boundary condition:

$$\left[K\frac{\partial M}{\partial Z} + M\right]_{Z=1} = 0$$

Then $$L\left\{\left[K\frac{\partial M}{\partial Z} + M\right]_{Z=1}\right\} = L\{0\}$$

$$\left[K\frac{\partial \tilde{M}}{\partial Z} + \tilde{M}\right]_{Z=1} = 0$$

Put solution of $\tilde{M}$, we get:

$$\frac{\partial \tilde{M}}{\partial Z} = C_1\theta e^{\theta Z} + C_2\phi e^{\phi Z}$$

$$\Rightarrow \left[K\left(C_1\theta e^{\theta Z} + C_2\phi e^{\phi Z}\right) + C_1 e^{\theta Z} + C_2 e^{\phi Z} + {}^{M_{I0}}\!/_{(q-R)}\right]_{Z=1} = 0$$

$$\Rightarrow K\left(C_1\theta e^{\theta} + C_2\phi e^{\phi}\right) + C_1 e^{\theta} + C_2 e^{\phi} = -{}^{M_{I0}}\!/_{(q-R)}$$

$$\Rightarrow (1+K\theta)C_1 e^{\theta} + (1+K\phi)C_2 e^{\phi} = -{}^{M_{I0}}\!/_{(q-R)}$$

From:

$$\left[K\frac{\partial M}{\partial Z} + M\right]_{Z=0} = B_1 M - B_2\big|_{Z=0}$$

$$L\left[K\frac{\partial M}{\partial Z} + M\right]_{Z=0} = L\{B_1 M - B_2\}_{Z=0}$$

$$\left[K\frac{\partial \tilde{M}}{\partial Z} + \tilde{M}\right]_{Z=0} = B_1 L\{M\}_{Z=0} - B_2 L\{1\}$$

$$= B_1\tilde{M}_{Z=0} - B_2\int_0^\infty e^{-qT}dT$$

$$= B_1\tilde{M}_{Z=0} - B_2\frac{e^{-qT}}{-q}\Big|_0^\infty$$

$$= B_1\tilde{M}_{Z=0} - B_2\left(0 - 1/-q\right)$$

$$\left[K\frac{\partial\tilde{M}}{\partial Z} + \tilde{M}\right]_{Z=0} = \left[B_1\tilde{M} - B_2/q\right]_{Z=0}$$

$$\left[K\left(C_1\theta e^{\theta Z} + C_2\phi e^{\phi Z}\right) + C_1e^{\theta Z} + C_2e^{\phi Z} + \frac{M_{I0}}{(q-R)}\right]_{Z=0}$$

$$= B_1\left(C_1e^{\theta Z} + C_2e^{\phi Z} + \frac{M_{I0}}{(q-R)}\right)_{Z=0} - \frac{B_2}{q}$$

$$\Rightarrow (1+K\theta-B_1)C_1 + (1+K\phi-B_1)C_2 = \frac{M_{I0}q(B_1-1) - B_2(q-R)}{q(q-R)}$$

Thus:

$$(1+K\theta)C_1e^{\theta} + (1+K\phi)C_2e^{\phi} = -M_{I0}/(q-R) \qquad \text{——————1}$$

$$(1+K\theta-B_1)C_1 + (1+K\phi-B_1)C_2 = \frac{M_{I0}q(B_1-1) - B_2(q-R)}{q(q-R)} \qquad \text{——— 2}$$

From 1:

$$C_2 = \frac{1}{(1+K\phi)e^{\phi}}\left[-\frac{M_{I0}}{q-R} - (1+K\theta)C_1e^{\theta}\right]$$

Put this into 2, we get:

$$(1+K\theta-B_1)C_1 - \frac{(1+K\phi-B_1)}{(1+K\phi)e^{\phi}}\left[\frac{M_{I0}}{q-R} + (1+K\theta)C_1e^{\theta}\right] = \frac{M_{I0}q(B_1-1) - B_2(q-R)}{q(q-R)}$$

$$C_1 = \frac{M_{I0}B_1q - (1+K\phi)(qM_{I0} + e^{\phi}(q(M_{I0}B_1 - B_2 - M_{I0}) + B_2R))}{q(q-R)\left[(1+K\phi-B_1)(1+K\theta)e^{\theta} - (1+K\theta-B_1)(1+K\phi)e^{\phi}\right]}$$

$$C_2 = \frac{(1+K\theta)(qM_{I0} + e^{\theta}(q(M_{I0}B_1 - B_2 - M_{I0}) + B_2R)) - M_{I0}B_1q}{q(q-R)\left[(1+K\phi-B_1)(1+K\theta)e^{\theta} - (1+K\theta-B_1)(1+K\phi)e^{\phi}\right]}$$

From the definition of inverse Laplace transform:

$$L^{-1}\left[\tilde{M}\right] = M = \frac{1}{2\pi i}\int_{\gamma-i\infty}^{\gamma+i\infty}e^{qT}\tilde{M}dq$$

Therefore:

$$M = \frac{1}{2\pi i}\int_{\gamma-i\infty}^{\gamma+i\infty}e^{qT}\left(C_1e^{\theta Z} + C_2e^{\phi Z} + M_{I0}/(q-R)\right)dq$$

$$M = \frac{1}{2\pi i}\int_{\gamma-i\infty}^{\gamma+i\infty}e^{qT}\left(C_1e^{\theta Z} + C_2e^{\phi Z}\right)dq + L^{-1}\left[M_{I0}/(q-R)\right]$$

$$M = M_{I0}e^{RT}$$

$$+\frac{1}{2\pi i}\int_{\gamma-i\infty}^{\gamma+i\infty}e^{qT}\left[\frac{L\phi e^{\theta Z} + M\theta e^{\phi Z}}{q(q-R)\left[(1+K\phi-B_1)(1+K\theta)e^{\theta} - (1+K\theta-B_1)(1+K\phi)e^{\phi}\right]}\right]dq$$

Where:

$$L\phi = M_{I0}B_1q - (1+K\phi)(qM_{I0} + e^{\phi}(q(M_{I0}B_1 - B_2 - M_{I0}) + B_2R))$$

$$M\theta = (1+K\theta)(qM_{I0} + e^{\theta}(q(M_{I0}B_1 - B_2 - M_{I0}) + B_2R)) - M_{I0}B_1q = -L\theta$$

Replace q to q-*1/4k*, then:

d(q-1/4K)=dq-d(1/4K)
=dq

$$\theta = \frac{-1}{2K} + \sqrt{\frac{q-R}{K}}$$

$$\phi = \frac{-1}{2K} - \sqrt{\frac{q-R}{K}}$$

Consider $q(q-R)\left[(1+K\phi-B_1)(1+K\theta)e^{\theta} - (1+K\theta-B_1)(1+K\phi)e^{\phi}\right]$

$$= (q-\frac{1}{4K})(q-R-\frac{1}{4K})e^{-1/2K}\begin{bmatrix} e^{\sqrt{(q-R)/K}} - e^{-\sqrt{(q-R)/K}} + K\phi(e^{\sqrt{(q-R)/K}} - e^{-\sqrt{(q-R)/K}}) \\ -B_1(e^{\sqrt{(q-R)/K}} - e^{-\sqrt{(q-R)/K}}) + K\theta(e^{\sqrt{(q-R)/K}} - e^{-\sqrt{(q-R)/K}}) \\ +K^2\theta\phi(e^{\sqrt{(q-R)/K}} - e^{-\sqrt{(q-R)/K}}) \\ -B_1K\theta e^{\sqrt{q-R/K}} + B_1K\phi e^{-\sqrt{q-R/K}} \end{bmatrix}$$

$$= (q-\frac{1}{4K})(q-R-\frac{1}{4K})e^{-1/2K}\begin{bmatrix} 2\sinh\sqrt{(q-R)/K} + 2K\phi\sinh\sqrt{(q-R)/K} \\ -2B_1\sinh\sqrt{(q-R)/K} \\ +2K\theta\sinh\sqrt{(q-R)/K} + 2K^2\theta\phi\sinh\sqrt{(q-R)/K} \\ -B_1Ke^{\sqrt{(q-R)/K}}(-1/2K + \sqrt{(q-R)/K}) \\ +B_1Ke^{-\sqrt{(q-R)/K}}(-1/2K - \sqrt{(q-R)/K}) \end{bmatrix}$$

$$= (q-\frac{1}{4K})(q-R-\frac{1}{4K})e^{-1/2K}\begin{bmatrix} -2(K(q-R)-1/4)\sinh\sqrt{(q-R)/K} - 2B_1\sinh\sqrt{\frac{q-R}{K}} \\ +\frac{B_1K}{2K}(e^{\sqrt{(q-R)/K}} - e^{-\sqrt{(q-R)/K}}) \\ -B_1K\sqrt{\frac{q-R}{K}}(e^{\sqrt{(q-R)/k}} + e^{-\sqrt{(q-R)/k}}) \end{bmatrix}$$

$$= (q-\frac{1}{4K})(q-R-\frac{1}{4K})e^{-1/2K}\begin{bmatrix} -2(K(q-R)-1/4)\sinh\sqrt{\frac{q-R}{K}} - B_1\sinh\sqrt{\frac{q-R}{K}} \\ -2B_1K\sqrt{\frac{q-R}{K}}\cosh\sqrt{\frac{q-R}{K}} \end{bmatrix}$$

Now

$$\theta = -1/2K + \sqrt{(q-R)/K}$$

$$\phi = -1/2K - \sqrt{(q-R)/K}$$

Also:

$$L\phi = M_{I0}B_1(q-\frac{1}{4K}) - (1+K\phi)((q-\frac{1}{4K})M_{I0} + e^{\phi}((q-\frac{1}{4K})(M_{I0}B_1 - B_2 - M_{I0}) + B_2R))$$

$$M\theta = (1+K\theta)((q-\frac{1}{4K})M_{I0} + e^{\theta}((q-\frac{1}{4K})(M_{I0}B_1 - B_2 - M_{I0}) + B_2R)) - M_{I0}B_1(q-\frac{1}{4K})$$

Thus:

$$C = M_{I0}e^{RT} + \frac{1}{2\pi i}\int_{\gamma-i\infty}^{\gamma+i\infty}\left[\frac{e^{(q-1/4K)T}\left(L\phi e^{\theta Z} + M\theta e^{\phi Z}\right)}{(q-\frac{1}{4K})e^{-1/2K}(q-R-\frac{1}{4K})\begin{bmatrix}-2(K(q-R)-1/4)\sinh\sqrt{\frac{q-R}{K}} - B_1\sinh\sqrt{\frac{q-R}{K}}\\ -2B_1K\sqrt{\frac{q-R}{K}}\cosh\sqrt{\frac{q-R}{K}}\end{bmatrix}}\right]dq$$

In Laplace transform, there is a rule that:

$$f(x) = \sum_{k=1}^{n}\frac{R(\lambda_k)}{Q'(\lambda_k)}\exp^{\lambda_k x}$$

For $Q(p) = \text{constant}^*(p-\lambda_1)(p-\lambda_2)\ldots(p-\lambda_n)$

$$\text{And } L[f(x)] = \frac{R(p)}{Q(p)}$$

$$\text{Consider } \tilde{M}(Z,q) = C_1e^{\theta Z} + C_2e^{\phi Z} + {M_{I0}}/{(q-R)}$$

Put $q=q-1/4K$, we get:

$$\tilde{M}(Z,q-1/4K) = \frac{M_{I0}}{q-R-\frac{1}{4K}} + \frac{L\phi e^{\theta Z} + M\theta e^{\phi Z}}{(q-\frac{1}{4K})e^{-1/2K}(q-R-\frac{1}{4K})\begin{bmatrix}-2(K(q-R)-1/4)\sinh\sqrt{\frac{q-R}{K}}\\ -B_1\sinh\sqrt{\frac{q-R}{K}}\\ -2B_1K\sqrt{\frac{q-R}{K}}\cosh\sqrt{\frac{q-R}{K}}\end{bmatrix}}$$

$$\text{Consider: } Q(q-\frac{1}{4K}) = (q-\frac{1}{4K})e^{-1/2K}(q-R-\frac{1}{4K})\begin{bmatrix}-2(K(q-R)-1/4)\sinh\sqrt{\frac{q-R}{K}}\\ -B_1\sinh\sqrt{\frac{q-R}{K}}\\ -2B_1K\sqrt{\frac{q-R}{K}}\cosh\sqrt{\frac{q-R}{K}}\end{bmatrix}$$

Then $Q=0$ has roots at $q-1/4K=0$, $q-R-1/4K=0$, or said $q=1/4K$, $q=R+1/4K$ and roots of equation:

$$-2(K(q-R)-1/4)\sinh\sqrt{\frac{q-R}{K}} - B_1\sinh\sqrt{\frac{q-R}{K}} - 2B_1K\sqrt{\frac{q-R}{K}}\cosh\sqrt{\frac{q-R}{K}} = 0$$

$$\Rightarrow \tanh\sqrt{\frac{q-R}{K}} = \frac{2B_1K\sqrt{(q-R)/K}}{0.5-2K(q-R)-B_1}$$

for variable $q-1/4K$

For q less than R, $\sqrt{(q-R)/K}$ is not real, however:

$$\tanh\sqrt{\frac{q-R}{K}} = \tanh(i\sqrt{\frac{R-q}{K}}) = \frac{e^{i\sqrt{\frac{R-q}{K}}} - e^{-i\sqrt{\frac{R-q}{K}}}}{e^{i\sqrt{\frac{R-q}{K}}} + e^{-i\sqrt{\frac{R-q}{K}}}}$$

$$= \frac{\cos\sqrt{\frac{R-q}{K}} + i\sin\sqrt{\frac{R-q}{K}} - \cos\sqrt{\frac{R-q}{K}} + i\sin\sqrt{\frac{R-q}{K}}}{\cos\sqrt{\frac{R-q}{K}} + i\sin\sqrt{\frac{R-q}{K}} + \cos\sqrt{\frac{R-q}{K}} - i\sin\sqrt{\frac{R-q}{K}}}$$

$$= i\tan\sqrt{\frac{R-q}{K}}$$

$$\Rightarrow i\tan\sqrt{\frac{R-q}{K}} = \frac{2B_1K\sqrt{\frac{q-R}{K}}}{0.5-2K(q-R)-B_1}$$

$$\tan\sqrt{-(q-R)/K} = \frac{2B_1K\sqrt{q-R/K}}{\sqrt{-1}(0.5-2K(q-R)-B_1)} = \frac{2B_1K\sqrt{-(q-R)/K}}{0.5-2K(q-R)-B_1}$$

Thus, Q can be written as follows:

$$Q(q-1/4K) = e^{-\gamma/2K}(q-1/4K)(q-R-1/4K)(q-a_1)...(q-a_n)$$

for $a_1,...a_n$ are roots of

$$\tanh\sqrt{\frac{q-R}{K}} = \frac{2B_1K\sqrt{(q-R)/K}}{0.5-2K(q-R)-B_1} \text{ for } q \text{ is real and larger than } R$$

$$\tan\sqrt{\frac{-(q-R)}{K}} = \frac{2B_1K\sqrt{-(q-R)/K}}{0.5-2K(q-R)-B_1} \text{ for } q \text{ is real and less than } R$$

Applying the rule of Laplace transform with variable *q-1/4K*, we get:

$$M(Z,T) = L^{-1}\left\{\frac{M_{I0}}{q-R-\frac{1}{4K}}\right\}$$

$$+ \sum_{q-\frac{1}{4K}=0}^{a_n} \frac{\left[L\phi e^{\theta Z} + M\theta e^{\phi Z}\right]e^{(q-1/4K)T}}{\frac{\partial}{\partial(q-1/4K)}\left\{(q-R-\frac{1}{4K})(q-\frac{1}{4K})e^{-\gamma/2K}\begin{bmatrix}-2(K(q-R)-\frac{1}{4})\sinh\sqrt{\frac{q-R}{K}} - B_1\sinh\sqrt{\frac{q-R}{K}} \\ -2B_1K\sqrt{\frac{q-R}{K}}\cosh\sqrt{\frac{q-R}{K}}\end{bmatrix}\right\}}$$

$$M(Z,T) = M_{I0}e^{RT} + \sum_{q-\frac{1}{4K}=0}^{a_n} \frac{\left[L\phi e^{\theta Z} + M\theta e^{\phi Z}\right]e^{(q-1/4k)T}}{\frac{\partial}{\partial q}\left\{(q-R-\frac{1}{4K})(q-\frac{1}{4K})e^{-\gamma/2K}\begin{bmatrix}-2(K(q-R)-\frac{1}{4})\sinh\sqrt{\frac{q-R}{K}} \\ -B_1\sinh\sqrt{\frac{q-R}{K}} \\ -2B_1K\sqrt{\frac{q-R}{K}}\cosh\sqrt{\frac{q-R}{K}}\end{bmatrix}\right\}}$$

For the summation over *q-1/4k=0* to *q-1/4k=a_n*, we can rewrite it as from *q=1/4k*, *q=R+1/4K* to *q=a'_n*, for *a'_i = a_i+R+1/4k*, or we can say *a'_i* are roots of $\tanh\sqrt{\frac{q-R}{K}} = \frac{2B_1K\sqrt{(q-R)/K}}{0.5-2K(q-R)-B_1}$ with variable *q*.

We, specially, separate contribution of the summation when *q* are *1/4K* and *R+1/4K*, when q is *R+1/4K*, we have:

$$\theta = \frac{-1+\sqrt{4K(R+1/4K-R)}}{2K} = 0$$

$$\phi = \frac{-1-\sqrt{4K(R+1/4K-R)}}{2K} = -1/K$$

$$L\phi = M_{I0}B_1(R+\frac{1}{4K}-\frac{1}{4K}) - (1+K(\frac{-1}{K}))(...)$$
$$= M_{I0}B_1R$$

$$M\theta = 1^*((R+\frac{1}{4K}-\frac{1}{4K})M_{I0} + e^0((R+\frac{1}{4K}-\frac{1}{4K})(M_{I0}B_1 - B_2 - M_{I0}) + B_2R)$$
$$- M_{I0}B_1(R+\frac{1}{4K}-\frac{1}{4K})$$
$$= 0$$

$$\frac{\partial}{\partial q}\left[(q-\frac{1}{4K})(q-R-\frac{1}{4K})\begin{pmatrix}(1+K\theta)(1+K\phi-B_1)e^{\theta}\\-(1+K\phi)(1+K\theta-B_1)e^{\phi}\end{pmatrix}\right]\Bigg|_{q=R+1/4K}$$
$$= (R+\frac{1}{4K}-\frac{1}{4K})\left[1^*(1+K(\frac{-1}{K})-B_1)e^0 - (1+K(\frac{-1}{K}))(...)\right]$$
$$= -RB_1$$

Thus, the contribution of summation at $q=R+1/4K$ is:

$$\frac{M_{I0}B_1\mathrm{Re}^{0^*Z}}{-B_1R}e^{(R+1/4K-1/4K)T} = -M_{I0}e^{RT}$$

when q is $1/4K$, we have:

$$\theta = \frac{-1+\sqrt{4K(1/4K-R)}}{2K} = \frac{-1+\sqrt{1-4KR}}{2K} = \theta_1$$

$$\phi = \frac{-1-\sqrt{4K(1/4K-R)}}{2K} = \frac{-1-\sqrt{1-4KR}}{2K} = \phi_1$$

$$L\phi_1 = M_{I0}B_1(\frac{1}{4K}-\frac{1}{4K})$$
$$-(1+K\phi_1)((\frac{1}{4K}-\frac{1}{4K})M_{I0} + e^{\phi_1}((\frac{1}{4K}-\frac{1}{4K})(M_{I0}B_1 - B_2 - M_{I0}) + B_2R))$$
$$= -(1+K\phi_1)e^{\phi_1}B_2R$$

$$M\theta_1 = (1+K\theta_1)((\frac{1}{4K}-\frac{1}{4K})M_{I0} + e^{\theta_1}((\frac{1}{4K}-\frac{1}{4K})(M_{I0}B_1 - B_2 - M_{I0}) + B_2R))$$
$$- M_{I0}B_1(\frac{1}{4K}-\frac{1}{4K})$$
$$= (1+K\theta_1)e^{\theta_1}B_2R$$

$$\frac{\partial}{\partial q}\left[(q-\frac{1}{4K})(q-R-\frac{1}{4K})\left((1+K\theta)(1+K\phi-B_1)e^{\theta} - (1+K\phi)(1+K\theta-B_1)e^{\phi}\right)\right]\Bigg|_{q=1/4K}$$
$$= (\frac{1}{4K}-R-\frac{1}{4K})\left((1+K\theta_1)(1+K\phi_1-B_1)e^{\theta_1} - (1+K\phi_1)(1+K\theta_1-B_1)e^{\phi_1}\right)$$
$$= -R\left((1+K\theta_1)(1+K\phi_1-B_1)e^{\theta_1} - (1+K\phi_1)(1+K\theta_1-B_1)e^{\phi_1}\right)$$
$$Let \quad a_1(\theta_1,\phi_1) = (1+K\theta_1)(1+K\phi_1-B_1)e^{\theta_1} - (1+K\phi_1)(1+K\theta_1-B_1)e^{\phi_1}$$

Thus, the contribution of summation from $q=1/4K$ is:

$$\frac{e^{0^*T}\left[-(1+K\phi_1)e^{\phi_1}B_2\,\mathrm{Re}^{\theta_1Z} + (1+K\theta_1)e^{\theta_1}B_2\,\mathrm{Re}^{\phi_1Z}\right]}{-Ra_1(\theta_1,\phi_1)}$$
$$= \frac{B_2\left[(1+K\phi_1)e^{\phi_1}e^{\theta_1Z} - (1+K\theta_1)e^{\theta_1}e^{\phi_1Z}\right]}{a_1(\theta_1,\phi_1)}$$

Therefore, M becomes:

$$M(Z,T)=\frac{B_2\left[(1+K\phi_1)e^{\phi_1 Z}e^{\theta_1 Z}-(1+K\theta_1)e^{\theta_1 Z}e^{\phi_1 Z}\right]}{a_1(\theta_1,\phi_1)}$$

$$+\sum_{q=a_1}^{a_n}\frac{\left[L\phi e^{\theta Z}+M\theta e^{\phi Z}\right]e^{(q-1/4K)T}}{\frac{\partial}{\partial q}\left\{(q-R-\frac{1}{4K})(q-\frac{1}{4K})e^{-1/2K}\left[\begin{array}{l}-2(K(q-R)-1/4)\sinh\sqrt{\frac{q-R}{K}}-B_1\sinh\sqrt{\frac{q-R}{K}}\\-2B_1K\sqrt{\frac{q-R}{K}}\cosh\sqrt{\frac{q-R}{K}}\end{array}\right]\right\}}$$

where the summation is over all the poles, except q=1/4K and q=R+1/4K , those poles are the roots of the equations

$$\tanh\sqrt{\frac{q-R}{K}}=\frac{2B_1K\sqrt{(q-R)/K}}{0.5-2K(q-R)-B_1}\quad\text{for q is real and larger than R}$$

$$\tan\sqrt{\frac{-(q-R)}{K}}=\frac{2B_1K\sqrt{-(q-R)/K}}{0.5-2K(q-R)-B_1}\quad\text{for q is real and less than R}$$

Consider $f(q)=\tan\sqrt{\frac{-(q-R)}{K}}-\frac{2B_1K\sqrt{-(q-R)/K}}{0.5-2K(q-R)-B_1}$ for q-R is negative and $a_1 \ldots a_n$ are roots of *f(q)*, put $q_m=-m^2\pi^2K+R$, *m* is integer, we have:

$$f(q_m)=\tan\sqrt{\frac{m^2\pi^2K}{K}}-\frac{2B_1K\sqrt{\frac{m^2\pi^2K}{K}}}{0.5-2K(-m^2\pi^2K)-B_1}$$

$$=\tan(m\pi)-\frac{2B_1Km\pi}{0.5+2K^2m^2\pi^2-B_1}$$

$$=\frac{-2B_1}{1/2Km\pi+2Km\pi-B_1/Km\pi}$$

$$\lim_{m\to\infty}f(q_m)=\frac{-2B_1}{0+\infty-0}$$

$$=0$$

This means *f(q)* has infinite roots, and thus *M* has infinite poles when *q-R* is less than zero. For *q-R>0* and *q* is real number, consider $L\phi e^{\theta Z}+M\theta e^{\phi Z}$:

$$=M_{I0}B_1(q-\frac{1}{4K})(e^{\theta Z}-e^{\phi Z})-(q-\frac{1}{4K})M_{I0}\left[(1+K\phi)e^{\theta Z}-(1+K\theta)e^{\phi Z}\right]$$

$$-\left[(q-\frac{1}{4K})(M_{I0}B_1-B_2-M_{I0})+B_2R\right]\left[(1+K\phi)e^{\phi}e^{\theta Z}-(1+K\theta)e^{\theta}e^{\phi Z}\right]$$

$$e^{\theta Z}-e^{\phi Z}=e^{-Z/2K}(e^{\sqrt{\frac{q-R}{K}}Z}-e^{-\sqrt{\frac{q-R}{K}}Z})=2e^{\frac{-Z}{2K}}\sinh\sqrt{\frac{q-R}{K}}Z$$

$$(1+K\phi)e^{\theta Z}-(1+K\theta)e^{\phi Z}=\frac{1}{2}(e^{\theta Z}-e^{\phi Z})-\sqrt{K(q-R)}(e^{\theta Z}+e^{\phi Z})$$

$$=2e^{\frac{-Z}{2K}}\left[\frac{1}{2}\sinh\sqrt{\frac{q-R}{K}}Z-\sqrt{K(q-R)}\cosh\sqrt{\frac{q-R}{K}}Z\right]$$

$$(1+K\phi)e^{\phi}e^{\theta Z}-(1+K\theta)e^{\theta}e^{\phi Z}$$

$$=\frac{1}{2}\left[e^{\phi}e^{\theta Z}-e^{\theta}e^{\phi Z}\right]-\sqrt{K(q-R)}\left[e^{\phi}e^{\theta Z}+e^{\theta}e^{\phi Z}\right]$$

$$=-2e^{\frac{-(1+Z)}{2K}}\left[\frac{1}{2}\sinh(\sqrt{\frac{q-R}{K}}(1-Z))+\sqrt{K(q-R)}\cosh(\sqrt{\frac{q-R}{K}}(1-Z))\right]$$

$L\phi e^{\theta Z}+M\theta e^{\phi Z}$ now becomes:

$$= 2e^{\frac{-Z}{2K}}\left\{\begin{array}{l} M_{I0}B_1(q-\frac{1}{4K})(\sinh\sqrt{\frac{q-R}{K}}Z)-(q-\frac{1}{4K})M_{I0}\left[\begin{array}{l}\frac{1}{2}\sinh\sqrt{\frac{q-R}{K}}Z \\ -\sqrt{K(q-R)}\cosh\sqrt{\frac{q-R}{K}}Z\end{array}\right] \\ +e^{\frac{-1}{2K}}\left[(q-\frac{1}{4K})(M_{I0}B_1-B_2-M_{I0})+B_2R\right]\left[\begin{array}{l}\frac{1}{2}\sinh(\sqrt{\frac{q-R}{K}}(1-Z)) \\ +\sqrt{K(q-R)}\cosh(\sqrt{\frac{q-R}{K}}(1-Z))\end{array}\right]\end{array}\right\}$$

$$= 2e^{\frac{-Z}{2K}}\left\{\begin{array}{l}(q-\frac{1}{4K})M_{I0}\left[(B_1-\frac{1}{2})\sinh\sqrt{\frac{q-R}{K}}Z+\sqrt{K(q-R)}\cosh\sqrt{\frac{q-R}{K}}Z\right] \\ +e^{\frac{-1}{2K}}\left[(q-\frac{1}{4K})(M_{I0}B_1-B_2-M_{I0})+B_2R\right]\left[\begin{array}{l}\frac{1}{2}\sinh(\sqrt{\frac{q-R}{K}}(1-Z)) \\ +\sqrt{K(q-R)}\cosh(\sqrt{\frac{q-R}{K}}(1-Z))\end{array}\right]\end{array}\right\}$$

For q-R<0 and q is real number, Then:

$$\textit{From } \theta = -1/2K + i\sqrt{(R-q)/K}\,;\ \phi = -1/2K - i\sqrt{(R-q)/K}$$

$$\Rightarrow \theta = \bar{\phi} \textit{ by the definition that } \bar{Z} = a - bi \textit{ when } Z = a + bi$$

We can easily prove that:

$$\overline{L\phi e^{\theta Z}} = L\theta e^{\phi Z} = -M\theta e^{\phi Z}$$

Therefore:

$$\begin{aligned} L\phi e^{\theta Z} + M\theta e^{\phi Z} &= L\phi e^{\theta Z} - \overline{L\phi e^{\theta Z}} \\ &= 2\,\mathrm{Im}\left[L\phi e^{\theta Z}\right]i \end{aligned}$$

Then:

$$L\phi = M_{I0}B_1(q-\frac{1}{4K})-(1+K\phi)((q-\frac{1}{4K})M_{I0}+e^{\phi}((q-\frac{1}{4K})(M_{I0}B_1-B_2-M_{I0})+B_2R))$$

$$=(q-\frac{1}{4K})\left[\begin{array}{l}M_{I0}B_1 \\ -(1+K\phi)(M_{I0}+e^{\phi}(M_{I0}B_1-B_2-M_{I0}))\end{array}\right]-e^{\phi}(1+K\phi)B_2R$$

$$=(q-\frac{1}{4K})\left[\begin{array}{l}M_{I0}B_1 \\ -(\frac{1}{2}-i\sqrt{K(R-q)})(M_{I0}+e^{\frac{-1}{2K}}(\cos\sqrt{\frac{R-q}{K}}-i\sin\sqrt{\frac{R-q}{K}})(M_{I0}B_1-B_2-M_{I0})\end{array}\right]$$

$$-(\frac{1}{2}-i\sqrt{K(R-q)})e^{\frac{-1}{2K}}B_2R(\cos\sqrt{\frac{R-q}{K}}-i\sin\sqrt{\frac{R-q}{K}})$$

$$e^{\theta Z} = e^{\frac{-Z}{2K}}(\cos(\sqrt{\frac{R-q}{K}}Z)+i\sin(\sqrt{\frac{R-q}{K}}Z))$$

Thus $\mathrm{Im}[L\phi e^{\theta Z}]$ become:

$$= e^{\frac{-Z}{2K}}\left\{\begin{array}{l}(q-\frac{1}{4K})\sqrt{K(R-q)}e^{\frac{-1}{2K}}(M_{I0}B_1-B_2-M_{I0})\left[\begin{array}{l}\cos(\sqrt{\frac{R-q}{K}}Z)\cos\sqrt{\frac{R-q}{K}}\\+\sin(\sqrt{\frac{R-q}{K}}Z)\sin\sqrt{\frac{R-q}{K}}\end{array}\right]\\+\frac{e^{\frac{-1}{2K}}}{2}(q-\frac{1}{4K})(M_{I0}B_1-B_2-M_{I0})\left[\begin{array}{l}\cos(\sqrt{\frac{R-q}{K}}Z)\sin\sqrt{\frac{R-q}{K}}\\-\sin(\sqrt{\frac{R-q}{K}}Z)\cos\sqrt{\frac{R-q}{K}}\end{array}\right]\\+\frac{e^{\frac{-1}{2K}}B_2R}{2}\left[\cos(\sqrt{\frac{R-q}{K}}Z)\sin\sqrt{\frac{R-q}{K}}-\sin(\sqrt{\frac{R-q}{K}}Z)\cos\sqrt{\frac{R-q}{K}}\right]\\+\sqrt{K(R-q)}e^{\frac{-1}{2K}}B_2R\left[\cos(\sqrt{\frac{R-q}{K}}Z)\cos\sqrt{\frac{R-q}{K}}+\sin(\sqrt{\frac{R-q}{K}}Z)\sin\sqrt{\frac{R-q}{K}}\right]\\+(q-\frac{1}{4K})M_{I0}\sqrt{K(R-q)}\cos(\sqrt{\frac{R-q}{K}}Z)+(q-\frac{1}{4K})M_{I0}(B_1-\frac{1}{2})\sin(\sqrt{\frac{R-q}{K}}Z)\end{array}\right\}$$

$$= e^{\frac{-Z}{2K}}\left\{\begin{array}{l}M_{I0}(q-\frac{1}{4K})\left[\sqrt{K(R-q)}\cos(\sqrt{\frac{R-q}{K}}Z)+(B_1-\frac{1}{2})\sin(\sqrt{\frac{R-q}{K}}Z)\right]\\+e^{\frac{-1}{2K}}\left\{\begin{array}{l}\left[(q-\frac{1}{4K})\sqrt{K(R-q)}(M_{I0}B_1-B_2-M_{I0})+\sqrt{K(R-q)}B_2R\right]\cos(\sqrt{\frac{R-q}{K}}(1-Z))\\+\left[\frac{1}{2}(q-\frac{1}{4K})(M_{I0}B_1-B_2-M_{I0})+\frac{B_2R}{2}\right]\sin(\sqrt{\frac{R-q}{K}}(1-Z))\end{array}\right.\end{array}\right\}$$

$$= e^{\frac{-Z}{2K}}\left\{\begin{array}{l}M_{I0}(q-\frac{1}{4K})\left[\sqrt{K(R-q)}\cos(\sqrt{\frac{R-q}{K}}Z)+(B_1-\frac{1}{2})\sin(\sqrt{\frac{R-q}{K}}Z)\right]\\+e^{\frac{-1}{2K}}\left[(q-\frac{1}{4K})(M_{I0}B_1-B_2-M_{I0})+B_2R\right]\left[\begin{array}{l}\sqrt{K(R-q)}\cos(\sqrt{\frac{R-q}{K}}(1-Z))\\+\frac{1}{2}\sin(\sqrt{\frac{R-q}{K}}(1-Z))\end{array}\right]\end{array}\right\}$$

Note: as $q = R$, since $\sqrt{K(R-q)}$, $\sin(\sqrt{\frac{R-q}{K}}Z)$, and $\sin(\sqrt{\frac{R-q}{K}}(1-Z))$ are all equal to zero.

Thus $Im[L\phi e^{\theta Z}] = 0$ at $q = R$.
At poles, consider:

$$\frac{\partial}{\partial q}\left\{e^{-\gamma_{2k}}(q-R-\frac{1}{4K})(q-\frac{1}{4K})\left[\begin{array}{l}-2(K(q-R)-\frac{1}{4})\sinh\sqrt{\frac{q-R}{K}}-B_1\sinh\sqrt{\frac{q-R}{K}}\\-2B_1K\sqrt{\frac{q-R}{K}}\cosh\sqrt{\frac{q-R}{K}}\end{array}\right]\right\}$$

$$= \frac{\partial(q-1/4K)(q-R-1/4K)}{\partial q} e^{-1/2K} \begin{bmatrix} -2(K(q-R)-1/4)\sinh\sqrt{\frac{q-R}{K}} - B_1 \sinh\sqrt{\frac{q-R}{K}} \\ -2B_1 K\sqrt{\frac{q-R}{K}}\cosh\sqrt{\frac{q-R}{K}} \end{bmatrix}$$

$$+(q-\frac{1}{4K})(q-R-\frac{1}{4K})e^{-1/2K}\frac{\partial}{\partial q}\begin{bmatrix} -2(K(q-R)-1/4)\sinh\sqrt{\frac{q-R}{K}} - B_1 \sinh\sqrt{\frac{q-R}{K}} \\ -2B_1 K\sqrt{\frac{q-R}{K}}\cosh\sqrt{\frac{q-R}{K}} \end{bmatrix}$$

Note that at pole, $-2(K(q-R)-\frac{1}{4})\sinh\sqrt{\frac{q-R}{K}} - B\sinh\sqrt{\frac{q-R}{K}} - 2Bk\sqrt{\frac{q-R}{K}}\cosh\sqrt{\frac{q-R}{K}} = 0,$

and thus :

$$= (q-\frac{1}{4K})(q-R-\frac{1}{4K})e^{-1/2K}\frac{\partial}{\partial q}\begin{bmatrix} -2(K(q-R)-1/4)\sinh\sqrt{\frac{q-R}{K}} - B_1 \sinh\sqrt{\frac{q-R}{K}} \\ -2B_1 K\sqrt{\frac{q-R}{K}}\cosh\sqrt{\frac{q-R}{K}} \end{bmatrix}$$

$$= (q-\frac{1}{4K})(q-R-\frac{1}{4K})e^{-1/2K}\begin{bmatrix} -2(K(q-R)-1/4)(\frac{1}{2\sqrt{K(q-R)}})\cosh\sqrt{\frac{q-R}{K}} \\ -2K\sinh\sqrt{\frac{q-R}{K}} - B_1(\frac{1}{2\sqrt{K(q-R)}})\cosh\sqrt{\frac{q-R}{K}} \\ -2B_1K(\frac{1}{2\sqrt{K(q-R)}})\cosh\sqrt{\frac{q-R}{K}} \\ -2B_1K(\frac{1}{2\sqrt{K(q-R)}})\sqrt{\frac{q-R}{K}}\sinh\sqrt{\frac{q-R}{K}} \end{bmatrix}$$

$$= (q-\frac{1}{4K})(q-R-\frac{1}{4K})e^{-1/2K}\begin{bmatrix} (\frac{1}{2\sqrt{K(q-R)}})\begin{Bmatrix} -2(K(q-R)-\frac{1}{4}) \\ -B_1 - 2B_1K \end{Bmatrix}\cosh\sqrt{\frac{q-R}{K}} \\ -(2K+B_1)\sinh\sqrt{\frac{q-R}{K}} \end{bmatrix}$$

As q-R is negative:

$$\cosh\sqrt{\frac{q-R}{K}} = \cosh i\sqrt{\frac{-(q-R)}{K}} = \frac{e^{i\sqrt{\frac{-(q-R)}{K}}} + e^{-i\sqrt{\frac{-(q-R)}{K}}}}{2}$$

$$= \frac{1}{2}\left(\cos\sqrt{\frac{-(q-R)}{K}} + i\sin\sqrt{\frac{-(q-R)}{K}} + \cos\sqrt{\frac{-(q-R)}{K}} - i\sin\sqrt{\frac{-(q-R)}{K}}\right)$$

$$= \cos\sqrt{\frac{-(q-R)}{K}}$$

$$\sinh\sqrt{\frac{q-R}{K}} = i\sin\sqrt{\frac{-(q-R)}{K}}$$

$$\therefore = (q-\frac{1}{4K})(q-R-\frac{1}{4K})e^{-1/2k}\begin{bmatrix}(\frac{1}{2\sqrt{K(q-R)}})\begin{Bmatrix}-2(K(q-R)-\frac{1}{4})\\-B_1-2B_1K\end{Bmatrix}\cos\sqrt{\frac{R-q}{K}}\\-(2K+B_1)i\sin\sqrt{\frac{R-q}{K}}\end{bmatrix}$$

$$= i(q-\frac{1}{4K})(q-R-\frac{1}{4K})e^{-1/2k}\left[\frac{2(K(q-R)-\frac{1}{4})+B_1+2B_1K}{2\sqrt{K(R-q)}}\cos\sqrt{\frac{R-q}{K}}-(2K+B_1)\sin\sqrt{\frac{R-q}{K}}\right]$$

Note: as q=R, the term $1\Big/\frac{\partial}{\partial}(...)=0$, thus the contribution of the summation at q=R is zero.

Therefore, solution of M as q less than R can be written as:

$$M(Z,T)=\frac{B_2\left[(1+K\phi_1)e^{\phi_1}e^{\theta_1 Z}-(1+K\theta_1)e^{\theta_1}e^{\phi_1 Z}\right]}{a_1(\theta_1,\phi_1)}$$

$$+\sum_{q=a_1}^{a_n}\frac{2i\,\mathrm{Im}[L\phi e^{\theta Z}]e^{(q-1/4k)T}}{\frac{\partial}{\partial q}\left\{(q-R-\frac{1}{4K})(q-\frac{1}{4K})e^{-1/2K}\begin{bmatrix}-2(K(q-R)-1/4)\sinh\sqrt{\frac{q-R}{K}}-B_1\sinh\sqrt{\frac{q-R}{K}}\\-2B_1K\sqrt{\frac{q-R}{K}}\cosh\sqrt{\frac{q-R}{K}}\end{bmatrix}\right\}}$$

$$M(Z,T)=\frac{B_2\left[(1+K\phi_1)e^{\phi_1}e^{\theta_1 Z}-(1+K\theta_1)e^{\theta_1}e^{\phi_1 Z}\right]}{a_1(\theta_1,\phi_1)}$$

$$+\sum_{q=a_1}^{a_n}\frac{2e^{\left[(q-\frac{1}{4K})T+\frac{1-Z}{2K}\right]}f(K,B_1,B_2,M_{10},Z,q)}{(q-\frac{1}{4K})(q-R-\frac{1}{4K})\left[\frac{2(K(q-R)-\frac{1}{4})+B_1+2B_1K}{2\sqrt{K(R-q)}}\cos\sqrt{\frac{R-q}{K}}-(2K+B_1)\sin\sqrt{\frac{R-q}{K}}\right]}$$

$$a_1(\theta_1,\phi_1)=(1+K\theta_1)(1+K\phi_1-B_1)e^{\theta_1}-(1+K\phi_1)(1+K\theta_1-B_1)e^{\phi_1}$$

$$\theta_1=(-1+\sqrt{1-4KR})/2K$$

$$\phi_1=(-1-\sqrt{1-4KR})/2K$$

As $\theta_1=\frac{-1+\sqrt{1-4KR}}{2K}$; $\phi_1=\frac{-1-\sqrt{1-4KR}}{2K}$, θ_1 and ϕ_1 are not real numbers when *1 - 4KR<0*.

Consider $a_1(\theta_1, \phi_1)$:

$$a_1(\theta_1,\phi_1)=(1+K\theta_1)(1+K\phi_1-B_1)e^{\theta_1}-(1+K\phi_1)(1+K\theta_1-B_1)e^{\phi_1}$$

$$=(KR-B_1(1+K\theta_1))e^{\theta_1}-(KR-B_1(1+K\phi_1))e^{\phi_1}$$

$$=(KR-B_1/2)(e^{\theta_1}-e^{\phi_1})-B_1\sqrt{1-4KR}(e^{\theta_1}+e^{\phi_1})/2$$

For 1-4KR>0, we have:

$$e^{\theta_1}-e^{\phi_1}=e^{-1/2K}(e^{\sqrt{1-4KR}/2K}-e^{-\sqrt{1-4KR}/2K})$$

$$=2e^{-1/2K}\sinh(\sqrt{1-4KR}/2K)$$

$$e^{\theta_1}+e^{\phi_1}=2e^{-1/2K}\cosh(\sqrt{1-4KR}/2K)$$

While 1-4KR<0, we have:

$$e^{\theta_1}-e^{\phi_1}=e^{-1/2K}(e^{i\sqrt{4KR-1}/2K}-e^{-i\sqrt{4KR-1}/2K})$$

$$=2ie^{-1/2K}\sin(\sqrt{1-4KR}/2K)$$

$$e^{\theta_1}+e^{\phi_1}=2e^{-1/2K}\cos(\sqrt{1-4KR}/2K)$$

Thus $a_1(\theta_1, \phi_1)$ become:

$$a_1(\theta_1,\phi_1) = e^{-1/2K}\left[(2KR - B_1)\sinh\frac{\sqrt{1-4KR}}{2K} - B_1\sqrt{1-4KR}\cosh\frac{\sqrt{1-4KR}}{2K}\right]$$

when *1 - 4KR > 0*

$$a_1(\theta_1,\phi_1) = ie^{-1/2K}\left[(2KR - B_1)\sin\frac{\sqrt{4KR-1}}{2K} - B_1\sqrt{4KR-1}\cos\frac{\sqrt{4KR-1}}{2K}\right]$$

when *1 - 4KR < 0*

Consider $(1+K\phi_1)e^{\phi_1}e^{\theta_1 Z} - (1+K\theta_1)e^{\theta_1}e^{\phi_1 Z}$:

$$= e^{\phi_1}e^{\theta_1 Z} - e^{\theta_1}e^{\phi_1 Z} + K(\phi_1 e^{\phi_1}e^{\theta_1 Z} - \theta_1 e^{\theta_1}e^{\phi_1 Z})$$

$$= \frac{1}{2}(e^{\phi_1}e^{\theta_1 Z} - e^{\theta_1}e^{\phi_1 Z}) - \frac{\sqrt{1-4KR}}{2}(e^{\phi_1}e^{\theta_1 Z} + e^{\theta_1}e^{\phi_1 Z})$$

For *1-4KR > 0*, we have:

$$e^{\phi_1}e^{\theta_1 Z} - e^{\theta_1}e^{\phi_1 Z} = \exp(\frac{-(1+Z)}{2K})\left(\exp(\frac{\sqrt{1-4KR}}{2K}(Z-1)) - \exp(\frac{-\sqrt{1-4KR}}{2K}(Z-1))\right)$$

$$= 2e^{\frac{(1+Z)}{2K}}\sinh\left(\frac{\sqrt{1-4KR}}{2K}(Z-1)\right)$$

$$e^{\phi_1}e^{\theta_1 Z} + e^{\theta_1}e^{\phi_1 Z} = 2e^{\frac{(1+Z)}{2K}}\cosh\left(\frac{\sqrt{1-4KR}}{2K}(Z-1)\right)$$

For *1-4KR < 0*, we have:

$$e^{\phi_1}e^{\theta_1 Z} - e^{\theta_1}e^{\phi_1 Z} = \exp(\frac{-(1+Z)}{2K})\left(\exp(\frac{i\sqrt{4KR-1}}{2K}(Z-1)) - \exp(\frac{-i\sqrt{4KR-1}}{2K}(Z-1))\right)$$

$$= 2ie^{\frac{(1+Z)}{2K}}\sin\left(\frac{\sqrt{4KR-1}}{2K}(Z-1)\right)$$

$$e^{\phi_1}e^{\theta_1 Z} + e^{\theta_1}e^{\phi_1 Z} = 2e^{\frac{(1+Z)}{2K}}\cos\left(\frac{\sqrt{4KR-1}}{2K}(Z-1)\right)$$

Thus, $(1+K\phi_1)e^{\phi_1}e^{\theta_1 Z} - (1+K\theta_1)e^{\theta_1}e^{\phi_1 Z}$ become:

$$= e^{\frac{-(1+Z)}{2K}}\left[\sinh\left(\frac{\sqrt{1-4KR}}{2K}(Z-1)\right) - \sqrt{1-4KR}\cosh\left(\frac{\sqrt{1-4KR}}{2K}(Z-1)\right)\right]$$

when *1 - 4KR > 0*

$$= ie^{\frac{-(1+Z)}{2K}}\left[\sin\left(\frac{\sqrt{4KR-1}}{2K}(Z-1)\right) - \sqrt{4KR-1}\cos\left(\frac{\sqrt{4KR-1}}{2K}(Z-1)\right)\right]$$

when *1 - 4KR < 0*

Therefore, the contribution of the summation, let be $G(K,B_1,B_2,R,Z)$ at node $q=1/4K$ now becomes:

$$G(K,B_1,B_2,R,Z) = B_2\frac{e^{\frac{-Z}{2K}}\left[\sinh\left(\frac{\sqrt{1-4KR}}{2K}(Z-1)\right) - \sqrt{1-4KR}\cosh\left(\frac{\sqrt{1-4KR}}{2K}(Z-1)\right)\right]}{\left[(2KR - B_1)\sinh\frac{\sqrt{1-4KR}}{2K} - B_1\sqrt{1-4KR}\cosh\frac{\sqrt{1-4KR}}{2K}\right]}$$

when *1 - 4KR > 0*

$$G(K,B_1,B_2,R,Z) = B_2\frac{e^{\frac{-Z}{2K}}\left[\sin\left(\frac{\sqrt{4KR-1}}{2K}(Z-1)\right) - \sqrt{4KR-1}\cos\left(\frac{\sqrt{4KR-1}}{2K}(Z-1)\right)\right]}{\left[(2KR - B_1)\sin\frac{\sqrt{4KR-1}}{2K} - B_1\sqrt{4KR-1}\cos\frac{\sqrt{4KR-1}}{2K}\right]}$$

when *1 - 4KR < 0*

Solution of $M(Z,T)$ now becomes:

$$C(Z,T) = G(K,B_1,B_2,R,Z) + \sum_{q=a_1}^{a_n} \frac{2e^{\left[(q-\frac{1}{4K})T+\frac{1-Z}{2K}\right]} f(K,B_1,B_2,M_{I0},R,Z,q)}{(q-\frac{1}{4K})(q-R-\frac{1}{4K})h(K,B_1,R,q)}$$

a_i are the roots of $\tanh\sqrt{\frac{q-R}{K}} = \frac{2B_1K\sqrt{(q-R)/K}}{0.5-2K(q-R)-B_1}$ for q larger than R, and

$\tan\sqrt{\frac{-(q-R)}{K}} = \frac{2B_1K\sqrt{-(q-R)/K}}{0.5-2K(q-R)-B_1}$ for q less than R,

where:

$$G(K,B_1,B_{2*},R,Z) = B_2 \frac{e^{\frac{-Z}{2K}}\left[\sinh\left(\frac{\sqrt{1-4KR}}{2K}(Z-1)\right) - \sqrt{1-4KR}\cosh\left(\frac{\sqrt{1-4KR}}{2K}(Z-1)\right)\right]}{\left[(2KR-B_1)\sinh\frac{\sqrt{1-4KR}}{2K} - B_1\sqrt{1-4KR}\cosh\frac{\sqrt{1-4KR}}{2K}\right]}$$

when $1 - 4KR > 0$

$$G(K,B_1,B_{2*},R,Z) = B_2 \frac{e^{\frac{-Z}{2K}}\left[\sin\left(\frac{\sqrt{4KR-1}}{2K}(Z-1)\right) - \sqrt{4KR-1}\cos\left(\frac{\sqrt{4KR-1}}{2K}(Z-1)\right)\right]}{\left[(2KR-B_1)\sin\frac{\sqrt{4KR-1}}{2K} - B_1\sqrt{4KR-1}\cos\frac{\sqrt{4KR-1}}{2K}\right]}$$

when $1 - 4KR < 0$

When q is larger than R:

$$h(K,B_1,R,q) = \frac{-2(K(q-R)-\frac{1}{4}) - B_1 - 2B_1K}{2\sqrt{K(q-R)}}\cosh\sqrt{\frac{q-R}{K}} - (2K+B_1)\sinh\sqrt{\frac{q-R}{K}}$$

$$f(K,B_1,B_2,M_{I0},Z,R,q) = (q-\frac{1}{4K})M_{I0}\left[(B_1-\frac{1}{2})\sinh\sqrt{\frac{q-R}{K}}Z + \sqrt{K(q-R)}\cosh\sqrt{\frac{q-R}{K}}Z\right]$$

$$+ e^{\frac{-1}{2K}}\left[(q-\frac{1}{4K})(M_{I0}B_1 - B_2 - M_{I0}) + B_2R\right]\left[\begin{array}{l}\frac{1}{2}\sinh(\sqrt{\frac{q-R}{K}}(1-Z)) \\ +\sqrt{K(q-R)}\cosh(\sqrt{\frac{q-R}{K}}(1-Z))\end{array}\right]$$

When q is less than R:

$$h(K,B_1,R,q) = \frac{2(K(q-R)-\frac{1}{4}) + B_1 + 2B_1K}{2\sqrt{K(R-q)}}\cos\sqrt{\frac{R-q}{K}} - (2K+B_1)\sin\sqrt{\frac{R-q}{K}}$$

$$f(K,B_1,B_2,M_{I0},Z,R,q) = M_{I0}(q-\frac{1}{4K})\left[\sqrt{K(R-q)}\cos(\sqrt{\frac{R-q}{K}}Z) + (B_1-\frac{1}{2})\sin(\sqrt{\frac{R-q}{K}}Z)\right]$$

$$+ e^{\frac{-1}{2K}}\left[(q-\frac{1}{4K})(M_{I0}B_1 - B_2 - M_{I0}) + B_2R\right]\left[\begin{array}{l}\sqrt{K(R-q)}\cos(\sqrt{\frac{R-q}{K}}(1-Z)) \\ +\frac{1}{2}\sin(\sqrt{\frac{R-q}{K}}(1-Z))\end{array}\right]$$

References

1. Al-Niami, A. N. S. and Rushton, K. R. "Dispersion in stratified porous media: analytical solutions". *Water Resources Research,* Vol. 15. No. 5, 1044-1048 (1979).

2. Alshawabkeh, A. and Adrian, D. D. "Analytical water quality model for a sinusoidally varying BOD discharge concentrtaion". *Water Researches*, Vol. 31. No. 5, 1207-1215 (1997).

3. Bahr, J. M. and Rubin, J., "Direct comparison of kinetics and local equilibrium formulations for solute transport affected by surface reactions". *Water Resources Research,* Vol. 23, 438-452 (1987).

4. Barry, D. A. "Analytical solution of a convection-dispersion model with time-dependent transport coefficients". *Water Resources Research,* Vol. 25. No. 12, 2407-2416 (1989).

5. Cao, Zhixian. "Turbulent bursting-based sediment entrainment function". *Journal of Hydraulic Engineering,* ASCE, 123(3)., 233-236 (1997).

6. Cao, Zhixian. "Equilibrium near-bed concentration of suspended sediment". *Journal of Hydraulic Engineering,* ASCE, 125(12)., 1270-1278 (1999).

7. Carroll, J. and Harms, I. H., "Uncertainty analysis of partition coefficients in a radionuclide transport model", *Water Research*, Vol. 33, No. 11, 2617-2626 (1999).

8. Celik, I., and Rodi, W. "Modeling suspension sediment transport in nonequilibrium situations", *Journal of Hydraulic Engineering,* ASCE, 114(10)., 1157-1191 (1989).

9. Chapra, S. C. *Surface water quality modeling*, McGraw-Hill (1997).

10. Cheng, K. J. "Bottom –boundary condition for nonequilibrium transport of sediment", *Journal of Geophysical research,* American Geophysical Union, Vol. 89, No. C5, 8209-8214 (1984).

11. Cheng, N, S., "Simplified settling velocity formula for sediment particle," *Journal of Hydraulic Engineering,* ASCE, 123(2)., 149-152 (1997).

12. Chiu, C. L., Jin, W., and Chen, Y.C., "Mathematical models of distribution of sediment concentration", *Journal of Hydraulic Engineering,* Vol. 126, No. 1, 16-23 (2000).

13. Choy, B., and Reible, D. D., *Diffusion models of environmental transport,* Lewis Publishers, (1999).

14. Civil Engineering Department of HKSAR., *Environmental impact assessment study for disposal of contaminated mud in East Sha Chau Marine Borrow Pit,* ERM-Hong Kong, LTD, (1997).

15. Connolly, J. P., Zahakos, H. A., Benaman, J., Ziegler, C. K., Rhea, J. R. and Russell, K., "A model of PCB fate in the upper Hudson River". *Environmental Science and Technology,* Vol. 34, No. 19, 4076-4087 (2000).

16. Cvetkovic , V. and Dagan, G., "Transport of kinetically sorbing solute by steady random velocity in hetrogeneous porous formations". *Journal of Fluid Mechanics,* Vol 265, 189-215 (1994).

17. DePinto, J. V., Lick, W. and Paul, J. F. *Transport and Transformation of Contaminants Near the Sediment-Water Interface,* Lewis Publishers, (1994).

18. Einstein, H. A., "The Bed-load function for sediment transportation in open channel flow", *Technical Bulletin No. 1026, U.S. Dep. of Agriculture, Washington, D.C.,* (1950).

19. Engelund, F., and FredsØe, J., "A sediment transport model for straight alluvial channels", *Nordic Hydrology,* 7, 293-306 (1976).

20. Flury, M., Wu, Q. J., Wu, L., and Xu, L., "Analytical solution for solute transport with depth-dependent transformation or sorption coefficients", *Water Resources Research,* Vol 34, No. 11, 2931-2937 (1998).

21. Formica, S. J., Baron, J. A., Thibodeaux, L. J. and Valsaraj, K. T. "PCB transport into lake sediments. Conceptual model and laboratory simulation". *Enviornmental Science and Technlogy,* Vol 22, No. 12, 1435-1440 (1988).

22. Han, Q. W., and He, M. M., *Initiation of motion and critical velocity for sediment particles,* Science Press, Printed in China, in Chinese (1999).

23. *Handbook of Mathematical Functions*, National Bureau of Standards, Applied Mathematical Series 55, (1966).

24. Polyanin, A. D. and Manzhirov, A. V. *Handbook of Integral Equations*, CRC Press. (1998).

25. Hjelmfelt, A. T. and Lenau, C. W. "Nonequilibrium transport of suspended sediment". *Journal of Hydraulic Division,* Am. Soc. Civil Eng., 96(HY7)., 1567-1586 (1970).

26. Huang, S. L. and Wan, Zhao-hui "Study on sorption of heavy metal pollutants by sediment particles". *Journal of Hydrodynamics, Ser. B*, Vol. 3, 9-23 (1997).

27. Hwang, B. G., Jun, K. S., Lee, Y. D. and Lung, W. S. "Importance of DOC in sediments for contaminant transport modeling". *Water Science Technology,* Vol. 38, No. 11, 193-199 (1998).

28. Jobson, H. E. and Sayre, W. W. "Vertical transfer in open channel flow". *Journal of hydraulic Division,* Vol. 96, No. 3, 703-724 (1970).

29. Leji, F. J. and Van Genuchten, M. Th. "Approximate analytical solutions for solute transport in two-layer porous media". *Transport in Porous Media*, Vol 18, 65-85 (1995).

30. Liu, C., Ball, W. P. and Ellis, J. H. "An analytical solution to the one-dimensional solute advection-dispersion equation in multi-layer porous media". *Transport in Porous Media*, Vol 30, 25-43 (1998).

31. Lokenath, D. *Integral transforms and their applications.* CRC Press, Inc, 1995.

32. Luke, Y. L. *Mathematical functions and their approximations.* Academic Press, Inc, 1975.

33. Mei, C. C. "Nonuniform diffusion of suspension sediment". *Journal of Hydraulic Division,* Am Soc. Civil Eng., 95(HY1)., 581-584 (1969).

34. Ng, C. O. "Chemical transport associated with discharge of contaminated fine particles to a steady open-channel flow". *Physics of Fluids,* Vol. 12, No. 1, 136-144 (2000a).

35. Ng, C. O. "Dispersion in sediment-laden stream flow". *Journal of Engineering Mechanics,* Vol. 126, No 8, 779-786 (2000b).

36. Ng, C. O. and Yip, T. L. "Effects of kinetic sorptive exchange on solute transport in open-channel flow". *Journal of Fluid Mechanics,* Vol. 446, 321-345 (2001).

37. O'Conner, D. J. "Models of sorptive toxic substances in freshwater system I, II and III". *Journal of Environmental Engineering*, Vol. 114, No. 3, 507-574 (1988).

38. Oliver, D. R. "The sedimentation suspension of closely-sized spherical particles". *Chemical Engineering Science*, Vol. 15, 230-242, see pg 3.16 in Van Rijn (1993).

39. Prakash, A. "Analytical modeling of contaminant transport through vadose and saturated soil zones". *Journal of Hydraulic Engineering*, October 2000, 773-777 (2000).

40. Richardson, Y. F., and Zaki, W. N. "Sedimentation and fluidization". *Part I. Trans. Inst. Chem. Eng*, Vol. 32, (35-53).

41. Runkel, R. L. "Solution of the advection-dispersion equation: continuous load of finite duration". *Journal of environmental engineering*, September 1996, 830-832 (1996).

42. Schnoor, J. L. *Environmental Modeling: Fate and Transport of Pollutants in Water, Air and Soil,* John Wiley & Sons, Inc

43. Smedt, F. De., Vuksanovic, V., Meerbeeck, S. V. and Reyns, D. "A time dependent flow model for heavy metals in the Scheldt estuary". *Hydrobiologia,* Vol. 366, 143-155 (1998).

44. Smith. J. D. and Mclean. S. R. "Spatially averaged flow over a wavy surface". *Journal of Geophysical Research*, Vol. 82, No. 12, 1735-1746 (1977).

45. Thomann, R. V. and Mueller, J. A. *Principles of surface water quality modeling and control*, HarperCollins, (1987).

46. Tkalitch, P. V., Chen, W. and Tay, J. H. "Modeling of heavy metals in a reservoir with diffusive bottom layer". *Water Science Technology,* Vol. 34, No. 7-8, 117-123 (1996).

47. Valocchi, A. J. "Validity of the local equilibrium assumption for modeling sorbing solute transport through homogeneous soils". *Water Resources Research,* Vol. 21, 808-820 (1985).

48. Van Rijn, L. C. "Sediment transport, part II: suspended load transport". *Journal of Hydraulic Engineering,* Vol. 110, No. 11, 1613-1641 (1984).

49. Van Rijn, L. C. *Principles of sediment transport in rivers, estuaries and coastal seas,* Aqua Publications, (1993).

50. Wai, O. W. H. and Lu, Q. "Gradient-Adaptive -Sigma (GAS). grid for 3D mass-transport modeling". *Journal of Hydraulic Engineering,* Vol. 125, No. 2, 141-151 (1999).

51. Wu, S. C. and Gschwend, P. M. "Sorption kinetics of hydrophobic organic compounds to natural sediment ". *Environmental Science and Technology*, Vol. 20, 717-725 (1986).

52. Wei, Z. "Research on deposition process of sediment in two-dimensional, steady, uniform flow". *M. Sc. Diss*, WUHEE, (1981). see pg. 62 in Zhang and Xie (1993).

53. Yang, C. T. *Sediment Transport: Theory and Practice*, McGraw-Hill Companies, Inc, (1996).

54. Zhang, Q. "Diffusion Process of sedimentation in open channel flow and its application".

55. *Journal of Sediment Research*, (1980).

56. Zhang, R. and Xie, J. *Sedimentation research in China: systematic selections*, China and Power Press, (1993).

57. Zyserman, J. A. and FredsØe, J. "Data analysis of bed concentration of suspended sediment". *Journal of Hydraulic Engineering*, Vol. 120, No. 9, 1021-1042 (1994).